

The CORVET complex: compositions, function, and impact on cellular behaviour

Caspar T. H. Jonker

The CORVET complex: compositions, function, and impact on cellular behaviour

Caspar Theodorus Hugo Jonker 2016

Paranimfen

Gudo J.D. Jonker

Timo E.F. Kujjt

The work described in this thesis was performed in the department of cell biology of the University Medical Center Utrecht, Faculty of Medicine, Utrecht University, The Netherlands with financial support from NWO (VICI 918.56.611).

ISBN

978-90-393-6642-4

Printed by

BOXPress | proefschriftmaken.nl

Printing of this thesis was financially supported by the Stichting tot bevordering van de Electronenmicroscopie in Nederland (SEN).

Cover artwork

Juliëtte Jonker

The CORVET complex: compositions, function, and impact on cellular behaviour

Het CORVET complex: samenstelling, functie, en invloed op cellulair gedrag
(met een samenvatting in het Nederlands)

Proefschrift

ter verkrijging van de graad van doctor aan de Universiteit Utrecht op
gezag van de rector magnificus, prof. dr. G.J. van der Zwaan, ingevolge
het besluit van het college voor promoties in het openbaar te
verdedigen op donderdag 10 november 2016 des middags te 2.30 uur

door

Caspar Theodorus Hugo Jonker

geboren op 18 mei 1986 te Delft

Promotor:

Prof. dr. J. Klumperman

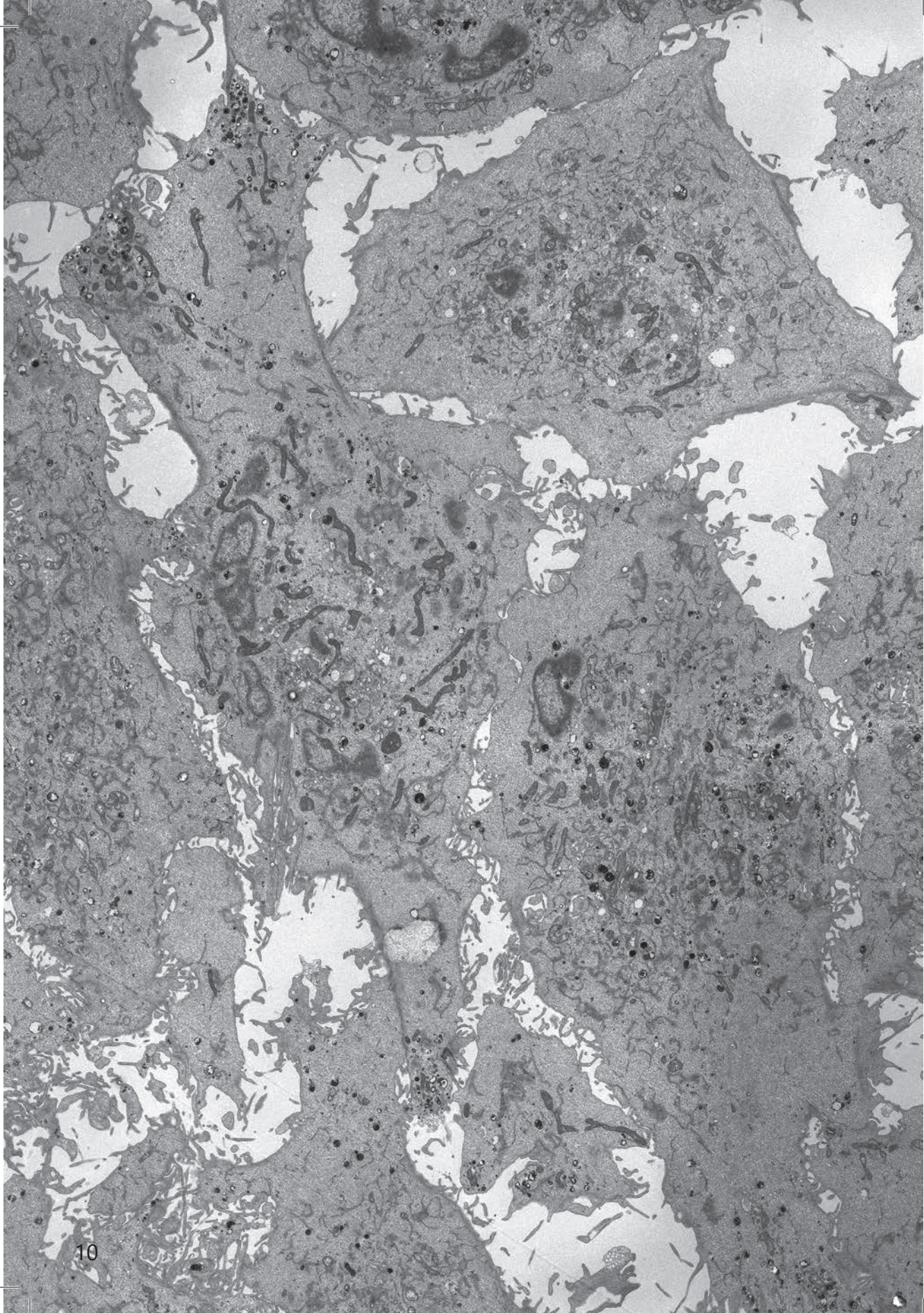
Table of contents

Abbreviations		7
Chapter 1	General Introduction	11
Chapter 2	Characterization of the mammalian CORVET and HOPS complexes and their modular restructuring for endosome specificity.	39
Chapter 3	A complex of Vps3 and Vps8 controls integrin trafficking from early to recycling endosomes and regulates cell adhesion, spreading, and migration.	61
Chapter 4	A Vps8-dependent apical recycling pathway is required for polarized cell organization.	89
Chapter 5	The Smad4 chaperone and CORVET subunit TGFBRAP1/Vps3 has a dual role in TGF β receptor signalling and trafficking.	111
Chapter 6	An adapted protocol to overcome endosomal damage caused by polyethylenimine (PEI) mediated transfections.	129
Chapter 7	Summarizing Discussion	147
Nederlandse Samenvatting		156
Dankwoord/Acknowledgements		159
Curriculum Vitae		167

List of abbreviations

AP	adaptor protein	ESCRT	endosomal sorting complex required for transport
APPL1	adaptor protein, phosphotyrosine interacting with PH domain and leucine zipper 1	Fig	figure
ARC	Arthrogryposis renal dysfunction cholestasis	FYVE domain	Fab1, YOTB, Vac1 and EEA1 domain
ARE	apical recycling endosome	GA	glutaraldehyde
Arf	ADP-ribosylation factor	GAP	GTPase-activating protein
Arl	Arf-like	GDF	growth and differentiation factor
ATP	adenosine triphosphate	GDP	guanosine diphosphate
BAR	bin-amphiphysin	GEF	guanine nucleotide exchange factor
BC	bile canaliculus	GFP	green fluorescent protein
BSA	bovine serum albumin	GST	glutathione S-transferase
BMP	bone morphogenetic protein	GTP	guanosine triphosphate
CCV	clathrin coated vesicle	GTPase	GTP hydrolase
ChIP-seq	chromatin immunoprecipitation sequencing	h	hour
CIE	clathrin independent endocytosis	HeLa	Henrietta Lacks
CI-MPR	cation-independent mannose 6-phosphate receptor	HOPS	homotypic fusion and protein sorting
CLEAR	coordinated lysosomal expression and regulation	HRP	horseradish peroxidase
CME	clathrin mediated endocytosis	ICB	Intracellular bridge
CRE	common recycling endosome	IEM	immuno-electron microscopy
coIP	co-immunoprecipitation	IF	immunofluorescence microscopy
CORVET	class-C core vesicle-endosome tethering	IGG	immunoglobulin G
DAG	diacylglycerol	ILV	intraluminal vesicle
DNA	desoxyribonucleic acid	IP	immunoprecipitation
ECM	extracellular matrix	KD	knockdown
EE	early endosome	LAMP	lysosome-associated membrane protein
EEA1	early endosome antigen 1	LE	late endosome
ELISA	enzyme-linked immunosorbent assay	LMP	lysosomal membrane protein
EM	electron microscopy	LRO	lysosome-related organelle
		Min	minute
		MPR	mannose-6-phosphate receptor
		mRNA	messenger RNA

MTC	multi-subunit tethering complex	SNARE	soluble NSF (N-ethylmaleimide-sensitive factor) attachment protein receptors
MTOC	microtubule-organizing center		
mTORC1	mammalian target of rapamycin complex 1	SNX	sorting nexin
MVB	multi-vesicular body	STX	syntaxin
nm	nanometer	TEM	transmission electron microscope
PBS	phosphate buffer	TFEB	transcription factor EB
PCR	polymerase chain reaction	TGFβ	transforming growth factor beta
PEI	Polyethylenimine	TGFBR	transforming growth factor beta receptor
PFA	paraformaldehyde	TGFBRAP1	transforming growth factor beta receptor associated protein 1
pH	power of hydrogen	TGN	trans-golgi network
PI(x)P	phosphatidylinositol x-phosphate	Tf	transferrin
PI(x)K	phosphatidylinositol x kinase	TfR	transferrin receptor
PLD	phospholipase D	μm	micrometer
PM	plasma membrane	V-ATPase	vacuolar ATP hydrolase
Q-SNARE	glutamine contributing SNARE	VAMP	vesicle-associated membrane protein
qPCR	quantitative PCR	VIPAS39	VPS33B Interacting Protein, Apical-Basolateral Polarity Regulator, Spe-39 Homolog
Rab	Ras-related in brain	Vps	vacuolar protein sorting
RE	recycling endosome	WB	western blot
RILP	Rab7-interacting lysosomal protein	WT	Wild type
RNA	ribonucleic acid		
RNAi	RNA interference		
R-SNARE	arginine contributing SNARE		
RT-PCR	real-time PCR		
SAC	sub-apical compartment		
SARA	Smad anchor for receptor activation		
Scr	scrambled		
SD	standard deviation		
SDS-PAGE	sodium dodecyl sulphate polyacrylamide gel electrophoresis		
SEM	standard error of the mean		
siRNA	small interfering RNA		
SM	Sec1/Munc18		
SMAD	small mothers against decapentaplegic		



Chapter 1

General Introduction

Caspar T. H. Jonker & Judith Klumperman

The endolysosomal network

Endocytosis is the process of internalization of macromolecules, fluids and membrane components from the extracellular space through invagination of the plasma membrane. After endocytic vesicles bud off from the plasma membrane (PM) they fuse with an early endosome (EE) where cargo is sorted towards the degradative pathway or the recycling pathway. When recycled, cargo travels back to the PM either directly from an EE or via specialized recycling endosomes (REs). Material that is not recycled stays in EEs, which mature into late endosomes (LE). LEs are able to fuse with lysosomes allowing the content to be degraded by hydrolases (fig. 1).

The limiting membrane of each compartment in the endolysosomal system has a unique protein and lipid composition. An essential component of the membrane composition is the fusion machinery, which ensures membrane fusion takes place at the correct site and involves the correct membranes. Organelles can only fuse with a limited number of other compartments or vesicles, which makes fusion proteins highly specific for a given membrane, which is why they are often used as markers to identify compartments. The main players of the membrane fusion machinery are Rab (Ras Analog in Brain) proteins, tethering complexes, and soluble NSF attachment protein receptor (SNARE) proteins. Rab proteins are small molecular switches that upon activation are recruited to a specific membrane. Here, they recruit effector proteins such as lipid kinases and tethering complexes. Tethering complexes are large protein complexes that

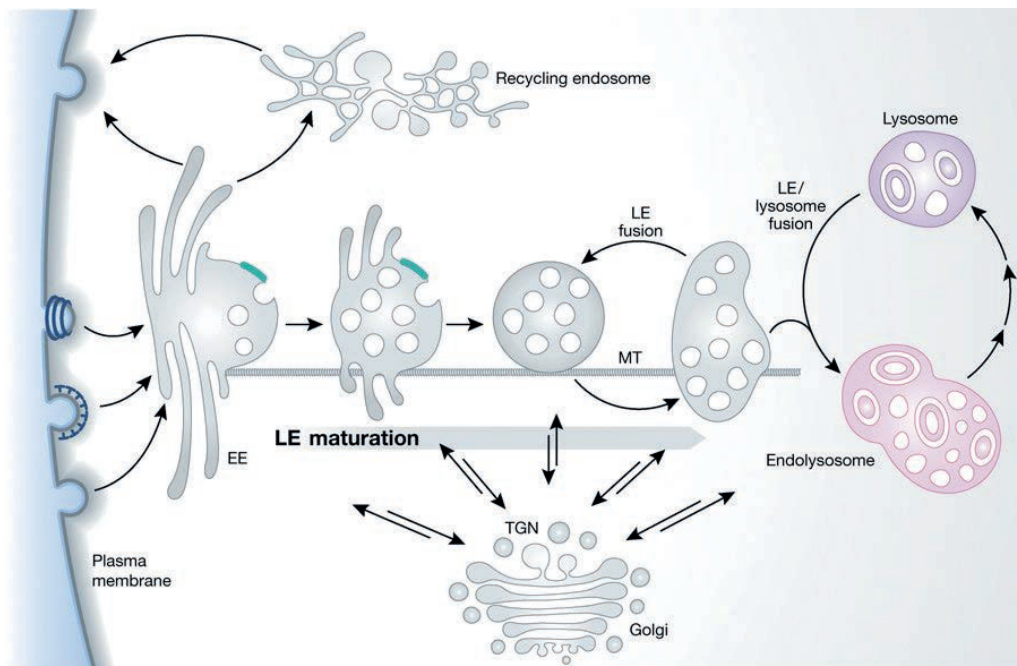


Figure 1. Schematic overview of the endolysosomal system. Endocytosis starts with the formation of vesicles via clathrin mediated endocytosis (CME) or clathrin independent endocytosis (CIE), which fuse with early endosomes (EEs). EEs are sorting stations where cargo is sorted towards the degradative or recycling pathways. Cargo destined for recycling enters tubules where vesicles bud off that travel either directly, or via specialized recycling endosomes (REs) back to the plasma membrane. EEs mature into late endosomes (LEs) which form intraluminal vesicles containing cytosolic cargo to be degraded. LEs can then fuse with hydrolase-containing lysosomes that degrade their content. Image from (79).

establish the first contact between two membranes. This interaction safeguards fusion specificity and brings membranes in close proximity to allow SNARE proteins to mediate membrane fusion. SNARE proteins located on opposite tethered membranes can form a stable trans-complex. The assembly of the trans-SNARE complex together with the assistance of interacting proteins, drives fusion of the tethered membranes. Together the membrane fusion machinery maintains the specificity of fusion events at each compartment and thereby regulates its content and identity. Here we will discuss in detail the entire endolysosomal system and the role of the membrane fusion machinery in its regulation.

Endocytic vesicle formation

At the onset of endocytosis, formation of a vesicle from the PM depends on the type, size, state and location of the cargo, but can also occur independent of cargo (1). The different types of endocytosis are characterized by the morphology of endocytic vesicles using electron microscopy (EM) techniques and by cargo specificity. The best characterized type of endocytosis is clathrin mediated endocytosis (CME), defined by the formation of 50-100nm clathrin coated vesicles (CCVs), which by EM have a visible lattice of clathrin surrounding the membrane (2). Clathrin is a cytosolic protein complex that is recruited to the site of endocytosis by the general adaptor protein AP2 or by cargo-specific AP1 (3). At the site of endocytosis (or nucleation site) specialized proteins initiate membrane bending and interact with cell-surface receptor tails and AP2 (4–6). AP2 then recruits additional adapter proteins to mediate cargo selection (7–9). Next, clathrin is recruited and polymerizes into a lattice of hexagons and pentagons that stabilizes the increased membrane curvature generated by CALM/AP180, Epsins and BAR-domain proteins (10–12). The BAR-domain containing proteins recruit dynamin, which mediates the fission of the vesicle from the plasma membrane (13–15). After the release from the PM, the clathrin lattice is disassembled and the vesicle proceeds to its target endosome (16).

Despite being the best understood form of endocytosis, the entire mechanism of CCV formation is not completely elucidated. CME is illustrative of the complexity of forming a vesicle containing the correct cargo from the correct site at the PM. Other (clathrin-independent) forms of endocytosis (CIE) have been identified by their morphology, cargo and regulatory proteins, but have a similar function: concentration of cargo at the PM and producing a vesicle that can enter the endolysosomal system.

Early endosomes

For all types of endocytosis, the first station after internalization are EEs. At EEs cargo is sorted towards either degradation in lysosomes or recycling to the PM, hence, EEs are also known as sorting endosomes. However, in addition to sorting, EEs also have roles in cellular processes such as receptor mediated signaling (Box 1). EEs are dynamic compartments that are generally characterized as 100-500nm diameter vacuoles from which multiple tubules emerge (17). In addition to their morphology, EEs are characterized by a mildly acidic pH (~6.0) that allows the dissociation of ligands from their receptors (18,19), and by the time it takes for endocytosed material to reach the endosome, which for EEs is 1-5 minutes depending on cell type (20–22). However, the most widely used method to identify EEs is to visualize key marker proteins. For EEs this is Rab5, which operates as the regulator for membrane fusion (fig. 2) (23,24).

Activation and recruitment of Rab5 to EEs is mediated by Rabex-5, which localizes to

Box 1. The endolysosomal system and TGF β signaling

Transforming growth factor-beta (TGF β) is a cytokine belonging to the TGF- β superfamily of growth factors, which modulate expression of hundreds of genes and thereby regulate cellular processes such as cell proliferation, tissue homeostasis and cell motility (199,200). TGF β signaling starts with binding of TGF β to type II cell surface receptors (TGFBRII), which induces complex formation with type I (TGFBR I) receptors. TGFBR I and TGFBR II are continuously endocytosed independent of ligand binding (201–203), although endocytosis can be triggered by ligand binding. (204–206). After internalization into EEs, activated receptor complexes associate with Smad Anchor for Receptor Activation (SARA), which is recruited to EEs by binding PI3P via its FYVE-domain (207). In addition SARA binds Smad2 and thereby facilitates recruitment of Smad2 and Smad3 to the activated TGF β receptor complex on endosomes (207–209). Since SARA-mediated Smad activation can only occur at EEs, endocytosis is a crucial step in TGF β signaling (203,209,210). At EEs, the Smad2/3 complex then binds Smad4, after which the entire Smad2/3/4 complex shuttles to the nucleus to modulate the expression of an extensive amount of genes (199,211–213).

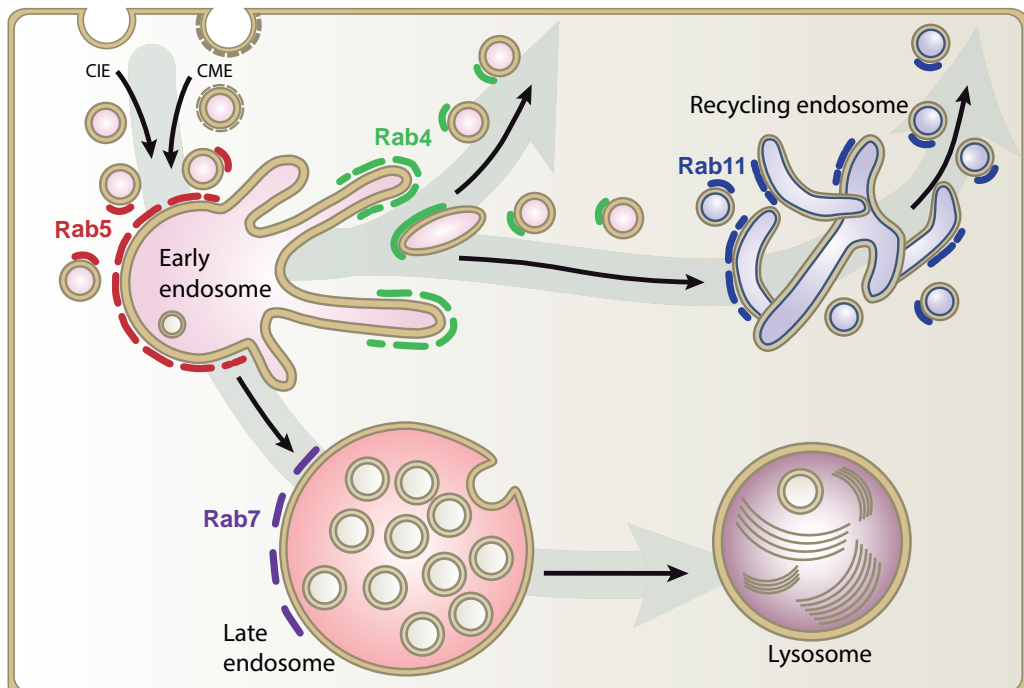


Figure 2. Rab localizations in the endolysosomal system. Rab-proteins are commonly used markers to distinguish endosomal compartments. At EEs, Rab5 is present on the vacuole, while Rab4 concentrates on the tubular domains. Rab4 is also present on recycling vesicles that transport cargo to the PM for fast recycling or to the RE for slow recycling. The RE is positive for Rab11, which regulates fusion of vesicles with the RE as well as transport from the RE to the PM. Upon maturation of an EE to a LE, Rab5 is replaced by Rab7, inducing movement to the perinuclear area and allowing fusion with lysosomes where cargo is degraded by lysosomal hydrolases. CME: clathrin mediated endocytosis; CIE: clathrin independent endocytosis.

EEs by binding ubiquitin on ubiquitinated endocytosed cargo (25–28). Rab5 and Rabex-5 recruit a series of effector proteins such as the tethering factor EEA1 (29) and the lipid kinase Vps34 (30,31). These proteins stabilize Rabex-5 on the membrane causing a positive feedback loop on the EE localization of Rabex-5, Rab5 and their effector proteins (32). In addition, Vps34 generates phosphatidylinositol-3-phosphate (PI3P), leading to increased recruitment of effector molecules (31,32). The positive feedback loop of Rab5 activation establishes EE membrane identity and recruits proteins necessary for proper fusion of endocytic vesicles with EEs and homotypic fusion between EEs.

The Rab5 positive feedback loop is interrupted on EE tubules, from where recycling takes place. Rabenosyn-5, which is recruited by the Rab5 feedback loop, is thought to facilitate segregation of cargo into the tubules, which are marked by Rab4 (fig. 2) (33) (34). The exact mechanism of generating Rab4 membrane domains on a Rab5-positive compartment, is poorly understood. The only other event where the Rab5 positive feedback loop is broken is during maturation of an EE to a LE, which is discussed below.

Endocytic recycling

Depending in cell type, it is estimated that endocytosis is responsible for the internalization of 0,5 to 1,8 times the total cell surface area per hour (35). This amount of uptake is counterbalanced by the continuous recycling of endocytosed material and membrane to the PM. The fast turnover of membrane components through endocytosis and recycling allows precise control of the composition of the PM, and therefore is vital for cellular processes at the PM such as cell-matrix attachment, cell-cell adhesion, cell migration, signal transduction, cell division and establishment of cell polarity.

From EEs there are 2 main recycling routes. Cargo can either be transported back to the PM directly (also called “fast recycling” or “short-loop recycling”), or indirectly via REs (also called “slow recycling” or “long-loop recycling”) (fig. 2). These separate recycling pathways allow molecules to be separately returned to the PM at different rates. Fast recycling transport molecules to the PM around 1-5 min after endocytosis, while slow recycling takes on average 10-15 min (36,37). Not all cargo is completely separated over the two recycling pathways, transferrin receptors (TfRs) for example travel through both fast and slow recycling pathways (37) while distinct integrins are recycled separately (38–42) (Box 2).

Fast Recycling

During fast recycling, vesicles pinch off from tubular membrane regions on EEs and fuse with the PM. Fast recycling is regulated by Rab4, which resides on EE tubules and EE-derived recycling vesicles(43–45). Dominant negative mutants of Rab4 inhibit recycling of endocytosed cargo such as transferrin (Tf) (43,44), the most widely used marker for endocytic recycling. Hence, Rab4 is often used as a specific marker for fast recycling. However, this is challenged by studies that show that siRNA mediated knockdown of Rab4 has a positive effect on Tf recycling (46), whereas overexpression of Rab4 has a negative effect (47). In addition, Rab4 is present on REs but not the PM (34,48,49) and some cargos travel to REs via a Rab4 positive intermediate (50–53). Together these data indicate that Rab4 is not exclusively involved in fast recycling, but also in transport from EEs to REs.

Slow recycling

Slow recycling requires 2 steps: transport from EEs to REs and transport from REs to the PM. REs are heterogeneous and dynamic compartments, consisting mainly of a collection of tubules and vesicles (17,54). In most cell types REs are found in the perinuclear area near the microtubule organizing center (MTOC) (55,56). However, in other cell types such as HeLa, REs have a more dispersed localization (57), and in polarized cells REs localize near the apical PM (58,59). The main marker for REs is the small GTPase Rab11, the main regulator of fusion with REs and recycling from REs (60–63) (fig. 2). Additional markers are the SNARE Cellubrevin/VAMP3 and the Rab11 family interacting proteins (Rab11-FIPs) (55,64–66).

The route from EEs to REs requires Rab4 and Sorting nexin 4 (SNX4), which both localize to the tubular domains of EEs and REs. SNX4 regulates transport of EE-derived vesicles by recruiting KIBRA, a protein that interacts with the motor protein dynein (67). siRNA mediated depletion of SNX4 results in rerouting of TfRs to LEs and lysosomes, showing that SNX4 knockdown blocks exit from EEs and thus inhibits the fast and slow recycling pathway. In contrast, depletion of the Rab effector protein RAB11FIP5, which mediates transport of TfRs from EEs to REs, does not inhibit fast recycling, and therefore likely acts downstream from SNX4 (68). The pathway between EEs and REs is poorly described and specific regulatory proteins for this pathway are not yet identified.

Transport from REs to the PM can occur via several distinct pathways. For example, in HeLa cells TfRs travel from REs to the PM in separate vesicles than MHCI and other clathrin-independent endocytosed (CIE) cargo (69). Although both pathways depend on Rab11 (70,71), it has become increasingly clear that these pathways are separately regulated. Unlike TfR recycling, recycling of CIE cargo requires Arf6 and Rab8. Arf6 is recruited to REs by MICAL-L1 and activates phospholipase D (PLD), which generates diacylglycerol (DAG) and phosphatidic acid (PA) that assist fission of vesicles from REs and fusion of vesicles with the PM (72,73). The Arf6 dependent pathway of CIE cargo likely involves a subpopulation of REs. This is in agreement with studies that show multiple subsets of Rab11 positive REs in one cell, as well as multiple distinct domains in the same RE region (64,69,74–76). Polarized epithelial cells contain separate recycling compartments for apical and basolateral cargo, which are needed for proper recycling to distinct membrane domains (Box3) (77). Subcompartmentalization of the recycling system in non-polarized cells most likely has a similar regulatory function, but the details of this system are poorly understood.

Endosomal maturation and late endosomes

Proteins that are not recycled to the PM accumulate in the main body of EEs. Here, ubiquitinated membrane proteins recruit the endosomal sorting required for transport (ESCRT) complex that induces inward-budding of the limiting membrane, producing intraluminal vesicles (ILVs) (78). Membrane proteins, cytoplasmic proteins, RNAs and lipids are targeted for lysosomal degradation via these ILV's. Formation of ILVs is initiated on EEs and increases upon maturation of an EE to a LE. A single LE can have over 30 ILVs, which is why LEs are also referred to as multivesicular bodies (MVBs) (17,79). Maturation of EEs to LEs is accompanied by their movement to the perinuclear area. In addition, maturing EEs lose their tubular domains resulting in a spherical compartment with a diameter of 0,2-1,0 μ M (17).

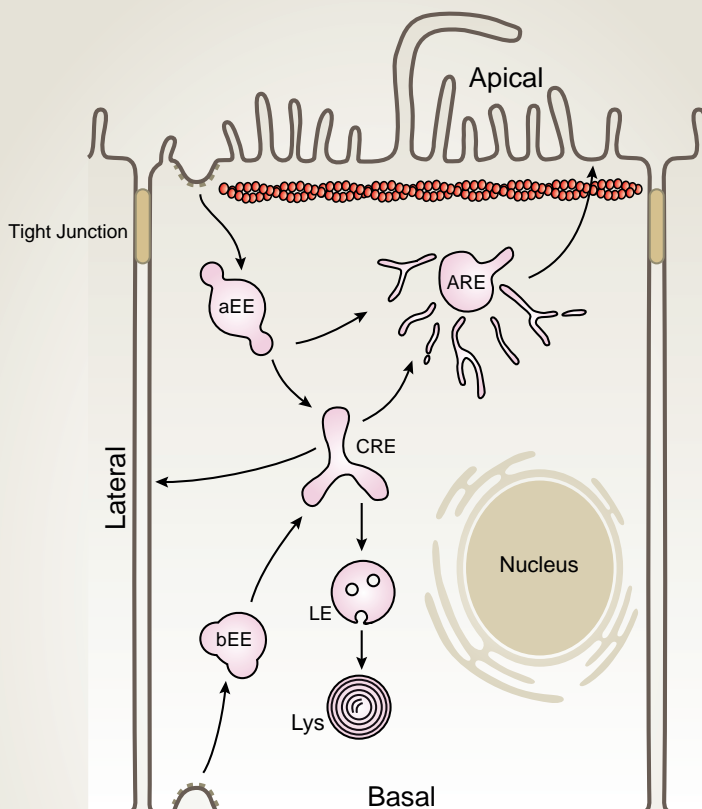
Box 2. Fast and slow integrin recycling

Integrins are transmembrane cell surface proteins that establish the adhesion of cells to the extracellular matrix (ECM) (214). Integrins connect to the ECM as heterodimers (one alpha and one beta subunit). In vertebrates, 24 different integrin pairs exist that each have distinct substrate specificity (40,215). Constitutive endocytosis and regulated recycling of integrins determines the availability of integrin heterodimers at the PM and thereby regulates cellular processes such as cell adhesion and migration (42,216,217). Recycling of integrins occurs via fast or slow recycling pathways depending heterodimer composition, conformation (active or inactive) and ligand binding. Recycling of the majority of integrins depends on Rab11, thus involving slow recycling via REs. However, cellular triggers can alter the recycling of integrins. For example, growth factor stimulation of fibroblasts induces the Rab11-independent fast recycling of $\alpha v\beta 3$, while $\alpha 5\beta 1$ recycling remains Rab11-dependent (218). By regulating recycling, substrate specific adhesion of cells and integrin-mediated signaling are regulated (216,219). Integrins can adopt an active or inactive conformation, which defines the affinity for ECM ligands. For $\beta 1$ integrins the activation state does not alter endocytosis rates, but does influence recycling. Active $\beta 1$ integrins recycle via Rab11-positive REs, while inactive $\beta 1$ integrins recycle directly from EEs to the PM (41). This mechanism increases the pool of inactive and decreases active $\beta 1$ integrin at the PM, as a feedback mechanism for integrin activation (42).

During maturation of endosomes, the Rab5 dependent positive-feedback loop that maintains EE membrane identity is interrupted by replacing Rab5 with Rab7, the main regulator of LE fusion (fig. 2) (80). The cytosolic proteins Ccz1 and SAND1/mon1 bind activated Rab5 and PI3P, thereby displacing Rabex-5 and facilitating the recruitment of activated Rab7 (81–83). The timing of the Rab5-to-Rab7 conversion depends on the PI3P levels of the EE, ensuring that the conversion does not take place too early (84). Membrane associated Rab7 recruits its own set of effector molecules marking the final conversion to a functional LE. Rab7 effector molecules include the Rab7-interacting lysosomal protein (RILP), which binds p150glued and thereby recruits dynein motors for movement to the perinuclear area (85). In addition, RILP recruits the homotypic fusion and protein sorting (HOPS) tethering complex, which regulates fusion events at LEs and lysosomes (86–88). Rab7 also recruits the retromer complex, which facilitates the recycling of proteins to the trans Golgi network (TGN) (89,90).

The conversion to a LE is accompanied by a decrease in pH from 6.8-5.9 in EEs to 6.0-4.9 in LEs. The vacuolar-type H⁺ ATPase (V-ATPase), a transmembrane proton pump complex, actively transports protons across the limiting membrane of the endosome thereby decreasing the luminal pH, which is necessary for optimal activation of lysosomal hydrolases (91). The drop in pH is coupled to an increased transport of hydrolases and lysosomal membrane proteins (LMPs) to LEs (92). Multiple routes exist for the delivery of hydrolases and LMPs to LEs and lysosomes. Mannose-6-phosphate receptors (MPR) regulate the transport of the majority of lysosomal enzymes from the TGN to lysosomes (93,94). Newly synthesized, Mannose-6-phosphate (M6P) containing proteins bind to MPRs and are sorted into clathrin coated vesicles at the TGN that fuse with endosomes (95–97). In the acidified endosomal environment MPRs dissociate from their ligand and recycle to the TGN for another round of transport (89,98). LMPs are transported in an MPR-independent manner to lysosomes and instead rely on a tyrosine- or di-leucine based

Box 3. Recycling in polarized cells



Polarized epithelial cells have an apical and basolateral PM that are separated by junctions that inhibit mixing of membrane domains. Endocytosed cargo from the apical domain is transported to apical EEs and basolateral cargo to basolateral EEs (220–222). From there fast recycling can occur back to the original PM domains. For the slow recycling pathway, both apical and basolateral cargo is transported to the common recycling endosome (CRE) (223). At the CRE, basolateral cargo is transported directly to the basolateral PM while apical cargo travels from CRE to a specialized apical recycling endosome (ARE) to reach the apical PM (59,224,225). These separated recycling routes are necessary to maintain the distinction between the PM domains (226–228). Like in non-polarized cells, Rab11 is a key regulator for recycling in polarized cells. Rab11 regulates vesicular transport to and from the apically localized AREs (229–233). In contrast, recycling from the CRE does not depend on Rab11, but relies on Rab8 and Rab10 (234,235). Despite being differentially regulated, it is still unclear whether the ARE and CRE are separate compartments or different membrane domains of the same compartment (222,228,236).

sorting motif that interacts with GGAs and the adaptor protein AP-1 at the TGN, enabling traffic to endosomes (99,100). Alternatively, LMPs can reach lysosomes through an indirect pathway via the PM followed by clathrin mediated endocytosis (101). A third route for the transport of LMPs directly from the TGN to LEs in an AP-1 and clathrin independent manner requires VAMP7 and Vps41, which assist in the fusion with LEs (102). The recruitment of fusion machinery and transport of lysosomal proteins to LEs prepares for the fusion of LEs with lysosomes.

Lysosomes

Lysosomes are ubiquitous acidic organelles that are the main site for degradation in the cell. Lysosomes receive cargo from autophagic pathways by fusing with autophagosomes, and from the endosomal pathway by fusing with LEs. Degradation of cargo starts in LEs (79,103), but the majority of the proteolytic activity takes place after fusion of a LE with a lysosome (104,105). Fusion of a LE with an acidic lysosome (pH 4.5-5.0) results in a further drop of the luminal pH and a rise in Ca²⁺ levels triggering the maturation of precursor hydrolases (106,107). Lysosomes contain over 50 different lysosomal hydrolases which degrade the content including the lipids of the ILVs (108). Heavily glycosylated LMPs protect the limiting membrane of the lysosome from its own hydrolytic activity. In addition, LMPs have a diversity of functions that are required for lysosome integrity, lipid homeostasis and the maintenance of an optimal milieu for lysosomal hydrolases (101,109–111).

The past few years have changed the dogma that lysosomes are just passive endpoints of the endocytic pathway completely. Recent data shows that lysosomes are active signaling compartments that modulate cellular lysosomal and autophagic activity. For example, detection of amino acid levels inside the lysosomal lumen is performed by a complex of Rag GTPases, Ragulator and the vacuolar-type H⁺ ATPase (V-ATPase) (112–114), which regulate the lysosomal recruitment of the mTOR complex 1 (mTORC1) in nutrient rich conditions. After recruitment, mTORC1 binds and phosphorylates Transcription Factor EB (TFEB), a master regulator of lysosomal biogenesis (115,116). Lysosomal recruitment inhibits translocation of TFEB to the nucleus, thereby blocking its function in upregulating genes of the Coordinated Lysosomal Expression and Regulation (CLEAR) network (115,117). By contrast, during starvation mTORC1 is not recruited to the lysosome and does not phosphorylate TFEB, which can therefore freely translocate to the nucleus to upregulate cellular lysosomal and autophagic activity (115).

Membrane fusion

Transport specificity and maintenance of membrane identity in the endolysosomal system is controlled by an elaborate membrane fusion machinery. Three main protein groups are crucial for membrane fusion: Rab proteins, Tethering complexes and SNARE proteins (fig. 3). Together these proteins ensure proper fusion at the correct site and between correct membranes.

Rab proteins

Rab proteins are the largest group of the Ras superfamily of small monomeric G proteins and key factors in determining organelle membrane identity (118,119). Rab proteins cycle between a GTP bound (active) and GDP bound (inactive) state, which are catalyzed by Guanine-nucleotide exchange factors (GEFs) and GTPase-activating proteins (GAPs) (120,121). The GTP/GDP cycles of Rab proteins regulate their membrane localization. In the cytosol Rab proteins are kept in a soluble inactive (GDP-bound) state through interaction with Rab GDP-dissociation inhibitors (Rab-GDI) (122,123). Membrane targeting occurs by prenylation of Rab proteins on their C-terminus, followed by GEF-mediated stabilization on the membrane (27,124,125). The activation state of Rab proteins controls their ability to recruit various effector proteins such as tethering factors and lipid kinases (126). The combination of controllable membrane targeting and effector recruitment establish Rab proteins as master regulators of intracellular trafficking and membrane identity.

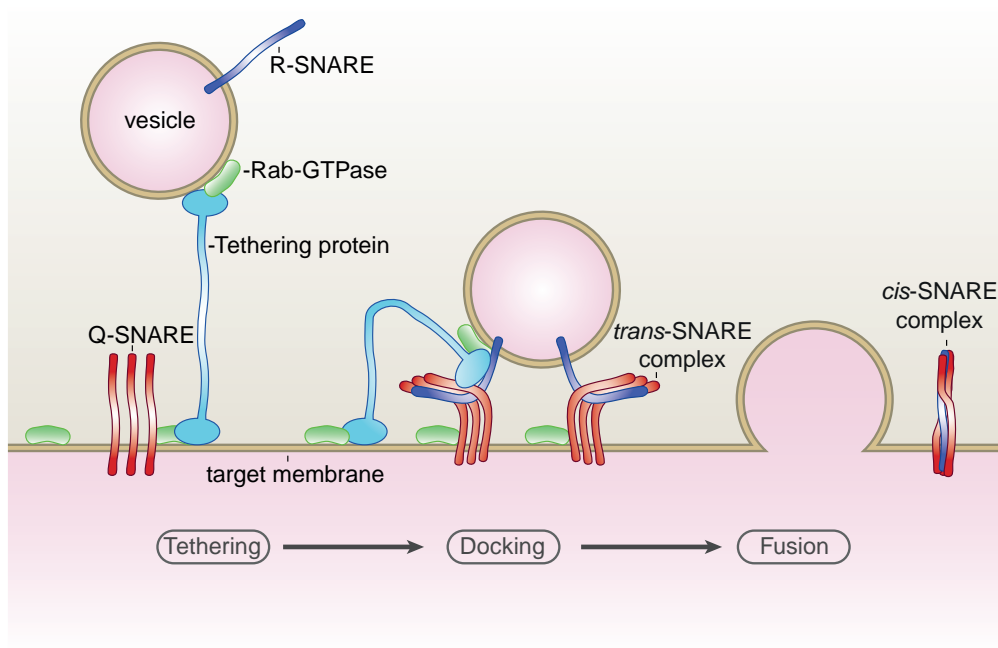


Figure 3. Schematic overview of membrane fusion. Membrane fusion requires the coordinated action of Rab proteins, tethering factors and SNARE proteins. Before fusion, Rab-GTPases are recruited to the membrane and in turn recruit other fusion machinery such as SNAREs and tethers. Membrane fusion starts with tethering proteins establishing the first connection between two membranes. Tethers bring the membranes in close proximity to allow formation of trans-SNARE complexes. The trans-SNARE complex undergoes a conformational change that pulls membranes together leading to fusion of the membranes.

Tethering factors

Tethering factors mediate the docking of a vesicle or compartment to its target membrane. This reflects the first contact between two membranes and therefore the first regulatory step to ensure specificity of membrane fusion (127–129). Rab or Arl GTPases recruit tethers to specific membrane domains (130–132), where they are able to dock incoming vesicles, recruit effector proteins and assist in SNARE complex formation (29,127,133–136). Tethering factors can be divided into two main groups: multisubunit tethering complexes (MTCs) and long coiled-coil proteins (137,138). The coiled coil tethering factors are large hydrophilic homodimers that consist of a head and tail domain that interact with two opposite membranes (137). The length to span the distance between two membranes is provided by an elongated coiled coil domain, which in some cases reaches over 400nm (137,139). Multisubunit tethering complexes (MTCs) are a heterogenic group of protein complexes that consist of up to 10 subunits. Despite their higher molecular weight, the compact structure of MTCs results in a limited reach of maximally 30nm, preventing them to reach over equally long distances as the coiled coil tethers (140–142). However, the presence of multiple subunits permits additional regulatory roles in membrane fusion. For example, MTCs promote SNARE assembly (140), movement along microtubules (85,86), endosome maturation (79), coat protein interaction (143) and membrane bending (144,145). Moreover, some MTCs share subunits between complexes (146,147) and independent roles for individual MTC subunits have been described (102). Together these characteristics indicate that the role of MTCs comprises more than tethering alone, as will be discussed below in detail for the CORVET and HOPS tethering complexes.

SNARE proteins

After tethering, SNARE proteins located on the two opposing membranes mediate the actual membrane fusion. SNARE proteins are grouped into two types, Q-SNAREs (Glutamine contributing SNAREs) and R-SNAREs (Arginine contributing SNAREs) (148). To form a SNARE complex, three Q-SNAREs on the target (acceptor) membrane and one R-SNARE on the incoming vesicle (donor) membrane form a trans-complex between the membranes (149,150). Pairing of the Q-SNAREs and R-SNAREs in the trans-SNARE complex only provides limited specificity for membrane fusion. Several SNARE proteins can engage in non-functional but stable SNARE complexes *in vitro* (151,152), emphasizing that Rab proteins and tethering factors are additionally important to determine fusion specificity (153). Formation of the trans-SNARE complex is regulated by SNARE-interacting Sec1/Munc18 (SM) proteins, since removal of SM proteins completely perturbs membrane fusion (150,154). In addition, SM proteins are implicated in membrane bending, SNARE complex stabilization and lipid mixing (155). During trans-SNARE complex formation, the individual unstructured SNARE proteins form a stable bundle of four α -helices (156,157). This folding process, named “zippering”, exerts force on the opposite membranes pulling them together (158). Although the exact stoichiometry of SNARE mediated fusion is still unsure, the assembly of one SNARE complex supplies around one third of the force necessary to fuse two membranes, suggesting that three SNARE complexes are sufficient for membrane fusion (159). After membrane fusion the bundled SNARE complex resides in the fused membrane as a cis-SNARE complex, which needs to be disassembled. This requires ATP-hydrolysis and is mediated by the cis-SNARE complex binding proteins NSF and its adapter SNAP, after which the individual SNAREs are primed for a new round of fusion (160,161).

Tethering complexes of the endolysosomal system: CORVET, HOPS and Vps33B/VIPAS39

Since this thesis focusses on the CORVET and HOPS tethering complexes, these complexes are described here in detail.

1

The HOPS complex

The Homotypic fusion and protein sorting (HOPS) complex is a multisubunit tethering complex that was originally described in yeast (162). Mammalian HOPS consist of six subunits, Vps41, Vps39, Vps11, Vps16, Vps18 and Vps33A, of which four core subunits (11, 16, 18 and 33A) are shared with the class-C core vacuole endosome transport (CORVET) complex (142,163,164). Cryo-EM studies on the molecular structure of the HOPS complex revealed an elongated, curved complex, in which the core subunits are located in the center between Vps39 and Vps41 (142) (fig. 4). In yeast, Vps41 and Vps39 both interact with the Rab7 homologue Ypt7, suggesting that Vps41 and Vps39 interact with two opposing Ypt7-positive membranes to mediate tethering. In mammals, recruitment of Vps39 and Vps41 to membranes is regulated by interaction with Rab7 as well as Rab7 effector proteins, indicating that in mammals HOPS regulates fusion events at Rab7-positive LEs as well (87,162,165–172). Knockdown of Vps39 or Vps41 indeed inhibits LE and lysosomal fusion events, resulting in accumulation of LEs that are unable to fuse with each other or with lysosomes (88). Moreover, the HOPS complex is one of the few MTC's for which a positive effect on fusion is directly demonstrated since a reconstituted HOPS complex accelerates the SNARE mediated fusion between liposomes (173–175). Apart from membrane tethering and fusion, the HOPS complex also mediates other events at LEs and lysosomes. For example, in yeast the Sec1/Munc18 (SM) protein and HOPS component Vps33p binds lysosomal SNAREs and ensures the correct pairing of SNARE proteins in a process named “proofreading” (135,176). In addition, the HOPS complex facilitates anterograde transport of LEs and lysosomes via interactions with Arl8b and its effector SKIP, which bind kinesins (177), as well as retrograde transport of LEs via interactions with the Rab7 effector protein RILP, which binds the dynein motor complex (85–87,165). Together with the connection to coat proteins (166), the ESCRT machinery (178), the actin cytoskeleton (179,180) and the individual roles of HOPS subunits (102), these additional functions indicate that the HOPS complex is more than a tether, it is a hub for many critical functions on the LE membrane.

The CORVET complex

Like the HOPS complex, the CORVET complex was originally described in yeast and consists of the same core subunits as the HOPS complex, with the addition of Vps3p and Vps8p (181) (fig. 4). Although CORVET subunits are well conserved from yeast to mammals, the mammalian homolog of Vps3p has only recently been identified as TGF β -Receptor associated protein 1 (TGFBRAP1), now also known as Vps3 (182,183). In the CORVET complex, Vps8 and Vps3 are located on opposite sides of the complex, similar to Vps41 and Vps39 in HOPS (142,171). Since Vps8 and Vps3 show homology to Vps41 and Vps39, respectively, they were modelled into the CORVET structure based on the positions of Vps41 and Vps39 in the HOPS complex (142). In yeast, Vps3p and Vps8p interact with Vps21, the yeast Rab5 ortholog, which is required for recruitment of the complex to endosomes (181,184–186). This interaction is conserved since in

mammalian cells Vps8 interacts with Rab5, localizing the CORVET to EEs (87,182,187). At EEs, the CORVET complex mediates the homotypic fusion of EEs (182). Despite high homology of CORVET and HOPS, their interaction partners and membrane localizations are surprisingly separate. For example, the HOPS binding protein RILP does not interact with the CORVET complex (86,87,165), ensuring that CORVET remains upstream of LEs. Although the CORVET complex is less extensively studied than the HOPS complex, it is speculated that CORVET, like HOPS, has a broader array of functions than tethering alone.

Vps33B and VIPAS39

All HOPS and CORVET subunits are well conserved and all eight subunits are found in mammals, with the addition of two subunits, Vps33B and VIPAS39 (also known as VIPAR or SPE-39) (147,188,189). These proteins are homologous to Vps33A and Vps16 respectively, but are not included in the CORVET or HOPS complex (fig. 3). Vps33B and VIPAS39 strongly interact with each other and this interaction is required for their membrane localization (190,191). The Vps33B/VIPAS39 complex localizes to both LEs and REs (87,191,192). Both VIPAS39 and Vps33B interact with RILP recruiting them to LEs. In addition, Vps33B interacts with Rab11 and the SNARE VAMP3 on REs (87). Mutations in Vps33B and VIPAS39 underlie Arthrogryposis Renal dysfunction Cholestasis (ARC) syndrome, a multisystem disorder that is characterized by neurogenic arthrogryposis multiplex congenita, renal tubular dysfunction and neonatal

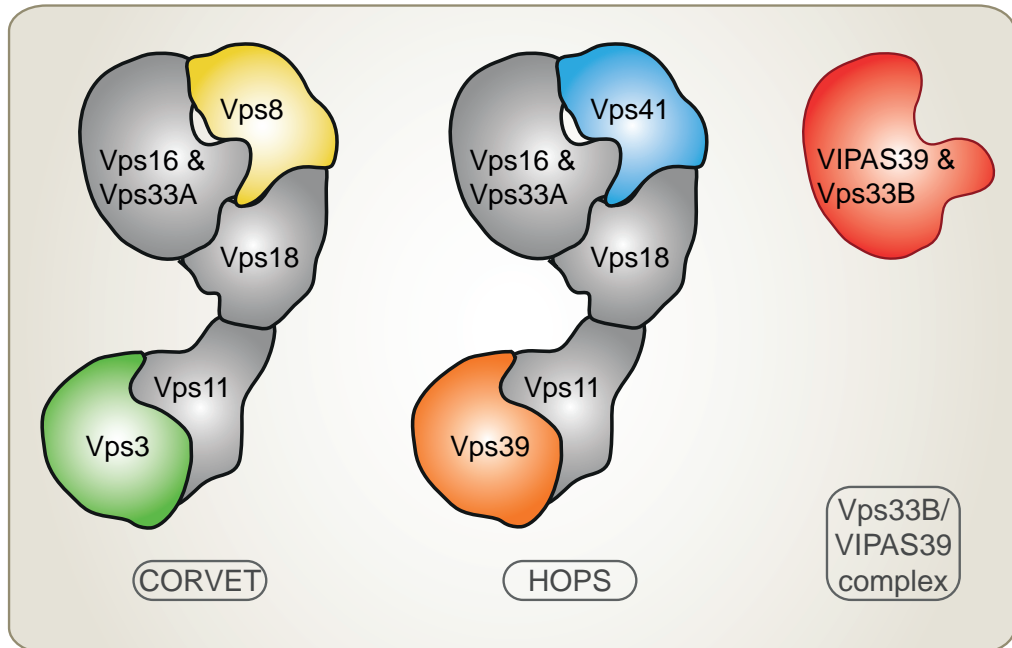


Figure 4. Schematic representation of the CORVET, HOPS and Vps33B/VIPAS39 complexes. CORVET and HOPS are related tethering complexes each consisting of six subunits. CORVET and HOPS share a core of 4 proteins (Vps11, Vps16, Vps18, Vps33A) and have two complex specific subunits (Vps8 and Vps3 (also named TRAP1 or TGFBRAP1) for CORVET and Vps41 and Vps39 for HOPS). In mammalian cells a third complex next to the CORVET and HOPS exists, consisting of Vps33B and VIPAS39 (also named VIPAR or SPE-39), which are homologues to Vps33A and Vps16 respectively. Structures based on Cryo EM studies on HOPS (142).

cholestasis (191,193,194). These phenotypes are at least in part attributed to the role of VIPAS39 and Vps33B at the RE, since the disease-causing mutations result in the mislocalization of apical membrane proteins in renal cells and hepatocytes (191,193,194). Additionally, perturbation of Vps33B and VIPAS39 impairs the formation of alpha-granules in platelets, which is likely caused by the disruption of LE function in megakaryocytes (195–197). These functions have caused speculation on the participation of Vps33B and VIPAS39 in alternative HOPS/CORVET complexes (198), but no evidence for this has been found to date. This positions the Vps33B/VIPAS39 complex as a separate complex from HOPS and CORVET.

Scope of this thesis

The endolysosomal system is positioned on the crossroad of the intracellular and extracellular environment and is therefore crucial to regulate many cellular processes. Proper function of the endolysosomal system greatly depends on the concept of membrane identity; the controlled protein and lipid composition of all organellar membranes. To maintain this identity requires exact timing and regulation of membrane fusion, organelle motility and signaling, together regulating transport inside the cell. Multi-subunit tethering complexes such as CORVET and HOPS are increasingly implicated as interaction hubs for many aspects of membrane fusion, organelle motility and signaling. In this thesis we investigate the structure and function of the mammalian CORVET complex by focusing on subunits Vps3 and Vps8.

Compared to yeast, the composition of the mammalian CORVET and HOPS complexes are less well described. In **chapter 2** we investigate the mammalian CORVET and HOPS complexes and the mammalian specific VIPAS39/Vps33B complex and unravel their molecular architecture. We show that CORVET and HOPS differ in their ability to bind RILP. The CORVET specific subunit Vps3 prevents binding of RILP to Vps11 in CORVET, while replacement of Vps3 with the HOPS-specific Vps39 allows binding of RILP to Vps11 in HOPS. Interaction of the HOPS complex with regulating proteins such as RILP and Arl8b connect LEs and lysosomes to motor complexes mediating retrograde and anterograde movement.

In **chapter 3** we investigate the roles of the CORVET-specific subunits Vps3 and Vps8 in more detail. We reveal that in addition to their role in the CORVET complex, these 2 proteins form a separate complex that localizes to EE-derived, Rab4-positive recycling vesicles. We reveal an unexpected role for the Vps3/8 complex regulating integrin transport from EEs to REs together with the VIPAS39/Vps33B complex and VAMP3. Knocking down the Vps3/8 or VIPAS39/Vps33B complexes impairs integrin recycling as well as integrin-mediated processes such as cell migration, attachment, spreading and focal adhesion formation.

Recycling in polarized cells is markedly different from non-polarized cells to accommodate separate recycling routes from the apical and basolateral PM (Box 3). The VIPAS39/Vps33B complex is involved in recycling of apical proteins in polarized cells and interacts with Vps3 and Vps8. Having established a role for Vps3 and Vps8 in endosomal recycling in non-polarized cells, in **chapter 4** we investigate the role of Vps8 in a polarized cell model. We show that Vps8 localizes to apical EEs and the specialized Rab11-positive apical recycling endosome (ARE). Overexpression of Vps8 induces association of EEs with the ARE indicating a tethering role in the transport between these compartments. Knockdown of Vps8 interferes with correct apical-basal polarization of HepG2 cells and the front-rear polarization of HeLa cells during directed cell migration. In addition we show that knockdown of Vps8 results in impaired abscission during cytokinesis, a defect that is similar to known defects in apical recycling.

Before TGFBRAP1 was identified as the CORVET-specific subunit Vps3, it was shown to function in the TGF β pathway as a Smad4 chaperone. As a consequence, the role of Vps3 as a Smad4 chaperone has not yet been studied in the context of its endosomal functions. In **chapter 5** we investigate the role of Vps3 and Vps8 in the TGF β pathway. We show that Vps3 and Vps8 knockdown decreases Smad4 recruitment to endosomes and leads to intracellular accumulation of TGF β receptor II. These findings suggest a role for Vps3 as well as the Vps3/8 complex and the CORVET complex in the TGF β signaling pathway.

During our studies on endosomal transport we recognized that commonly used approaches to overexpress or knock down proteins affect the integrity of the endolysosomal system. In **chapter 6** we reveal that PEI-mediated transfections, which are used extensively in cell biology research, cause a reduction in the number of EEA1-positive EEs while the number and integrity of lysosomes remain unaltered. However, the reduction in EE numbers is temporary and can be easily overcome by including a chase period in the transfection protocol. These observations resulted in an alternative protocol for overexpression using PEI.

Finally in **chapter 7** the main results of this thesis are summarized and discussed.

References

1. Doherty GJ, McMahon HT. Mechanisms of endocytosis. *Annu Rev Biochem.* 2009;78:857–902.
2. Pearse BM. Clathrin: a unique protein associated with intracellular transfer of membrane by coated vesicles. *Proc Natl Acad Sci U S A.* 1976 Apr;73(4):1255–1259.
3. Zaremba S, Keen JH. Assembly polypeptides from coated vesicles mediate reassembly of unique clathrin coats. *J Cell Biol.* 1983 Nov;97(5 Pt 1):1339–1347.
4. Hollopeter G, Lange JJ, Zhang Y, Vu TN, Gu M, Ailion M, et al. The membrane-associated proteins FCHO and SGIP are allosteric activators of the AP2 clathrin adaptor complex. *elife.* 2014 Oct 10;3.
5. Henne WM, Boucrot E, Meinecke M, Evergren E, Vallis Y, Mittal R, et al. FCHO proteins are nucleators of clathrin-mediated endocytosis. *Science.* 2010 Jun 4;328(5983):1281–1284.
6. Stimpson HE, Toret CP, Cheng AT, Pauly BS, Drubin DG. Early-arriving Syp1p and Ede1p function in endocytic site placement and formation in budding yeast. *Mol Biol Cell.* 2009 Nov;20(22):4640–4651.
7. Kelly BT, McCoy AJ, Späte K, Miller SE, Evans PR, Höning S, et al. A structural explanation for the binding of endocytic dileucine motifs by the AP2 complex. *Nature.* 2008 Dec 18;456(7224):976–979.
8. Collins BM, McCoy AJ, Kent HM, Evans PR, Owen DJ. Molecular architecture and functional model of the endocytic AP2 complex. *Cell.* 2002 May 17;109(4):523–535.
9. Traub LM, Bonifacino JS. Cargo recognition in clathrin-mediated endocytosis. *Cold Spring Harb Perspect Biol.* 2013 Nov 1;5(11):a016790.
10. Ford MG, Mills IG, Peter BJ, Vallis Y, Praefcke GJ, Evans PR, et al. Curvature of clathrin-coated pits driven by epsin. *Nature.* 2002 Sep 26;419(6905):361–366.
11. Miller SE, Mathiasen S, Bright NA, Pierre F, Kelly BT, Kladt N, et al. CALM regulates clathrin-coated vesicle size and maturation by directly sensing and driving membrane curvature. *Dev Cell.* 2015 Apr 20;33(2):163–175.
12. Peter BJ, Kent HM, Mills IG, Vallis Y, Butler PJ, Evans PR, et al. BAR domains as sensors of membrane curvature: the amphiphysin BAR structure. *Science.* 2004 Jan 23;303(5657):495–499.
13. Roux A, Uyhazi K, Frost A, De Camilli P. GTP-dependent twisting of dynamin implicates constriction and tension in membrane fission. *Nature.* 2006 May 25;441(7092):528–531.
14. Sweitzer SM, Hinshaw JE. Dynamin undergoes a GTP-dependent conformational change causing vesiculation. *Cell.* 1998 Jun 12;93(6):1021–1029.
15. Ferguson SM, Raimondi A, Paradise S, Shen H, Mesaki K, Ferguson A, et al. Coordinated actions of actin and BAR proteins upstream of dynamin at endocytic clathrin-coated pits. *Dev Cell.* 2009 Dec;17(6):811–822.
16. Schlossman DM, Schmid SL, Braell WA, Rothman JE. An enzyme that removes clathrin coats: purification of an uncoating ATPase. *J Cell Biol.* 1984 Aug;99(2):723–733.
17. Klumperman J, Raposo G. The complex ultrastructure of the endolysosomal system. *Cold Spring Harb Perspect Biol.* 2014 Oct;6(10):a016857.
18. Davis CG, Goldstein JL, Südhof TC, Anderson RG, Russell DW, Brown MS. Acid-dependent ligand dissociation and recycling of LDL receptor mediated by growth factor homology region. *Nature.* 1987 Apr 29;326(6115):760–765.
19. Maxfield FR, McGraw TE. Endocytic recycling. *Nat Rev Mol Cell Biol.* 2004 Feb 1;5(2):121–132.
20. De Wit H, Lichtenstein Y, Geuze HJ, Kelly RB, van der Sluijs P, Klumperman J. Synaptic vesicles form by budding from tubular extensions of sorting endosomes in PC12 cells. *Mol Biol Cell.* 1999 Dec;10(12):4163–4176.
21. Tooze J, Hollinshead M. Tubular early endosomal networks in AtT20 and other cells. *J Cell Biol.* 1991 Nov;115(3):635–653.
22. Schmid SL, Fuchs R, Male P, Mellman I. Two distinct subpopulations of endosomes involved in membrane recycling and transport to lysosomes. *Cell.* 1988 Jan 15;52(1):73–83.
23. Rybin V, Ullrich O, Rubino M, Alexandrov K, Simon I, Seabra MC, et al. GTPase activity of Rab5 acts as a timer for endocytic membrane fusion. *Nature.* 1996 Sep 19;383(6597):266–269.
24. Gorvel JP, Chavrier P, Zerial M, Gruenberg J. rab5 controls early endosome fusion in vitro. *Cell.* 1991 Mar 8;64(5):915–925.
25. Mattera R, Bonifacino JS. Ubiquitin binding and conjugation regulate the recruitment of Rabex-5 to early endosomes. *EMBO J.* 2008 Oct 8;27(19):2484–2494.

26. Horiuchi H, Lippé R, McBride HM, Rubino M, Woodman P, Stenmark H, et al. A novel Rab5 GDP/GTP exchange factor complexed to Rabaptin-5 links nucleotide exchange to effector recruitment and function. *Cell*. 1997 Sep 19;90(6):1149–1159.
27. Blümer J, Rey J, Dehmelt L, Mazel T, Wu YW, Bastiaens P, et al. RabGEFs are a major determinant for specific Rab membrane targeting. *J Cell Biol*. 2013 Feb 4;200(3):287–300.
28. Barr F, Lambright DG. Rab GEFs and GAPs. *Curr Opin Cell Biol*. 2010 Aug;22(4):461–470.
29. Christoforidis S, McBride HM, Burgoyne RD, Zerial M. The Rab5 effector EEA1 is a core component of endosome docking. *Nature*. 1999 Feb 18;397(6720):621–625.
30. Stack JH, DeWald DB, Takegawa K, Emr SD. Vesicle-mediated protein transport: regulatory interactions between the Vps15 protein kinase and the Vps34 PtdIns 3-kinase essential for protein sorting to the vacuole in yeast. *J Cell Biol*. 1995 Apr;129(2):321–334.
31. Christoforidis S, Miaczynska M, Ashman K, Wilm M, Zhao L, Yip SC, et al. Phosphatidylinositol-3-OH kinases are Rab5 effectors. *Nat Cell Biol*. 1999 Aug;1(4):249–252.
32. Zerial M, McBride H. Rab proteins as membrane organizers. *Nat Rev Mol Cell Biol*. 2001 Feb;2(2):107–117.
33. De Renzis S, Sönnichsen B, Zerial M. Divalent Rab effectors regulate the sub-compartmental organization and sorting of early endosomes. *Nat Cell Biol*. 2002 Feb;4(2):124–133.
34. Sönnichsen B, De Renzis S, Nielsen E, Rietdorf J, Zerial M. Distinct membrane domains on endosomes in the recycling pathway visualized by multicolor imaging of Rab4, Rab5, and Rab11. *J Cell Biol*. 2000 May 15;149(4):901–914.
35. Steinman RM, Mellman IS, Muller WA, Cohn ZA. Endocytosis and the recycling of plasma membrane. *J Cell Biol*. 1983 Jan;96(1):1–27.
36. Mayor S, Presley JF, Maxfield FR. Sorting of membrane components from endosomes and subsequent recycling to the cell surface occurs by a bulk flow process. *J Cell Biol*. 1993 Jun;121(6):1257–1269.
37. Hao M, Maxfield FR. Characterization of rapid membrane internalization and recycling. *J Biol Chem*. 2000 May 19;275(20):15279–15286.
38. Morgan MR, Byron A, Humphries MJ, Bass MD. Giving off mixed signals--distinct functions of alpha5beta1 and alphavbeta3 integrins in regulating cell behaviour. *IUBMB Life*. 2009 Jul;61(7):731–738.
39. Woods AJ, White DP, Caswell PT, Norman JC. PKD1/PKCmu promotes alphavbeta3 integrin recycling and delivery to nascent focal adhesions. *EMBO J*. 2004 Jul 7;23(13):2531–2543.
40. Margadant C, Monsuur HN, Norman JC, Sonnenberg A. Mechanisms of integrin activation and trafficking. *Curr Opin Cell Biol*. 2011 Oct;23(5):607–614.
41. Arjonen A, Alanko J, Veltel S, Ivaska J. Distinct recycling of active and inactive $\beta 1$ integrins. *Traffic*. 2012 Apr;13(4):610–625.
42. De Franceschi N, Hamidi H, Alanko J, Sahgal P, Ivaska J. Integrin traffic- the update. *J Cell Sci*. 2015 Mar 1;128(5):839–852.
43. McCaffrey MW, Bielli A, Cantalupo G, Mora S, Roberti V, Santillo M, et al. Rab4 affects both recycling and degradative endosomal trafficking. *FEBS Lett*. 2001 Apr 20;495(1-2):21–30.
44. Yudowski GA, Puthenveedu MA, Henry AG, von Zastrow M. Cargo-mediated regulation of a rapid Rab4-dependent recycling pathway. *Mol Biol Cell*. 2009 Jun;20(11):2774–2784.
45. De Wit H, Lichtenstein Y, Kelly RB, Geuze HJ, Klumperman J, van der Sluijs P. Rab4 regulates formation of synaptic-like microvesicles from early endosomes in PC12 cells. *Mol Biol Cell*. 2001 Nov;12(11):3703–3715.
46. Deneka M, Neeft M, Popa I, van Oort M, Sprong H, Oorschot V, et al. Rabaptin-5/alpha/rabaptin-4 serves as a linker between rab4 and gamma(1)-adaptin in membrane recycling from endosomes. *EMBO J*. 2003 Jun 2;22(11):2645–2657.
47. Van Der Sluijs P, Hull M, Zahraoui A, Tavitian A, Goud B, Mellman I. The small GTP-binding protein rab4 is associated with early endosomes. *Proc Natl Acad Sci U S A*. 1991 Jul 15;88(14):6313–6317.
48. Sheff DR, Daro EA, Hull M, Mellman I. The receptor recycling pathway contains two distinct populations of early endosomes with different sorting functions. *J Cell Biol*. 1999 Apr 5;145(1):123–139.
49. Nagelkerken B, Van Anken E, Van Raak M, Gerez L, Mohrmann K, Van Uden N, et al. Rabaptin4, a novel effector of the small GTPase rab4a, is recruited to perinuclear recycling vesicles. *Biochem J*. 2000 Mar 15;346 Pt 3:593–601.
50. Li H, Li HF, Felder RA, Periasamy A, Jose PA. Rab4 and Rab11 coordinately regulate the recycling of angiotensin

- II type I receptor as demonstrated by fluorescence resonance energy transfer microscopy. *J Biomed Opt.* 2008 Jun;13(3):031206.
51. Ward ES, Martinez C, Vaccaro C, Zhou J, Tang Q, Ober RJ. From sorting endosomes to exocytosis: association of Rab4 and Rab11 GTPases with the Fc receptor, FcRn, during recycling. *Mol Biol Cell.* 2005 Apr;16(4):2028–2038.
 52. Van der Sluijs P, Hull M, Webster P, Måle P, Goud B, Mellman I. The small GTP-binding protein rab4 controls an early sorting event on the endocytic pathway. *Cell.* 1992 Sep 4;70(5):729–740.
 53. Daro E, van der Sluijs P, Galli T, Mellman I. Rab4 and cellubrevin define different early endosome populations on the pathway of transferrin receptor recycling. *Proc Natl Acad Sci U S A.* 1996 Sep 3;93(18):9559–9564.
 54. Mesaki K, Tanabe K, Obayashi M, Oe N, Takei K. Fission of tubular endosomes triggers endosomal acidification and movement. *PLoS ONE.* 2011 May 10;6(5):e19764.
 55. Van Ijzendoorn SC. Recycling endosomes. *J Cell Sci.* 2006 May 1;119(Pt 9):1679–1681.
 56. Yamashiro DJ, Tycko B, Fluss SR, Maxfield FR. Segregation of transferrin to a mildly acidic (pH 6.5) para-Golgi compartment in the recycling pathway. *Cell.* 1984 Jul;37(3):789–800.
 57. Delevoeye C, Miserey-Lenkei S, Montagnac G, Gilles-Marsens F, Paul-Gilloteaux P, Giordano F, et al. Recycling endosome tubule morphogenesis from sorting endosomes requires the kinesin motor KIF13A. *Cell Rep.* 2014 Feb 13;6(3):445–454.
 58. Hoekstra D, Tyteca D, van Ijzendoorn SC. The subapical compartment: a traffic center in membrane polarity development. *J Cell Sci.* 2004 May 1;117(Pt 11):2183–2192.
 59. Brown PS, Wang E, Aroeti B, Chapin SJ, Mostov KE, Dunn KW. Definition of distinct compartments in polarized Madin-Darby canine kidney (MDCK) cells for membrane-volume sorting, polarized sorting and apical recycling. *Traffic.* 2000 Feb;1(2):124–140.
 60. Ullrich O, Reinsch S, Urbé S, Zerial M, Parton RG. Rab11 regulates recycling through the pericentriolar recycling endosome. *J Cell Biol.* 1996 Nov;135(4):913–924.
 61. Horgan CP, McCaffrey MW. The dynamic Rab11-FIPs. *Biochem Soc Trans.* 2009 Oct;37(Pt 5):1032–1036.
 62. Takahashi S, Kubo K, Waguri S, Yabashi A, Shin HW, Katoh Y, et al. Rab11 regulates exocytosis of recycling vesicles at the plasma membrane. *J Cell Sci.* 2012 Sep 1;125(Pt 17):4049–4057.
 63. Ren M, Xu G, Zeng J, De Lemos-Chiarandini C, Adesnik M, Sabatini DD. Hydrolysis of GTP on rab11 is required for the direct delivery of transferrin from the pericentriolar recycling compartment to the cell surface but not from sorting endosomes. *Proc Natl Acad Sci U S A.* 1998 May 26;95(11):6187–6192.
 64. Radhakrishna H, Donaldson JG. ADP-ribosylation factor 6 regulates a novel plasma membrane recycling pathway. *J Cell Biol.* 1997 Oct 6;139(1):49–61.
 65. Tarbutton E, Peden AA, Junutula JR, Prekeris R. Class I FIPs, Rab11-binding proteins that regulate endocytic sorting and recycling. *Meth Enzymol.* 2005;403:512–525.
 66. Horgan CP, Oleksy A, Zhdanov AV, Lall PY, White IJ, Khan AR, et al. Rab11-FIP3 is critical for the structural integrity of the endosomal recycling compartment. *Traffic.* 2007 Apr;8(4):414–430.
 67. Traer CJ, Rutherford AC, Palmer KJ, Wassmer T, Oakley J, Attar N, et al. SNX4 coordinates endosomal sorting of TfnR with dynein-mediated transport into the endocytic recycling compartment. *Nat Cell Biol.* 2007 Dec;9(12):1370–1380.
 68. Schonteich E, Wilson GM, Burden J, Hopkins CR, Anderson K, Goldenring JR, et al. The Rip11/Rab11-FIP5 and kinesin II complex regulates endocytic protein recycling. *J Cell Sci.* 2008 Nov 15;121(Pt 22):3824–3833.
 69. Naslavsky N, Weigert R, Donaldson JG. Characterization of a nonclathrin endocytic pathway: membrane cargo and lipid requirements. *Mol Biol Cell.* 2004 Aug;15(8):3542–3552.
 70. Powelka AM, Sun J, Li J, Gao M, Shaw LM, Sonnenberg A, et al. Stimulation-dependent recycling of integrin beta1 regulated by ARF6 and Rab11. *Traffic.* 2004 Jan;5(1):20–36.
 71. Weigert R, Yeung AC, Li J, Donaldson JG. Rab22a regulates the recycling of membrane proteins internalized independently of clathrin. *Mol Biol Cell.* 2004 Aug;15(8):3758–3770.
 72. Huttner WB, Zimmerberg J. Implications of lipid microdomains for membrane curvature, budding and fission. *Curr Opin Cell Biol.* 2001 Aug;13(4):478–484.
 73. Jovanovic OA, Brown FD, Donaldson JG. An effector domain mutant of Arf6 implicates phospholipase D in endosomal membrane recycling. *Mol Biol Cell.* 2006 Jan;17(1):327–335.

74. Baetz NW, Goldenring JR. Rab11-family interacting proteins define spatially and temporally distinct regions within the dynamic Rab11a-dependent recycling system. *Mol Biol Cell*. 2013 Mar;24(5):643–658.
75. Baetz NW, Goldenring JR. Distinct patterns of phosphatidylserine localization within the Rab11a-containing recycling system. *Cell Logist*. 2014 Apr 3;4:e28680.
76. Kobayashi H, Fukuda M. Arf6, Rab11 and transferrin receptor define distinct populations of recycling endosomes. *Commun Integr Biol*. 2013 Sep 1;6(5):e25036.
77. Thompson A, Nessler R, Wisco D, Anderson E, Winckler B, Sheff D. Recycling endosomes of polarized epithelial cells actively sort apical and basolateral cargos into separate subdomains. *Mol Biol Cell*. 2007 Jul;18(7):2687–2697.
78. Hurley JH. The ESCRT complexes. *Crit Rev Biochem Mol Biol*. 2010 Dec;45(6):463–487.
79. Huotari J, Helenius A. Endosome maturation. *EMBO J*. 2011 Aug 31;30(17):3481–3500.
80. Rink J, Ghigo E, Kalaidzidis Y, Zerial M. Rab conversion as a mechanism of progression from early to late endosomes. *Cell*. 2005 Sep 9;122(5):735–749.
81. Kinchen JM, Ravichandran KS. Identification of two evolutionarily conserved genes regulating processing of engulfed apoptotic cells. *Nature*. 2010 Apr 1;464(7289):778–782.
82. Nordmann M, Cabrera M, Perz A, Bröcker C, Ostrowicz C, Engelbrecht-Vandré S, et al. The Mon1-Ccz1 complex is the GEF of the late endosomal Rab7 homolog Ypt7. *Curr Biol*. 2010 Sep 28;20(18):1654–1659.
83. Poteryaev D, Datta S, Ackema K, Zerial M, Spang A. Identification of the switch in early-to-late endosome transition. *Cell*. 2010 Apr 30;141(3):497–508.
84. Vieira OV, Bucci C, Harrison RE, Trimble WS, Lanzetti L, Gruenberg J, et al. Modulation of Rab5 and Rab7 recruitment to phagosomes by phosphatidylinositol 3-kinase. *Mol Cell Biol*. 2003 Apr;23(7):2501–2514.
85. Jordens I, Fernandez-Borja M, Marsman M, Dusseljee S, Janssen L, Calafat J, et al. The Rab7 effector protein RILP controls lysosomal transport by inducing the recruitment of dynein-dynactin motors. *Curr Biol*. 2001 Oct 30;11(21):1680–1685.
86. Van der Kant R, Fish A, Janssen L, Janssen H, Krom S, Ho N, et al. Late endosomal transport and tethering are coupled processes controlled by RILP and the cholesterol sensor ORP1L. *J Cell Sci*. 2013 Aug 1;126(Pt 15):3462–3474.
87. Van der Kant R, Jonker CT, Wijdeven RH, Bakker J, Janssen L, Klumperman J, et al. Characterization of the mammalian CORVET and HOPS complexes and their modular restructuring for endosome specificity. *J Biol Chem*. 2015 Oct 13;
88. Pols MS, ten Brink C, Gosavi P, Oorschot V, Klumperman J. The HOPS proteins hVps41 and hVps39 are required for homotypic and heterotypic late endosome fusion. *Traffic*. 2013 Feb;14(2):219–232.
89. Bonifacino JS, Hurley JH. Retromer. *Curr Opin Cell Biol*. 2008 Aug;20(4):427–436.
90. Rojas R, van Vlijmen T, Mardones GA, Prabhu Y, Rojas AL, Mohammed S, et al. Regulation of retromer recruitment to endosomes by sequential action of Rab5 and Rab7. *J Cell Biol*. 2008 Nov 3;183(3):513–526.
91. Weisz OA. Acidification and protein traffic. *Int Rev Cytol*. 2003;226:259–319.
92. Maxfield FR, Yamashiro DJ. Endosome acidification and the pathways of receptor-mediated endocytosis. *Adv Exp Med Biol*. 1987;225:189–198.
93. Braulke T, Bonifacino JS. Sorting of lysosomal proteins. *Biochim Biophys Acta*. 2009 Apr;1793(4):605–614.
94. Qian M, Sleat DE, Zheng H, Moore D, Lobel P. Proteomics analysis of serum from mutant mice reveals lysosomal proteins selectively transported by each of the two mannose 6-phosphate receptors. *Mol Cell Proteomics*. 2008 Jan;7(1):58–70.
95. Doray B, Ghosh P, Griffith J, Geuze HJ, Kornfeld S. Cooperation of GGAs and AP-1 in packaging MPRs at the trans-Golgi network. *Science*. 2002 Sep 6;297(5587):1700–1703.
96. Klumperman J, Hille A, Veenendaal T, Oorschot V, Stoorvogel W, von Figura K, et al. Differences in the endosomal distributions of the two mannose 6-phosphate receptors. *J Cell Biol*. 1993 Jun;121(5):997–1010.
97. Van Meel E, Klumperman J. Imaging and imagination: understanding the endo-lysosomal system. *Histochem Cell Biol*. 2008 Mar;129(3):253–266.
98. Arighi CN, Hartnell LM, Aguilar RC, Haft CR, Bonifacino JS. Role of the mammalian retromer in sorting of the cation-independent mannose 6-phosphate receptor. *J Cell Biol*. 2004 Apr;165(1):123–133.
99. Hunziker W, Geuze HJ. Intracellular trafficking of lysosomal membrane proteins. *Bioessays*. 1996 May;18(5):379–389.

100. Höning S, Griffith J, Geuze HJ, Hunziker W. The tyrosine-based lysosomal targeting signal in lamp-1 mediates sorting Golgi-derived clathrin-coated vesicles. *EMBO J.* 1996 Oct 1;15(19):5230–5239.
101. Saftig P, Klumperman J. Lysosome biogenesis and lysosomal membrane proteins: trafficking meets function. *Nat Rev Mol Cell Biol.* 2009 Sep;10(9):623–635.
102. Pols MS, van Meel E, Oorschot V, ten Brink C, Fukuda M, Swetha MG, et al. hVps41 and VAMP7 function in direct TGN to late endosome transport of lysosomal membrane proteins. *Nat Commun.* 2013;4:1361.
103. Tjelle TE, Brech A, Juvet LK, Griffiths G, Berg T. Isolation and characterization of early endosomes, late endosomes and terminal lysosomes: their role in protein degradation. *J Cell Sci.* 1996 Dec;109 (Pt 12):2905–2914.
104. Pillay CS, Elliott E, Dennison C. Endolysosomal proteolysis and its regulation. *Biochem J.* 2002 May 1;363(Pt 3):417–429.
105. Futter CE, Pearse A, Hewlett LJ, Hopkins CR. Multivesicular endosomes containing internalized EGF-EGF receptor complexes mature and then fuse directly with lysosomes. *J Cell Biol.* 1996 Mar;132(6):1011–1023.
106. Mellman I, Fuchs R, Helenius A. Acidification of the endocytic and exocytic pathways. *Annu Rev Biochem.* 1986;55:663–700.
107. Luzio JP, Gray SR, Bright NA. Endosome-lysosome fusion. *Biochem Soc Trans.* 2010 Dec;38(6):1413–1416.
108. Kolter T, Sandhoff K. Lysosomal degradation of membrane lipids. *FEBS Lett.* 2010 May 3;584(9):1700–1712.
109. Eskelinen EL, Tanaka Y, Saftig P. At the acidic edge: emerging functions for lysosomal membrane proteins. *Trends Cell Biol.* 2003 Mar;13(3):137–145.
110. Kundra R, Kornfeld S. Asparagine-linked oligosaccharides protect Lamp-1 and Lamp-2 from intracellular proteolysis. *J Biol Chem.* 1999 Oct 22;274(43):31039–31046.
111. Barriocanal JG, Bonifacino JS, Yuan L, Sandoval IV. Biosynthesis, glycosylation, movement through the Golgi system, and transport to lysosomes by an N-linked carbohydrate-independent mechanism of three lysosomal integral membrane proteins. *J Biol Chem.* 1986 Dec 15;261(35):16755–16763.
112. Kim E, Goraksha-Hicks P, Li L, Neufeld TP, Guan KL. Regulation of TORC1 by Rag GTPases in nutrient response. *Nat Cell Biol.* 2008 Aug;10(8):935–945.
113. Zoncu R, Bar-Peled L, Efeyan A, Wang S, Sancak Y, Sabatini DM. mTORC1 senses lysosomal amino acids through an inside-out mechanism that requires the vacuolar H(+)-ATPase. *Science.* 2011 Nov 4;334(6056):678–683.
114. Sancak Y, Peterson TR, Shaul YD, Lindquist RA, Thoreen CC, Bar-Peled L, et al. The Rag GTPases bind raptor and mediate amino acid signaling to mTORC1. *Science.* 2008 Jun 13;320(5882):1496–1501.
115. Settembre C, Zoncu R, Medina DL, Vetrini F, Erdin S, Erdin S, et al. A lysosome-to-nucleus signalling mechanism senses and regulates the lysosome via mTOR and TFEB. *EMBO J.* 2012 Mar 7;31(5):1095–1108.
116. Sancak Y, Bar-Peled L, Zoncu R, Markhard AL, Nada S, Sabatini DM. Ragulator-Rag complex targets mTORC1 to the lysosomal surface and is necessary for its activation by amino acids. *Cell.* 2010 Apr 16;141(2):290–303.
117. Palmieri M, Impey S, Kang H, di Ronza A, Pelz C, Sardiello M, et al. Characterization of the CLEAR network reveals an integrated control of cellular clearance pathways. *Hum Mol Genet.* 2011 Oct 1;20(19):3852–3866.
118. Wennerberg K, Rossman KL, Der CJ. The Ras superfamily at a glance. *J Cell Sci.* 2005 Mar 1;118(Pt 5):843–846.
119. Wandinger-Ness A, Zerial M. Rab proteins and the compartmentalization of the endosomal system. *Cold Spring Harb Perspect Biol.* 2014 Nov;6(11):a022616.
120. Wu X, Bradley MJ, Cai Y, Kümmel D, De La Cruz EM, Barr FA, et al. Insights regarding guanine nucleotide exchange from the structure of a DENN-domain protein complexed with its Rab GTPase substrate. *Proc Natl Acad Sci U S A.* 2011 Nov 15;108(46):18672–18677.
121. Cherfils J, Zeghouf M. Regulation of small GTPases by GEFs, GAPs, and GDIs. *Physiol Rev.* 2013 Jan;93(1):269–309.
122. Gavriliuk K, Itzen A, Goody RS, Gerwert K, Kötting C. Membrane extraction of Rab proteins by GDP dissociation inhibitor characterized using attenuated total reflection infrared spectroscopy. *Proc Natl Acad Sci U S A.* 2013 Aug 13;110(33):13380–13385.
123. Ullrich O, Stenmark H, Alexandrov K, Huber LA, Kaibuchi K, Sasaki T, et al. Rab GDP dissociation inhibitor as a general regulator for the membrane association of rab proteins. *J Biol Chem.* 1993 Aug 25;268(24):18143–18150.
124. Wu YW, Oesterlin LK, Tan KT, Waldmann H, Alexandrov K, Goody RS. Membrane targeting mechanism of Rab GTPases elucidated by semisynthetic protein probes. *Nat Chem Biol.* 2010 Jul;6(7):534–540.
125. Pylypenko O, Rak A, Durek T, Kushnir S, Dursina BE, Thomae NH, et al. Structure of doubly prenylated Ypt1:GDI

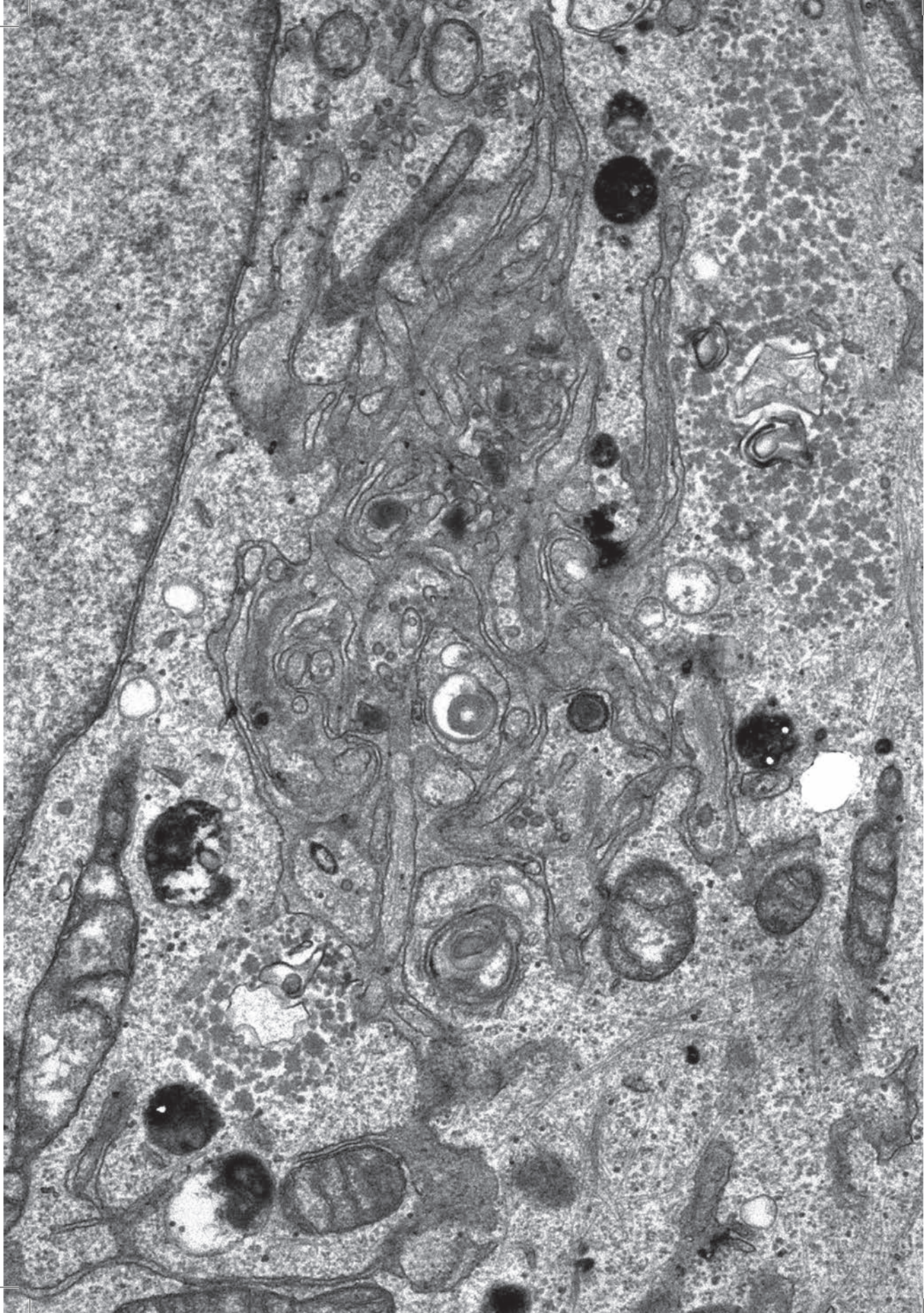
- complex and the mechanism of GDI-mediated Rab recycling. *EMBO J.* 2006 Jan 11;25(1):13–23.
126. Wittinghofer A, Franken SM, Scheidig AJ, Rensland H, Lautwein A, Pai EF, et al. Three-dimensional structure and properties of wild-type and mutant H-ras-encoded p21. *Ciba Found Symp.* 1993;176:6–21; discussion 21.
127. Pfeffer SR. Transport-vesicle targeting: tethers before SNAREs. *Nat Cell Biol.* 1999 May;1(1):E17–E22.
128. Guo W, Sacher M, Barrowman J, Ferro-Novick S, Novick P. Protein complexes in transport vesicle targeting. *Trends Cell Biol.* 2000 Jun;10(6):251–255.
129. Cao X, Ballew N, Barlowe C. Initial docking of ER-derived vesicles requires Uso1p and Ypt1p but is independent of SNARE proteins. *EMBO J.* 1998 Apr 15;17(8):2156–2165.
130. Stenmark H. Rab GTPases as coordinators of vesicle traffic. *Nat Rev Mol Cell Biol.* 2009 Aug;10(8):513–525.
131. Derby MC, Gleeson PA. New insights into membrane trafficking and protein sorting. *Int Rev Cytol.* 2007;261:47–116.
132. Guo W, Roth D, Walch-Solimena C, Novick P. The exocyst is an effector for Sec4p, targeting secretory vesicles to sites of exocytosis. *EMBO J.* 1999 Feb 15;18(4):1071–1080.
133. Shorter J, Beard MB, Seemann J, Dirac-Svejstrup AB, Warren G. Sequential tethering of Golgins and catalysis of SNAREpin assembly by the vesicle-tethering protein p115. *J Cell Biol.* 2002 Apr 1;157(1):45–62.
134. Malsam J, Satoh A, Pelletier L, Warren G. Golgin tethers define subpopulations of COPI vesicles. *Science.* 2005 Feb 18;307(5712):1095–1098.
135. Starai VJ, Hickey CM, Wickner W. HOPS proofreads the trans-SNARE complex for yeast vacuole fusion. *Mol Biol Cell.* 2008 Jun;19(6):2500–2508.
136. Ohya T, Miaczynska M, Coskun U, Lommer B, Runge A, Drechsel D, et al. Reconstitution of Rab- and SNARE-dependent membrane fusion by synthetic endosomes. *Nature.* 2009 Jun 25;459(7250):1091–1097.
137. Gillingham AK, Munro S. Long coiled-coil proteins and membrane traffic. *Biochim Biophys Acta.* 2003 Aug 18;1641(2-3):71–85.
138. Whyte JR, Munro S. Vesicle tethering complexes in membrane traffic. *J Cell Sci.* 2002 Jul 1;115(Pt 13):2627–2637.
139. Munro S. The golgin coiled-coil proteins of the Golgi apparatus. *Cold Spring Harb Perspect Biol.* 2011 Jun 1;3(6).
140. Ren Y, Yip CK, Tripathi A, Huie D, Jeffrey PD, Walz T, et al. A structure-based mechanism for vesicle capture by the multisubunit tethering complex Dsl1. *Cell.* 2009 Dec 11;139(6):1119–1129.
141. Hsu SC, Hazuka CD, Roth R, Foletti DL, Heuser J, Scheller RH. Subunit composition, protein interactions, and structures of the mammalian brain sec6/8 complex and septin filaments. *Neuron.* 1998 Jun;20(6):1111–1122.
142. Bröcker C, Kuhlee A, Gatsogiannis C, Balderhaar HJ, Hönscher C, Engelbrecht-Vandré S, et al. Molecular architecture of the multisubunit homotypic fusion and vacuole protein sorting (HOPS) tethering complex. *Proc Natl Acad Sci U S A.* 2012 Feb 7;109(6):1991–1996.
143. Zolov SN, Lupashin VV. Cog3p depletion blocks vesicle-mediated Golgi retrograde trafficking in HeLa cells. *J Cell Biol.* 2005 Feb 28;168(5):747–759.
144. Hui E, Johnson CP, Yao J, Dunning FM, Chapman ER. Synaptotagmin-mediated bending of the target membrane is a critical step in Ca(2+)-regulated fusion. *Cell.* 2009 Aug 21;138(4):709–721.
145. Martens S, Kozlov MM, McMahon HT. How synaptotagmin promotes membrane fusion. *Science.* 2007 May 25;316(5828):1205–1208.
146. Solinger JA, Spang A. Tethering complexes in the endocytic pathway: CORVET and HOPS. *FEBS J.* 2013 Jun;280(12):2743–2757.
147. Balderhaar HJ, Ungermann C. CORVET and HOPS tethering complexes - coordinators of endosome and lysosome fusion. *J Cell Sci.* 2013 Mar 15;126(Pt 6):1307–1316.
148. Fasshauer D, Sutton RB, Brunger AT, Jahn R. Conserved structural features of the synaptic fusion complex: SNARE proteins reclassified as Q- and R-SNAREs. *Proc Natl Acad Sci U S A.* 1998 Dec 22;95(26):15781–15786.
149. Söllner T, Whiteheart SW, Brunner M, Erdjument-Bromage H, Geromanos S, Tempst P, et al. SNAP receptors implicated in vesicle targeting and fusion. *Nature.* 1993 Mar 25;362(6418):318–324.
150. Südhof TC, Rothman JE. Membrane fusion: grappling with SNARE and SM proteins. *Science.* 2009 Jan 23;323(5913):474–477.
151. Fasshauer D, Antonin W, Margittai M, Pabst S, Jahn R. Mixed and non-cognate SNARE complexes. Characterization of assembly and biophysical properties. *J Biol Chem.* 1999 May 28;274(22):15440–15446.

152. Yang B, Gonzalez L, Prekeris R, Steegmaier M, Advani RJ, Scheller RH. SNARE interactions are not selective. Implications for membrane fusion specificity. *J Biol Chem*. 1999 Feb 26;274(9):5649–5653.
153. Grosshans BL, Ortiz D, Novick P. Rabs and their effectors: achieving specificity in membrane traffic. *Proc Natl Acad Sci U S A*. 2006 Aug 8;103(32):11821–11827.
154. Carr CM, Rizo J. At the junction of SNARE and SM protein function. *Curr Opin Cell Biol*. 2010 Aug 1;22(4):488–495.
155. Rizo J, Südhof TC. The membrane fusion enigma: SNAREs, Sec1/Munc18 proteins, and their accomplices--guilty as charged? *Annu Rev Cell Dev Biol*. 2012;28:279–308.
156. Sutton RB, Fasshauer D, Jahn R, Brunger AT. Crystal structure of a SNARE complex involved in synaptic exocytosis at 2.4 Å resolution. *Nature*. 1998 Sep 24;395(6700):347–353.
157. Hayashi T, McMahon H, Yamasaki S, Binz T, Hata Y, Südhof TC, et al. Synaptic vesicle membrane fusion complex: action of clostridial neurotoxins on assembly. *EMBO J*. 1994 Nov 1;13(21):5051–5061.
158. Li F, Pincet F, Perez E, Eng WS, Melia TJ, Rothman JE, et al. Energetics and dynamics of SNAREpin folding across lipid bilayers. *Nat Struct Mol Biol*. 2007 Oct;14(10):890–896.
159. Cohen FS, Melikyan GB. The energetics of membrane fusion from binding, through hemifusion, pore formation, and pore enlargement. *J Membr Biol*. 2004 May 1;199(1):1–14.
160. Söllner T, Bennett MK, Whiteheart SW, Scheller RH, Rothman JE. A protein assembly-disassembly pathway in vitro that may correspond to sequential steps of synaptic vesicle docking, activation, and fusion. *Cell*. 1993 Nov 5;75(3):409–418.
161. Mayer A, Wickner W, Haas A. Sec18p (NSF)-Driven Release of Sec17p (α -SNAP) Can Precede Docking and Fusion of Yeast Vacuoles. *Cell*. 1996 Apr;85(1):83–94.
162. Wurmser AE, Sato TK, Emr SD. New component of the vacuolar class C-Vps complex couples nucleotide exchange on the Ypt7 GTPase to SNARE-dependent docking and fusion. *J Cell Biol*. 2000 Oct 30;151(3):551–562.
163. Sato TK, Rehling P, Peterson MR, Emr SD. Class C Vps protein complex regulates vacuolar SNARE pairing and is required for vesicle docking/fusion. *Mol Cell*. 2000 Sep;6(3):661–671.
164. Nickerson DP, Brett CL, Merz AJ. Vps-C complexes: gatekeepers of endolysosomal traffic. *Curr Opin Cell Biol*. 2009 Aug 1;21(4):543–551.
165. Lin X, Yang T, Wang S, Wang Z, Yun Y, Sun L, et al. RILP interacts with HOPS complex via VPS41 subunit to regulate endocytic trafficking. *Sci Rep*. 2014 Dec 2;4:7282.
166. Rehling P, Darsow T, Katzmann DJ, Emr SD. Formation of AP-3 transport intermediates requires Vps41 function. *Nat Cell Biol*. 1999 Oct;1(6):346–353.
167. Cabrera M, Langemeyer L, Mari M, Rethmeier R, Orban I, Perz A, et al. Phosphorylation of a membrane curvature-sensing motif switches function of the HOPS subunit Vps41 in membrane tethering. *J Cell Biol*. 2010 Nov 15;191(4):845–859.
168. Hickey CM, Stroupe C, Wickner W. The major role of the Rab Ypt7p in vacuole fusion is supporting HOPS membrane association. *J Biol Chem*. 2009 Jun 12;284(24):16118–16125.
169. Ostrowicz CW, Bröcker C, Ahnert F, Nordmann M, Lachmann J, Peplowska K, et al. Defined subunit arrangement and rab interactions are required for functionality of the HOPS tethering complex. *Traffic*. 2010 Oct;11(10):1334–1346.
170. Stroupe C, Collins KM, Fratti RA, Wickner W. Purification of active HOPS complex reveals its affinities for phosphoinositides and the SNARE Vam7p. *EMBO J*. 2006 Apr 19;25(8):1579–1589.
171. Plemel RL, Lobingier BT, Brett CL, Angers CG, Nickerson DP, Paulsel A, et al. Subunit organization and Rab interactions of Vps-C protein complexes that control endolysosomal membrane traffic. *Mol Biol Cell*. 2011 Apr 15;22(8):1353–1363.
172. Peralta ER, Martin BC, Edinger AL. Differential effects of TBC1D15 and mammalian Vps39 on Rab7 activation state, lysosomal morphology, and growth factor dependence. *J Biol Chem*. 2010 May 28;285(22):16814–16821.
173. Mima J, Hickey CM, Xu H, Jun Y, Wickner W. Reconstituted membrane fusion requires regulatory lipids, SNAREs and synergistic SNARE chaperones. *EMBO J*. 2008 Aug 6;27(15):2031–2042.
174. Stroupe C, Hickey CM, Mima J, Burfeind AS, Wickner W. Minimal membrane docking requirements revealed by reconstitution of Rab GTPase-dependent membrane fusion from purified components. *Proc Natl Acad Sci U S A*. 2009 Oct 20;106(42):17626–17633.
175. Hickey CM, Wickner W. HOPS initiates vacuole docking by tethering membranes before trans-SNARE complex

- assembly. *Mol Biol Cell*. 2010 Jul 1;21(13):2297–2305.
176. Lobingier BT, Merz AJ. Sec1/Munc18 protein Vps33 binds to SNARE domains and the quaternary SNARE complex. *Mol Biol Cell*. 2012 Dec;23(23):4611–4622.
177. Khatteer D, Raina VB, Dwivedi D, Sindhwani A, Bahl S, Sharma M. The small GTPase Arl8b regulates assembly of the mammalian HOPS complex on lysosomes. *J Cell Sci*. 2015 May 1;128(9):1746–1761.
178. Bugnicourt A, Froissard M, Sereti K, Ulrich HD, Haguenaer-Tsapis R, Galan JM. Antagonistic roles of ESCRT and Vps class C/HOPS complexes in the recycling of yeast membrane proteins. *Mol Biol Cell*. 2004 Sep;15(9):4203–4214.
179. Richardson SC, Winistorfer SC, Poupon V, Luzio JP, Piper RC. Mammalian late vacuole protein sorting orthologues participate in early endosomal fusion and interact with the cytoskeleton. *Mol Biol Cell*. 2004 Mar;15(3):1197–1210.
180. Poupon V, Stewart A, Gray SR, Piper RC, Luzio JP. The role of mVps18p in clustering, fusion, and intracellular localization of late endocytic organelles. *Mol Biol Cell*. 2003 Oct;14(10):4015–4027.
181. Peplowska K, Markgraf DF, Ostrowicz CW, Bange G, Ungermann C. The CORVET tethering complex interacts with the yeast Rab5 homolog Vps21 and is involved in endo-lysosomal biogenesis. *Dev Cell*. 2007 May;12(5):739–750.
182. Perini ED, Schaefer R, Stöter M, Kalaidzidis Y, Zerial M. Mammalian CORVET is required for fusion and conversion of distinct early endosome subpopulations. *Traffic*. 2014 Dec;15(12):1366–1389.
183. Lachmann J, Glaubke E, Moore PS, Ungermann C. The Vps39-like TRAP1 is an effector of Rab5 and likely the missing Vps3 subunit of human CORVET. *Cell Logist*. 2014 Dec;4(4):e970840.
184. Horazdovsky BF, Cowles CR, Mustol P, Holmes M, Emr SD. A novel RING finger protein, Vps8p, functionally interacts with the small GTPase, Vps21p, to facilitate soluble vacuolar protein localization. *J Biol Chem*. 1996 Dec 27;271(52):33607–33615.
185. Markgraf DF, Ahnert F, Arlt H, Mari M, Peplowska K, Epp N, et al. The CORVET subunit Vps8 cooperates with the Rab5 homolog Vps21 to induce clustering of late endosomal compartments. *Mol Biol Cell*. 2009 Dec;20(24):5276–5289.
186. Balderhaar HJ, Lachmann J, Yavavli E, Bröcker C, Lürick A, Ungermann C. The CORVET complex promotes tethering and fusion of Rab5/Vps21-positive membranes. *Proc Natl Acad Sci U S A*. 2013 Mar 5;110(10):3823–3828.
187. Epp N, Ungermann C. The N-terminal domains of Vps3 and Vps8 are critical for localization and function of the CORVET tethering complex on endosomes. *PLoS ONE*. 2013 Jun 20;8(6):e67307.
188. Klinger CM, Klute MJ, Dacks JB. Comparative genomic analysis of multi-subunit tethering complexes demonstrates an ancient pan-eukaryotic complement and sculpting in Apicomplexa. *PLoS ONE*. 2013 Sep 27;8(9):e76278.
189. Gissen P, Johnson CA, Gentle D, Hurst LD, Doherty AJ, O’Kane CJ, et al. Comparative evolutionary analysis of VPS33 homologues: genetic and functional insights. *Hum Mol Genet*. 2005 May 15;14(10):1261–1270.
190. Tornieri K, Zlatich SA, Mullin AP, Werner E, Harrison R, L’hernault SW, et al. Vps33b pathogenic mutations preferentially affect VIPAS39/SPE-39-positive endosomes. *Hum Mol Genet*. 2013 Dec 20;22(25):5215–5228.
191. Smith H, Galmes R, Gogolina E, Straatman-Iwanowska A, Reay K, Banushi B, et al. Associations among genotype, clinical phenotype, and intracellular localization of trafficking proteins in ARC syndrome. *Hum Mutat*. 2012 Dec;33(12):1656–1664.
192. Zhu GD, Salazar G, Zlatich SA, Fiza B, Doucette MM, Heilman CJ, et al. SPE-39 family proteins interact with the HOPS complex and function in lysosomal delivery. *Mol Biol Cell*. 2009 Feb;20(4):1223–1240.
193. Gissen P, Johnson CA, Morgan NV, Stapelbroek JM, Forshew T, Cooper WN, et al. Mutations in VPS33B, encoding a regulator of SNARE-dependent membrane fusion, cause arthrogryposis-renal dysfunction-cholestasis (ARC) syndrome. *Nat Genet*. 2004 Apr;36(4):400–404.
194. Cullinane AR, Straatman-Iwanowska A, Zaucker A, Wakabayashi Y, Bruce CK, Luo G, et al. Mutations in VIPAR cause an arthrogryposis, renal dysfunction and cholestasis syndrome phenotype with defects in epithelial polarization. *Nat Genet*. 2010 Apr;42(4):303–312.
195. Lo B, Li L, Gissen P, Christensen H, McKiernan PJ, Ye C, et al. Requirement of VPS33B, a member of the Sec1/Munc18 protein family, in megakaryocyte and platelet alpha-granule biogenesis. *Blood*. 2005 Dec 15;106(13):4159–4166.
196. Urban D, Li L, Christensen H, Pluthero FG, Chen SZ, Puhacz M, et al. The VPS33B-binding protein VPS16B is required in megakaryocyte and platelet alpha-granule biogenesis. *Blood*. 2012 Dec 13;120(25):5032–5040.
197. Bem D, Smith H, Banushi B, Burden JJ, White IJ, Hanley J, et al. VPS33B regulates protein sorting into and maturation of alpha-granule progenitor organelles in mouse megakaryocytes. *Blood*. 2015 Jul 9;126(2):133–143.
198. Spang A. Membrane Tethering Complexes in the Endosomal System. *Frontiers in cell and developmental biology*.

- 2016 May 9;4:35.
199. Derynck R, Zhang YE. Smad-dependent and Smad-independent pathways in TGF-beta family signalling. *Nature*. 2003 Oct 9;425(6958):577–584.
200. Le Roy C, Wrana JL. Clathrin- and non-clathrin-mediated endocytic regulation of cell signalling. *Nat Rev Mol Cell Biol*. 2005 Feb;6(2):112–126.
201. Ehrlich M, Shmueli A, Henis YI. A single internalization signal from the di-leucine family is critical for constitutive endocytosis of the type II TGF-beta receptor. *J Cell Sci*. 2001 May;114(Pt 9):1777–1786.
202. Lu Z, Murray JT, Luo W, Li H, Wu X, Xu H, et al. Transforming growth factor beta activates Smad2 in the absence of receptor endocytosis. *J Biol Chem*. 2002 Aug 16;277(33):29363–29368.
203. Di Guglielmo GM, Le Roy C, Goodfellow AF, Wrana JL. Distinct endocytic pathways regulate TGF-beta receptor signalling and turnover. *Nat Cell Biol*. 2003 May;5(5):410–421.
204. Anders RA, Doré JJ, Arline SL, Garamszegi N, Leof EB. Differential requirement for type I and type II transforming growth factor beta receptor kinase activity in ligand-mediated receptor endocytosis. *J Biol Chem*. 1998 Sep 4;273(36):23118–23125.
205. Anders RA, Arline SL, Doré JJ, Leof EB. Distinct endocytic responses of heteromeric and homomeric transforming growth factor beta receptors. *Mol Biol Cell*. 1997 Nov;8(11):2133–2143.
206. Garamszegi N, Doré JJ, Penheiter SG, Edens M, Yao D, Leof EB. Transforming growth factor beta receptor signaling and endocytosis are linked through a COOH terminal activation motif in the type I receptor. *Mol Biol Cell*. 2001 Sep;12(9):2881–2893.
207. Tsukazaki T, Chiang TA, Davison AF, Attisano L, Wrana JL. SARA, a FYVE domain protein that recruits Smad2 to the TGFbeta receptor. *Cell*. 1998 Dec 11;95(6):779–791.
208. Itoh F, Divecha N, Brocks L, Oomen L, Janssen H, Calafat J, et al. The FYVE domain in Smad anchor for receptor activation (SARA) is sufficient for localization of SARA in early endosomes and regulates TGF-beta/Smad signalling. *Genes Cells*. 2002 Mar;7(3):321–331.
209. Hayes S, Chawla A, Corvera S. TGF beta receptor internalization into EEA1-enriched early endosomes: role in signaling to Smad2. *J Cell Biol*. 2002 Sep 30;158(7):1239–1249.
210. Rajagopal R, Ishii S, Beebe DC. Intracellular mediators of transforming growth factor beta superfamily signaling localize to endosomes in chicken embryo and mouse lenses in vivo. *BMC Cell Biol*. 2007 Jun 25;8:25.
211. Feng XH, Derynck R. Specificity and versatility in $\text{tgf-}\beta$ signaling through Smads. *Annu Rev Cell Dev Biol*. 2005;21:659–693.
212. Wrana JL. Regulation of Smad activity. *Cell*. 2000 Jan 21;100(2):189–192.
213. Shi Y, Massagué J. Mechanisms of TGF-beta signaling from cell membrane to the nucleus. *Cell*. 2003 Jun 13;113(6):685–700.
214. Hynes RO. Integrins: bidirectional, allosteric signaling machines. *Cell*. 2002 Sep 20;110(6):673–687.
215. Pellinen T, Ivaska J. Integrin traffic. *J Cell Sci*. 2006 Sep 15;119(Pt 18):3723–3731.
216. Caswell PT, Norman JC. Integrin trafficking and the control of cell migration. *Traffic*. 2006 Jan;7(1):14–21.
217. Caswell P, Norman J. Endocytic transport of integrins during cell migration and invasion. *Trends Cell Biol*. 2008 Jun;18(6):257–263.
218. Roberts M, Barry S, Woods A, van der Sluijs P, Norman J. PDGF-regulated rab4-dependent recycling of α v β 3 integrin from early endosomes is necessary for cell adhesion and spreading. *Curr Biol*. 2001 Sep 18;11(18):1392–1402.
219. White DP, Caswell PT, Norman JC. α v β 3 and α 5 β 1 integrin recycling pathways dictate downstream Rho kinase signaling to regulate persistent cell migration. *J Cell Biol*. 2007 May 7;177(3):515–525.
220. Drubin DG, Nelson WJ. Origins of cell polarity. *Cell*. 1996 Feb 9;84(3):335–344.
221. Balda MS, Matter K. Tight junctions. *J Cell Sci*. 1998 Mar;111 (Pt 5):541–547.
222. Sheff DR, Kroschewski R, Mellman I. Actin dependence of polarized receptor recycling in Madin-Darby canine kidney cell endosomes. *Mol Biol Cell*. 2002 Jan;13(1):262–275.
223. Wang E, Brown PS, Aroeti B, Chapin SJ, Mostov KE, Dunn KW. Apical and basolateral endocytic pathways of MDCK cells meet in acidic common endosomes distinct from a nearly-neutral apical recycling endosome. *Traffic*. 2000 Jun;1(6):480–493.

224. Golachowska MR, Hoekstra D, van IJendoorn SC. Recycling endosomes in apical plasma membrane domain formation and epithelial cell polarity. *Trends Cell Biol.* 2010 Oct;20(10):618–626.
225. Apodaca G, Katz LA, Mostov KE. Receptor-mediated transcytosis of IgA in MDCK cells is via apical recycling endosomes. *J Cell Biol.* 1994 Apr;125(1):67–86.
226. Mostov K, Su T, ter Beest M. Polarized epithelial membrane traffic: conservation and plasticity. *Nat Cell Biol.* 2003 Apr;5(4):287–293.
227. Weisz OA, Rodriguez-Boulan E. Apical trafficking in epithelial cells: signals, clusters and motors. *J Cell Sci.* 2009 Dec 1;122(Pt 23):4253–4266.
228. Mellman I, Nelson WJ. Coordinated protein sorting, targeting and distribution in polarized cells. *Nat Rev Mol Cell Biol.* 2008 Nov;9(11):833–845.
229. Roland JT, Bryant DM, Datta A, Itzen A, Mostov KE, Goldenring JR. Rab GTPase-Myo5B complexes control membrane recycling and epithelial polarization. *Proc Natl Acad Sci U S A.* 2011 Feb 15;108(7):2789–2794.
230. Roland JT, Kenworthy AK, Peranen J, Caplan S, Goldenring JR. Myosin Vb interacts with Rab8a on a tubular network containing EHD1 and EHD3. *Mol Biol Cell.* 2007 Aug;18(8):2828–2837.
231. Lapiere LA, Kumar R, Hales CM, Navarre J, Bhartur SG, Burnette JO, et al. Myosin vb is associated with plasma membrane recycling systems. *Mol Biol Cell.* 2001 Jun;12(6):1843–1857.
232. Perez Bay AE, Schreiner R, Mazzoni F, Carvajal-Gonzalez JM, Gravotta D, Perret E, et al. The kinesin KIF16B mediates apical transcytosis of transferrin receptor in AP-1B-deficient epithelia. *EMBO J.* 2013 Jul 31;32(15):2125–2139.
233. Goldenring JR, Smith J, Vaughan HD, Cameron P, Hawkins W, Navarre J. Rab11 is an apically located small GTP-binding protein in epithelial tissues. *Am J Physiol.* 1996 Mar;270(3 Pt 1):G515–G525.
234. Babbey CM, Ahktar N, Wang E, Chen CC, Grant BD, Dunn KW. Rab10 regulates membrane transport through early endosomes of polarized Madin-Darby canine kidney cells. *Mol Biol Cell.* 2006 Jul;17(7):3156–3175.
235. Schuck S, Gerl MJ, Ang A, Manninen A, Keller P, Mellman I, et al. Rab10 is involved in basolateral transport in polarized Madin-Darby canine kidney cells. *Traffic.* 2007 Jan;8(1):47–60.
236. Tzaban S, Massol RH, Yen E, Hamman W, Frank SR, Lapiere LA, et al. The recycling and transcytotic pathways for IgG transport by FcRn are distinct and display an inherent polarity. *J Cell Biol.* 2009 May 18;185(4):673–684.



Chapter 2

Characterization of the mammalian CORVET and HOPS complexes and their modular restructuring for endosome specificity

Rik van der Kant^{*,1,3}, Caspar TH Jonker^{*,2}, Ruud H Wijdeven¹, Jeroen Bakker¹, Lennert Janssen¹, Judith Klumperman², Jacques Neefjes¹

* shared first author

¹ Division of Cell Biology, Netherlands Cancer Institute; Amsterdam; 1066 CX; The Netherlands

² Department of Cell Biology, Center for Molecular Medicine, University Medical Center Utrecht, the Netherlands.

³ Current Address; Department of Cellular and Molecular Medicine; University of California-San Diego; La Jolla; CA92093, USA

J Biol Chem. 2015 Dec; 290(51):30280-90

Abstract

Trafficking of cargo through the endosomal system depends on endosomal fusion events mediated by SNARE proteins, Rab-GTPases and multi-subunit tethering complexes. The CORVET and HOPS tethering complexes respectively regulate early- and late-endosomal tethering and have been characterized in detail in yeast, where their sequential membrane targeting and assembly is well understood. Mammalian CORVET and HOPS subunits significantly differ from their yeast homologues and novel proteins with high homology to CORVET/HOPS subunits have evolved. However, an analysis of the molecular interactions between these subunits in mammals is lacking. Here, we provide a detailed analysis of interactions within the mammalian CORVET and HOPS, as well as an additional endosomal-targeting complex (VIPAS39/ VPS33B) that does not exist in yeast. We show that core interactions within CORVET and HOPS are largely conserved, but that the membrane-targeting module in HOPS has significantly changed to accommodate binding to mammalian-specific RAB7 interacting lysosomal protein (RILP). Arthrogyrosis-Renal dysfunction-Cholestasis (ARC) -syndrome associated mutations in VPS33B selectively disrupt recruitment to late endosomes by RILP or binding to its partner VIPAS39. Within the shared core of CORVET/HOPS, we find that VPS11 acts as a molecular switch that binds either CORVET specific TGFBRAP1 or HOPS specific VPS39/RILP thereby allowing selective targeting of these tethering complexes to early- or late endosomes to time fusion events in the endo/lysosomal pathway.

Introduction

The endocytic pathway is a dynamic system in which vesicles are continuously fusing, moving and budding in order to deliver their cargo to the correct compartment. After internalization, endocytic cargo is delivered to the early endosome (EE) from which it can be recycled or degraded (1). Cargo destined for degradation such as internalized nutrients, activated growth receptors and endocytosed pathogens are targeted to the late endosomes (LE) and lysosomes where the acidic environment and resident proteases allow for degradation. Rab5 (EE) and Rab7 (LE) are master regulators of endosomal transport and fusion and regulate cargo flux through the endocytic system in conjunction with multi-subunit motor- and tethering complexes. In yeast, EE and LE tethering is regulated by the CORVET (class C core vacuole/endosome tethering) and HOPS (Homotypic fusion and vacuole Protein Sorting) complexes respectively, that have been characterized in high detail (2–8). Both complexes consist of a shared core (vps16, vps18, vps11, vps33) that associates with CORVET specific (vps3 and vps8) or HOPS specific (vps39 and vps41) subunits. These different subunits target the complexes to membranes by interaction with respectively vps21 (yeast Rab5) and Ypt7 (yeast Rab7) (6,7). In addition, vps41 can also bind lipids (9). Apparent homologues of CORVET and HOPS subunits in mammals have been implicated in endosomal maturation (10), EE fusion (11) and fusion of lysosomes with late endosomes, phagosomes or autophagosomes (12–14). Based on sequence alignment, homologs of all eight yeast HOPS and CORVET subunits are present in mammalian cells with the addition of two novel homologues; VIPAS39 (a.k.a. SPE-39 or VIPAR) and VPS33B. Recently it was shown that mammalian VPS8 and TGFBRAP1 are the vps8 and vps3 homologues (11) and the mammalian CORVET therefore consists of VPS8, TGFBRAP1, VPS18, VPS16, VPS33A and VPS11, whereas HOPS consists of VPS41, VPS39, VPS18, VPS16, VPS33A and VPS11. While VPS33B was initially

shown to interact with HOPS subunits (15), more recent data suggest that VPS33B and VIPAS39 form a separate complex (12).

The organization of these mammalian complexes has only partly been addressed with seemingly conflicting results and hampered the interpretation of functional experiments in which roles of specific or multiple units are addressed (16–26). Furthermore, it is not known what drives membrane specificity of these complexes in mammals. Here we provide an extensive map of the mammalian CORVET, HOPS and VPS33B/VIPAS39 complexes describing their inter-subunit interactions and membrane recruitment. In agreement with Wartosch et al. we find that VIPAS39 and VPS33B are not part of the CORVET or HOPS complex but assemble in a distinct complex. We find that the CORVET complex is prevented from recruitment to LE (in line with its function at the EE). Within the HOPS complex there are multiple RILP-binding modules and pathogenic (Arthrogryposis-Renal dysfunction-Cholestasis (ARC) -syndrome) mutations in VPS33B disrupt VPS33B/VIPAS39 complex assembly or RILP dependent LE recruitment. Within the shared CORVET/HOPS core, VPS11 can bind TGFBRAP1 (CORVET) as well as VPS39 (HOPS) and these subunits likely compete for binding to VPS11 in the core of the CORVET/HOPS complex, thereby driving the membrane-specific assembly and tethering capability of these complexes.

Results

Characterization and definition of the mammalian CORVET, HOPS and VPS33B/VIPAS39 complex.

The yeast CORVET and HOPS complexes are assembled from eight different proteins (a Vps16/Vps33/Vps18/Vps11 core with Vps3/Vps8 or Vps39/Vps41). Mammals do not possess eight, but ten homologues to the yeast CORVET/HOPS subunits. Two mammalian homologues for yeast Vps33 exist (VPS33A and VPS33B) as well as an additional protein with weak homology to Vps16 (VIPAS39). To probe the interactions between the ten putative CORVET/HOPS subunits and determine the topology of the different subunits in the CORVET/HOPS complexes, we performed an extensive array of co-immunoprecipitations (IP) in human MeIJuSo cells with antibodies against endogenous VIPAS39, VPS33B, VPS11, VPS16, VPS8 and VPS33A (fig. 1a) (antibodies specific for other components were either not available or did not work for IP). We observed extensive interactions between VPS11, VPS16, VPS8, TGFBRAP1 and VPS33A. In contrast, VIPAS39 and VPS33B interacted with each other, but not with any of the other canonical CORVET/HOPS subunits in line with recent data (12).

To further map the HOPS complex and define possible interactions between VIPAS39 and VPS33B with HOPS components that we could not map in endogenous-pull down experiments, we ectopically co-expressed all six putative HOPS complex subunits as well as VPS33B and VIPAS39 as tagged proteins. We have previously shown that expression levels of these tagged proteins in our systems are low (comparable to endogenous) and that the tagged-subunits incorporate into functional complexes (27).

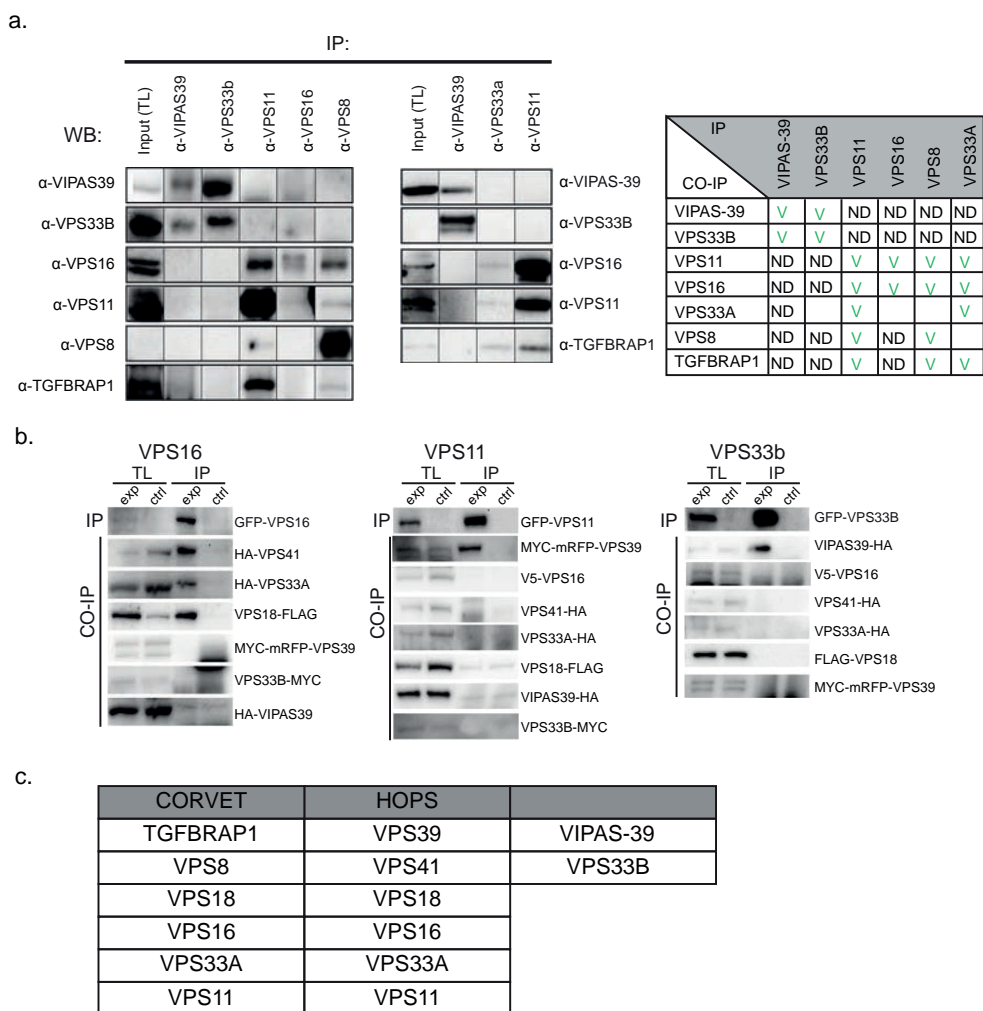


Figure 1. Biochemical definition of mammalian CORVET, HOPS and VPS33B/VIPAS39. (a) MelJuSo lysates were immunoprecipitated (IP) by indicated antibodies and analyzed by WB using indicated antibodies. Each panel represents an independent experiment. Upper left panel: MelJuSo cell lysates were generated (at which point a total lysate TL fraction was taken) and divided over five fractions and an immunoprecipitation was performed on each lysate using one of the indicated antibodies (generating five experimental conditions, horizontal axis). The five experimental conditions were run on the same blot with the same exposures for each detection antibody. A separate gel was run for each detection antibody (on the vertical axis). From these blots cut-outs were taken and grouped to compose the figure panel. Top right panel: same as left panel, with three experimental conditions. The table (lower panel) summarizes results from the IP experiments. Checkmark indicates interaction detected, ND= not detected, empty boxes are not tested. (b) Lysates of MelJuSo cells expressing 8 tagged (experimental condition, exp) or 7 tagged subunits (control condition (ctrl) not-expressing the GFP-tagged subunit) were IP'ed with anti-GFP (to pull down VPS16, VPS11, or VPS33B respectively) and analyzed by WB. Shown are total lysates (TL) for experimental and control lanes and the IP'ed fraction for experimental and control lanes. (c) Summary of experimental data A-E, VIPAS39 and VPS33B do not interact with HOPS complex subunits.

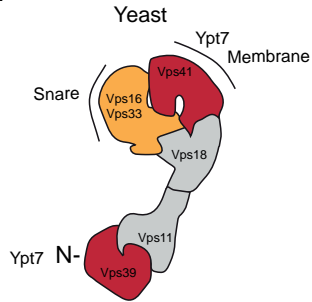
We pulled down GFP-VPS16, GFP-VPS11 or GFP-VPS33B and detected associated proteins by Western blotting with antibodies against the different epitope-tags (fig. 1b) GFP-VPS16 specifically interacted with VPS41, VPS18 and VPS33A. In addition, GFP-VPS11 interacted with VPS39. In contrast to the endogenous co-IP (fig. 1a), no interactions between the two groups (VPS16/41/18/33a and VPS11/39) were observed. A pull down-experiment with GFP-VPS11 also failed to detect interactions between GFP-VPS11 and endogenous VPS16/VPS33a (data not shown). This may reflect a limitation of the over-expression system or an interference with normal interactions by the associated tags. In line with the endogenous IP (fig. 1a), we again observed strong interactions between VPS33B and VIPAS39, but not with any other subunit of the HOPS complex. This suggests that mammalian HOPS consist of VPS11/VPS16/VPS18/VPS33A/ VPS39/ VPS41 whereas VPS33B/VIPAS39 assemble in a distinct complex (fig. 1c). Furthermore, the observation that tagged-subunits recapitulate in large part endogenous interactions indicates we can use these constructs for further detailed mapping of the respective complexes.

A high-detail interaction map of the mammalian HOPS complex

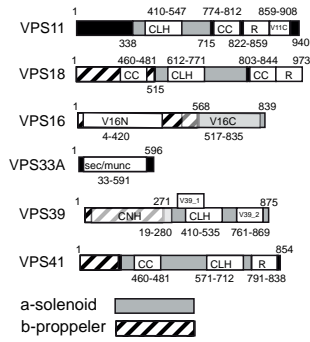
The yeast HOPS complex resembles a seahorse shaped complex with a head (Vps16/Vps33/Vps41/Vps18) and a tail (Vps11/Vps39) and interactions within the complex have been extensively mapped (6,7) (fig. 2a). No structure for the mammalian HOPS complex is available, yet our experiments (fig. 1) suggest that interactions within the head (VPS16/VPS33/VPS41/VPS18) and tail (VPS39/VPS11) are conserved from yeast to mammal. To study the interactions within the proposed head of the mammalian HOPS complex, we expressed tagged-truncation mutants of a particular subunit (domain organizations based on STRING 9.1 <http://string-db.org/>) depicted in figure 2b and assessed interactions with the three other head proteins by co-IP experiments (fig. 2c, summarized in 2d). We observed that VPS16 is a central protein in the head since its C-terminus binds VPS33A while the N-terminal segment binds to VPS41 and VPS18. The Ring finger (R) domains of VPS18 and VPS41 interact with the N-terminus of VPS16 possibly acting in a tripartite-interaction.

Different from yeast, the mammalian HOPS complex is not recruited to membranes by RAB7 (Ypt7 in yeast), but by binding to the RAB7 effector RILP that has no apparent ortholog in yeast (27,28). To evaluate membrane targeting of the mammalian HOPS complex, we mapped the minimal domains for membrane recruitment of distinct subunits by expressing tagged truncation mutants and assessed their recruitment to RILP-containing LE (fig. 2e). In addition to VPS41 (32), we observed that small domains of various HOPS subunits could be recruited to RILP (summarized in fig. 2f, 2g). This suggests that RILP could act as a scaffold in the assembly of the HOPS complex or that interactions within the mammalian HOPS complex are further stabilized via secondary interactions of its subunits with RILP. In assembly, our data suggest that interactions within the HOPS complex are reasonably conserved from yeast to mammals, yet the complex has significantly evolved to accommodate a shift from RAB7 to binding to RAB7 effector RILP instead, possibly reflecting higher-order regulation such as the concomitant binding of the dynein-motor complex (27).

a.



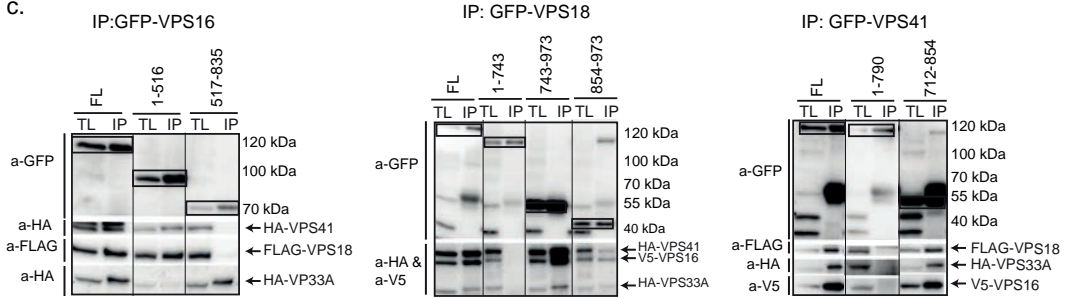
b.



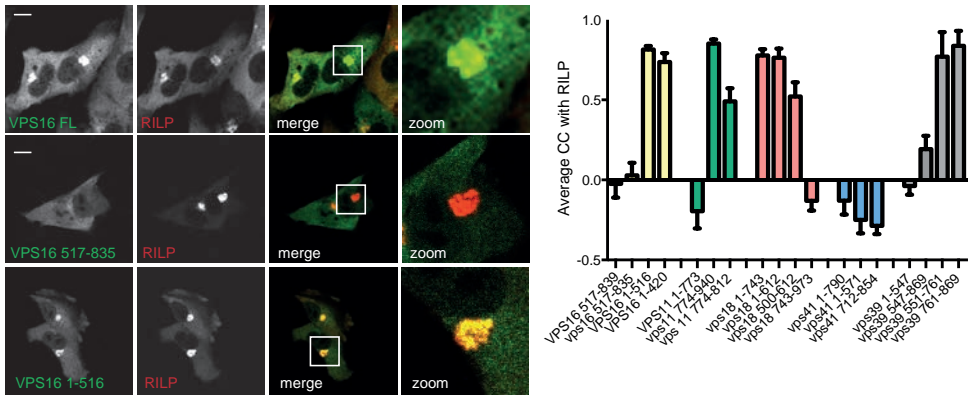
d.

IP	CO-IP		
	VPS16	VPS41	VPS33A
VPS16 FL	✓	✓	✓
VPS 16 1-516	✓	✓	ND
VPS 16 517-835	ND	ND	✓
VPS18 FL	✓	✓	✓
VPS18 1-743	ND	ND	ND
VPS18 743-973	✓	✓	✓
VPS18 854-973	✓	✓	✓
VPS41 FL	✓	✓	✓
VPS 41 1-790	ND	ND	ND
VPS41 712-854	✓	✓	✓

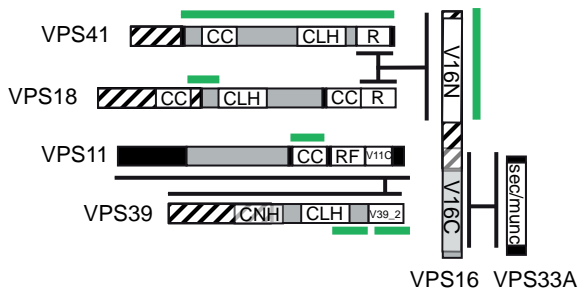
c.



e.



f.



g.

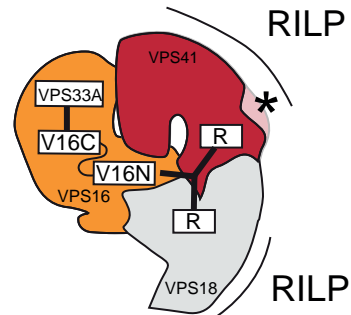


Figure 2. Interactions within the mammalian HOPS complex. (a) Structure of the yeast HOPS complex. Yeast HOPS interacts with Ypt-7 via Vps41 and the N-terminus of Vps39. (b) Domain organization of the mammalian HOPS complex subunit orthologs. CLH, clathrin heavy chain repeat; CC, coiled coil; R, Ring Finger; V11C, PFAM VPS11 C-terminus; V16N, PFAM VPS11 N-terminus; V16C, PFAM VPS11 C-terminus; V39_1, VPS39 domain 1; V39_2, VPS39 domain 2; CNH; Citron Homology. (c) Lysates of MeJuso cells co-expressing tagged-VPS constructs as indicated were IP'ed with anti-GFP antibodies and analyzed by WB using anti-HA, anti-Flag, anti-V5 and anti-GFP antibodies as indicated. Within each panel, experimental conditions were run on the same blot with the same exposures for each detection antibody and cut-outs were taken and grouped for presentation purposes. (d) Summarized results of Figure 2C. (e) MeJuso cells expressing GFP-VPS16 constructs (green) and mRFP-RILP (red). Scale bars: 10 μ m. Graphs show average correlation coefficient (CC) + s.e.m. (n>25) between different VPS truncation constructs and RILP. (f) Detailed map of domain interactions and membrane targeting modules (domains required for RILP binding in green) within the mammalian HOPS complex. (g) Interactions in the head domain of the mammalian HOPS complex superimposed on the known structure of the yeast HOPS complex.

VPS11 as the core receptor for HOPS and CORVET specific subunits.

We have shown that TGFBRAP1 and VPS8 endogenously bind core CORVET/HOPS subunits including VPS11 and VPS16 (fig. 1a) and that VPS11 and VPS16 are recruited to LE by RILP ((27), fig. 2e). This argued that overexpression of RILP, via their secondary interactions with VPS11 or VPS16, might attract VPS8 and TGFBRAP1 to LE. However, when RILP and VPS8 or TGFBRAP1 were co-expressed, the latter were not recruited to RILP but remained localized to EE (fig. 3a) similar to VPS8 and TGFBRAP1 expression alone (fig. 3b). This indicates an active mechanism that prevents recruitment of TGFBRAP1 and VPS8 to LE even in the presence of RILP. We therefore asked how CORVET- versus HOPS-specific protein binding to the core of the complex is regulated to assure correct targeting and sequential activity in endosomal maturation. Since TGFBRAP1 and VPS39 have high sequence homology, their competitive binding to the same subunit in the CORVET/HOPS core suggests a mechanism for sequential binding. A likely candidate for a common binding partner in the core of the CORVET/HOPS complex would be VPS11, as we already identified interactions between VPS11 and VPS39 (fig. 1). In line with our endogenous IP with VPS11 antibodies, an interaction between TGFBRAP1 and GFP-VPS11 was observed (fig. 3c) and co-expression of VPS11 and TGFBRAP1 resulted in the recruitment of cytosolic GFP-VPS11 to EE (fig. 3d). To map the interactions between TGFBRAP1 and VPS39 with VPS11, we expressed tagged-truncation mutants of VPS11 and assessed putative interactions (Figure 4A-B). TGFBRAP1 and VPS39 bound to the same domain in VPS11 (fig. 4a, 4b), implying that these two proteins might compete for VPS11 binding (fig. 4c). As TGFBRAP1 binds VPS11 and VPS11 binds RILP, we argued that a RILP-VPS11-TGFBRAP1 interaction could exist that could induce (erroneous) recruitment of TGFBRAP1 to LE. However, when VPS11 was co-expressed with TGFBRAP1 and RILP, VPS11 was exclusively recruited to EE and no longer recruited to LE (even though high levels of RILP were present) (fig. 4d). This suggests a regulatory mechanism in which binding of TGFBRAP1 to VPS11 in the CORVET complex prevents VPS11 binding to RILP, thereby blocking the targeting of VPS11 to LE and premature assembly of the HOPS complex on LE. Such a mechanism would safeguard a sequential assembly of the CORVET and HOPS and thereby time the fusion events of EE and LE.

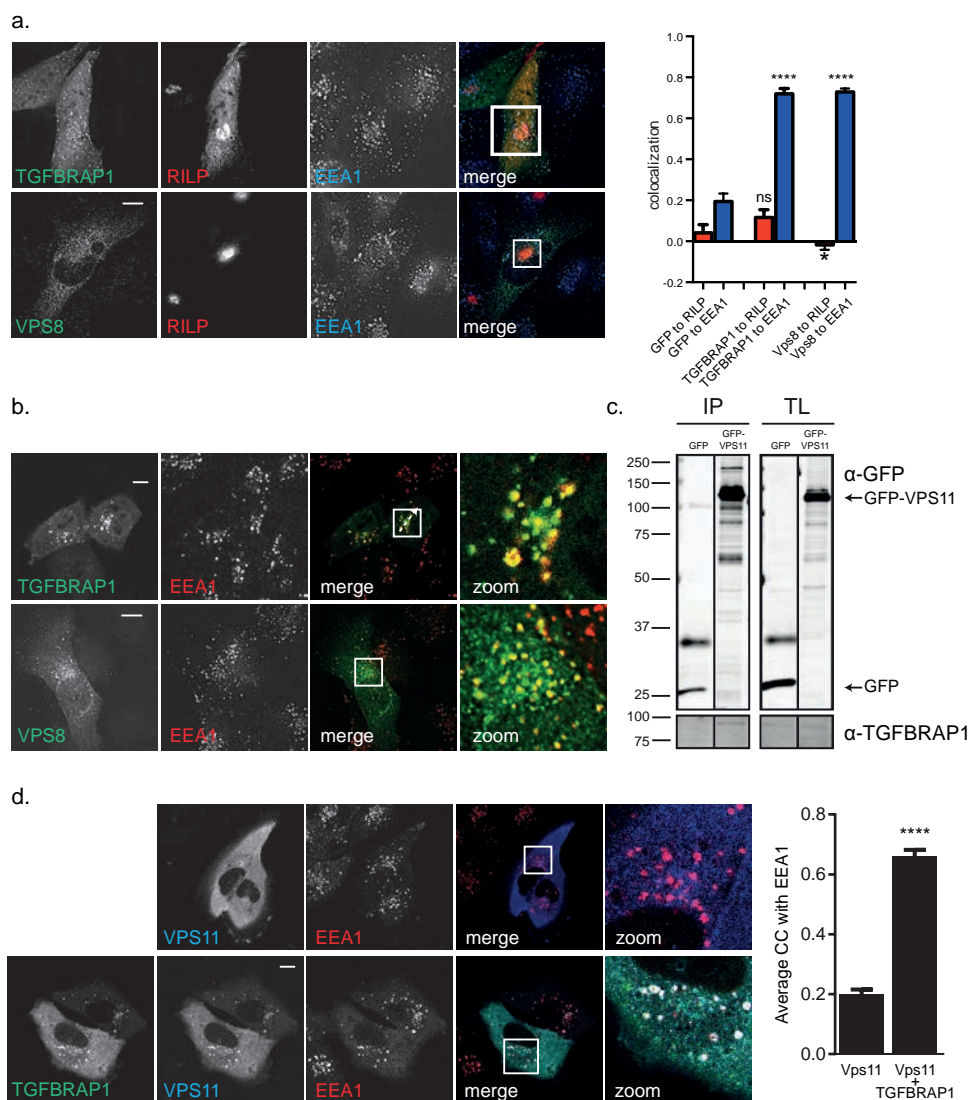


Figure 3. VPS11 interacts with CORVET specific subunits. (a) MelJuSo cells co-expressing mRFP-RILP (Red) and GFP-TGFBRAP1 or HA-VPS8 (green) were fixed, stained with antibodies against EEA1 (and anti-HA for VPS8) and imaged by CLSM. Scale bars: 10 μ m. Graphs show average correlation coefficient (CC) + s.e.m. ($n > 25$) for RILP or EEA1 and GFP, TGFBRAP1 or VPS8. Asterisks indicate significance to GFP control ((**** $p \leq 0.0001$, * $p \leq 0.05$, ns = not significant). (b) MelJuSo cells co-expressing GFP-TGFBRAP1 or HA-VPS8 were fixed, stained with antibodies against EEA1 (and anti-HA for VPS8) and imaged by CLSM. Scale bars: 10 μ m. (c) Lysates of MelJuSo cells expressing GFP or GFP-VPS11 were IP'ed with anti-GFP and analyzed by WB using anti-GFP and anti-TGFBRAP1 antibodies. Experimental conditions were run on the same blot with the same exposures for each detection antibody and cut-outs were taken and grouped for presentation purposes. (d) MelJuSo cells expressing mRFP-VPS11 (blue) or co-expressing mRFP-VPS11 (blue) and GFP-TGFBRAP1 (green) were fixed, stained with antibodies against EEA1 (red) and imaged by CLSM. Scale bars: 10 μ m. Graphs show average correlation coefficient (CC) + s.e.m. ($n > 25$) between VPS11 and EEA1 +/- ectopically expressed TGFBRAP1 (**** $p \leq 0.0001$).

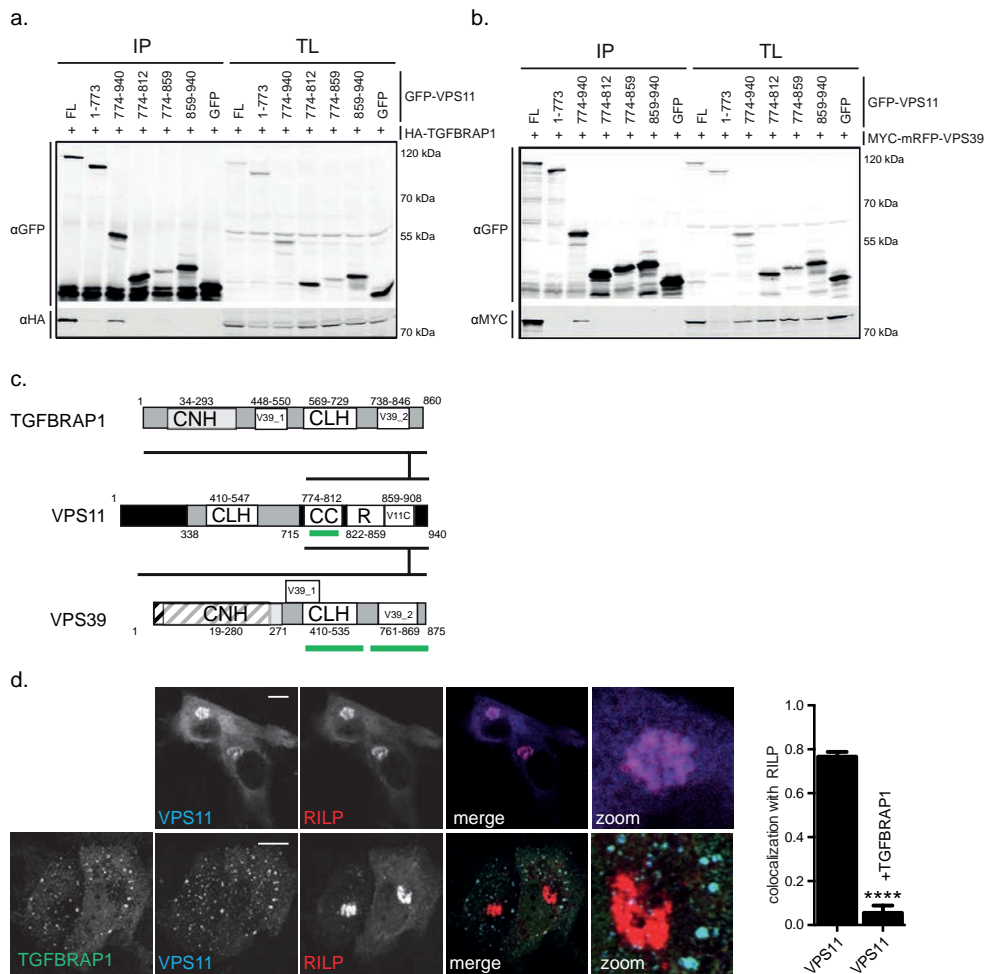


Figure 4. CORVET and HOPS specific assembly via VPS11. Lysates of HEK293 cells co-expressing GFP-VPS11 constructs (as indicated) and HA-TGFBRAP1 (**a**) or MYC-mRFP-VPS39 (**b**) constructs were IP'ed with anti-GFP before SDS-PAGE and WB and probed with anti-GFP and anti-HA or anti-MYC antibodies. (**c**) Detailed map of interactions between TGFBRAP1, VPS39 and VPS11. TGFBRAP1 and VPS11 both bind to the same region in VPS11 indicating competitive binding. Domains that contribute to RILP binding are indicated in green. (**d**) MeJuSo cells expressing GFP-VPS11 (blue) and HA-RILP (red) +/- GFP-TGFBRAP1 (green) were fixed, stained with antibodies against HA and FLAG and imaged by CLSM. Scale bars: 10 μ m. Graphs show average correlation coefficient (CC) + s.e.m. (n>25) between VPS11 and RILP in the +/- ectopically expressed TGFBRAP1 (**** p < 0.0001).

2

ARC mutations specifically disrupt VPS33B-VIPAS39 interactions or complex recruitment to late endosomes by RILP.

Published data regarding the role of VPS33B and VIPAS39 as members of the HOPS complex are seemingly conflicting (12,15). Our endogenous IP data (fig. 1a) as well as our IP's with tagged subunits (fig. 1b) indicated that VPS33B and VIPAS39 did not interact with other HOPS subunits. To further substantiate the existence of a separate VPS33B/VIPAS39 complex, we depleted CORVET/HOPS subunits by siRNA and assessed the effects on the stability of their endogenous interaction partners by western blot (WB) (fig. 5a). Silencing of VPS16 significantly decreased VPS33A and VPS11 protein levels, while VPS33B and VIPAS39 levels did not decrease (fig. 5a). Similarly, silencing of VPS33B compromised VIPAS39 levels without affecting VPS16, VPS33A or VPS11 (fig. 5a). These findings reinforce the notion that VPS33B and VIPAS39 assemble into a separate complex.

Interestingly, autosomal recessive mutations in VPS33B or VIPAS39 cause ARC syndrome (22,29), a fatal multisystem disorder characterized by defects in apical transport in polarized cells. In line with this, VPS33B and VIPAS39 have previously been shown to function at RAB11 positive recycling endosomes (20,21). Under steady-state conditions VPS33B and VIPAR do not significantly localize to LE (21) but we have shown that these proteins can be recruited to LE by RILP (27). In line with a function of VPS33B and VIPAR at the LE, it was recently shown that VPS33B is important for the maturation of the α -granule, a specialized late endosomal compartment (30). Therefore, we investigated whether pathogenic mutations in VPS33B could still be recruited to LE by RILP. We studied two pathogenic mutations of VPS33B, a single amino-acid substitution mutant (VPS33B L30P) and a truncation mutant (VPS33B 1-437) and mapped the effect on VPS33B-VIPAS39 interactions as well as RILP-dependent membrane recruitment. The truncated mutant of VPS33B (1-437) did not interact with VIPAS39 (fig. 5b, (21)), but was still recruited to LE by RILP, indicating that VPS33B can bind RILP independent of VIPAS39 (fig. 5c). The L30P mutation in VPS33B had a different effect; although VPS33B L30P still interacted with VIPAS39 (fig. 5b), it failed to be recruited to LE by RILP (fig. 5c, (27)). Thus, our results indicate that two specific mutations in VPS33B as found in ARC patients, affect assembly with VIPAS39 (VPS33B 1-437) or LE recruitment of the VPS33B-VIPAS39 complex (VPS33B L30P) by RILP (Figure 5D).

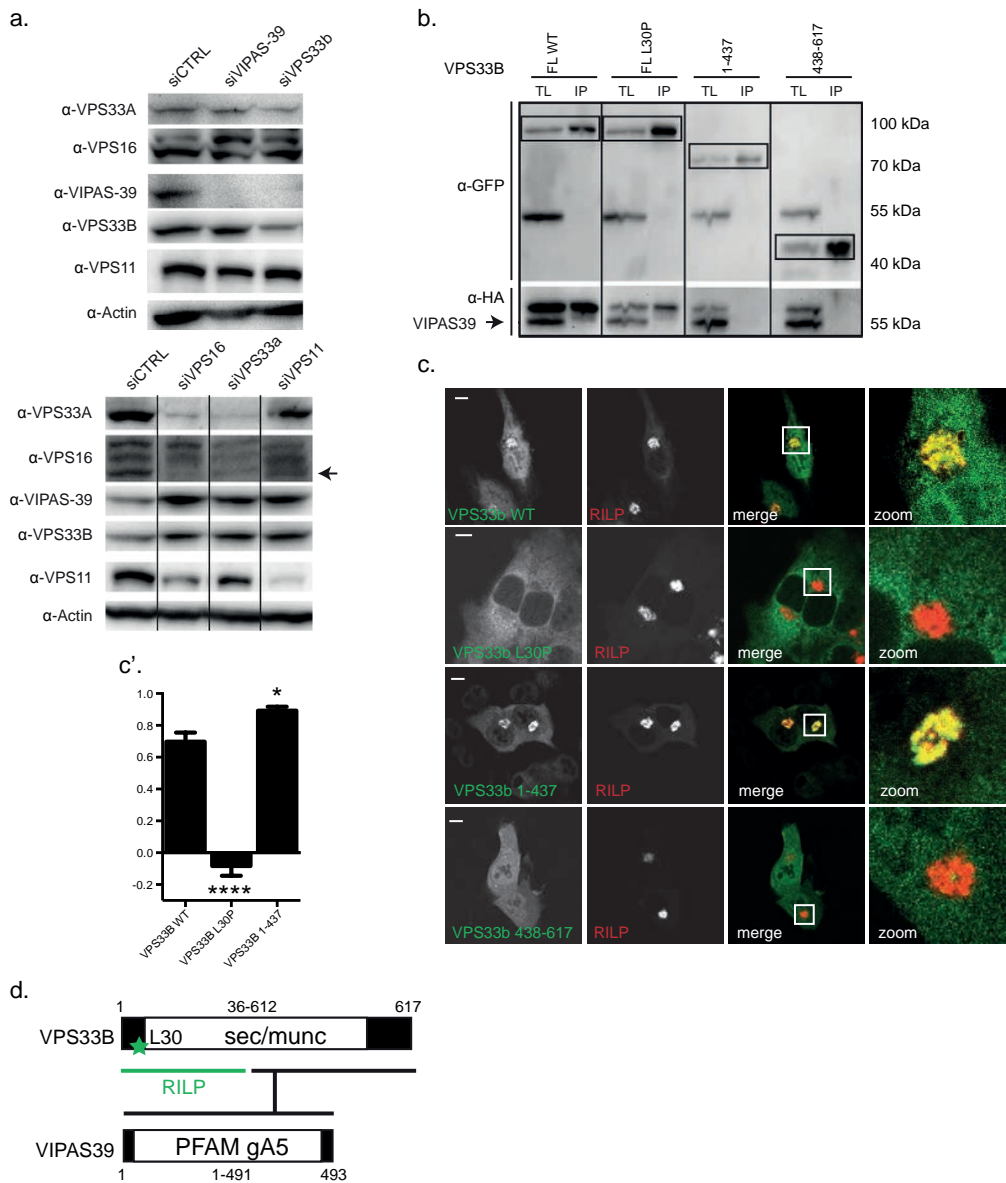


Figure 5. VPS33B and VIPAS39 are not HOPS complex subunits and mutations in VPS33B differentially affect VPS33B interactions with VIPAS39 and RILP. (a) Lysates of MeJuSo cells silenced for indicated HOPS subunits were analyzed by WB using anti-VPS16, anti-VPS33B, anti-VIPAS39, anti-VPS11, anti-VPS33 and anti-Actin (as loading control) antibodies as indicated. Within each panel, experimental conditions were run on the same blot with the same exposures for each detection antibody and cut-outs were taken and grouped for presentation purposes. (b) IP with anti-GFP from lysates of MeJuSo cells co-expressing GFP-VPS33B mutants and HA-VIPAS39 (as indicated) were analyzed by WB using anti-GFP and anti-HA antibodies. Experimental conditions were run on the same blot with the same exposures for each detection antibody and cut-outs were taken and grouped for presentation purposes. (c) MeJuSo cells expressing GFP-VPS33B constructs (green) and mRFP-RILP (red) were fixed and imaged by CLSM. Scale bars: 10 μ m. Correlation coefficient was calculated from plot profiles measuring RILP intensity and GFP intensity over a vector through the cells. Graphs show the average correlation coefficient (CC) + s.e.m. (n>25) between VPS33B constructs and RILP (* $p \leq 0.05$, **** $p \leq 0.0001$, ns = not significant, when compared to VPS33B wt). (d) Summary of VPS33B domains involved in interactions with RILP (green) and VIPAS39. Asterisks indicates L30 residue (mutated in ARC syndrome) required for VPS33B recruitment to RILP.

Discussion

We have investigated the interactions between the proposed mammalian subunits of the multi-subunit CORVET and HOPS tethering complexes, and found –with modifications- that the organization of these complexes is largely conserved from yeast to mammals (fig. 6a). As in yeast, the mammalian HOPS complex consists of VPS16, VPS11, VPS33A, VPS18, VPS41 and VPS39. We confirm that TGFBRAP1 and VPS8 are the mammalian CORVET specific subunits (with TGFBRAP1 as the yeast *vps3* ortholog) (11,31). In contrast to previous data (15) however, our data indicates that VIPAS39 and VPS33B, two CORVET/HOPS subunit homologues not present in yeast, are not part of CORVET/HOPS as also suggested by others (12,20,32). We cannot formally exclude the occurrence of transient interactions of VPS33B and/or VIPAS39 with CORVET/HOPS or the existence of VPS33B/VIPAS39-HOPS interactions in other cellular systems. However, the existence of a VPS33/VIPAS39 complex independent of other core subunits might explain why only mutations in VPS33B and VIPAS39 but not any of other HOPS subunits are associated to ARC syndrome (20–22,29) and why all HOPS complex subunits –but not VPS33B and VIPAS39- are required for Ebola-virus infection (18). Conservation of these separate complexes is not apparent in all organisms. For example, in *C. elegans* the two VPS33 homologues (VPS33.1 and VPS33.2) are present in HOPS (VPS33.1) and CORVET (VPS33.2) (33). It is unclear however whether VPS33.1 and VPS33.2 are direct orthologous for mammalian VPS33A and VPS33B or reflect other evolutionary divergence. Similar to mammals, *Drosophila* VPS33A (Car) and VPS33B have distinct functions (34) and *Drosophila* VPS16 interacts with VPS33A, whereas *Drosophila* VIPAS39 interacts with VPS33B (35). However, *Drosophila* VIPAS39 also interacted with VPS18 suggesting that VIPAS39/VPS33B in *Drosophila* can interact with CORVET/HOPS core subunits (35). In mice, mutations in VPS33A yielded hypopigmentation and mild platelet-deficiency, but did not cause ARC indicating that VPS33A and VPS33B functions do not completely overlap in mice (36). This suggests that VPS33B/VIPAS39 interactions might have gradually diverted from that of CORVET/HOPS during mammalian evolution. Yet, functions of VIPAS39 seem conserved between different organisms. For example, the observation that *Drosophila* lacking VIPAS39 (*dVPS16*) have a profound defect in phagosomal acidification is in line with our observation that VIPAS39 functions at LE compartments (27). Here we report that ARC-syndrome mutations in VPS33B differentially affect the binding of VPS33b to VIPAS39 or membrane recruitment of VPS33B to RILP. This consolidates the finding that VPS33B/VIPAS39 function at LE (30) as well as recycling endosomes (15,20,21), and that both membrane binding and VIPAS39 binding are needed for correct VPS33B function.

We show that HOPS subunits have evolved to accommodate binding to the RAB7 effector RILP (for a mammalian model superimposed on the yeast structure see figure 3G). The N-terminus of yeast *vps39* that binds Ypt7 is poorly conserved in the mammalian VPS39 ortholog, which might explain why the mammalian HOPS complex has shifted to bind RAB7 effectors such as RILP (27,28) and PLEKHM1 (14,37). The HOPS complex binds RILP on either side of the complex (VPS39/VPS11 in the tail and VPS41/VPS18 in the head) and may bridge RILP molecules on opposing vesicles. Since VPS33A in the head of HOPS also binds to SNAREs (38), a connection between two vesicles will then support tethering and subsequent fusion. It is interesting to note that the HOPS complex can also bind the GTPase Arl8b on lysosomes (19,39) and PLEKHM1 on LE, phagosomes and autophagosomes (14,37), possibly tethering these vesicles with RILP containing organelles

(fig. 6b). RAB7-RILP concomitantly binds the HOPS complex and the dynein-motor complex for retrograde transport (27), whereas the Arl8b effector SKIP also concomitantly regulates HOPS binding and anterograde transport by kinesin (39), indicating that timing of vesicle tethering is likely coupled to their transport.

We found that binding of TGFBRAP1 to VPS11 prevents the interaction of VPS11 with RILP and erroneous recruitment of CORVET complexes to RILP-bearing LE. This might provide an important regulatory step in the conversion of CORVET to HOPS complexes (fig. 5) where TGFBRAP1 in CORVET would have to release VPS11, thereby allowing VPS11 to bind VPS39 and recruit the entire HOPS complex to RAB7-RILP during RAB5 (EE) to RAB7 (LE) conversion. Specific targeting of tethering complexes by modulation of targeting subunits was recently also shown for GARP and EARP tethering on Golgi and EE respectively, indicating this might be a common mechanism in the regulation of vesicular fusion (40). TGFBRAP1 to VPS39 exchange might further be regulated by proteins such as MON1-CCZ1 (fig. 6b) that are recruited by CORVET, interact with VPS39 and act as activators of RAB7 (41–43) and signalling pathways such as the TGF β pathway that has been shown to intersect with TGFBRAP1 and VPS39 function (44–46).

In conclusion, we describe the molecular architecture of the mammalian CORVET, HOPS and VIPAS39/VPS33B complexes. We find that different ARC syndrome mutations affect VIPAS39-VPS33B or VPS33B-RILP interactions, indicating that this complex has a function at the LE. Through mapping of the CORVET and HOPS complexes we found that within the shared CORVET/HOPS core, VPS11 is a molecular switch that, depending on its interacting proteins (TGFBRAP1 or VPS39), determines targeting of CORVET and HOPS to EE and LE.

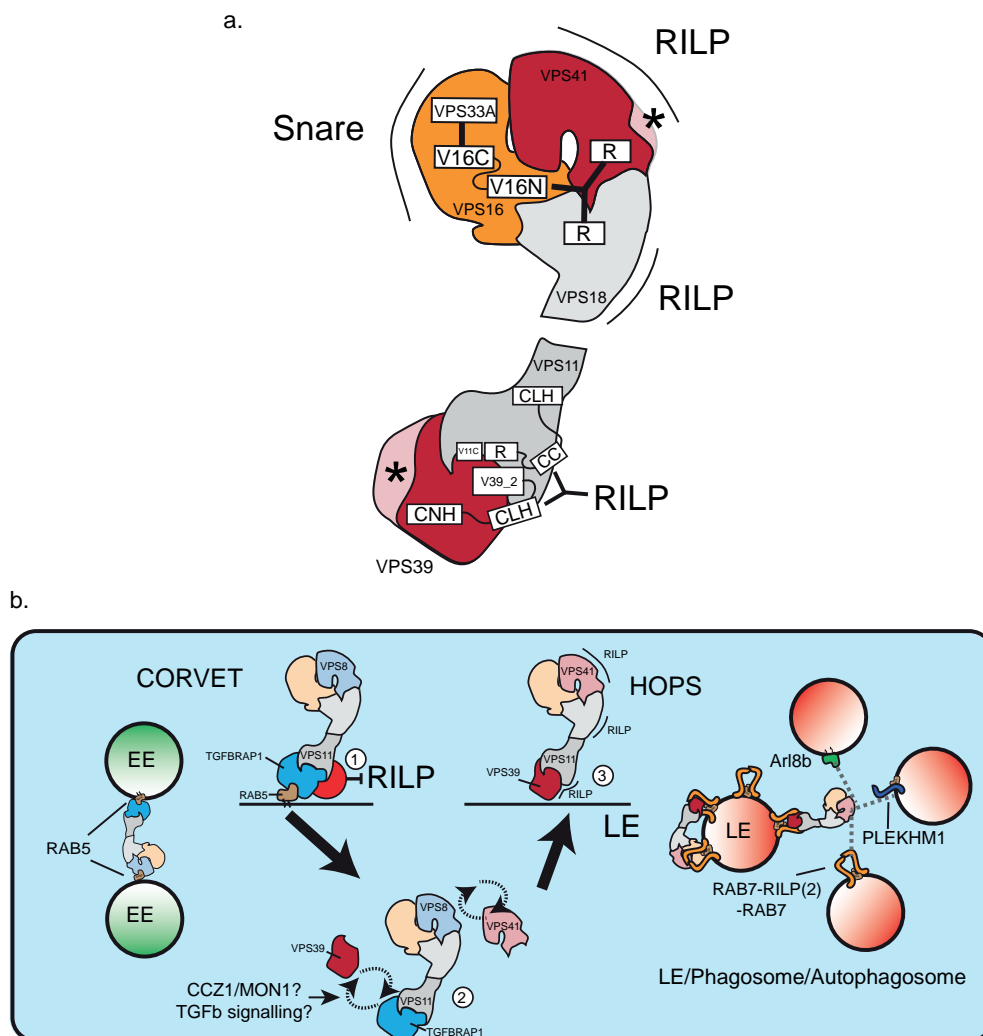


Figure 6. Model of membrane binding specificity of the CORVET and HOPS complex and their conversion during maturation. (a) Model of the mammalian HOPS complex superimposed on the yeast structure, depicting RILP-binding domains. Asterisks indicate poorly conserved regions in the N-terminus of VPS39 and loss of lipid-binding motif of VPS41 that have altered membrane targeting in the mammalian complex. **(b)** The CORVET complex binds to RAB5 on EE and (1) within this complex, TGFBRAP1 binding to VPS11 prevent association of VPS11 to RILP. (2) To allow RAB7-RILP binding, TGFBRAP1 is replaced by VPS39, possibly controlled by CCZ1/MON1 and TGF β signaling. Replacement of VPS8 with VPS41 adds an additional RILP-binding motif, completing the conversion of CORVET to HOPS complex from RAB5- to RAB7- during endosomal maturation (3). Both the head and tail of mammalian HOPS can bind the homodimer RAB7-RILP. There may be two conditions; an inactive conformation where HOPS binds back to RILP on the same vesicle failing to contact a fusion partner; and an active conformation in which RILP-HOPS contacts other vesicles (LE, phagosomes or autophagosomes containing HOPS interactors such as ARL8b, PLEKHM1 or RILP) for tethering and subsequent fusion.

Materials and Methods

Reagents

Rabbit anti-GFP and rabbit anti-mRFP antibodies were generated in house using purified His-mRFP or His-GFP recombinant proteins, respectively. Cross-reactivity has been excluded by Western blot analyses with various mRFP- or GFP-labelled fusion proteins. Other antibodies used were: mouse anti-CD63 (47), mouse anti-EEA1 (ab2900, Abcam) mouse anti-V5 and anti-V5-HRP (R96025, R96125 Invitrogen), anti-Myc (2278P, Cell signaling) anti-Myc-HRP (NB600-302H Novus), anti-HA (12013819001, Roche) and anti-HA-HRP (ab1190, Abcam), anti-FLAG (M2) and anti-FLAG-HRP (F3165, A8592 Sigma) anti-VPS33A (C1C3) (GTX119416, GeneTex), anti-VPS33b (12195-1-AP, Proteintech), anti-VPS11 (19140-1-AP, Proteintech), anti-TGFBRAP1 (SC-13134 Santa Cruz) anti-VPS41 (13869-1-AP, Proteintech), anti-VPS8 (HPA036871, Sigma), anti-VPS16 (17776-1-AP Proteintech), Anti-VIPAS39 was a gift of V. Faundez (Center for Translational Social Neuroscience, Emory University, Atlanta). Fluorescent and HRP-conjugated secondary antibodies were obtained from Invitrogen.

Constructs

RAB7 and RILP (48) and full length VPS constructs and GFP-VPS33b L30P (27) have been described previously. GFP-VPS16 and GFP-VPS18 were gifts from Chengyu Liang (Department of Molecular Microbiology and Immunology, University of Southern California, Los Angeles). VPS33a was a gift of V. Faundez (Center translational social neuroscience, Emory University, Atlanta), Vps39 was a gift of J. Bonifacino (National Institute of Health, Bethesda, MD). HA-VPS8 was purchased from Origene and inserted into pcDNA3.2-HA/DEST vector (Invitrogen) using Gateway recombination cloning. Truncation constructs were generated by PCR using these respective cut sites, donor vectors, forward primer and reverse primer,

VPS33b 1-437, Xho1-BamH1 GFP-C1 cccaCTCGAGCCATGGCTTTTCCCCATCG and cccaGGATCCTCACAGATTGGAGAAGGTTAGCA VPS33b 438-617, EcoR1-BamH1 GFP-C1 CCCAGAATTCCTGCGAAGAGCTGGGCTCCT and CCCAGGATCCTCAGGCTTTCACCTCACTCA mVPS16 1-516, EcoR1-Asp718 GFP-C1 cccaGAATTCATGGACTGTTACTACTGCGAA and cccaGGTACCTCAACCAGGCGTGTCACCCAGCT mVPS16 1-420, EcoR1-BamH1 GFP-C1, cccaGAATTCATGGACTGCTACACGGCGAA and cccaGGATCCTCAGTGCACGAAGCTGTCGGGTG mVPS16 517-835, EcoR1-BamH1 GFP-C1 cccaGAATTCCTTACTCCGACATTGCTGC and cccaGGATCCTCATTGTGCCCTGGCCCGTTGAA mVPS16 517-839, EcoR1-EcoR1 GFP-C1 cccaGAATTCCTTACTCCGACATTGCTGC and cccaGAATTCCTCACTTCTTGGGCTTGTVPS41 1-790, Xho1-BamH1 GFP-C1 cccaCTCGAGCCATGGCGGAAGCAGAGGAGCA and cccaGGATCCTCAGATGTTCTCCTCATCAACAA VPS41 1-571, Xho1-BamH1 GFP-C1 cccaCTCGAGCCATGGCGGAA-GCAGAGGAGCA and cccaGGATCCTCAAAGCATGTCAACAGCTTTCT VPS41 712-854, BglII-EcoR1 GFP-C1 cccaAGATCTGGCTTGTTAAACAACATTGG and cccaGAATTCCTATTTTTTCATCTCCAAAA VPS11 1-773, Xho1-EcoR1 GFP-C1 cccaCTCGAGCCATGGCGGCTACCTGCAGTG and cccaGAATTCCTCAGTCCCTGATGACGGAGA VPS11 774-940, EcoR1-BamH1 GFP-C1 cccaGAATTCCTACCTGGTCCAAAAACTACA and cccaGGATCCTCAAGTGCCCTCCTGGAGTGCA VPS11 774-812, EcoR1-BamH1 GFP-C1 cccaGAATTCCTACCTGGTCCAAAAACTACA and cccaGGATCCTCAGGCCTTGAGCTTTGGATCT VPS11 774-859, EcoR1-BamH1 GFP-C1 cccaGAATTCCTACCTGGTCCAAAAACTACA and

cccaGGATCCTCAGGTGGGGCAGTCAGCATCAC VPS11 859-940, EcoR1-BamH1 GFP-C1
 cccaGAATTCCACCTGCCTCCCTGAAAACCG and cccaGGATCCTCAAGTGCCCTCCTGGAGTGCA
 VPS18 1-743, EcoR1-BamH1 GFP-C1 CCCAGAATTCCATGGCGTCCATCCTGGATGA and
 CCCAGGATCCTTAATCAGGAAAGAAGGGCA VPS18 1-612, EcoR1-BamH1 GFP-C1
 CCCAGAATTCCATGGCGTCCATCCTGGATGA and cccaGGATCCTCAATCTACAAGCTGGCGGGGGAT
 VPS18 500-612, EcoR1-BamH1 GFP-C1 cccaGAATTCCAGCCGGCTT-GGGGCTCTGCA and
 cccaGGATCCTCAATCTACAAGCTGGCGGGGGAT VPS18 743-973, EcoR1-BamH1 GFP-C1
 CCCAGAATTCCGATTTTCGTACCATCGACCA and cccaGGATCCTCACAGCCAAGCTGAGCTGCTCCT
 VPS18 854-973, EcoR1-BamH1 GFP-C1 cccaGAATTCCGGCACTGTGGAGCCCCAGGA and
 cccaGGATCCTCACAGCCAAGCTGAGCTGCTCCT VPS39 551-761, EcoR1-BamH1 GFP-C1
 cccaGAATTCCCTGCATTTGATTTCTCCTA and cccaGGATCCTCATAGTTCCAGCTTGATTGG
 VPS39 761-869, EcoR1-BamH1 GFP-C1 cccaGAA-TTCCCTACTGGAGCCAAAAGCCAA and
 cccaGGATCCTCAATTGGGGTATCTTGCAAATG

Cell culture and microscopy

MelJuSo cells were cultured in Iscove's modified Dulbecco's medium (IMDM; Invitrogen) supplemented with 8% FCS in a 5% CO₂ humidified culture hood at 37°C. HEK293 cells were cultured in Dulbecco's modified eagle medium (DMEM; Invitrogen) supplemented with 8% FCS in a 5% CO₂ humidified culture hood at 37°C. All specimens were analyzed by confocal laser-scanning microscopes (TCS-SP1, TCS-SP2, or AOBS; Leica) equipped with HCX Plan-Apochromat 63× NA 1.32 and HCX Plan-Apochromat lbd.bl 63× NA 1.4 oil-corrected objective lenses (Leica) using LCS (Leica) acquisition software or Deltavision wide field microscope (Applied Precision) with a 100/1.4A immersion objective. Widefield images were deconvolved using SoftWorx software (Applied Precision).

Transfection

Expression constructs were transfected using Effectene reagents (Qiagen) according to manufacturer's instructions. For silencing, cells were transfected with Dharmafect1 (Thermo Fisher Scientific) with siRNA's (ON-TARGETplus SMARTpool) against VPS16, VPS33B, VPS33A, SPE-39 or control siRNA (Thermo Fisher Scientific).

Microscopy sample preparation

Transfected cells were fixed 24h post-transfection with 4% formaldehyde in PBS for 15 min and permeabilized for 10 min with 0.05% Triton X-100 in PBS at room temperature. Non-specific binding of antibodies was blocked by 0.5%BSA in PBS for 40 min, after which cells were incubated with primary antibodies in 0.5%BSA in PBS for 1h at room temperature. After washing three times with PBS, primary antibodies were visualized with Alexa-Fluor secondary antibody conjugates antibodies in 0.5%BSA in PBS for 30min at room temperature (Invitrogen). After three washes with PBS, samples were mounted in Vectashield mounting medium (Vector Laboratories).

Protein immunoprecipitation

MelJuSo cells were washed with ice-cold PBS and scraped into cell lysis buffer (50mM Tris-HCl, 150mM NaCl, 5mM MgCl₂, 1% NP40, 10% glycerol, pH 7.4) supplemented with complete EDTA-free Protease Inhibitor Cocktail. Cell lysates were obtained by incubation on ice for 10

min followed by centrifugation for clearing. The supernatants were incubated for 2h with respective antibodies followed by capture with protein G-Sepharose 4 FF resin and washed extensively with wash-buffer (50mM Tris, 150mM NaCl, 5mM MgCl₂, 10% glycerol, pH 7.4). For GFP-tagged pulldown, GFP-TRAP beads were used (Chromotek). All experiments were repeated multiple times. To compose the figure panels, inserts from a single experiment containing all the experimental conditions (and all the transfected constructs) are composed as described in the figure legends.

Statistical analysis

For calculation of correlation coefficients the signal intensity over a vector was plotted using the plot profile tool in ImageJ (<http://imagej.nih.gov/ij/index.html>) in respective fluorescence channels. Correlation coefficient for colocalization assays were calculated from plot profiles measuring intensity for the indicated fluorescence channels over a vector through the cells (as in (27)). Correlation coefficients for the two plots were calculated in Excel using the function:

$$\text{correl}(x, y) = \frac{\sum(x - \bar{x})(y - \bar{y})}{\sqrt{(\sum(x - \bar{x})^2)(\sum(y - \bar{y})^2)}}$$

Statistical testing was performed in Graphpad Prism 6 using a one-way Anova with Tukey's multiple comparison test for significance.

Acknowledgments

We thank C. Liang, J. Bonifacino, V. Faundez, and S. Zlatić for kindly providing reagents. This work is supported by a European Research Council Advanced Grant; and a TOP grant from The Netherlands Organization for Scientific Research – Chemical Sciences. We thank Romain Galmes and Peter van der Sluijs for valuable discussions and Rene Schriwanek for preparation of EM figures.

Conflict of interest

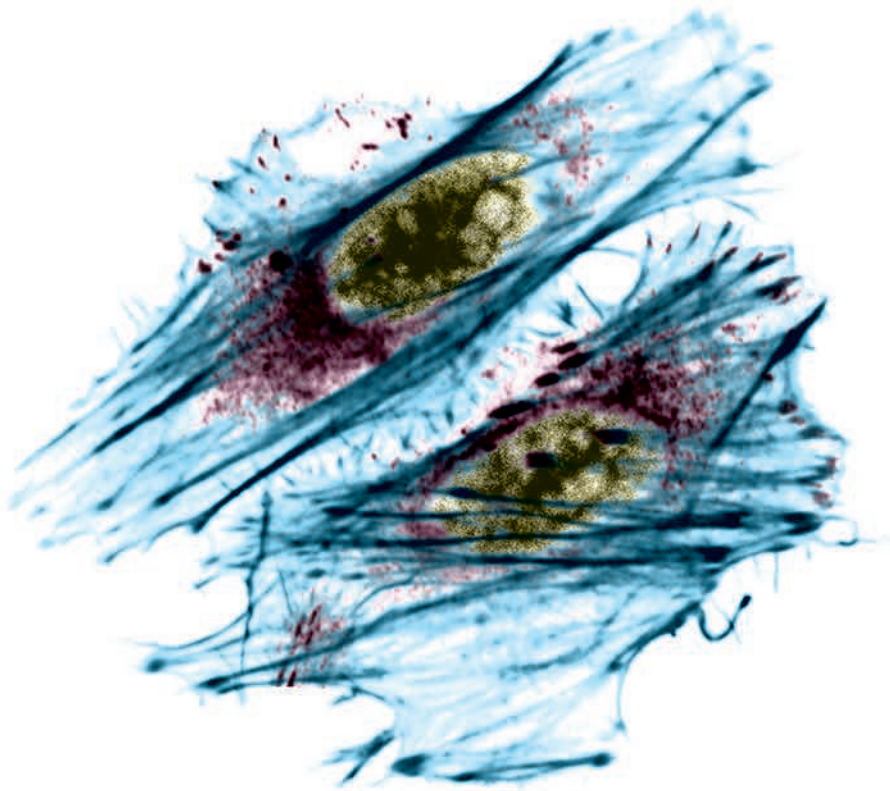
The authors declare that they have no conflicts of interest with the contents of this article.

References

1. Stenmark H. Rab GTPases as coordinators of vesicle traffic. *Nat Rev Mol Cell Biol.* 2009 Aug;10(8):513–525.
2. Wickner W. Membrane fusion: five lipids, four SNAREs, three chaperones, two nucleotides, and a Rab, all dancing in a ring on yeast vacuoles. *Annu Rev Cell Dev Biol.* 2010;26:115–136.
3. Sato TK, Rehling P, Peterson MR, Emr SD. Class C Vps protein complex regulates vacuolar SNARE pairing and is required for vesicle docking/fusion. *Mol Cell.* 2000 Sep;6(3):661–671.
4. Wurmser AE, Sato TK, Emr SD. New component of the vacuolar class C-Vps complex couples nucleotide exchange on the Ypt7 GTPase to SNARE-dependent docking and fusion. *J Cell Biol.* 2000 Oct 30;151(3):551–562.
5. Nakamura N, Hirata A, Ohsumi Y, Wada Y. Vam2/Vps41p and Vam6/Vps39p are components of a protein complex on the vacuolar membranes and involved in the vacuolar assembly in the yeast *Saccharomyces cerevisiae*. *J Biol Chem.* 1997 Apr 25;272(17):11344–11349.
6. Plemel RL, Lobingier BT, Brett CL, Angers CG, Nickerson DP, Paulsel A, et al. Subunit organization and Rab interactions of Vps-C protein complexes that control endolysosomal membrane traffic. *Mol Biol Cell.* 2011 Apr 15;22(8):1353–1363.
7. Ostrowicz CW, Bröcker C, Ahnert F, Nordmann M, Lachmann J, Peplowska K, et al. Defined subunit arrangement and rab interactions are required for functionality of the HOPS tethering complex. *Traffic.* 2010 Oct;11(10):1334–1346.
8. Bröcker C, Kuhlee A, Gatsogiannis C, Balderhaar HJ, Hönscher C, Engelbrecht-Vandré S, et al. Molecular architecture of the multisubunit homotypic fusion and vacuole protein sorting (HOPS) tethering complex. *Proc Natl Acad Sci U S A.* 2012 Feb 7;109(6):1991–1996.
9. Cabrera M, Langemeyer L, Mari M, Rethmeier R, Orban I, Perz A, et al. Phosphorylation of a membrane curvature-sensing motif switches function of the HOPS subunit Vps41 in membrane tethering. *J Cell Biol.* 2010 Nov 15;191(4):845–859.
10. Rink J, Ghigo E, Kalaidzidis Y, Zerial M. Rab conversion as a mechanism of progression from early to late endosomes. *Cell.* 2005 Sep 9;122(5):735–749.
11. Perini ED, Schaefer R, Stöter M, Kalaidzidis Y, Zerial M. Mammalian CORVET is required for fusion and conversion of distinct early endosome subpopulations. *Traffic.* 2014 Dec;15(12):1366–1389.
12. Wartosch L, Günesdogan U, Graham SC, Luzio JP. Recruitment of VPS33A to HOPS by VPS16 Is Required for Lysosome Fusion with Endosomes and Autophagosomes. *Traffic.* 2015 Jul;16(7):727–742.
13. Jiang P, Nishimura T, Sakamaki Y, Itakura E, Hatta T, Natsume T, et al. The HOPS complex mediates autophagosome-lysosome fusion through interaction with syntaxin 17. *Mol Biol Cell.* 2014 Apr;25(8):1327–1337.
14. McEwan DG, Popovic D, Gubas A, Terawaki S, Suzuki H, Stadel D, et al. PLEKHM1 regulates autophagosome-lysosome fusion through HOPS complex and LC3/GABARAP proteins. *Mol Cell.* 2015 Jan 8;57(1):39–54.
15. Zhu GD, Salazar G, Zlatic SA, Fiza B, Doucette MM, Heilman CJ, et al. SPE-39 family proteins interact with the HOPS complex and function in lysosomal delivery. *Mol Biol Cell.* 2009 Feb;20(4):1223–1240.
16. Chirivino D, Del Maestro L, Formstecher E, Hupé P, Raposo G, Louvard D, et al. The ERM proteins interact with the HOPS complex to regulate the maturation of endosomes. *Mol Biol Cell.* 2011 Feb 1;22(3):375–385.
17. Liang C, Lee JS, Inn KS, Gack MU, Li Q, Roberts EA, et al. Beclin1-binding UVRAG targets the class C Vps complex to coordinate autophagosome maturation and endocytic trafficking. *Nat Cell Biol.* 2008 Jul;10(7):776–787.
18. Carette JE, Raaben M, Wong AC, Herbert AS, Obernosterer G, Mulherkar N, et al. Ebola virus entry requires the cholesterol transporter Niemann-Pick C1. *Nature.* 2011 Sep 15;477(7364):340–343.
19. Garg S, Sharma M, Ung C, Tuli A, Barral DC, Hava DL, et al. Lysosomal trafficking, antigen presentation, and microbial killing are controlled by the Arf-like GTPase Arl8b. *Immunity.* 2011 Aug 26;35(2):182–193.
20. Smith H, Galmes R, Gogolina E, Straatman-Iwanowska A, Reay K, Banushi B, et al. Associations among genotype, clinical phenotype, and intracellular localization of trafficking proteins in ARC syndrome. *Hum Mutat.* 2012 Dec;33(12):1656–1664.
21. Cullinane AR, Straatman-Iwanowska A, Zaucker A, Wakabayashi Y, Bruce CK, Luo G, et al. Mutations in VIPAR cause an arthrogryposis, renal dysfunction and cholestasis syndrome phenotype with defects in epithelial polarization. *Nat Genet.* 2010 Apr;42(4):303–312.
22. Gissen P, Johnson CA, Morgan NV, Stapelbroek JM, Forshew T, Cooper WN, et al. Mutations in VPS33B, encoding a regulator of SNARE-dependent membrane fusion, cause arthrogryposis-renal dysfunction-cholestasis (ARC)

- syndrome. *Nat Genet.* 2004 Apr;36(4):400–404.
23. Lo B, Li L, Gissen P, Christensen H, McKiernan PJ, Ye C, et al. Requirement of VPS33B, a member of the Sec1/Munc18 protein family, in megakaryocyte and platelet alpha-granule biogenesis. *Blood.* 2005 Dec 15;106(13):4159–4166.
 24. Van Luijn MM, Kreft KL, Jongsma ML, Mes SW, Wierenga-Wolf AF, van Meurs M, et al. Multiple sclerosis-associated CLEC16A controls HLA class II expression via late endosome biogenesis. *Brain.* 2015 Jun;138(Pt 6):1531–1547.
 25. Tornieri K, Zlatic SA, Mullin AP, Werner E, Harrison R, L'hernault SW, et al. Vps33b pathogenic mutations preferentially affect VIPAS39/SPE-39-positive endosomes. *Hum Mol Genet.* 2013 Dec 20;22(25):5215–5228.
 26. Pols MS, van Meel E, Oorschot V, ten Brink C, Fukuda M, Swetha MG, et al. hVps41 and VAMP7 function in direct TGN to late endosome transport of lysosomal membrane proteins. *Nat Commun.* 2013;4:1361.
 27. Van der Kant R, Fish A, Janssen L, Janssen H, Krom S, Ho N, et al. Late endosomal transport and tethering are coupled processes controlled by RILP and the cholesterol sensor ORP1L. *J Cell Sci.* 2013 Aug 1;126(Pt 15):3462–3474.
 28. Lin X, Yang T, Wang S, Wang Z, Yun Y, Sun L, et al. RILP interacts with HOPS complex via VPS41 subunit to regulate endocytic trafficking. *Sci Rep.* 2014 Dec 2;4:7282.
 29. Gissen P, Johnson CA, Gentle D, Hurst LD, Doherty AJ, O’Kane CJ, et al. Comparative evolutionary analysis of VPS33 homologues: genetic and functional insights. *Hum Mol Genet.* 2005 May 15;14(10):1261–1270.
 30. Bem D, Smith H, Banushi B, Burden JJ, White IJ, Hanley J, et al. VPS33B regulates protein sorting into and maturation of α -granule progenitor organelles in mouse megakaryocytes. *Blood.* 2015 Jul 9;126(2):133–143.
 31. Lachmann J, Glaubke E, Moore PS, Ungermann C. The Vps39-like TRAP1 is an effector of Rab5 and likely the missing Vps3 subunit of human CORVET. *Cell Logist.* 2014 Dec;4(4):e970840.
 32. Graham SC, Wartosch L, Gray SR, Scourfield EJ, Deane JE, Luzio JP, et al. Structural basis of Vps33A recruitment to the human HOPS complex by Vps16. *Proc Natl Acad Sci U S A.* 2013 Aug 13;110(33):13345–13350.
 33. Solinger JA, Spang A. Tethering complexes in the endocytic pathway: CORVET and HOPS. *FEBS J.* 2013 Jun;280(12):2743–2757.
 34. Akbar MA, Ray S, Krämer H. The SM protein Car/Vps33A regulates SNARE-mediated trafficking to lysosomes and lysosome-related organelles. *Mol Biol Cell.* 2009 Mar;20(6):1705–1714.
 35. Pulipparacharuvil S, Akbar MA, Ray S, Sevrioukov EA, Haberman AS, Rohrer J, et al. Drosophila Vps16A is required for trafficking to lysosomes and biogenesis of pigment granules. *J Cell Sci.* 2005 Aug 15;118(Pt 16):3663–3673.
 36. Suzuki T, Oiso N, Gautam R, Novak EK, Panthier JJ, Suprabha PG, et al. The mouse organellar biogenesis mutant buff results from a mutation in Vps33a, a homologue of yeast vps33 and Drosophila carnation. *Proc Natl Acad Sci U S A.* 2003 Feb 4;100(3):1146–1150.
 37. McEwan DG, Richter B, Claudi B, Wigge C, Wild P, Farhan H, et al. PLEKHM1 regulates Salmonella-containing vacuole biogenesis and infection. *Cell Host Microbe.* 2015 Jan 14;17(1):58–71.
 38. Lobingier BT, Merz AJ. Sec1/Munc18 protein Vps33 binds to SNARE domains and the quaternary SNARE complex. *Mol Biol Cell.* 2012 Dec;23(23):4611–4622.
 39. Khatter D, Raina VB, Dwivedi D, Sindhwani A, Bahl S, Sharma M. The small GTPase Arl8b regulates assembly of the mammalian HOPS complex on lysosomes. *J Cell Sci.* 2015 May 1;128(9):1746–1761.
 40. Schindler C, Chen Y, Pu J, Guo X, Bonifacino JS. EARP is a multisubunit tethering complex involved in endocytic recycling. *Nat Cell Biol.* 2015 May;17(5):639–650.
 41. Nordmann M, Cabrera M, Perz A, Bröcker C, Ostrowicz C, Engelbrecht-Vandré S, et al. The Mon1-Ccz1 complex is the GEF of the late endosomal Rab7 homolog Ypt7. *Curr Biol.* 2010 Sep 28;20(18):1654–1659.
 42. Poteryaev D, Datta S, Ackema K, Zerial M, Spang A. Identification of the switch in early-to-late endosome transition. *Cell.* 2010 Apr 30;141(3):497–508.
 43. Kinchen JM, Ravichandran KS. Identification of two evolutionarily conserved genes regulating processing of engulfed apoptotic cells. *Nature.* 2010 Apr 1;464(7289):778–782.
 44. Felici A, Würthner JU, Parks WT, Giam LR, Reiss M, Karpova TS, et al. TLP, a novel modulator of TGF-beta signaling, has opposite effects on Smad2- and Smad3-dependent signaling. *EMBO J.* 2003 Sep 1;22(17):4465–4477.
 45. Messler S, Kropp S, Episkopou V, Felici A, Würthner J, Lemke R, et al. The TGF- β signaling modulators TRAP1/TGFBRAP1 and VPS39/Vam6/TLP are essential for early embryonic development. *Immunobiology.* 2011 Mar;216(3):343–350.
 46. Würthner JU, Frank DB, Felici A, Green HM, Cao Z, Schneider MD, et al. Transforming growth factor-beta receptor-

- associated protein 1 is a Smad4 chaperone. *J Biol Chem.* 2001 Jun 1;276(22):19495–19502.
47. Vennegoor C, Calafat J, Hageman P, van Buitenen F, Janssen H, Kolk A, et al. Biochemical characterization and cellular localization of a formalin-resistant melanoma-associated antigen reacting with monoclonal antibody NK1/C-3. *Int J Cancer.* 1985 Mar 15;35(3):287–295.
 48. Jordens I, Fernandez-Borja M, Marsman M, Dusseljee S, Janssen L, Calafat J, et al. The Rab7 effector protein RILP controls lysosomal transport by inducing the recruitment of dynein-dynactin motors. *Curr Biol.* 2001 Oct 30;11(21):1680–1685.



Chapter 3

A complex of Vps3 and Vps8 controls integrin trafficking from early to recycling endosomes and regulates cell adhesion, spreading, and migration

Caspar TH Jonker^{1, §}, R. Galmes^{1, 2, §}, T. Veenendaal¹, C. ten Brink¹, R.E.N. van der Welle¹, J. de Rooij³, A.A. Peden⁴, P. van der Sluijs¹, C. Margadant⁵, J. Klumperman^{1,*}

* Corresponding author

§ Both authors contributed equally

¹ Department of Cell Biology, Center for Molecular Medicine, University Medical Center Utrecht, the Netherlands.

² Current address: UCL Cancer Institute, University College London, 72 Huntley Street, London, WC1E 6DD, UK.

³ Department of Molecular Cancer Research, Center for Molecular Medicine, University Medical Center Utrecht, Heidelberglaan 100, 3584 CX Utrecht, the Netherlands.

⁴ Department of Biomedical Science, the University of Sheffield, Sheffield, S10 2TN, UK.

⁵ Department of Molecular Cell Biology, Sanquin Research, Amsterdam, the Netherlands.

Submitted

Abstract

Recycling endosomes maintain plasma membrane homeostasis and are important for cell polarity, migration, and cytokinesis. Yet, the molecular machineries that drive endocytic recycling remain largely unclear. Here we define a complex consisting of two CORVET complex subunits, Vps3 and Vps8, regulating vesicular transport from early to recycling endosomes. The Vps3/8 complex localizes to Rab4-positive recycling vesicles in a CORVET-independent manner and interacts with the Vps33B/VIPAS39 complex on Rab11-positive recycling endosomes. The SM protein Vps33B binds to VAMP3, identifying the first SNARE binding partner of the Vps33B/VIPAS39 complex. Depletion of Vps3/8 or Vps33B/VIPAS39 does not affect transferrin recycling, but delays integrin recycling, resulting in defects in cell adhesion, spreading, migration and focal adhesion formation. Since mutations in Vps33B/VIPAS39 cause Arthrogyryposis, Renal dysfunction and Cholestasis (ARC) syndrome, we suggest that the Vps3/8 complex is part of the molecular machinery regulating a specialized recycling pathway that is defective in ARC syndrome.

3

Introduction

The endolysosomal system is important for a variety of cellular processes, such as protein homeostasis, antigen presentation, signal transduction and cell migration. Hence, disruption of endolysosome function underlies a wide range of diseases, from lysosomal storage disorders to cancer and neurodegenerative disorders (1–3). The progression of cargo through the endolysosomal system, from early endosomes (EE) to late endosomes and lysosomes or from EEs to plasma membrane (PM) or recycling endosomes (REs), is tightly controlled by dedicated protein machinery. Membrane fusion is coordinated by the concerted action of Rab GTPases, tethers, Sec1/Munc18-like (SM) proteins and soluble NSF attachment protein receptors (SNAREs) (4,5). Rab GTPases drive the process by recruiting effector machinery proteins to specific membrane domains (6,7). Contact between opposing membranes is then initiated by tethering proteins, followed by SNARE mediated fusion.

EE-EE fusion is initiated by activation of Rab5, which recruits multiple effector proteins including the class C core vacuole/endosome tethering (CORVET) tethering complex (8–11). The multisubunit CORVET complex consists of a core (Vps11, Vps16, Vps18, Vps33A) which is shared with the late endosomal ‘Homotypic fusion and protein sorting’ (HOPS) tethering complex, and the two CORVET specific subunits Vps8 and Vps3 (also named TGFBRAP1 or TRAP1) (9,12). Recycling of endocytosed proteins and membranes from EEs is crucial to maintain PM homeostasis and essential for cell polarity, migration, and cytokinesis. Recycling occurs either directly from EEs to the PM (fast recycling) or indirectly via Rab11-positive REs (slow recycling) (13–15). Both pathways require Rab4, which resides on the EE vacuole as well as on the recycling vesicles that emerge from there (15–17). A complex consisting of Vps33B and VIPAS39, homologous of Vps33A and Vps16 respectively, binds to Rab11 and localizes to REs (18–20). Mutations in Vps33B or VIPAS39 underlie Arthrogyryposis, Renal dysfunction and Cholestasis (ARC) syndrome, a rare autosomal recessive multisystem disorder that at the cellular level affects the transport of apical and junctional proteins in polarized cells (18).

A poorly understood step in endosomal recycling is transport from EEs to REs. Since EEs are the major source of membranes for REs, we here studied a possible role for the CORVET complex in endosomal recycling. To our surprise we found that Vps3 and Vps8 form a CORVET-independent

A complex of Vps3 and Vps8 controls integrin trafficking from early to recycling endosomes and regulates cell adhesion, spreading, and migration.

complex on Rab4-positive recycling vesicles. The Vps3/8 complex interacts with Vps33B/VIPAS39 on REs by which a specialized recycling pathway is attained that we found to be required for integrin recycling and integrin dependent processes. Our data contribute to understanding the molecular basis of ARC syndrome and are of probable interest for integrin-dependent disorders, such as cancer metastasis.

Results

Vps3 and Vps8 localize to Rab4-and Rab11-positive recycling endosomes

The mammalian CORVET complex functions as a tether between EEs and is recruited to membranes via the interaction of Vps8 with Rab5 (8). To determine a possible role of the CORVET complex in endosomal recycling, we analysed the localization of the CORVET-specific subunits Vps3 and Vps8 in ultrastructural detail by expressing GFP-Vps3 and HA-Vps8 in HeLa cells and performing immuno-electron microscopy (IEM). By IEM we confirmed the localization of Vps3 and Vps8 on EEs (fig. 1a, left panel, arrow), but in addition found substantial label on EE-associated tubules and vesicles negative for endocytosed BSA-Au5 (fig. 1a, right panel, arrows). Since BSA-Au5 predominantly follows the degradative pathway to lysosomes, the absence of BSA-Au5 in Vps3 and Vps8-positive vesicles indicates these as recycling vesicles.

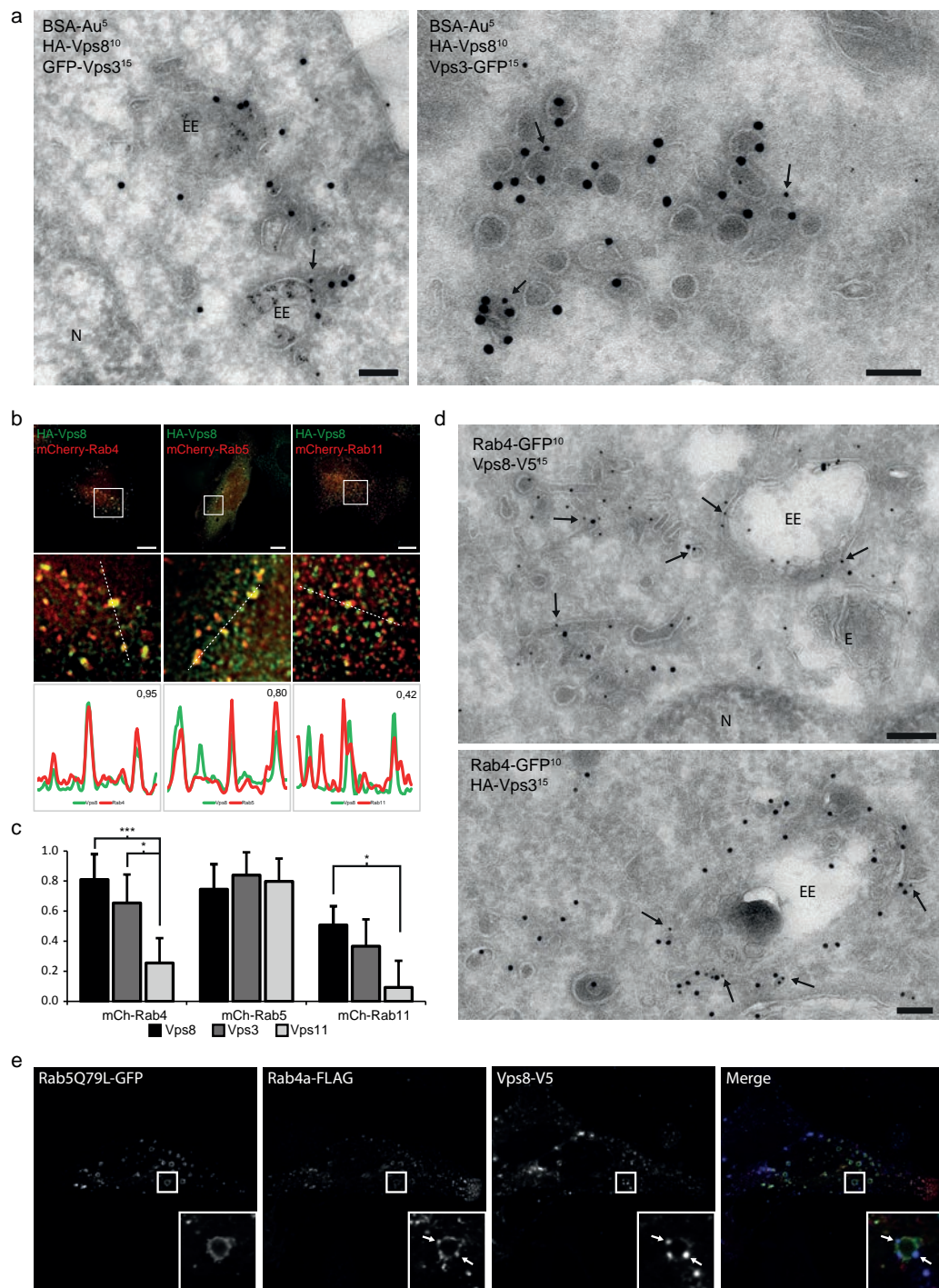
To investigate a putative association of the CORVET complex with recycling vesicles, we expressed GFP-Vps3, HA-Vps8 or GFP-Vps11 together with mCherry-tagged Rab proteins (Rab4, Rab5 or Rab11). Using quantitative immunofluorescence (IF) microscopy we found that Vps3 (fig. 1c, S1a) and Vps8 (fig. 1b, 1c) significantly colocalized with Rab5 and Rab4, which label EEs and EE-derived recycling vesicles, respectively (17,21). In addition, we found a partial colocalization with the RE marker Rab11 (fig. 1b, 1c, S1a). By contrast, the CORVET/HOPS core subunit GFP-Vps11 only overlapped with Rab5 (fig. 1c, S1b). Expression of Rab5Q79L increases the size of EEs (22), which facilitates the distinction of Rab5 and Rab4 subdomains by IF microscopy (21). Strikingly, we found that on Rab5Q79L-positive endosomes HA-Vps8 concentrated in FLAG-Rab4 containing patches (fig. 1e, arrows) and protrusions (fig. S1c, arrows). To unequivocally define whether Vps3 and Vps8 reside on the same vesicles as Rab4 we performed IEM of HeLa cells expressing HA-Vps8 or HA-Vps3 with GFP-Rab4. This revealed that Vps3 and Vps8 indeed localized on Rab4-positive tubules and vesicles (fig. 1a, 1d, arrows). Together these data show that Vps3 and Vps8 localize to EE-derived Rab4-positive recycling vesicles.

We conclude from these data that mammalian Vps3 and Vps8 localize to EEs as part of the CORVET complex and in addition to Rab4-positive recycling vesicles and partially to Rab11-positive REs independent of the CORVET core.

A Vps3/8 complex interacts with the Vps33B/VIPAS39 complex on REs

Previous studies showed that Vps3 and Vps8 interact with the core complex to form the CORVET complex. In addition, direct interactions between Vps3 and Vps8 were reported in yeast (23). In HeLa cells we revealed by co-immunoprecipitation (co-IP) a strong interaction between Vps8 and Vps3 (fig. 2a) and a mild interaction of Vps8 with Vps11 and Vps16. The strong interaction between Vps3 and Vps8 is indicative for a direct interaction between these two subunits.

The previously described Vps33B/VIPAS39 complex localizes to REs and interacts with Rab11 (8,9,18,19,24,25). Since Vps3 and Vps8 partially colocalized with Rab11 (fig. 1b, 1c) we studied



A complex of Vps3 and Vps8 controls integrin trafficking from early to recycling endosomes and regulates cell adhesion, spreading, and migration.

Figure 1. (a) IEM of HeLa cells expressing HA-Vps8 and GFP-Vps3 loaded with BSA-Au5. HA-Vps8 (10nm gold, arrows) and GFP-Vps3 (15nm gold) colocalize on EEs (left panel) and on vesicles negative for BSA-Au5 (right panel). EE=early endosome, N=Nucleus, Bar, 100nm. **(b)** HeLa cells expressing HA-Vps8 together with mCherry-Rab4, mCherry-Rab5 or mCherry-Rab11. HA-Vps8 colocalizes strongly with Rab4 and Rab5 and less with Rab11. **(c)** Quantification of triplicate experiments shown in (b) based on n>30 cells per condition. Error bars represent the standard error of the correlation coefficient (SEr). **(d)** IEM of HeLa cells expressing Rab4-GFP together with Vps8-V5 or HA-Vps3, showing colocalization of Rab4-GFP (10nm gold, arrows) with Vps8-V5 (15nm gold, top panel) and HA-Vps3 (15nm gold, bottom panel) on recycling tubules and vesicles. E=endosome EE=early endosome N=Nucleus. Bar, 200nm. **(e)** Immunofluorescence of HeLa cells expressing Rab5Q79L-GFP, Rab4-FLAG and Vps8-V5. Vps8 localizes to Rab4 positive patches on Rab5Q79L positive enlarged endosomes (arrows).

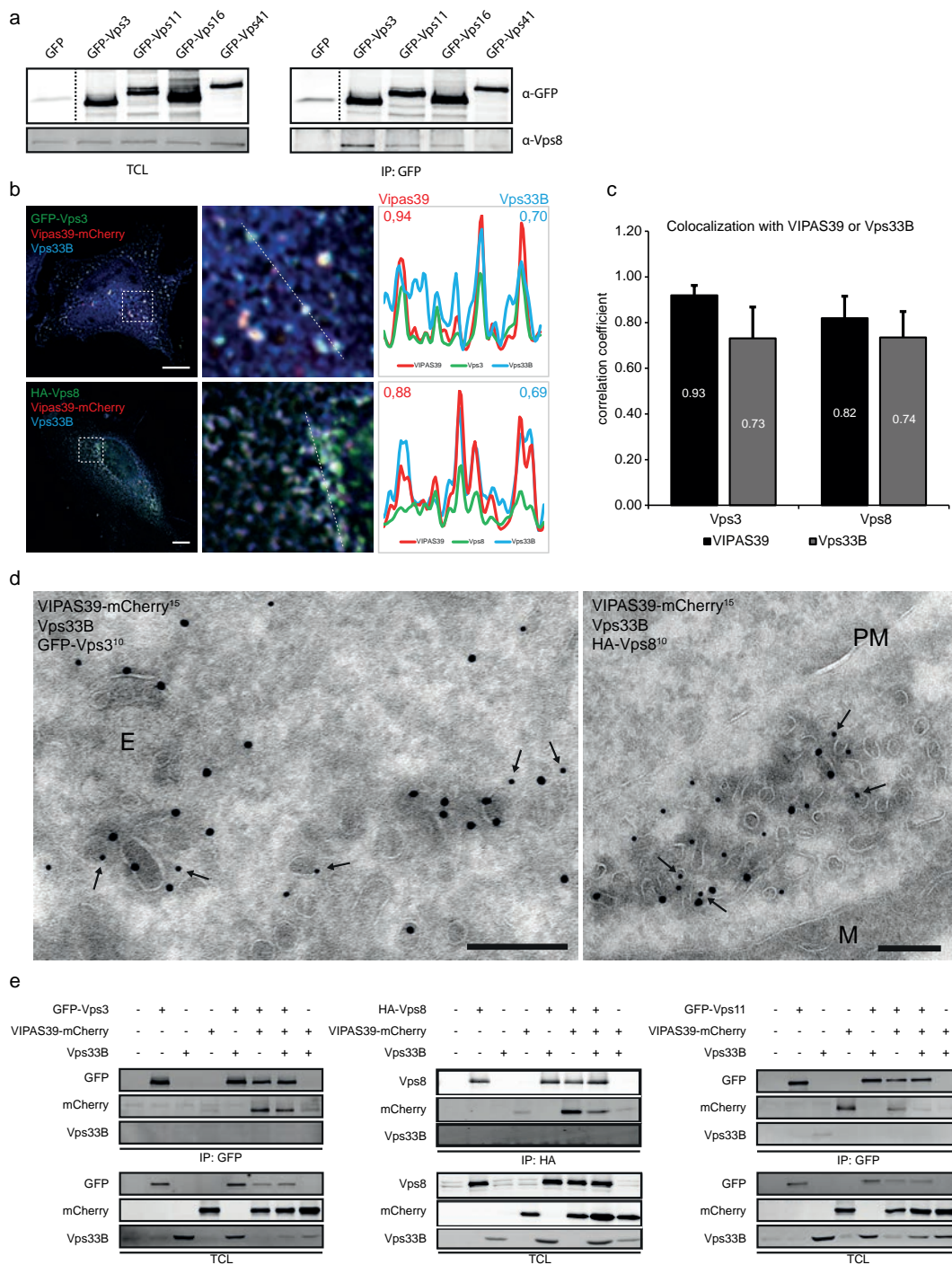
the localisation patterns of Vps8, Vps3 and Vps33B/VIPAS39 by quantitative IF microscopy. Co-expression of VIPAS39-mCherry and Vps33B with HA-Vps8 or GFP-Vps3 resulted in extensive co-localization of Vps3 or Vps8 with the Vps33B/VIPAS39 complex (fig. 2b, 2c). By IEM, these punctae of co-localization were, based on their morphology, unequivocally identified as recycling tubules and vesicles (fig. 2d).

To reveal a possible interaction between the Vps33B/VIPAS39 complex and Vps3 or Vps8 we performed co-IP experiments using HA-Vps8, GFP-Vps3, untagged Vps33B and VIPAS39-mCherry. VIPAS39 expression without co-expression of Vps33B causes cytoplasmic aggregates resulting in aspecific interactions of VIPAS39 with several HOPS and CORVET subunits (19). Hence, we only studied interactions with overexpressed VIPAS39 in the presence of overexpressed Vps33B, which leads to membrane recruitment of the Vps33B/VIPAS39 complex (18,19). This showed that both GFP-Vps3 and HA-Vps8 interacted with VIPAS39-mCherry, but not with Vps33B (fig. 2e). We performed similar experiments with GFP-Vps11, which did not interact with VIPAS39 or Vps33B (fig. 2e). Previous studies using endogenous proteins failed to detect specific interactions between Vps33B or VIPAS39 with any of the HOPS or CORVET subunits, including Vps3 and Vps8 (8,9). This suggests that the interaction between the Vps3/Vps8 and Vps33B/VIPAS39 complex is transient and remains below detection level in an endogenous system.

Taken together these data show that Vps3 and Vps8 interact with each other and that the Vps3/8 complex can interact with VIPAS39 in the presence of Vps33B. Since the core subunit Vps11 does not interact with VIPAS39 or Vps33B we conclude that the Vps3/Vps8 - Vps33B/VIPAS39 interactions occur independently from the CORVET core. Moreover, since Vps3 and Vps8 colocalize with the Vps33B/VIPAS39 complex we postulate that interaction between these complexes take place at REs.

Association of Vps33B with VAMP3 requires VIPAS39

Vps33B belongs to the family of SM proteins, which bind specific SNAREs and promote trans-SNARE complex formation(26,27), however, the Vps33B-interacting SNARE proteins are not yet identified. On occasion, SM protein-SNARE interactions can prevent premature degradation of SNAREs (28–30). To identify SNARE binding partners of Vps33B we analysed protein levels of several post-Golgi SNAREs after knockdown of Vps33B. This revealed a decrease of the RE-associated SNARE VAMP3 (fig. 3a), while the trans-Golgi network (TGN) SNARE syntaxin6 and the late endosomal-lysosomal SNAREs VAMP7, syntaxin7 and syntaxin8 were unaffected. Analysis of VAMP3 protein levels showed that the downregulation of VAMP3 is not caused by increased lysosomal or proteasomal degradation, but correlated with downregulation of VAMP3 mRNA



3

Figure 2. (a) Immunoprecipitates of GFP-tagged Vps3, Vps11, Vps16 or Vps41 probed for interaction with endogenous Vps8. **(b)** Immunofluorescence of HeLa cells expressing VIPAS39-mCherry, untagged Vps33B and either GFP-Vps3 or HA-Vps8. Vps3 and Vps8 colocalize with both VIPAS39 and Vps33B (line profiles in right panel indicate colocalization correlation, correlation coefficients indicated: VIPAS39=red, Vps33B=blue). **(c)** Quantification of triplicate experiments shown in (b) based on $n \geq 30$ cells per condition by line profile correlations. The mean is calculated using Fishers' r to z transformation. Error bars represent SEr. **(d)** IEM analysis of HeLa cells expressing VIPAS39-mCherry (15nm gold), untagged Vps33B (not labelled) and either GFP-Vps3 (10nm gold, arrows) or HA-Vps8 (10nm gold, arrows). Vps3 and Vps8 colocalize with VIPAS39 on recycling vesicles and tubules. E=endosome, M=mitochondria, Bar, 200nm. **(e)** Immunoprecipitates of HA-Vps8, GFP-Vps3 or GFP-Vps11 probed for interaction with co-expressed VIPAS39-mCherry and Vps33B-HA/V5/his in HeLa cells. Vps8 and Vps3 show interaction with VIPAS39 in the presence of co-expressed Vps33B while Vps11 does not.

levels in Vps33B knockdown cells (fig. S2a, S2b). This suggests that VAMP3 is co-regulated with Vps33B at the transcriptional level, which is indicative for a molecular interaction between Vps33B and VAMP3 (31,32).

To demonstrate a possible molecular interaction between VAMP3 and Vps33B we performed co-IPs between VAMP3-GFP, VIPAS39-mCherry and Vps33B-HA-V5-His (fig. 3b). This revealed that VAMP3-GFP and Vps33B-HA-V5-His interact, but only in the presence of VIPAS39. No interaction was detected between VAMP3-GFP and VIPAS39-mCherry. To assess the specificity of the VAMP3-Vps33B interaction, we performed a GST-pulldown using GST-VAMP3 as bait and GST-VAMP7 as a control. We found that Vps33B-HA-V5-His interacts with GST-VAMP3, but not with GST-VAMP7 (fig. 3c, TCL in fig. S2c.). These results show that Vps33B interacts with VAMP3, but only in the presence of VIPAS39. In agreement with our protein interaction data, co-expression of Vps33B-HA/V5/His, VIPAS39-mCherry and VAMP3-GFP resulted in the colocalization of all three proteins (fig. 3d, upper panels), which was lost in the absence of VIPAS39-mCherry (fig. 3d, lower panels). Ultrastructural localization of Vps33B-HA/V5/His or VIPAS39-mCherry with VAMP3-GFP in HeLa cells clearly showed their co-localization on tubulo-vesicular membranes typical for REs (33) (fig. 3e).

These data identify VAMP3 as the first binding SNARE of Vps33B on REs. Since Vps3 and Vps8 interact with VIPAS39, the binding partner of Vps33B (18,20,34) (fig. 3f), collectively our data indicate that Rab4-Vps3/8-vesicles dock on REs by interaction between the Vps3/8 and Vps33B/VIPAS39 complexes, ultimately resulting in fusion in a Vps33B-VAMP3-dependent manner.

Vps3/8 and Vps33B/VIPAS39 complexes mediate $\alpha 5\beta 1$ integrin recycling

To define the role of Vps3/8 and Vps33B/VIPAS39 in recycling we depleted these proteins from HeLa cells and studied the effect on transferrin (Tf) recycling. Endocytosed Tf recycles either directly from EEs to the PM or indirectly from EEs via REs to the PM (35). HeLa cells knocked down for Vps33B, Vps3, Vps8 or a double knockdown of Vps3+8 were incubated with fluorescent Tf and dextran for two hours. A block in Tf recycling would increase the colocalization between Tf and dextran (36,37), however, none of the knockdowns induced this effect (fig. 4a). These results are in agreement with earlier observations showing that Vps3 is not essential for Tf recycling (8) and show that Vps8 and Vps33B/VIPAS39 are not required either.

VAMP3 is required for the recycling of several substrates including $\beta 1$ integrins (38,39). To study the role of Vps3/8 and Vps33B/VIPAS39 in recycling of $\beta 1$ integrins we used an established antibody-based integrin recycling assay (40). HeLa cells were knocked down for Vps33B

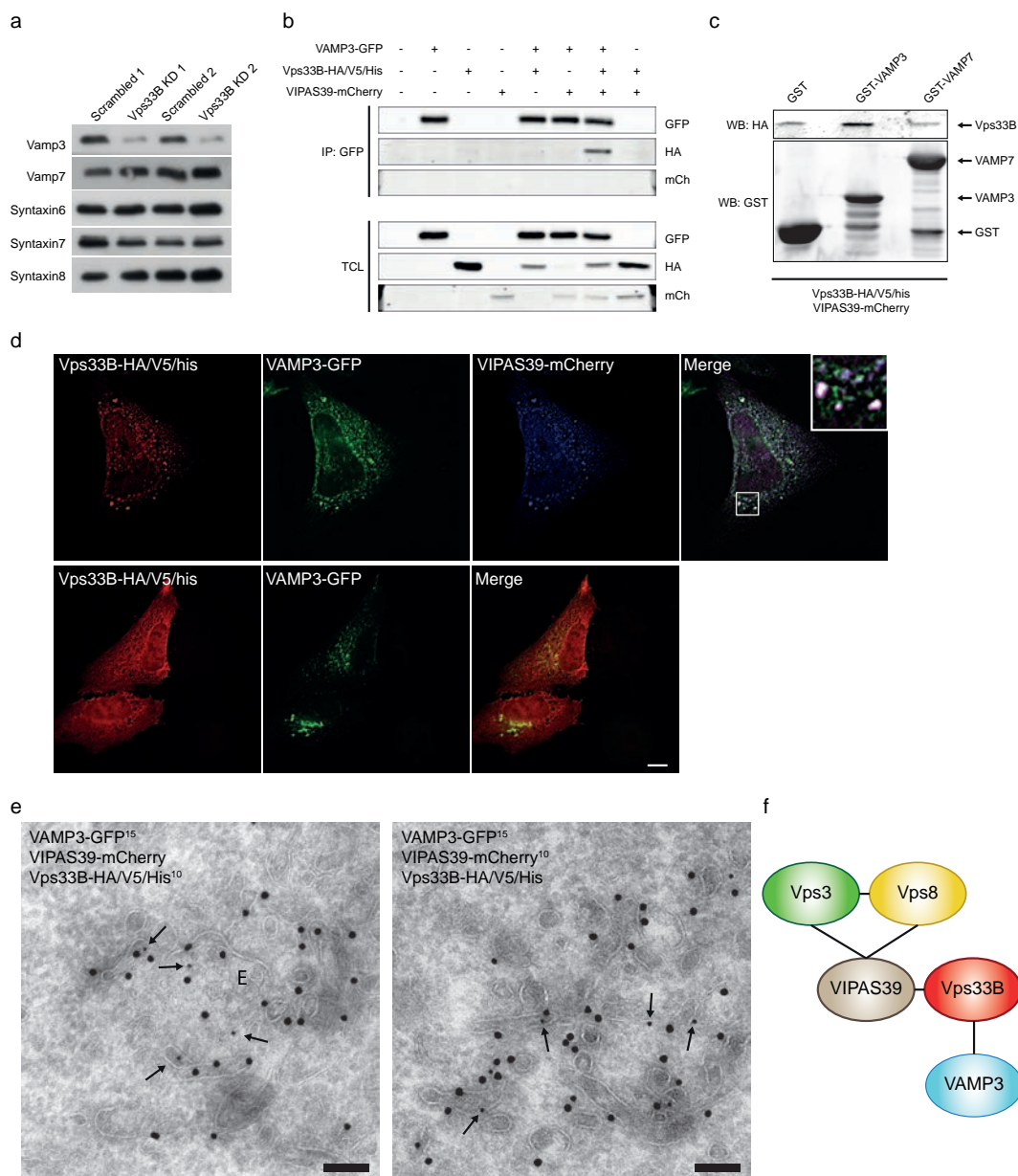


Figure 3. (a) HeLa cells knocked down for Vps33B using 2 different sets of siRNA were screened for selected SNARE protein levels by Western blotting. VAMP3 levels decrease dramatically while other SNARE proteins levels remained unaltered. (b) Immunoprecipitates of VAMP3-GFP probed for interaction with Vps33B-HA/V5/His or VIPAS39-mCherry. VAMP3 binds Vps33B only in the presence of VIPAS39. (c) GST-VAMP3 and GST-VAMP7 incubated with cell lysates of HeLa cells expressing Vps33B-HA/V5/His and VIPAS39-mCherry. Pull-down of GST shows binding of Vps33B to GST-VAMP3 but not GST-VAMP7. For complete blot including total cell lysates see fig. S2. (d) Immunofluorescence of HeLa cells expressing Vps33B-HA/V5/His, VAMP3-GFP and VIPAS39-mCherry (top panels) or expressing Vps33B-HA/V5/His and VAMP3-GFP (bottom panels). Vps33B is cytosolic without co-expression of VIPAS39. Co-expression of VIPAS39 induces colocalization of all three proteins. (e) IEM of HeLa cells expressing VAMP3-GFP (15nm gold), Vps33B-HA/V5/His and VIPAS39-mCherry (10nm gold, arrows). VAMP3 colocalizes with Vps33B (left panel) and with VIPAS39 (right panel) on recycling tubules. E=endosome, bars are 100nm. (f) Schematic overview of interactions between Vps3, Vps8, VIPAS39, Vps33B and VAMP3.

to inhibit formation of the Vps33B/VIPAS39 complex, or for Vps3+Vps8, to inhibit Vps3/8 complex formation. Cells were serum-starved overnight, labelled with anti- β 1-integrin, washed and chased for two hours. In the absence of serum, β 1 integrins accumulate in REs (fig. 4b, arrows). Interference with the Vps3/8 or Vps33B/VIPAS39 complex formation prevented this accumulation of β 1 integrins, which instead retained a dispersed distribution throughout the cell (fig. 4b). Using an adopted IEM protocol to visualize the antibody uptake as described above, we could identify the accumulations in control cells as clusters of recycling tubules and vesicles (fig. 4c, left panel). In the 3+8 knockdown cells β 1 integrins retained their localization to EEs and EE-associated vesicles (fig. 4c, right panel). Re-addition of serum induced integrin recycling in control cells resulting in the disappearance of intracellular accumulations while the localization of β 1 integrins in knockdown cells remained unchanged (fig. 4d, S3). Together these results imply that Vps3+8 or Vps33B knockdown prevents or delays β 1 integrins to reach the RE and prevents clearance of the intracellular pool of β 1 integrins.

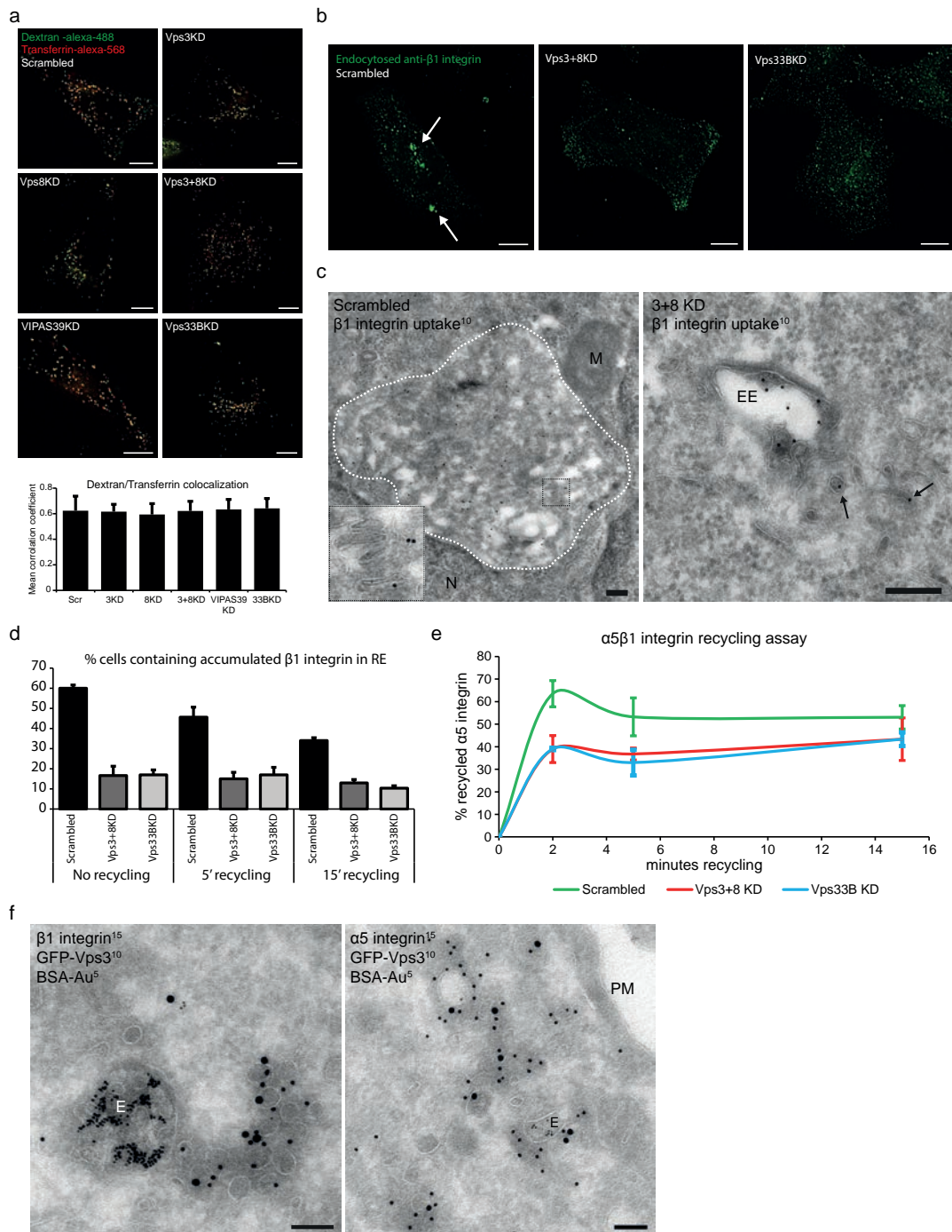
We next investigated the impact of Vps3+8 or Vps33B knockdown on the kinetics of integrin recycling by studying the fibronectin-binding integrin α 5 β 1 using surface biotinylation and capture-ELISA (41). In short, cells were surface-labelled with cleavable biotin and endocytosis was allowed for 30min in the absence of serum. Surface biotin was removed and recycling was induced by re-addition of serum. Surface biotin was removed again and the reduction of intracellular biotinylated α 5 integrin before and after recycling was quantified using capture-ELISA. This assay showed that knockdown of Vps33B or Vps3/8 resulted in a significant decrease of α 5 β 1 recycling, especially after short recycling times (fig. 4e). Finally, to verify that α 5 β 1 is indeed transported by Vps3/Vps8-positive recycling vesicles, we labelled the α 5 and β 1 subunits by IEM. Both subunits localized to Vps3/Vps8 positive recycling vesicles (fig. 4f), which is in agreement with the proposed role of Vps3/8 in α 5 β 1 integrin recycling.

Taken together, these data show that β 1 integrins are incorporated into Vps3/Vps8-positive recycling vesicles and that Vps3/Vps8 together with Vps33B/VIPAS39 are required for efficient β 1 integrin recycling.

Perturbation of the Vps3/8 or Vps33B/VIPAS39 complex impairs integrin-dependent cell adhesion, spreading, focal adhesion formation and cell migration

Integrins are the primary receptors for extracellular matrix (ECM) proteins (42) and integrin recycling is an important mechanism to regulate cell adhesion and migration (43–45). To investigate whether the Vps3/Vps8 or Vps33B/VIPAS39 complexes are required for the regulation of integrin-dependent cell adhesion, we seeded HeLa cells knocked down for Vps33B or Vps3+8 on fibronectin (FN) or collagen-1 (Col-1) in the absence of serum. Non-adherent cells were washed away after 5, 15 or 30 minutes and the number of attached cells was quantified. This revealed that adhesion to both FN (fig. 5a) and Col-1 (fig. 5b) was significantly compromised in Vps33B or Vps3+8 knockdown cells. In parallel experiments we determined cell spreading on FN and Col-1 two hours after initial adhesion (fig. 5c). Quantification of the number of spread cells showed that in knockdown cells spreading was reduced on both FN and Col-1 (fig. 5d).

Integrin-mediated cell spreading is associated with the assembly of focal adhesions (FAs), that anchor the actin cytoskeleton to the ECM (46). To determine if Vps33B or Vps3+8 knockdown impacts FA formation, we quantified the number of FAs per cell from confocal images (fig. 5e). Consistent with reduced cell adhesion and spreading, Vps33B or Vps3+8 knockdown cells



3

A complex of Vps3 and Vps8 controls integrin trafficking from early to recycling endosomes and regulates cell adhesion, spreading, and migration.

Figure 4. (a) HeLa cells knocked down for Vps3, Vps8, VIPAS39, Vps33B or Vps3 and 8 combined were incubated with green fluorescent dextran and red fluorescent Tf for 2hrs. Quantifications of colocalization over 3 separate experiments with $n > 40$ cells showed no block of Tf recycling. Error bars represent standard deviation of the mean (SD). (b) Integrin recycling assay as described 24. HeLa cells knocked down for Vps3+8 or Vps33B were serum-starved overnight and subsequently incubated with anti- $\beta 1$ -integrin. After 2 hours uptake at 37°C, and labelling with fluorescent secondary antibodies, $\beta 1$ -integrins accumulate in REs (arrows). In knockdown cells no accumulation of integrin is found indicating that trafficking to the RE is blocked. (c) IEM of cells subjected to the integrin uptake assay as in (b) and immunogold labeled for endocytosed anti- $\beta 1$ -integrin (10 nm gold). Accumulations of endocytosed $\beta 1$ integrin are by IEM identified as a cluster of tubular membranes (left panel, cluster accented by white dashed line, inset shows magnification of membrane tubules). In knockdown cells, internalised $\beta 1$ integrin was found in EEs and associated vesicles (right panel, arrows). EE=early endosome, N=nucleus, M=mitochondria, bar, 200nm. (d) Quantification of (fig. S3) indicating the percentage of cells with accumulation of $\beta 1$ integrins in the RE. $n=300$ Cells per time point from 3 separate experiments. Error bars represent SD. (e) ELISA based recycling assay of surface biotinylated $\alpha 5$ integrin as described 24. HeLa cells knocked down for Vps3+8 or Vps33B show a decrease in recycling of $\alpha 5 \beta 1$ integrin compared to the control. Error bars represent SD. (f) IEM of HeLa cells loaded with BSA-Au5 expressing GFP-Vps3. GFP-Vps3 (10nm gold) colocalizes with endogenous $\beta 1$ integrin (15nm gold, left panel) and endogenous $\alpha 5$ -integrin (15nm gold, right panel). G=Golgi, PM=plasma membrane, M=mitochondria, bar is 100nm.

assembled less FAs, both on FN and Col-1 (fig. 5f). We next analysed cell motility by time-lapse microscopy (fig. 5g, arrows indicate migration direction). Knockdown of Vps33B or Vps3+8 resulted in reduced migration speed (fig. 5h) and migration distance (fig. 5i) on both Col-1 and FN. Moreover, analysis of cell morphology revealed that the knockdowns induced a tail retraction defect (fig. 5g, 5j), which is a known effect of impaired integrin trafficking (47).

Together these results show that interfering with the Vps3/8/33B/VIPAS39-dependent pathway leads to a variety of defects in integrin-dependent processes. This positions the Vps3/8/33B/VIPAS39 machinery as an important regulator for integrin turnover.

Discussion

Our study shows that Vps3 and 8 as well as Vps33B and VIPAS39 are required for integrin recycling. Previous studies on mammalian Vps3 and Vps8 revealed their importance in EE-EE fusion as part of the CORVET complex. We now show that Vps3 and Vps8 in addition to EEs also localize to Rab4-positive, EE-associated recycling vesicles and tubules that lack Vps11, a marker for the CORVET/HOPS core. By co-IP we find strong interactions between Vps3 and Vps8, suggesting they can form a complex without requiring additional core subunits. In addition we show that Vps3 and Vps8 can interact with the Vps33B/VIPAS39 complex. We therefore propose that Vps3 and Vps8 are recruited to EEs together with CORVET core components, after which they form a separate complex on Rab4-positive recycling vesicles. The Rab4/Vps3/8 vesicles set out to fuse with Rab11-positive REs, possibly via the interaction of Vps3/8 with the Vps33B/VIPAS39 complex (fig. 6). This model connects the Vps3/8 complex to the role of Vps33B and VIPAS39 in recycling, and implicates Vps3 and Vps8 as additional ARC syndrome targets, a model that is reinforced by the recent discovery of Vps8 mutations in patients suffering from arthrogryposis (48). Additionally, we show that the Vps33B/VIPAS39 complex interacts with the recycling endosomal SNARE VAMP3 via Vps33B, implicating VAMP3 as putative SNARE for the Vps3/8 to Vps33B/VIPAS39 recycling pathway. Finally, we show that the Vps3/Vps8 and Vps33B/VIPAS39 complexes are required for efficient recycling of $\beta 1$ integrins and that perturbation of these complexes impairs integrin-dependent cell adhesion, spreading, migration and FA assembly. By IEM we showed that Vps3 and Vps8 localize to Rab4-positive recycling vesicles. Rab4 has been

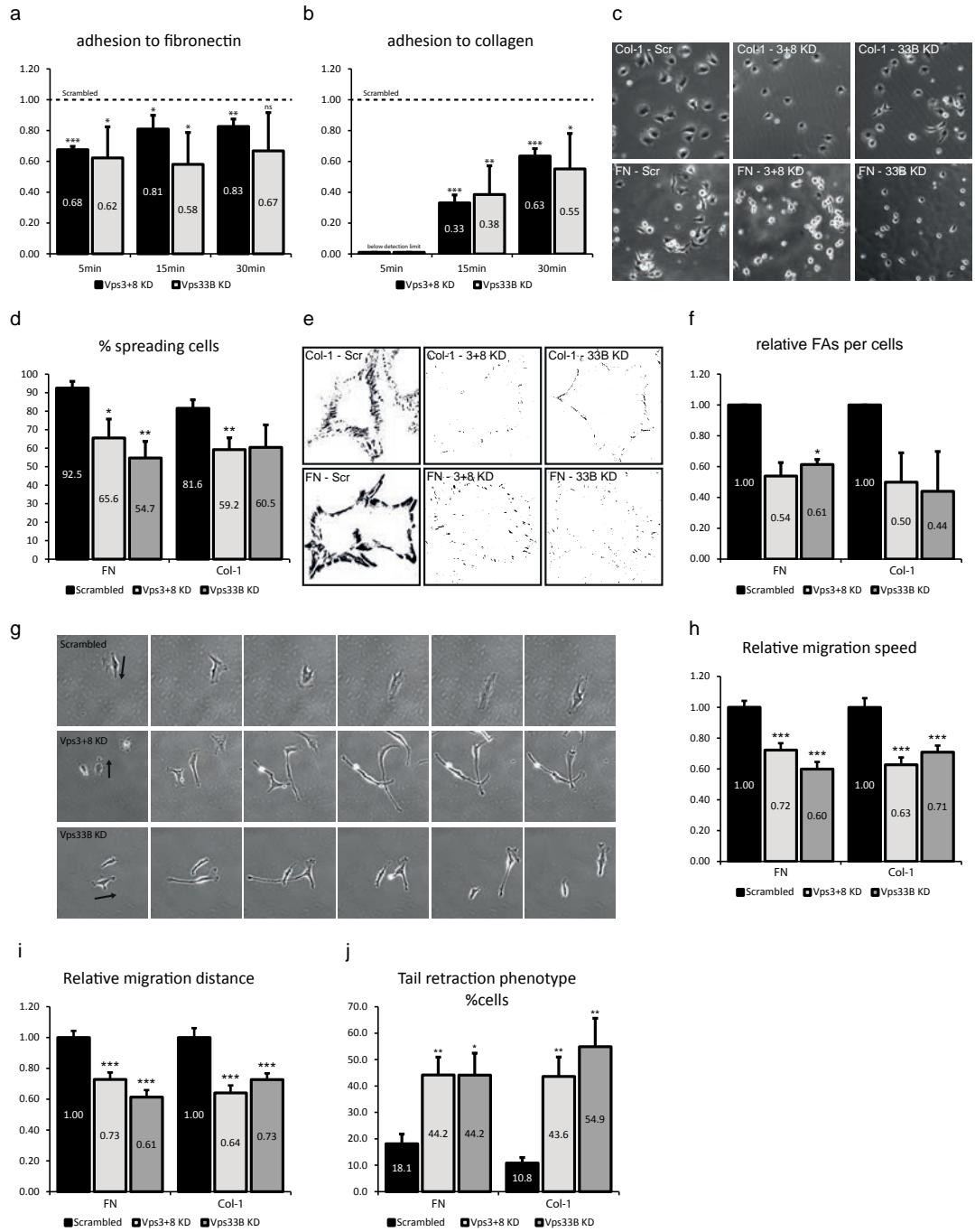


Figure 5. Cell adhesion assay. The number of adhered cells was assessed by PrestoBlue staining. Cells knocked down for Vps3+8 or Vps33B show a decreased capability to attach to collagen **(a)** or fibronectin **(b)**. Error bars indicate SD. **(c)** HeLa cells knocked down for Vps3+8 or Vps33B show decreased spreading compared to the control cells 2hrs after seeding on collagen- or fibronectin-coated surfaces. **(d)** Quantification of **(c)**. Error bars represent the SD. **(e)** Background-subtracted and thresholded confocal images of HeLa cells knocked down for Vps3+8 or Vps33B and stained with vinculin. Knockdown cells show a reduction in the number of FAs per cell both on collagen and fibronectin. **(f)** Quantification of **(e)**. **(g)** Time-lapse microscopy of HeLa cells knocked down for Vps3+8 or Vps33B (fibronectin condition, arrows indicate direction of migration) show defects in mean migration speed **(h)** and mean migration distance **(i)** on both collagen and fibronectin. Error bars represent the standard error of the mean (SEM). **(j)** The percentage of cells showing an elongated tail during cell migration increases significantly in knockdown cells on both collagen and fibronectin. Error bars represent SD.

implicated in both short-loop recycling from EEs to the PM, as well as in long-loop recycling from EEs to Rab11-positive REs (13,15–17,21,49,50). Since Vps3+8 knockdown prevents transport of $\beta 1$ integrins to REs (fig. 4b, 4d), we conclude that the Vps3/Vps8 complex is involved in transport from EEs to REs (fig. 6). Our model proposes a direct interaction of Vps3 and Vps8, as is demonstrated in fig. 2a. This direct interaction was found before (23), but seemed counterintuitive since in the current model of the CORVET complex Vps3 and Vps8 are located at opposite ends (51). The formation of a Vps3/Vps8 complex on recycling vesicles independent of the CORVET complex provides a functional and structural explanation for these findings. Interestingly, Vps39 and Vps41, the counterparts of Vps3 and Vps8 residing on the opposite ends of the HOPS complex, can also directly interact (23). It was hypothesized that this interaction takes place following late endosome- lysosome fusion after which the HOPS complex could obtain a closed post-fusion conformation (51,52). In analogy herewith, a closed post EE-EE fusion conformation of the CORVET complex could precede the direct interaction of Vps3 and Vps8 (fig. 6).

Endosomal tethering complexes interact with SNARE proteins to facilitate membrane fusion events. We found that Vps33B interacts with the SNARE VAMP3, an R-SNARE located on the TGN, EEs and REs (25,53–55). Previous studies have shown that endocytosed integrins recycle through VAMP3-positive REs(38)43 and that VAMP3 knockdown results in inhibition of cell migration and reduced $\beta 1$ -integrin levels at the PM (39). VAMP3 forms a transSNARE complex with syntaxin6 and knockdown of syntaxin6 leads to accumulation of integrins in VAMP3-positive REs (38). We show that Vps33B knockdown reduces the expression of VAMP3 but not of syntaxin6 and in contrast to the syntaxin6 knockdown phenotype results in a block in transport towards REs (Fig. 4), implicating a role for VAMP3 in the fusion of recycling vesicles with REs.

As crucial mechanisms to control integrin action at the PM, endocytosis and recycling of integrins are topic of intense research (45,56–58). Integrins use multiple recycling pathways depending on heterodimer composition, conformation (active or inactive) and ligand binding. A key question is how sorting to these different pathways is achieved. Interestingly, we found that disruption of the Vps3/Vps8 or Vps33B/VIPAS39 complexes had no effect on Tf recycling (fig. 4a), which like $\beta 1$ integrin also depends on Rab4 and Rab11 (13,36,40,44,59). However, recycling of $\beta 1$ integrins specifically depends on a NPXY motif that in EEs binds SNX17 and SNX31 to sort integrins into recycling vesicles and prevents lysosomal degradation (60–62). This suggests that within the Rab4/Rab11 pathway multiple subpathways might exist. Consistent with the previously postulated concept of EE-associated tubular sorting endosomes or networks, machinery proteins involved in cargo sorting might define subdomains on REs (33,63,64). As SM protein and VAMP3-interactor Vps33B is a putative candidate to define RE tubules specialized for integrin recycling,

even more since Vps33B interacts directly with integrin β -subunits (65). Since $\alpha 5\beta 1$ integrin recycling promotes invasive migration of cells (43,66–68), our data indicate a putative role for Vps3/8 and Vps33B/VIPAS39 dependent regulation of integrin recycling in cancer metastasis. Finally, our data contribute to the emerging view that multisubunit tethering complexes are dynamic in composition in order to facilitate multiple transport pathways (11,69). The increasing number of disease-causing mutations found in individual subunits illustrates the importance to understand the role of each subunit at a fundamental cellular level. Moreover, it will be of great interest to define additional cargo for the here portrayed specialized recycling pathway.

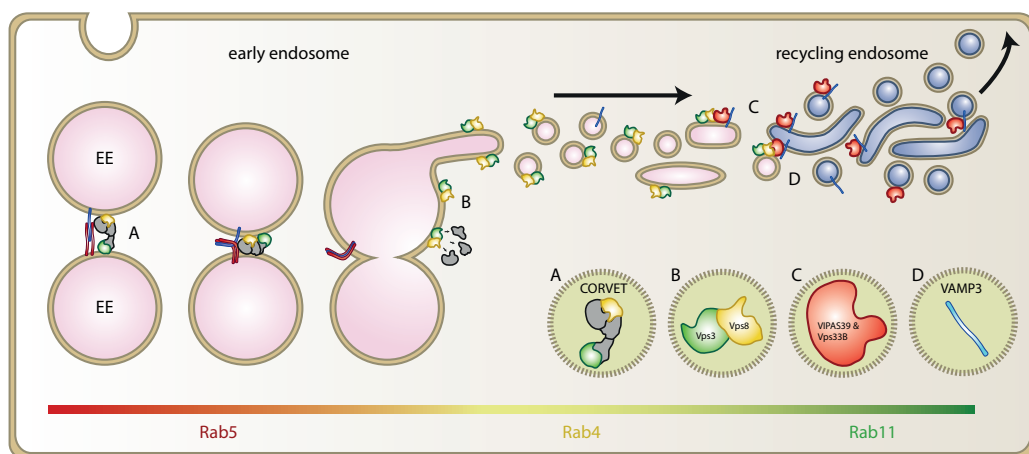


Figure 6. Model of the proposed function of the Vps3/8 and VIPAS39/Vps33B complex in endosomal recycling. The CORVET complex mediates the fusion between Rab5 positive EEs (A), after which it can adopt a closed conformation, allowing Vps3 and Vps8 to interact with each other. The resulting Vps3/Vps8 complex localizes to Rab4-positive vesicles emerging from EEs (B). The Vps3/8 complex on recycling vesicles interacts with the VIPAS39/Vps33B complex on Rab11-positive REs (C). The R-SNARE VAMP3 interacts with Vps33B and assists in the fusion of EE-derived vesicles with REs (D).

Materials and Methods

Cell culture and transfection

HeLa cells (ATCC clone ccl-2) were grown at 37°C and 5% CO₂ in Dulbecco's modified Eagle's medium (DMEM) supplemented with 10% heat inactivated Foetal Bovine Serum (FBS), 2mM L-Glutamin, 100U/mL penicillin and 100µg/mL streptomycin. Cells were transfected with cDNA using Effectene transfection reagent (Qiagen) according to the manufacturer's protocol. siRNA transfection was performed using HiPerfect transfection Reagent (Qiagen) according to manufacturer's protocol.

Antibodies

For immunofluorescence and IEM labelling: Mouse anti-HA (Covance), Mouse anti-β1-integrin (JB1A, Millipore), Mouse-anti-α5-integrin (VC5, BD biosciences), Goat anti-HA (Genscript), Rabbit anti-GFP (Acris), Rabbit-anti-mCherry was made on site as described (70), anti-Vps33B was generated by immunizing rabbits with a synthetic Vps33B peptide conjugated to KLH (sequence: ESKVSKLVTDKAAGKIT). Rabbit anti-goat IgG (NORDIC) or rabbit anti-mouse IgG (Z0412, Dako) was used to bridge between goat or mouse antibodies and protein-A gold (71). Fluorescent secondary antibodies were obtained from Invitrogen. For immunoprecipitation and Western blotting we used Mouse anti-GFP (Roche), Mouse anti-HA (Covance), Rabbit anti-mCherry, Rabbit anti-Vps33B and Rabbit anti-GFP (Abcam). Rabbit anti STX6, STX7, STX8, VAMP3 and VAMP7 were described (72). Fluorescent secondary antibodies were obtained from Li-Cor.

Reagents

5nm gold particles coupled to bovine serum albumin (BSA-Au5) and 10nm or 15nm gold particles conjugated to Protein A were made on site (Cell Microscopy Core, UMC Utrecht, The Netherlands). HA-Vps8, Vps8-V5 and Vps8-GFP, GFP-Rab4, mCherry-Rab4, FLAG-Rab4, mCherry-Rab5, mCherry-Rab7, mCherry-Rab11 and untagged Vps33B were cloned from cDNA purchased from Origen. HA-TGFBRAP1, GFP-TGFBRAP1, GFP-Vps11 and Vps41-GFP were a generous gift from Dr. J. Neefjes (NKI, Amsterdam, The Netherlands), VIPAS39-mCherry was a generous gift from Dr. P. Gissen (LMCB, UCL, London), Vps33B-HA-V5-His was a generous gift from Dr. V. Faundez (Cell Biology, Emory University, Atlanta, GA, USA), VAMP3-GFP, GST-VAMP3, GST-VAMP7 were generated by Andrew Peden (University of Sheffield, Sheffield, UK). Vps8, TGFBRAP1, Vps33B, VIPAS39, Vps11 and Vps41 SMARTPool siRNAs were purchased from Dharmacon. Fibronectin, Type-I collagen, bafilomycin A1 and poly-L-lysine were purchased from Sigma. MG132 was purchased from Enzo life sciences. EZ link Sulfo-NHS-SS-biotin was from Thermo Fisher. Complete protease inhibitors were purchased from Roche.

GST-Pulldown

GST-VAMP proteins were produced in Escherichia coli BL21 (DE3) grown at 30°C and immobilized on glutathione beads. HeLa cells expressing Vps33B-HA/V5/his were lysed for 30 to 60min at 4°C in 20mM HEPES pH 7.4, 100mM NaCl, 5mM MgCl₂, 1% TX-100 supplemented with leupeptin, aprotinin and PMSF. Lysates were centrifuged for 20min at 13000rpm at 4°C and supernatants were incubated for 2h at 4°C with GST-VAMP beads. Beads were washed with lysis buffer minus

protease inhibitors after which proteins were eluted using 1x sample buffer for 5min at 95°C. Eluted proteins were separated using SDS-PAGE and analysed using Western blotting.

Co-immuno-precipitation

Cells were washed in ice-cold PBS and scraped in lysis buffer (40mM TRIS pH7.4, 100mM NaCl, 0.1% TX-100, 5mM EDTA supplemented with complete protease inhibitors (Roche)). For VAMP3 immuno-precipitation, lysis buffer contained 20mM HEPES pH 7.4, 100mM NaCl, 5mM MgCl₂, 1% TX-100 supplemented with leupeptin, aprotinin and PMSF. Cells were lysed for 30 to 60min at 4°C followed by 20min centrifugation at 13000rpm at 4°C. Protein A beads were incubated with the desired antibody for 2hrs at 4°C, washed, and added to the collected supernatant. Beads and supernatant were incubated in a rotator at 4°C for 1hr. Beads were washed 6 times with lysis buffer minus protease inhibitors after which proteins were eluted using 1x sample buffer for 30min at 37°C. Eluted proteins were separated using SDS-PAGE and analysed by Western blotting.

Western blotting

Cells were washed in ice cold PBS and scraped in E1A lysis buffer (40mM TRIS pH7.4, 100mM NaCl, 0.1%TX-100, 5mMEDTA supplemented with complete protease inhibitors (Roche)). Cells were lysed for 30min at 4°C followed by 20min centrifugation at max speed at 4°C to remove cell debris. Proteins were eluted using 1.5x sample buffer for 30min at 37°C, separated on a 7.5 or 10% SDS-PAGE and transferred to Immobilon-FL PVDF membrane (Millipore). Membranes were blocked at room temperature using Odyssey blocking buffer in PBS (1:1) for 1hr and incubated with selected primary antibodies diluted in Odyssey blocking buffer in PBST 0.2% (1:1). Membranes were washed in PBST 0.1% and incubated with desired secondary antibodies diluted in Odyssey blocking buffer in PBST 0.2% (1:1) for 1hr at room temperature. Finally membranes were washed and imaged on an Odyssey imaging system (Li-Cor).

Degradation assay

To measure the effect of Vps33B depletion on degradation of VAMP3, HeLa cells were knocked down for Vps33B for 72hrs after which VAMP3 levels were assessed by Western blotting. Lysosomal degradation was inhibited by addition of 10nM Bafilomycin to the culture medium overnight. Proteasomal degradation was inhibited by addition of 20µM MG132 to the culture medium for 6hrs.

Immunofluorescence microscopy

HeLa cells grown on sterile glass coverslips were washed with ice-cold PBS and fixed with 4% paraformaldehyde (PFA) in PBS for 20min at room temperature (RT). Then, cells were permeabilized using 0.1% Triton-X100 in PBS for 5min and blocked for 15min using PBS supplemented with 1% BSA. Cells were labelled with primary antibodies diluted in blocking buffer at RT for 1hr, washed, and labelled with fluorescent secondary antibodies for 30min in the dark. For localization of endogenous VAMP3, cells were permeabilized and incubated with primary antibodies overnight in PBS containing 1% BSA and 0.1% Saponin. After labelling the cells were washed and mounted using Prolong Gold antifade reagent with DAPI and imaged on a DeltaVision wide field microscope using a 100x/1.4A immersion objective. Pictures were deconvolved using Softworx software and

A complex of Vps3 and Vps8 controls integrin trafficking from early to recycling endosomes and regulates cell adhesion, spreading, and migration.

analysed using FIJI ImageJ v1.48q.

Immuno-electron microscopy

Sample preparation, ultrathin cryosectioning and immunolabeling were described (71). In brief, HeLa cells were grown on 60mm dishes and fixed by the addition of freshly prepared 4% PFA in 0.1M Phosphate buffer pH 7.4 to an equal volume of culture medium for 10min, followed by postfixation with fresh 4% PFA overnight at 4°C. Fixed cells were washed in PBS containing 0.05M glycine and gently scraped in PBS containing 1% gelatine. Cells were pelleted in 12% gelatin in PBS which was then left to solidify on ice and cut into small blocks. The blocks were infiltrated overnight in 2.3M sucrose at 4°C, mounted on aluminium pins and frozen in liquid nitrogen. 70nm ultrathin cryosections were cut on a Leica ultracut UCT ultracryomicotome and picked up in a freshly prepared 1:1 mixture of 2.3M sucrose and 1.8% methylcellulose. Sections were then immunogold labelled with antibodies and protein A gold, contrasted and examined on a JEOL TEM 1010 electron microscope.

For antibody uptake IEM HeLa cells were serum-starved overnight in DMEM containing 0.01% BSA (D/B) and subsequently incubated at 4°C for 1hr with anti-β1-integrin (JB1A, Millipore) diluted in D/B to a final concentration of 10 µg/ml. Cells were transferred to pre-warmed D/B, and integrin endocytosis was allowed for 2hrs at 37°C after which cells were prepared for IEM as described above and labelled on section with Rabbit-ant-mouse IGG (Z0412, Dako) and protein A 10nm gold.

Stimulation-induced integrin recycling assay

Integrin recycling was analysed as described (40). In brief, HeLa cells were serum-starved overnight in DMEM containing 0.01% BSA (D/B) and subsequently incubated at 4°C for 1hr with anti-β1-integrin (JB1A, Millipore) diluted in D/B to a final concentration of 10µg/ml. Excess antibody was removed by 2 washes with cold D/B. Cells were then transferred to pre-warmed D/B, and integrin endocytosis was allowed for 2hrs at 37°C. Surface-bound antibodies that were not endocytosed were removed with 2 acid washes (0.5% Acetic acid, 0.5M NaCl) at 4°C. For recycling, cells were stimulated with pre-warmed D/B containing 20% FCS and internal accumulation of β1-integrin was monitored at indicated time points by fixation and preparation for immunofluorescence microscopy as described above.

Cell adhesion and spreading, quantification of focal adhesions, and cell migration assays

For cell adhesion assays, 48-well plates were coated with 10µg/ml FN or 3µg/ml Col-1, washed with PBS, and blocked with 2% BSA. Cells were seeded at a density of 5x10⁴ per well in serum-free DMEM. At the indicated time-points, non-adherent cells were washed away with PBS. Remaining cells were stained with Presto Blue, washed, transferred to a MDC SpectraMax M5e and absorbance was measured at 490nm.

For cell spreading assays and focal adhesion (FA) analysis, cells were seeded on FN or Col-1, fixed at the indicated time-points and the number of spread cells was counted. Confocal images of vinculin staining were acquired using fixed settings, background-subtracted and thresholded in ImageJ 1.44, and FA size and number were then determined using the 'analyze particles' function. For cell migration assays, cells were sparsely seeded on the indicated matrix proteins, and phase-contrast images were captured every 10min at 37°C and 5% CO₂ on a Widefield CCD system

using a 10x dry lens objective (Carl Zeiss MicroImaging). Migration tracks were generated using ImageJ 1.44, and the average displacement and migration speed were calculated from ~30 cells out of 3 independent experiments.

Integrin recycling and capture ELISA

Integrin recycling was investigated essentially as described earlier (41). Briefly, cells were transferred to ice, washed twice in PBS and surface-labeled at 4°C with 140 µg/ml NHS-SS-biotin. Internalization was allowed for 15min, after which the cells were washed with PBS, and remaining cell-surface biotin was removed with 20mM MesNa. Recycling of internalized proteins was then induced in DMEM/FCS at 37°C, whereafter biotin was removed from recycled proteins by a second reduction with MesNa, which was quenched with 20mM iodoacetamide. Cells were then washed twice in PBS and lysed in 1.5 NDLB buffer (150mM NaCl, 50mM Tris, 10mM NaF, 1.5mM Na₃VO₃, 5mM EDTA, 5mM EGTA, 1.5% Triton X-100, 0.75% Igepal CA-630, 1mM 4-(2-aminoethyl)benzylsulphonyl fluoride supplemented with complete protease inhibitors). Maxisorb 96-well plates (Life Technologies) were coated overnight with 5 µg/ml anti-integrin α5 in 0.05M Na₂CO₃ pH 9.6 at 4°C, and blocked in PBS/0.05% Tween-20 (PBS-T) with 5% BSA. Plates were incubated overnight with cell lysates at 4°C, washed with PBS-T, and incubated with HRP-streptavidin in PBS-T/1% BSA for 1hr at 4°C. After washing, biotinylated proteins were detected with ortho-phenylenediamine in a buffer containing 25.4mM Na₂HPO₄, 12.3mM citric acid (pH 5.4), and 0.003% H₂O₂. The reaction was terminated with 8 M H₂SO₄ and absorbance was read at 490nm.

Statistical analysis

For calculation of correlation coefficients of colocalization in immunofluorescence experiments the signal intensity over a vector was plotted using the plot profile tool in FIJI ImageJ in the green, red and where needed, the far-red channel. Correlation coefficients between two plots were calculated using the function:

$$\text{correl}(x, y) = \frac{\sum(x - \bar{x})(y - \bar{y})}{\sqrt{(\sum(x - \bar{x})^2)(\sum(y - \bar{y})^2)}}$$

Correlation coefficients were calculated between the channels from at least 30 cells taken from 3 separate experiments. Correlation coefficients were averaged as follows. Individual correlation coefficients (r) underwent Fisher r-to-z transformation according to the formula:

$$z_r = \frac{1}{2} \ln \left(\frac{1+r}{1-r} \right)$$

The mean of the z values was calculated and the resulting mean was transformed back to the mean correlation coefficient using:

$$r = \frac{e^{2z} - 1}{e^{2z} + 1}$$

A complex of Vps3 and Vps8 controls integrin trafficking from early to recycling endosomes and regulates cell adhesion, spreading, and migration.

To assess the significance between two mean correlation coefficients the z-score and P-value were calculated using:

$$z = \frac{\left(\frac{1}{2} \ln \frac{1+r_1}{1-r_1}\right) + \left(\frac{1}{2} \ln \frac{1+r_2}{1-r_2}\right)}{\sqrt{\frac{1}{n_1-3} + \frac{1}{n_2-3}}}$$

$$P(Z \leq z) = \int_{-\infty}^z \frac{1}{\sqrt{2\pi}} e^{-\frac{\mu^2}{2}} d\mu$$

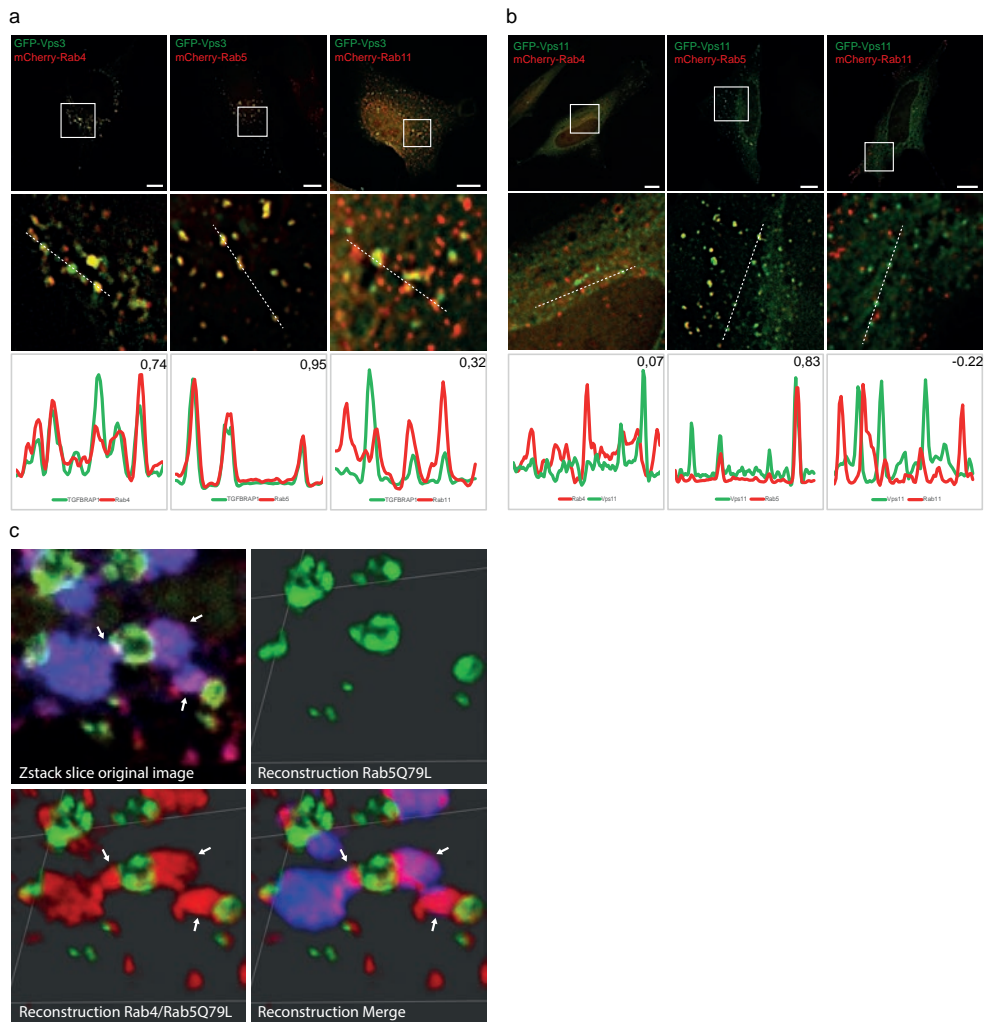
Acknowledgements

We thank Adam Grieve and Catherine Rabouille for fruitful discussions and reagents for the initial the integrin experiments. Our colleagues of the Center for Molecular Medicine and Cell Microscopy Core for discussions and assistance with electron microscopy and especially René Scriwanek for preparation of the electron micrographs. Paul Gissen, Victor Faundez and Sjaak Neefjes are kindly acknowledged for sharing critical reagents.

Author Contributions

C.T.H. Jonker designed and performed the experiments needed for figures 1-6, analysed the data, and wrote the paper. R. Galmes designed and performed the experiments needed for figures 1-3, analysed the data and made the Vps33B antibody and wrote the paper. T. Veenendaal performed experiments needed for figures 1a, 1d, 2d, 4c, 4f. C. ten Brink performed experiments needed for figures 4a and cloned constructs used in the manuscript. R.E.N. van der Welle performed experiments needed for figures 4e. J. de Rooij designed experiments needed for figure 4 and wrote the paper. A.A. Peden designed and performed the experiments for figure 3a and wrote the paper. P. van der Sluijs designed the experiments for figure 1b, 1c, 1e, cloned constructs, made the Vps33B antibody used in the manuscript and wrote the paper. C. Margadant designed and performed the experiments for figures 4-5, analysed the data and wrote the paper. J. Klumperman initiated and supervised the project, designed experiments for figures 1-4 and wrote the paper.

Supplemental figures



A complex of Vps3 and Vps8 controls integrin trafficking from early to recycling endosomes and regulates cell adhesion, spreading, and migration.

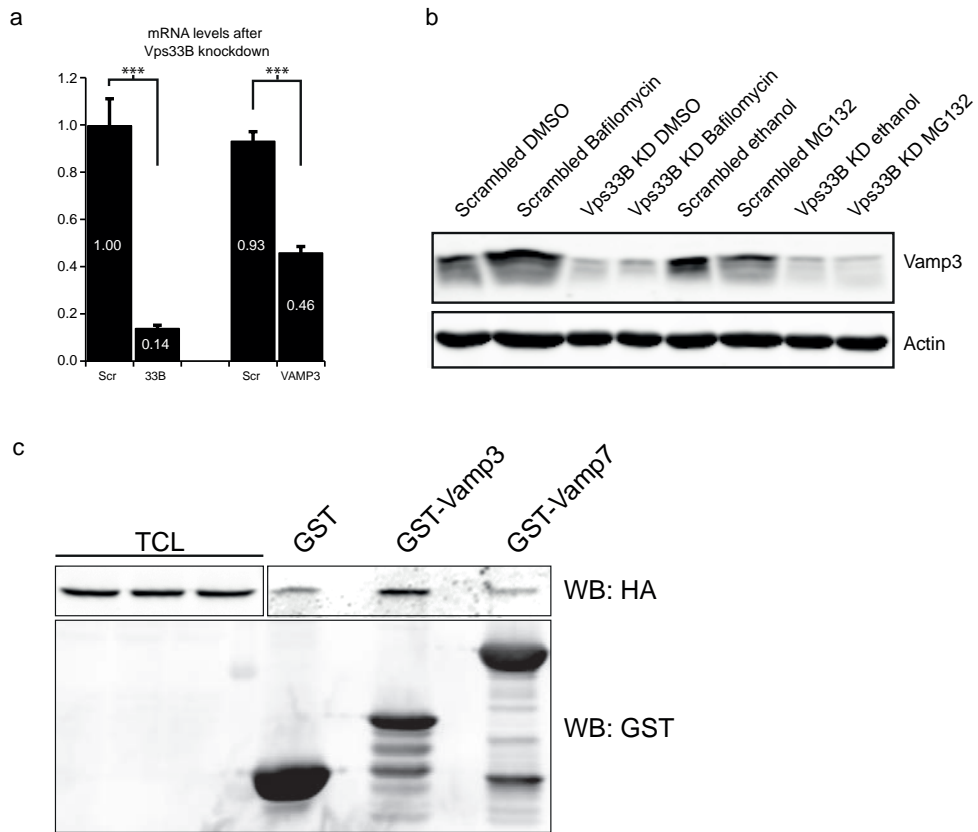


Figure S2. (a) Vps33B and VAMP3 mRNA levels of HeLa cells knocked down for Vps33B were measured in triplicate and plotted relative to scrambled conditions. VAMP3 mRNA levels are significantly decreased after Vps33B knockdown. Error bars represent SEM. **(b)** Lysosomal degradation was inhibited by addition of 10nM Bafilomycin and proteasomal degradation was inhibited by addition of 20μM MG132. None of the inhibitors restored the levels of VAMP3. **(c)** Blot including total cell lysates of VAMP-GST pull-down. GST-VAMP3 and GST-VAMP7 were incubated with cell lysates of HeLa cells expressing Vps33B-HA/V5/his and VIPAS39-mCherry. Pull-down of GST showed binding of Vps33B to GST-VAMP3 but not to GST-VAMP7.

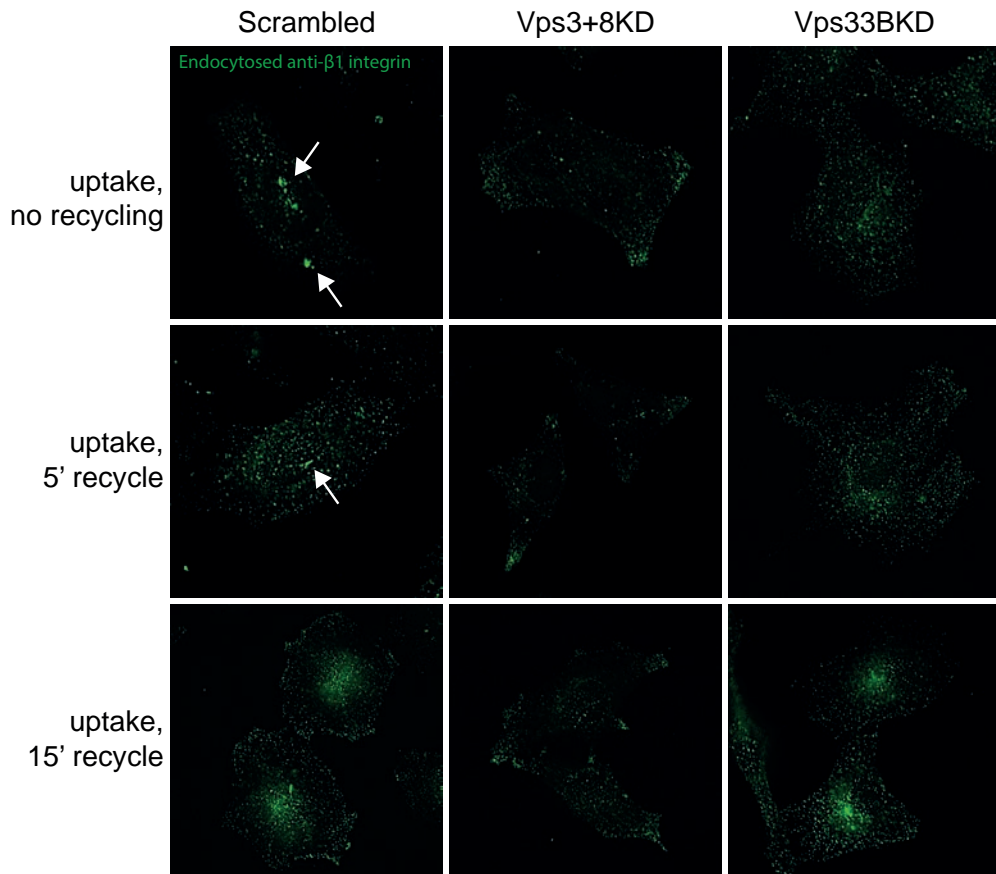


Figure S3. Integrin recycling assay as described 24. HeLa cells knocked down for Vps3+8 or Vps33B were serum-starved overnight and subsequently incubated with anti-β1-integrin. After 2hr uptake at 37°C, and labelling with fluorescent secondary antibodies, β1-integrins accumulate in REs (arrows). After addition of serum, β1-integrins are rapidly recycled and the accumulations disperse. Shown are time points before addition of serum (upper panels) 5 minutes after addition of serum (middle panels) and 15 minutes after addition of serum (lower panels). In knockdown cells no accumulation of integrins is observed indicating that trafficking to the REs is impaired.

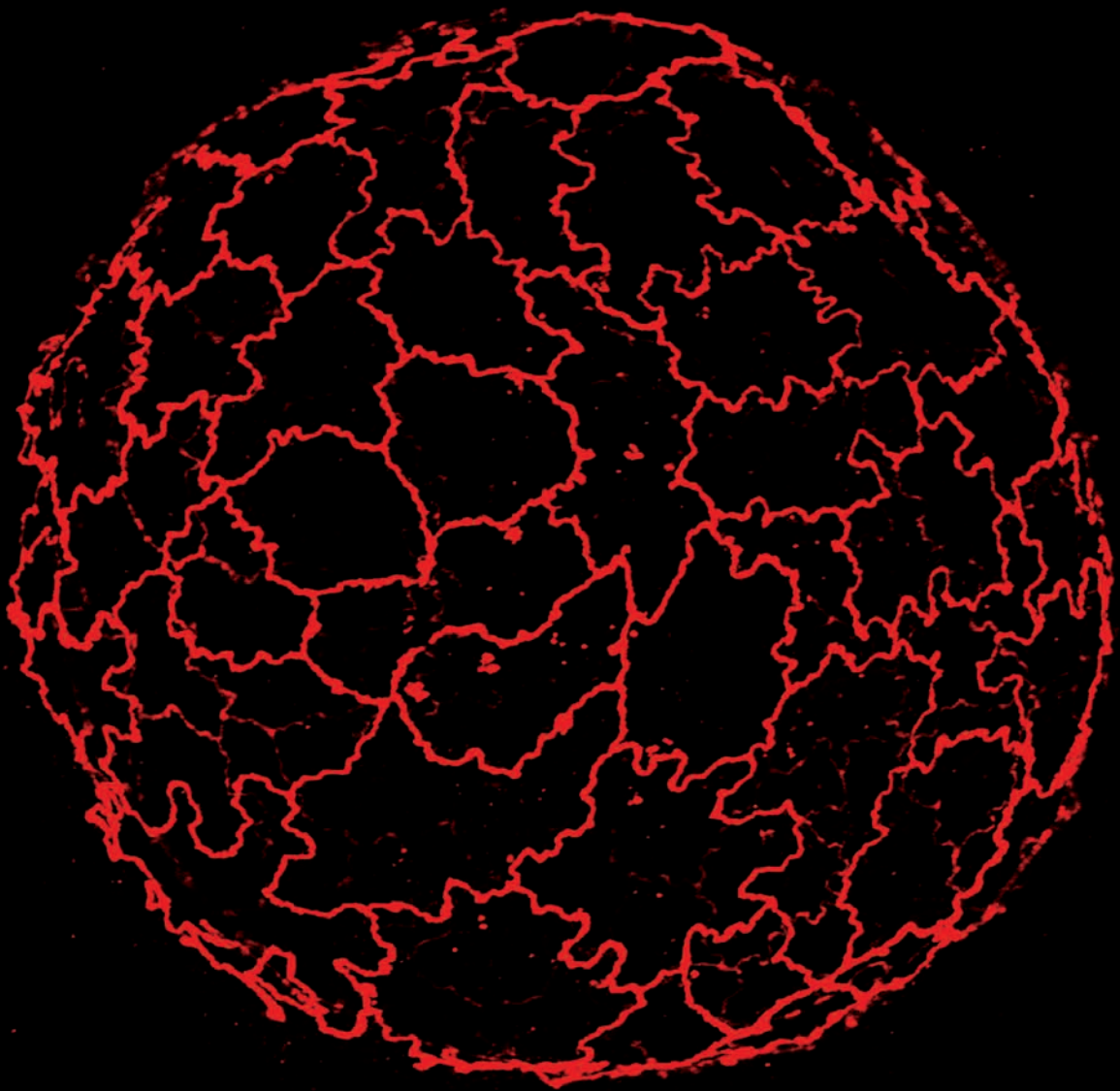
References

1. Boustany RM. Lysosomal storage diseases--the horizon expands. *Nat Rev Neurol*. 2013 Oct;9(10):583–598.
2. Neefjes J, van der Kant R. Stuck in traffic: an emerging theme in diseases of the nervous system. *Trends Neurosci*. 2014 Feb;37(2):66–76.
3. Mellman I, Yarden Y. Endocytosis and cancer. *Cold Spring Harb Perspect Biol*. 2013 Dec 1;5(12):a016949.
4. Epp N, Rethmeier R, Krämer L, Ungermann C. Membrane dynamics and fusion at late endosomes and vacuoles--Rab regulation, multisubunit tethering complexes and SNAREs. *Eur J Cell Biol*. 2011 Sep;90(9):779–785.
5. Rizo J, Südhof TC. The membrane fusion enigma: SNAREs, Sec1/Munc18 proteins, and their accomplices--guilty as charged? *Annu Rev Cell Dev Biol*. 2012;28:279–308.
6. Schimmöller F, Simon I, Pfeffer SR. Rab GTPases, directors of vesicle docking. *J Biol Chem*. 1998 Aug 28;273(35):22161–22164.
7. Jordens I, Marsman M, Kuijl C, Neefjes J. Rab proteins, connecting transport and vesicle fusion. *Traffic*. 2005 Dec;6(12):1070–1077.
8. Perini ED, Schaefer R, Stöter M, Kalaidzidis Y, Zerial M. Mammalian CORVET is required for fusion and conversion of distinct early endosome subpopulations. *Traffic*. 2014 Dec;15(12):1366–1389.
9. Van der Kant R, Jonker CT, Wijdeven RH, Bakker J, Janssen L, Klumperman J, et al. Characterization of the mammalian CORVET and HOPS complexes and their modular restructuring for endosome specificity. *J Biol Chem*. 2015 Oct 13;
10. Lachmann J, Glaubke E, Moore PS, Ungermann C. The Vps39-like TRAP1 is an effector of Rab5 and likely the missing Vps3 subunit of human CORVET. *Cell Logist*. 2014 Dec;4(4):e970840.
11. Spang A. Membrane Tethering Complexes in the Endosomal System. *Frontiers in cell and developmental biology*. 2016 May 9;4:35.
12. Klinger CM, Klute MJ, Dacks JB. Comparative genomic analysis of multi-subunit tethering complexes demonstrates an ancient pan-eukaryotic complement and sculpting in Apicomplexa. *PLoS ONE*. 2013 Sep 27;8(9):e76278.
13. Van der Sluijs P, Hull M, Webster P, Måle P, Goud B, Mellman I. The small GTP-binding protein rab4 controls an early sorting event on the endocytic pathway. *Cell*. 1992 Sep 4;70(5):729–740.
14. Ullrich O, Reinsch S, Urbé S, Zerial M, Parton RG. Rab11 regulates recycling through the pericentriolar recycling endosome. *J Cell Biol*. 1996 Nov;135(4):913–924.
15. Yudowski GA, Puthenveedu MA, Henry AG, von Zastrow M. Cargo-mediated regulation of a rapid Rab4-dependent recycling pathway. *Mol Biol Cell*. 2009 Jun;20(11):2774–2784.
16. McCaffrey MW, Bielli A, Cantalupo G, Mora S, Roberti V, Santillo M, et al. Rab4 affects both recycling and degradative endosomal trafficking. *FEBS Lett*. 2001 Apr 20;495(1-2):21–30.
17. De Wit H, Lichtenstein Y, Kelly RB, Geuze HJ, Klumperman J, van der Sluijs P. Rab4 regulates formation of synaptic-like microvesicles from early endosomes in PC12 cells. *Mol Biol Cell*. 2001 Nov;12(11):3703–3715.
18. Cullinane AR, Straatman-Iwanowska A, Zaucker A, Wakabayashi Y, Bruce CK, Luo G, et al. Mutations in VIPAR cause an arthrogryposis, renal dysfunction and cholestasis syndrome phenotype with defects in epithelial polarization. *Nat Genet*. 2010 Apr;42(4):303–312.
19. Smith H, Galmes R, Gogolina E, Straatman-Iwanowska A, Reay K, Banushi B, et al. Associations among genotype, clinical phenotype, and intracellular localization of trafficking proteins in ARC syndrome. *Hum Mutat*. 2012 Dec;33(12):1656–1664.
20. Zhu GD, Salazar G, Zlatich SA, Fiza B, Doucette MM, Heilman CJ, et al. SPE-39 family proteins interact with the HOPS complex and function in lysosomal delivery. *Mol Biol Cell*. 2009 Feb;20(4):1223–1240.
21. Sönnichsen B, De Renzis S, Nielsen E, Rietdorf J, Zerial M. Distinct membrane domains on endosomes in the recycling pathway visualized by multicolor imaging of Rab4, Rab5, and Rab11. *J Cell Biol*. 2000 May 15;149(4):901–914.
22. Wegner CS, Wegener CS, Malerød L, Pedersen NM, Progida C, Prodiga C, et al. Ultrastructural characterization of giant endosomes induced by GTPase-deficient Rab5. *Histochem Cell Biol*. 2010 Jan;133(1):41–55.
23. Plemel RL, Lobingier BT, Brett CL, Angers CG, Nickerson DP, Paulsel A, et al. Subunit organization and Rab interactions of Vps-C protein complexes that control endolysosomal membrane traffic. *Mol Biol Cell*. 2011 Apr 15;22(8):1353–1363.
24. Wartosch L, Günesdogan U, Graham SC, Luzio JP. Recruitment of VPS33A to HOPS by VPS16 Is Required for Lysosome

- Fusion with Endosomes and Autophagosomes. *Traffic*. 2015 Jul;16(7):727–742.
25. McMahon HT, Ushkaryov YA, Edelmann L, Link E, Binz T, Niemann H, et al. Cellubrevin is a ubiquitous tetanus-toxin substrate homologous to a putative synaptic vesicle fusion protein. *Nature*. 1993 Jul 22;364(6435):346–349.
 26. Südhof TC, Rothman JE. Membrane fusion: grappling with SNARE and SM proteins. *Science*. 2009 Jan 23;323(5913):474–477.
 27. De Wit H, Walter AM, Milosevic I, Gulyás-Kovács A, Riedel D, Sørensen JB, et al. Synaptotagmin-1 docks secretory vesicles to syntaxin-1/SNAP-25 acceptor complexes. *Cell*. 2009 Sep 4;138(5):935–946.
 28. Braun S, Jentsch S. SM-protein-controlled ER-associated degradation discriminates between different SNAREs. *EMBO Rep*. 2007 Dec;8(12):1176–1182.
 29. Carpp LN, Shanks SG, Struthers MS, Bryant NJ. Cellular levels of the syntaxin Tlg2p are regulated by a single mode of binding to Vps45p. *Biochem Biophys Res Commun*. 2007 Nov 23;363(3):857–860.
 30. Toonen RF, de Vries KJ, Zalm R, Südhof TC, Verhage M. Munc18-1 stabilizes syntaxin 1, but is not essential for syntaxin 1 targeting and SNARE complex formation. *J Neurochem*. 2005 Jun;93(6):1393–1400.
 31. Clark NL, Alani E, Aquadro CF. Evolutionary rate covariation reveals shared functionality and coexpression of genes. *Genome Res*. 2012 Apr;22(4):714–720.
 32. Fraser HB, Hirsh AE, Wall DP, Eisen MB. Coevolution of gene expression among interacting proteins. *Proc Natl Acad Sci U S A*. 2004 Jun 15;101(24):9033–9038.
 33. Klumperman J, Raposo G. The complex ultrastructure of the endolysosomal system. *Cold Spring Harb Perspect Biol*. 2014 Oct;6(10):a016857.
 34. Graham SC, Wartosch L, Gray SR, Scourfield EJ, Deane JE, Luzio JP, et al. Structural basis of Vps33A recruitment to the human HOPS complex by Vps16. *Proc Natl Acad Sci U S A*. 2013 Aug 13;110(33):13345–13350.
 35. Hao M, Maxfield FR. Characterization of rapid membrane internalization and recycling. *J Biol Chem*. 2000 May 19;275(20):15279–15286.
 36. Ren M, Xu G, Zeng J, De Lemos-Chiarandini C, Adesnik M, Sabatini DD. Hydrolysis of GTP on rab11 is required for the direct delivery of transferrin from the pericentriolar recycling compartment to the cell surface but not from sorting endosomes. *Proc Natl Acad Sci U S A*. 1998 May 26;95(11):6187–6192.
 37. Van Dam EM, Ten Broeke T, Jansen K, Spijkers P, Stoorvogel W. Endocytosed transferrin receptors recycle via distinct dynamin and phosphatidylinositol 3-kinase-dependent pathways. *J Biol Chem*. 2002 Dec 13;277(50):48876–48883.
 38. Riggs KA, Hasan N, Humphrey D, Raleigh C, Nevitt C, Corbin D, et al. Regulation of integrin endocytic recycling and chemotactic cell migration by syntaxin 6 and VAMP3 interaction. *J Cell Sci*. 2012 Aug 15;125(Pt 16):3827–3839.
 39. Luftman K, Hasan N, Day P, Hardee D, Hu C. Silencing of VAMP3 inhibits cell migration and integrin-mediated adhesion. *Biochem Biophys Res Commun*. 2009 Feb 27;380(1):65–70.
 40. Powelka AM, Sun J, Li J, Gao M, Shaw LM, Sonnenberg A, et al. Stimulation-dependent recycling of integrin beta1 regulated by ARF6 and Rab11. *Traffic*. 2004 Jan;5(1):20–36.
 41. Roberts M, Barry S, Woods A, van der Sluijs P, Norman J. PDGF-regulated rab4-dependent recycling of alphavbeta3 integrin from early endosomes is necessary for cell adhesion and spreading. *Curr Biol*. 2001 Sep 18;11(18):1392–1402.
 42. Hynes RO. Integrins: bidirectional, allosteric signaling machines. *Cell*. 2002 Sep 20;110(6):673–687.
 43. Caswell P, Norman J. Endocytic transport of integrins during cell migration and invasion. *Trends Cell Biol*. 2008 Jun;18(6):257–263.
 44. Caswell PT, Norman JC. Integrin trafficking and the control of cell migration. *Traffic*. 2006 Jan;7(1):14–21.
 45. De Franceschi N, Hamidi H, Alanko J, Sahgal P, Ivaska J. Integrin traffic- the update. *J Cell Sci*. 2015 Mar 1;128(5):839–852.
 46. Webb DJ, Parsons JT, Horwitz AF. Adhesion assembly, disassembly and turnover in migrating cells-- over and over and over again. *Nat Cell Biol*. 2002 Apr;4(4):E97–100.
 47. Theisen U, Straube E, Straube A. Directional persistence of migrating cells requires Kif1C-mediated stabilization of trailing adhesions. *Dev Cell*. 2012 Dec 11;23(6):1153–1166.
 48. Bayram Y, Karaca E, Coban Akdemir Z, Yilmaz EO, Tayfun GA, Aydin H, et al. Molecular etiology of arthrogyposis in multiple families of mostly Turkish origin. *J Clin Invest*. 2016 Feb 1;126(2):762–778.
 49. Sheff DR, Daro EA, Hull M, Mellman I. The receptor recycling pathway contains two distinct populations of early

- endosomes with different sorting functions. *J Cell Biol.* 1999 Apr 5;145(1):123–139.
50. Nagelkerken B, Van Anken E, Van Raak M, Gerez L, Mohrmann K, Van Uden N, et al. Rabaptin4, a novel effector of the small GTPase rab4a, is recruited to perinuclear recycling vesicles. *Biochem J.* 2000 Mar 15;346 Pt 3:593–601.
 51. Bröcker C, Kuhlee A, Gatsogiannis C, Balderhaar HJ, Hönscher C, Engelbrecht-Vandré S, et al. Molecular architecture of the multisubunit homotypic fusion and vacuole protein sorting (HOPS) tethering complex. *Proc Natl Acad Sci U S A.* 2012 Feb 7;109(6):1991–1996.
 52. Solinger JA, Spang A. Tethering complexes in the endocytic pathway: CORVET and HOPS. *FEBS J.* 2013 Jun;280(12):2743–2757.
 53. Galli T, Chilcote T, Mundigl O, Binz T, Niemann H, De Camilli P. Tetanus toxin-mediated cleavage of cellubrevin impairs exocytosis of transferrin receptor-containing vesicles in CHO cells. *J Cell Biol.* 1994 Jun;125(5):1015–1024.
 54. Jović M, Kean MJ, Dubankova A, Boura E, Gingras AC, Brill JA, et al. Endosomal sorting of VAMP3 is regulated by PI4K2A. *J Cell Sci.* 2014 Sep 1;127(Pt 17):3745–3756.
 55. Gordon DE, Mirza M, Sahlender DA, Jakovleska J, Peden AA. Coiled-coil interactions are required for post-Golgi R-SNARE trafficking. *EMBO Rep.* 2009 Aug;10(8):851–856.
 56. Jacquemet G, Hamidi H, Ivaska J. Filopodia in cell adhesion, 3D migration and cancer cell invasion. *Curr Opin Cell Biol.* 2015 Oct;36:23–31.
 57. Maritzen T, Schachtner H, Legler DF. On the move: endocytic trafficking in cell migration. *Cell Mol Life Sci.* 2015 Jun;72(11):2119–2134.
 58. Paul NR, Jacquemet G, Caswell PT. Endocytic Trafficking of Integrins in Cell Migration. *Curr Biol.* 2015 Nov 16;25(22):R1092–R1105.
 59. Arjonen A, Alanko J, Veltel S, Ivaska J. Distinct recycling of active and inactive $\beta 1$ integrins. *Traffic.* 2012 Apr;13(4):610–625.
 60. Margadant C, Kreft M, de Groot DJ, Norman JC, Sonnenberg A. Distinct roles of talin and kindlin in regulating integrin $\alpha 5 \beta 1$ function and trafficking. *Curr Biol.* 2012 Sep 11;22(17):1554–1563.
 61. Böttcher RT, Stremmel C, Meves A, Meyer H, Widmaier M, Tseng HY, et al. Sorting nexin 17 prevents lysosomal degradation of $\beta 1$ integrins by binding to the $\beta 1$ -integrin tail. *Nat Cell Biol.* 2012 Jun;14(6):584–592.
 62. Steinberg F, Heesom KJ, Bass MD, Cullen PJ. SNX17 protects integrins from degradation by sorting between lysosomal and recycling pathways. *J Cell Biol.* 2012 Apr 16;197(2):219–230.
 63. Peden AA, Oorschot V, Hesser BA, Austin CD, Scheller RH, Klumperman J. Localization of the AP-3 adaptor complex defines a novel endosomal exit site for lysosomal membrane proteins. *J Cell Biol.* 2004 Mar 29;164(7):1065–1076.
 64. Bonifacino JS, Rojas R. Retrograde transport from endosomes to the trans-Golgi network. *Nat Rev Mol Cell Biol.* 2006 Aug;7(8):568–579.
 65. Xiang B, Zhang G, Ye S, Zhang R, Huang C, Liu J, et al. Characterization of a Novel Integrin Binding Protein, VPS33B, Which Is Important for Platelet Activation and In Vivo Thrombosis and Hemostasis. *Circulation.* 2015 Dec 15;132(24):2334–2344.
 66. Caswell PT, Chan M, Lindsay AJ, McCaffrey MW, Boettiger D, Norman JC. Rab-coupling protein coordinates recycling of $\alpha 5 \beta 1$ integrin and EGFR1 to promote cell migration in 3D microenvironments. *J Cell Biol.* 2008 Oct 6;183(1):143–155.
 67. Caswell PT, Spence HJ, Parsons M, White DP, Clark K, Cheng KW, et al. Rab25 associates with $\alpha 5 \beta 1$ integrin to promote invasive migration in 3D microenvironments. *Dev Cell.* 2007 Oct;13(4):496–510.
 68. Muller PA, Caswell PT, Doyle B, Iwanicki MP, Tan EH, Karim S, et al. Mutant p53 drives invasion by promoting integrin recycling. *Cell.* 2009 Dec 24;139(7):1327–1341.

69. Pols MS, van Meel E, Oorschot V, ten Brink C, Fukuda M, Swetha MG, et al. hVps41 and VAMP7 function in direct TGN to late endosome transport of lysosomal membrane proteins. *Nat Commun.* 2013;4:1361.
70. Hagemeyer MC, Monastyrska I, Griffith J, van der Sluijs P, Voortman J, van Bergen en Henegouwen PM, et al. Membrane rearrangements mediated by coronavirus nonstructural proteins 3 and 4. *Virology.* 2014 Jun;458-459:125–135.
71. Slot JW, Geuze HJ. Cryosectioning and immunolabeling. *Nat Protoc.* 2007;2(10):2480–2491.
72. Gordon DE, Bond LM, Sahlender DA, Peden AA. A targeted siRNA screen to identify SNAREs required for constitutive secretion in mammalian cells. *Traffic.* 2010 Sep;11(9):1191–1204.



A Vps8-dependent apical recycling pathway is required for polarized cell organization

Chapter 4

Caspar TH Jonker¹, T. Veenendaal¹, C. ten Brink¹, P. Gosavi^{1,2}, R. Galmes^{1,3}, S.C. van IJendoorn⁴, J. Klumperman¹

¹ Department of Cell Biology; Center of Molecular Medicine; Utrecht, 3584 CX; The Netherlands

² Current Address; Biochemistry and Molecular Biology; The University of Melbourne; Victoria 3010; Australia

³ Current Address; UCL Cancer Institute, University College London, 72 Huntley Street, London, WC1E 6DD, UK.

⁴ Department of Cell Biology, University Medical Center Groningen, Groningen, 9713 AV; The Netherlands

Manuscript in preparation

Abstract

Previous studies in polarized epithelial cells showed that the VIPAS39/Vps33B complex is involved in recycling of apical and junctional proteins. Our recent findings (chapter 3) show that a complex of Vps3 and Vps8 together with the VIPAS39/Vps33B complex controls transport from early to recycling endosomes in non-polarized cells. This raises the question whether the Vps3/8 complex is also involved in apical recycling. Here we study the role of Vps8 in endosomal transport of polarized cells. We show that Vps8 localizes to early endosomes as well as apical recycling endosomes. Strikingly, overexpression of Vps8 induces recruitment of early endosomes to apical recycling endosomes, suggesting a role for Vps8 in tethering of these compartments. Furthermore, knockdown of Vps8 results in perturbation of cell polarity, prevents completion of cytokinesis and impairs polarization of cells during directed cell migration. These phenotypes are analogous to knockdown of the well-established recycling endosomal protein Rab11. We conclude that Vps8 is required for an apical recycling pathway essential for proper cell polarization.

Introduction

The endolysosomal system is the major membrane system of eukaryotic cells for uptake, recycling and degradation of extracellular molecules and plasma membrane (PM) constituents. In non-polarized cells endocytosed cargo is transported from the PM to early endosomes (EEs) and progresses to late endosomes (LEs) and lysosomes for degradation. Alternatively, cargo is transported from EEs to recycling endosomes (REs) for transport back to the PM. Specialized cell types have adapted their endolysosomal system to meet the requirements for cell type specific functions. In polarized epithelial cells the apical and basolateral PM are separated by junctions that inhibit mixing of membrane domains (chapter 1, Box3). After endocytosis, apical cargo enters apical EEs and basolateral cargo basolateral EEs (1–3). From each type of EE a direct, fast recycling pathway to the original PM can occur. In addition, indirect, slow recycling pathways exist that involve transport from either apical or basolateral EEs to a common recycling endosome (CRE) (4). From the CRE, basolateral cargo is transported back to the basolateral PM, while apical cargo travels via a specialized apical recycling endosome (ARE) to the apical PM (5–7). These separated recycling routes are necessary to maintain the distinction between the PM domains (8–10).

The transport from AREs to the apical PM is mediated by Rab11a (11–15), whereas recycling from the CRE to the basolateral PM relies on Rab8 and Rab10 (16,17). Despite this distinction, it is still unclear whether the ARE and CRE are truly separate compartments or different membrane domains of the same compartment (3,10,18).

Recent studies revealed a mammalian-specific vacuolar protein sorting (Vps) protein complex consisting of VIPAS39 and Vps33B, which interacts with Rab11a and is required for recycling of proteins to the apical PM (19–22). Mutations in Vps33B or VIPAS39 cause Arthrogyryposis Renal dysfunction Cholestasis (ARC) syndrome, a multisystem disorder that is characterized by neurogenic arthrogyryposis multiplex congenita, renal tubular dysfunction and neonatal cholestasis (19,20,23). ARC-causing mutations induce mislocalization of apical membrane proteins in renal cells and hepatocytes (19,20,23), illustrating the importance of the Vps33B/VIPAS39 complex in polarized transport.

VIPAS39 and Vps33B are homologous to Vps16 and Vps33A respectively, which are subunits of the

CORVET and HOPS tethering complexes. CORVET mediates fusion between EEs, whereas HOPS regulates fusion events at LEs. Recently, we found that the CORVET specific subunits Vps8 and Vps3 are required for transport of integrins from EEs to REs in non-polarized cells in a pathway independent of other CORVET subunits (chapter 3). Vps3 and Vps8 form a complex that interacts with the VIPAS39/Vps33B complex. These findings were the first to describe a role for Vps3 and Vps8 in recycling and add to a growing number of observations that subunits of the CORVET and related complexes can have individual roles in intracellular transport (24,25). Here we address the question whether the Vps3/8 complex is also required for apical recycling in polarized cells.

Results

Vps8 expression is increased in polarized cells and tissues

In HeLa cells, localization microscopy of endogenous Vps8 was hindered by low protein expression levels (chapter 3). Moreover, the pool of Vps8 that is localized to (endosomal) membranes in steady state is minimal compared to the amount of Vps8 present in the cytosol. To study Vps8 function in polarized cells we established protein expression levels in HepG2 cells. HepG2 cells are human hepatoma cells that develop a well-defined apical-basolateral polarity, making them a widely used model system for human hepatocytes. By western blotting we found that HeG2 cells have a 2-fold higher expression of endogenous Vps8 compared to HeLa cells (fig. 1a, 1b). Interestingly, an optimally polarized HepG2 cell line (pHepG2) presented even higher Vps8 levels (fig. 1a, 1b).

To investigate if high expression of Vps8 is a more general characteristic of polarized cell types, we consulted the ProteinAtlas immunohistological database (26). This revealed that protein expression levels of Vps8 are increased in various epithelial tissues including epithelial cells of the colon (fig. 1c, left panel), epididymis (middle panel) and the exocrine epithelium of the pancreas (right panel). Together these data show the propensity that Vps8 expression is increased in polarized cells.

Vps8 is enriched in the apical region of polarized cells

High expression of Vps8 in pHepG2 cells allowed detection of endogenous Vps8 using Immunofluorescence (IF) microscopy. Endogenous Vps8 localized throughout the cytosol, in discrete punctae, and was strikingly enriched near the apical PM (fig. 2a, left panel) delineated by the bile canaliculi (BC). Overexpression of HA-Vps8 resulted in a similar pattern, showing a clear accumulation of Vps8 just below the BC (fig. 2a, middle and right panel). Similarly, polarized LS174T-W4 cells and MDCK cells cultured in matrigel showed enrichment of Vps8 towards the apical PM (fig. 2b). Visualization of the cortical actin web lining the apical PM showed that Vps8 is localized just below the apical PM, since Vps8 and actin staining do not overlap (fig. 2b, line graphs). Together these data show that both endogenous and overexpressed Vps8 are enriched near the apical PM, below the cortical actin web in several polarized cell types.

To identify the Vps8-positive punctae we labeled MDCK cells with markers for the endosomal system. Endogenous Vps8 clearly overlaps with the EE marker EEA1 (fig. 2c, upper panels) but not with the TGN/late endosomal marker cation-independent mannose-6-phosphate receptor (CI-MPR) (fig. 2c, lower panels). Localization of Vps8 to EEs is in agreement with earlier observations in non-polarized cells by us and others (Chapter 3) (21,27). However, the apically enriched Vps8

did not completely overlap with EEA1, suggesting Vps8 is localized to an additional compartment in polarized cells.

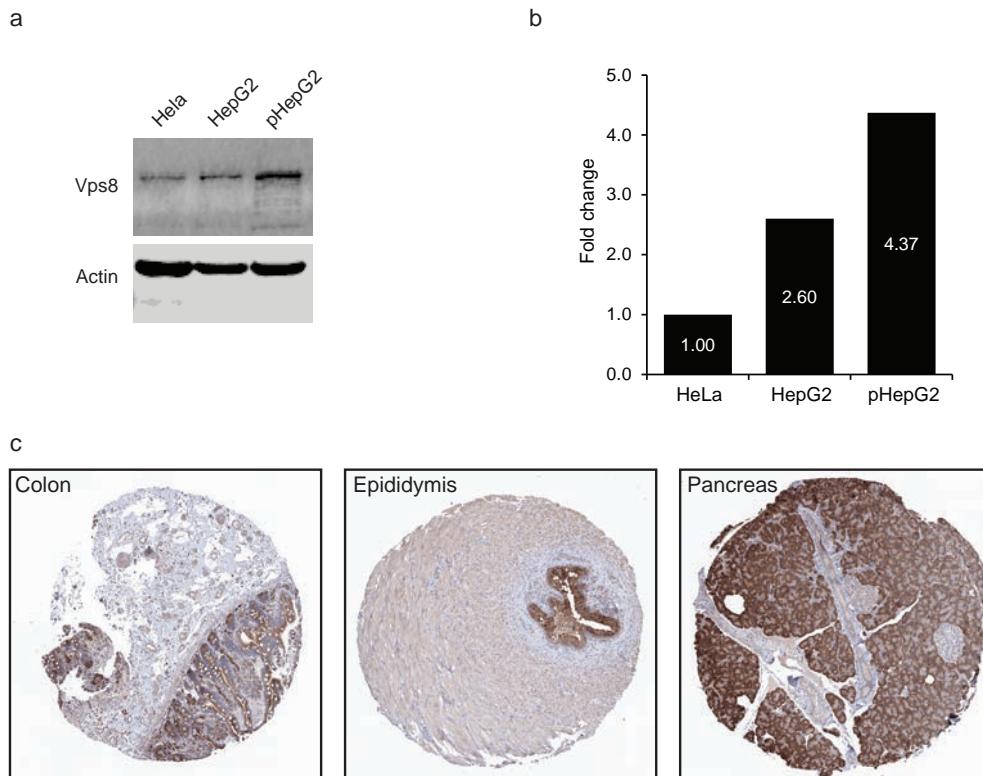


Figure 1 (a) HeLa cells, HepG2 cells and polarized HepG2 (pHepG2) cells were blotted for Vps8 and actin as a loading control. Polarized HepG2 cells express more Vps8 than HeLa cells or non-polarized HepG2 cells. Representative blot. (b) Quantification of (a), normalized to actin loading control. (c) Tissue microarray-based immunohistochemistry slides from the Human proteinatlas program (www.proteinatlas.org) (26,66) show an increase of Vps8 in polarized cells of various tissues. Surrounding tissue shows lower levels of Vps8 compared to the epithelial cells in colon (left), epididymis (middle) and exocrine pancreas (right). Bar 100 μ m.

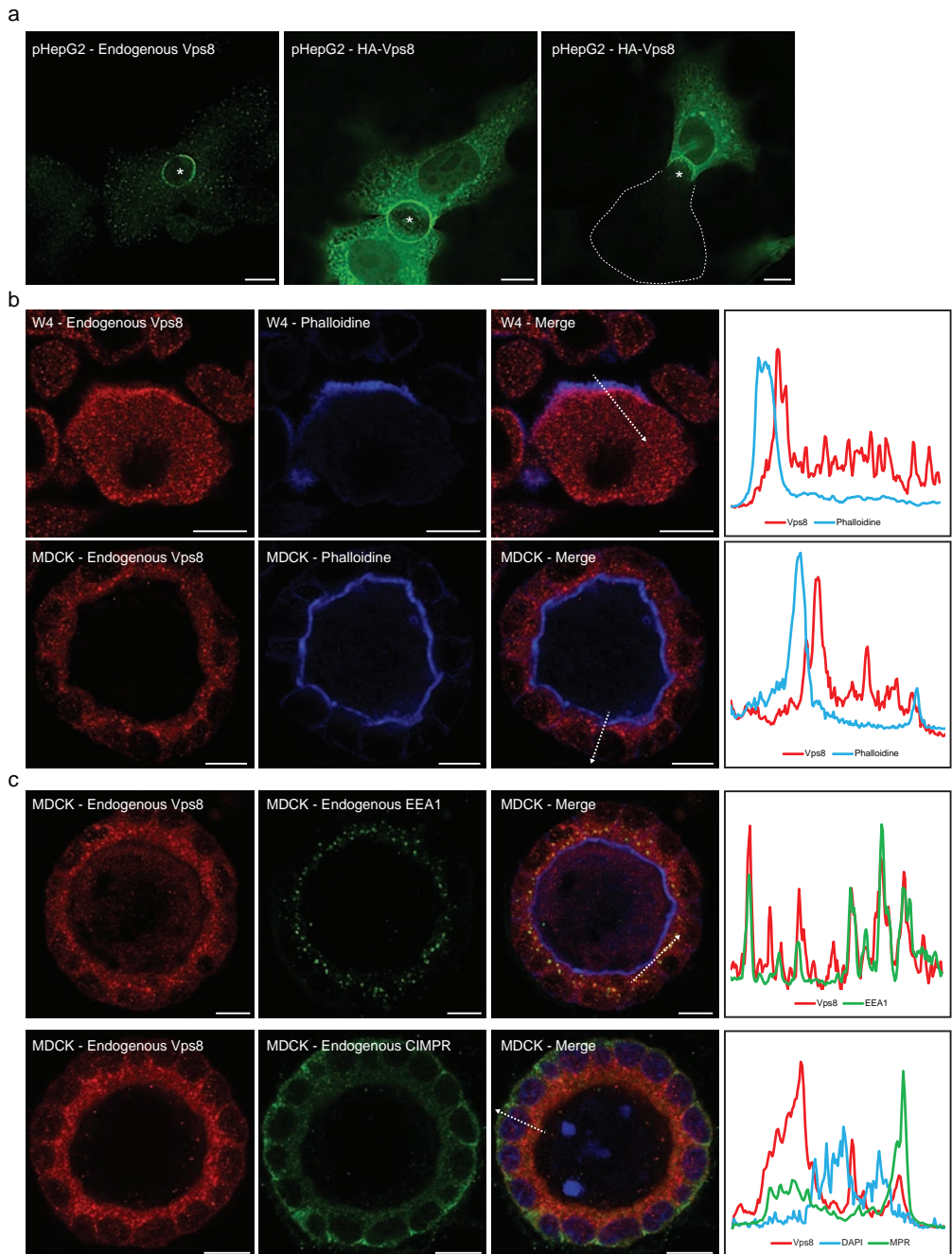


Figure 2 (a) pHepG2 cells labeled for endogenous Vps8 (left panel), or overexpressed with HA-Vps8 (middle and right panel) show accumulation of Vps8 under the apical PM forming the Bile Canalculus (marked with *) between two cells. Bar 10 μ m. (b) Endogenous Vps8 in polarized LS174T-W4 cells (upper panels) or polarized MDCK cells (lower panels) show enrichment of Vps8 near the apical PM marked by actin staining with phalloidine. Line quantifications show a high Vps8 signal in close proximity to the phalloidine signal that does not overlap. Bar 10 μ m. (c) Endogenous Vps8 colocalizes with EEA1 in polarized MDCK cells (upper panels) but not with CIMPR (lower panels) as indicated by the line quantifications. Bar 10 μ m.

Vps8 localizes to the apical recycling endosome in HepG2 cells

Enrichment of Vps8 near the apical membrane is reminiscent to the localization of the ARE, which is well described in pHepG2 cells (5,28,29). To investigate a potential overlap between Vps8 and the ARE, we expressed HA-Vps8 together with mCherry-Rab11, the main marker for ARE. This revealed a partial overlap between HA-Vps8 and the ARE (fig. 3a). The position of the ARE near the apical PM is dependent on an intact microtubular network (30). Treatment of pHepG2 cells expressing HA-Vps8 and mCherry-Rab11 for 2 hours with nocodazole caused both Vps8 and Rab11 to relocalize away from the apical PM to a dispersed localization throughout the cytosol (fig. 3b). These data strongly suggests that the Vps8 label overlapping with Rab11 localizes to membranes of the ARE. Additional labeling with EEA1 showed that Vps8 only colocalizes with mCherry-Rab11 close to the apical PM, whereas Vps8 and EEA1 also colocalize on EEs away from the apical PM (fig. 3c). To study the localization of Vps8 at higher resolution and within the context of membranes, we analyzed polarized HepG2 cells expressing HA-Vps8 using Immuno electron microscopy (IEM). This revealed that the pool of HA-Vps8 concentrating at the apical PM is membrane-bound (fig. 3d). The small tubulo-vesicular membranes positive for Vps8 are typical for REs (31). Together these results show that in polarized HepG2 cells Vps8 localizes to EEA1-positive EEs and the Rab11-positive ARE.

Vps8 tethers apical EEs to the ARE.

As shown in in figure 3c, a substantial quantity of EEA1-positive EEs localizes in close proximity to the Rab11-positive ARE. Previous studies in the same cell line showed a more dispersed localization of EEA1, also after overexpression of Rab11 (32). Similarly, we found that EEA1 does not significantly overlap with Rab11-positive ARE without co-expression of HA-Vps8 (fig. 4a). These observations suggest that expression of HA-Vps8 induces association of EEA1-positive EEs with the ARE. Indeed, co-expression of HA-Vps8 induced overlap between EEA1 and mCherry-Rab11 (fig. 4b, cells with *), while adjacent cells in the same sample not expressing HA-Vps8 maintained a dispersed localization of EEA1 (fig. 4b, cells without *). Quantification confirmed a significant increase of colocalization between EEA1 and Rab11 when cells co-express HA-Vps8 (fig.4c). These results indicate that overexpression of HA-Vps8 induces tethering of EEA1-positive EEs to Rab11-positive AREs.

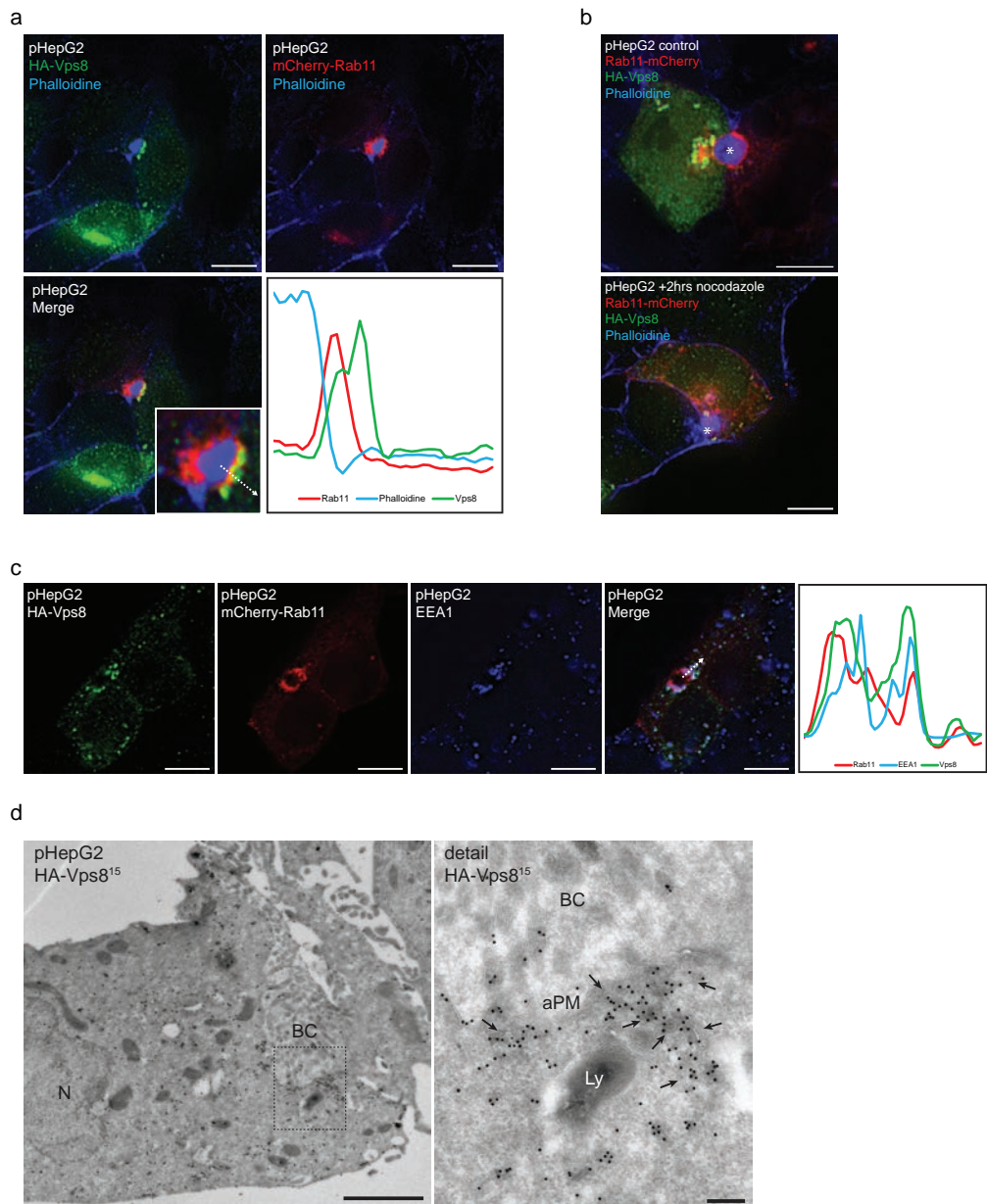


Figure 3 (a) Expression of HA-Vps8 and Rab11-mCherry in HepG2 cells results in their partial overlap near the apical PM. Bar 10µm. (b) Treatment of polarized HepG2 cells with 33µM nocodazole for 2hours disrupts the microtubular network and causes the HA-Vps8 signal and the Rab11-positive ARE to re-localize away from the apical PM. Bar 10µm. (c) Labeling of cells expressing HA-Vps8 and Rab11-mCherry with EEA1 reveals colocalization of Vps8 with EEA1 and Rab11. Bar 10µm. (d) IEM analysis of polarized HepG2 cells reveal that HA-Vps8 associates with tubules and vesicles of REs close to the BC (arrows indicate tubules, nearby lysosome (Ly) is negative). N=Nucleus, BC=Bile Canalliculus, Ly=Lysosome. Bar 2µm left panel, 200nm right panel.

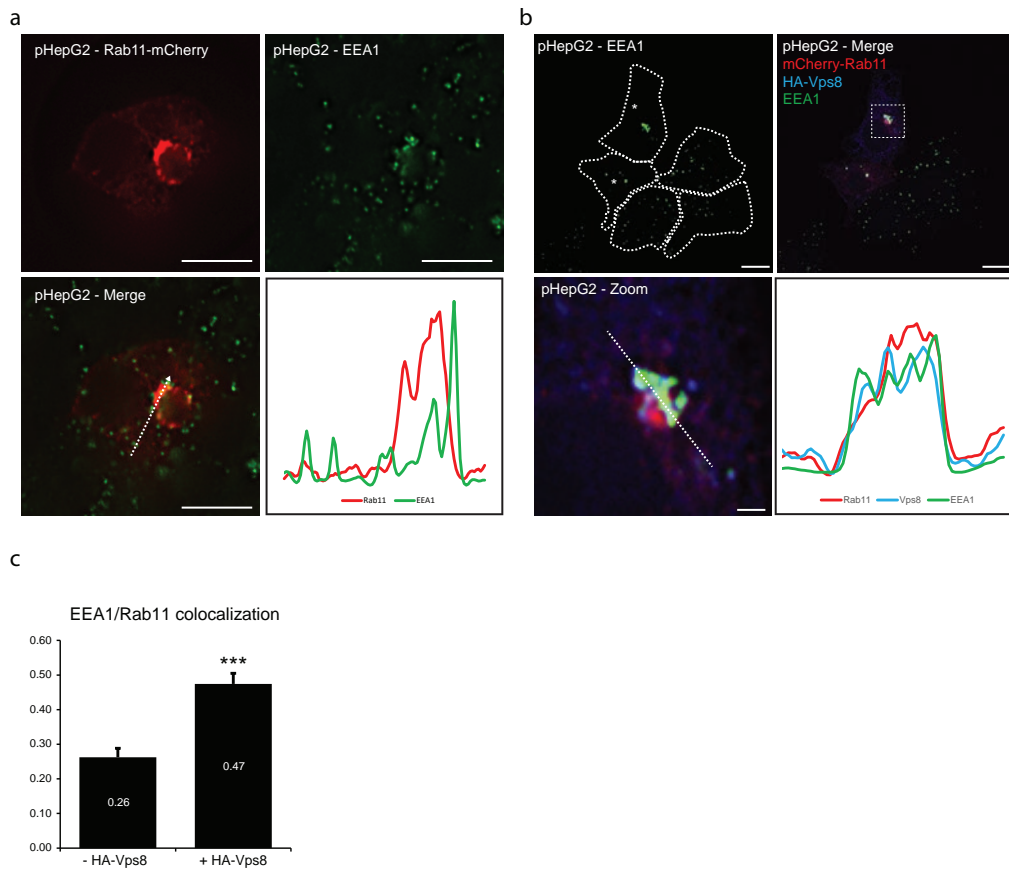


Figure 4 (a) Expression of Rab11-mCherry in HepG2 cells without co-expression HA-Vps8. Rab11 and EEA1 do not overlap. Bar 10 μ m. (b) Expression of Rab11-mCherry together with HA-Vps8 in HepG2 cells (marked with *) show high colocalization of Rab11, EEA1 and Vps8. Bar 10 μ m (c) Quantification of (a) and (b), colocalization between mCherry-Rab11 and EEA1 was measured using pixel based overlap. This shows a significant increase after co-expression of Vps8. Error bars represent the standard deviation of the mean (SD).

Vps8 is required for cell polarization

So far our data show that Vps8 is localized to EEs and the ARE and suggests a role in tethering of EE membranes to the ARE. This is in line with our previous data in non-polarized cells revealing that Vps8 in complex with Vps3 is required for vesicular transport from EEs to REs (chapter 3). Transport from the ARE to the apical PM is crucial for the establishment of cell polarity (5). To study a putative role for Vps8 in cell polarity we monitored the formation of BCs in HepG2 cells (fig. 5a, arrows). We visualized BCs with phalloidine and counted the number of BC per number of cells, an established method to evaluate the efficiency of cell polarization (33,34). Using this assay we found that knockdown of Vps8 significantly reduced the number of polarized cells (fig. 5b).

In addition to maintaining PM homeostasis in polarized cells, REs are also involved in cell migration by regulating the polarized distribution of integrins (the main extracellular matrix (ECM) anchoring proteins) (35–37) and for providing membrane for the generation of lamellopodia at the leading edge of a migrating cell (38). To study a putative role for Vps8 in migration-induced polarization we performed a directed cell migration assay using HeLa cells. Directed cell migration requires anterior to posterior polarization of the microtubular and endolysosomal networks and thereby induces polarization in non-polarized cell types such as HeLa. To investigate a possible role of Vps8 in this process, we knocked down Vps8 in HeLa cells and performed a wound healing assay. In this assay a scratch is made in a confluent layer of cells, resulting in directed migration of cells towards the wound (fig. 5c, red arrow shows the direction of the wound). Migration induced cell polarization is then quantified by measuring Golgi reorientation, which is the re-localization of the Golgi complex to the area between the nucleus and the leading edge of the cell (39). Knockdown of Vps8 led to a significant loss of Golgi reorientation (fig. 5d), as well as a reduced capability for wound closing after 20 hours (fig. 5e, 5f). Together these data show that Vps8 KD inhibits apical-basal cell polarization of HepG2 cells, as well as front-rear polarization of HeLa cells during cell migration.

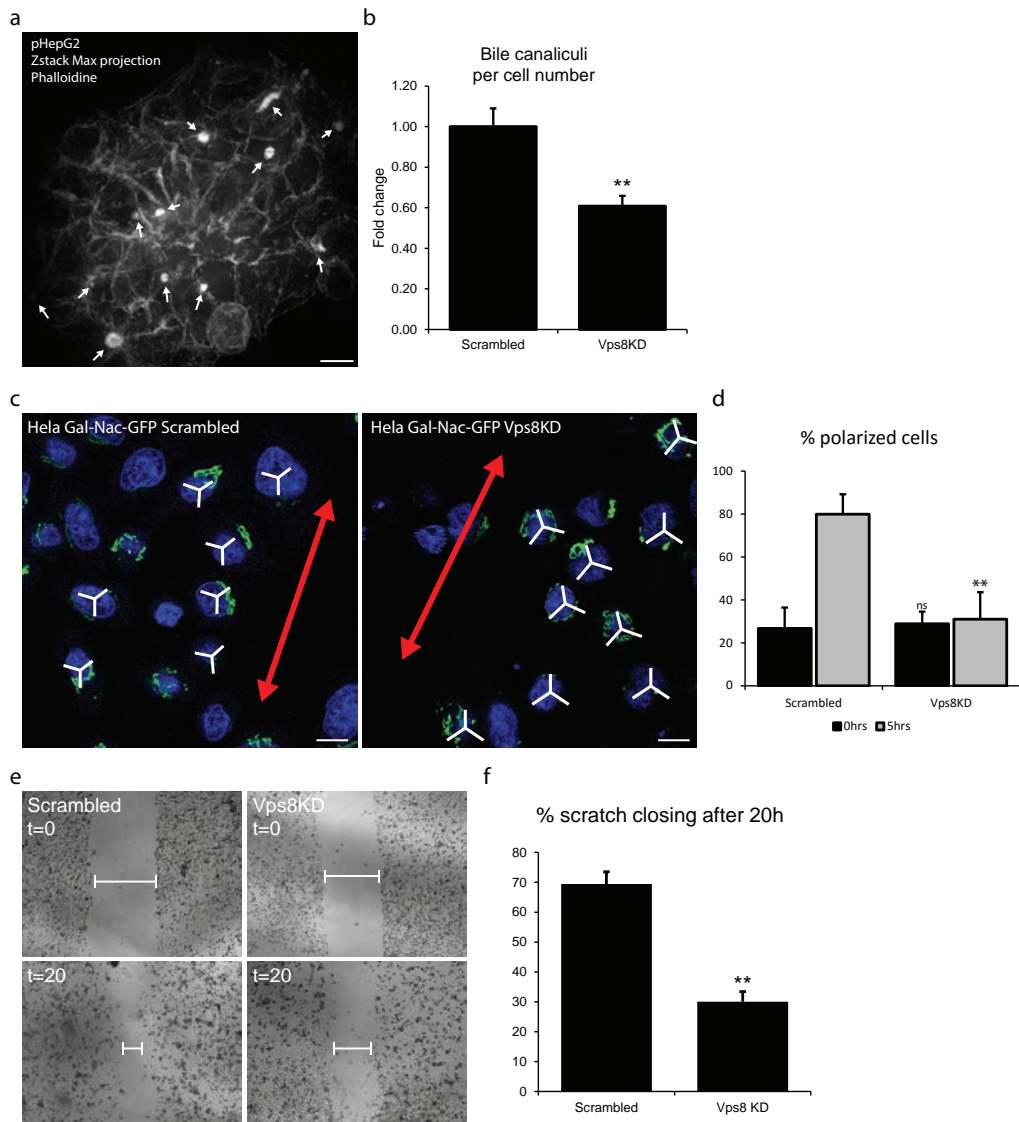


Figure 5 (a) Maximum projections of Zstacks taken from pHepG2 cells labeled with phalloidine show the formation of bile canaliculi (arrows). Bar 10µm (b) Quantification of BC's per number of cells represents the percentage of polarized cells. Knockdown of Vps8 or Vps3 and Vps8 shows a significant defect on cell polarization. (c) A Golgi reorientation assay on a confluent layer of HeLa cells shows decreased polarization of the Golgi (assessed by Golgi presence in 3 faces of the cell) towards the direction of the wound (wound direction indicated by red arrow) in scrambled treated cells (left panel) and Vps8KD cells (right panel). (d) Quantification of (c) shows a significant decrease in Golgi polarization 5 hours after application of the scratch. (e) Wound healing assay in a confluent layer of HeLa cells, 20 hours after the application of the scratch. Vps8 knockdown cells migrate less in the direction of the wound. (f) Quantification of (e) shows a significant decrease in wound closing.

Vps8 is required for completion of cytokinesis

During cytokinesis Rab11a positive vesicles travel to the intercellular bridge (ICB) for delivery of lipids and proteins required for the final stage of cell division (40–47). Completion of cytokinesis requires abscission of the ICB, a process that requires input from Rab11 positive REs (48). IF microscopy analysis of HepG2 cells revealed that endogenous Vps8 localizes to the ICB during late stages of cell division (fig. 6a), suggesting that Vps8 is involved in the abscission process. To test this hypothesis we knocked down Vps8 in HeLa cells and determined the amount of multinucleated cells, which is a measure for unsuccessful cell division (fig 6b). The knockdown of Vps8 increased the number of multinucleated cells more than 2-fold, indicating that cell division is impaired.

To determine at which stage the defect in cell division occurred, we used automated live cell microscopy to visualize defects in cytokinesis. Cells were synchronized by blocking cell division in the G1 phase using thymidine for 16 hours and subsequently released before imaging. Cells with Vps8 KD showed an overall increase in failure of abscission (fig. 6c, 6d left panel). Morphological analysis and quantification of individual cell divisions revealed that the defect predominantly occurs in the telophase (fig. 6d middle panel). Additionally, successful cell divisions were delayed, resulting in the significant increase of daughter cells that remained attached by the ICB more than 6 hours (fig. 6c, 6d right panel). These results show that similar to Rab11, Vps8 is required for the completion of cytokinesis. Cell division requires complete polarization of cells, which is in line with the role of Vps8 in recycling in polarized cells.

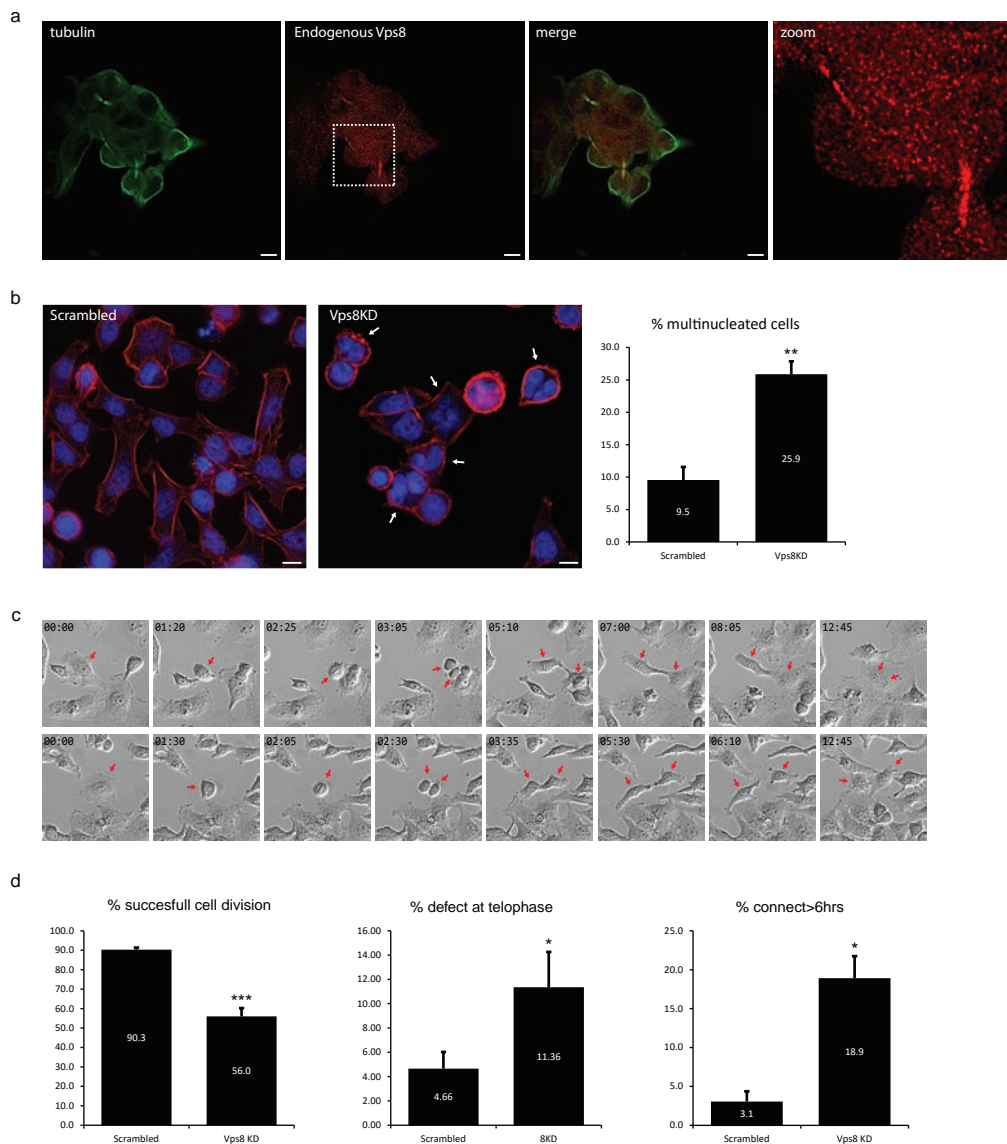


Figure 6 (a) Endogenous Vps8 and tubulin in HepG2 cells colocalize at the intercellular bridge (ICB) between 2 daughter cells during cytokinesis. Bar 10 μ m (b) 2 Hours after replating, Vps8KD cells show increased number of bi-, and multi-nucleated cells (arrows, middle panel) compared to the Scrambled treated cells (left panel). Quantification shows a more than twofold increase in the number of multinucleated cells (right panel). Bar 10 μ m (c) Stills taken from a time-lapse movie show an example failed abscission in a dividing cell in Vps8KD (red arrows, upper panels) and a normal abscission in scrambled cells (red arrows, lower panels). (d) Quantification of all cells in the timelapse movies show an overall decrease in success of cell division (left graph), an increase in defects at the telophase (middle graph) and an increase in cell divisions in which cells remain connected by the ICB for more than 6 hours (right graph).

Discussion

In this study we investigated the role of Vps8 in the endolysosomal system of polarized cells. We show that protein expression of Vps8 is increased in upon cell polarization and that Vps8 expression is increased in polarized cells of tissues such as the colon, epididymis and exocrine pancreas. High Vps8 expression allowed the detection of endogenous Vps8 using IF microscopy, which showed that Vps8 is localized to EEA1-positive EEs and Rab11-positive AREs. Overexpression of Vps8 showed this same localization pattern. Interestingly, overexpression of Vps8 in pHepG2 cells induced the recruitment of EEA1-positive EEs to Rab11-positive AREs, suggesting a role for Vps8 in the tethering of EE-derived membranes to the ARE. Pathways to and from the ARE are crucial for the establishment of cell polarity. Concomitantly, knockdown of Vps8 resulted in decreased apical-basal cell polarization of HepG2 cells and front-rear polarization of HeLa cells during directed cell migration. Finally, we found that, similar to Rab11, Vps8 localizes to the ICB between two daughter cells and knockdown of Vps8 reduces the efficiency of cell division. Like Rab11 deficiency, Vps8 mainly affects the telophase of cell division, slowing down or inhibiting the final abscission. Together our results show that Vps8 is required for cell polarization and we postulate that this is caused by regulating vesicular transport from EEs to the ARE. Our hypothesis is supported by the observation that defects in cell polarization after Vps8 knockdown result in very similar phenotypes to those caused by Rab11 deficiency.

We show that Vps8 localizes to EEA1-positive EEs as well as the Rab11-positive ARE. This unequivocally positions Vps8 in the apical recycling pathway. Since the CRE is Rab11 and EEA1 negative we do not expect an additional role for Vps8 in the basolateral pathway. However, further studies using basolateral and CRE-specific markers should be performed to formally rule out this possibility. In non-polarized cells, Vps8 functions in 2 separate complexes. Firstly, as part of the CORVET complex, Vps8 localizes to EEA1-positive EEs and regulates their homotypic fusion. Disruption of the CORVET complex alters the EE population, but does not inhibit transferrin recycling (27). Secondly, a separate complex of Vps3 and Vps8 localizes to EE-derived recycling vesicles and Rab11-positive REs and mediates transport from EEs to REs. Disruption of this complex inhibits the recycling of integrins but not transferrin (27) (chapter 3), indicating that the Vps3/8 complex is required for recycling of a subset of proteins only. Interestingly, the ARE is not involved in transport of transferrin (a basolateral recycling protein) either (7,49), providing a possible link between the Vps3/Vps8-mediated EE to RE pathway in non-polarized cells and apical EE to ARE transport in polarized cells. Together with the observed induction in EE-ARE tethering upon Vps8 overexpression, these results indicate a tethering role for Vps8 in apical EE to ARE transport as part of the Vps3/8 complex. The pathway between EEs and AREs in polarized epithelial cells is not well-characterized since the majority of transport between EEs and the ARE occurs via the CRE (4,28,50–52). Our studies provide a possible clue for a specialized machinery designed for an apical recycling pathway bypassing the CRE.

The Vps3/8 complex functions together with the Vps33B/VIPAS39 complex in the recycling of integrins in non-polarized cells (chapter 3). Mutations in Vps33B or VIPAS39 result in arthrogyrosis, renal dysfunction and cholestasis (ARC) syndrome, a rare autosomal recessive multisystemic disorder that primarily affects the liver, kidney, skin, and central nervous and musculoskeletal systems (19,20,23,53). On a cellular level, Vps33B or VIPAS39 localize to Rab11-positive REs and their disease-causing mutations causes mislocalization of apical and junctional

proteins and inhibit cell polarization (19,20). Our observations presented here connect Vps8 to the role of Vps33B and VIPAS39 in recycling of apical proteins, implicating Vps8 as an additional ARC syndrome target. The connection between Vps8 and ARC syndrome is supported by the recent discovery of Vps8 mutations in patients suffering from arthrogyposis (54).

During directed cell migration, cells polarize towards a given stimulus, which requires adjusting of their cytoskeletal and endolysosomal system (55). Here we show that knockdown of Vps8 in HeLa cells reduces this polarization and inhibits cell migration. In a previous study we showed that knockdown of Vps3 and Vps8 inhibited random cell migration as a result of decreased β 1 integrin recycling (chapter 3). Random migration of cells in 2D is promoted by β 1 integrin signaling pathways, whereas directed cell migration is promoted by signaling from β 3 integrins (56–58). Specific recycling of β 1 or β 3 integrins therefore regulates random or directed cell migration, respectively. Preliminary studies using IEM failed to detect β 3 integrins as cargo for the Vps3/8-dependent transport pathway (unpublished observations). Therefore, we do not think it likely that the reduction of directed cell migration presented here is caused by reduced β 3 integrin recycling. Determining the recycling efficiency of β 3 integrin after Vps8 knockdown could unequivocally exclude this hypothesis. In addition, identification of additional cargo of the Vps8-positive recycling vesicles is necessary to determine which proteins influence the front-rear polarization during directed cell migration.

Here we localized Vps8 to the site of abscission, providing the first ever link between Vps8 and cytokinesis. During cytokinesis, vesicular transport from Rab11-positive REs is needed to complete abscission (48,59–61). Knockdown of Vps8 reduced successful cytokinesis, similar to the effect of Rab11 knockdown (48). This suggests that disruption of Vps8 dependent transport to REs causes defects in cytokinesis. Alternatively, Rab35, an EE-protein that regulates Arf6-dependent recycling to the PM, is also required for successful abscission (62). However, dominant negative Rab35 expression results in severe accumulation of transferrin-positive endosomes (63), a phenotype that was not observed after Vps8 knockdown. Therefore we postulate that disruption of EE-to-RE transport by Vps8 knockdown results in the observed failed and delayed abscission. Taken together, our data show a role for Vps8 in the apical recycling pathway of polarized cells, which is important for induction of cellular polarity.

Materials & Methods

Cell culture and transfection

All cell lines were grown at 37°C and 5% CO₂. HeLa cells (ATCC clone ccl-2) were cultured in Dulbecco's modified Eagle's medium (DMEM) supplemented with 10% heat inactivated Fetal Bovine Serum (FBS), 2mM L-Glutamin, 100U/mL penicillin and 100µg/mL streptomycin (hereafter complete DMEM). MDCK cells were grown in 8-well chamber slides (Ibidi), pre coated with a thin layer of matrigel (BD-biosciences). Per well 10.000 cells were resuspended in 1x DMEM containing a final concentration of 20mM HEPES (Sigma), 56ug/mL collagen I (Sigma), 10% heat inactivated FBS, 100U/mL penicillin, 100µg/mL streptomycin, 2mM L-Glutamin and 50% Matrigel Basement Membrane Matrix (BD-biosciences). After solidifying overnight, fresh 1xDMEM containing 10%FBS and P/S was added on top of the matrix and refreshed every 48 hours. HepG2 cells were grown in complete DMEM. For imaging HepG2 cells were grown on glass coverslips coated with 30ug/mL Collagen to induce polarization. LS174T-W4 cells (64) were grown in RPMI1640 supplemented with 10% Tetracyclin-free heat inactivated FBS, 2mM L-Glutamin, 100U/mL penicillin and 100µg/mL streptomycin. Induction of polarization was achieved by addition of 1 ug/ml doxycycline to the culture medium for at least 16hours. HeLa cells were transfected with cDNA using Effectene transfection reagent (Qiagen) according to the manufacturer's protocol. HepG2 cells and LS174T-W4 cells were transfected using Polyethylenimine (PEI) in a ratio of 1/5 cDNA/PEI, using a protocol implementing a chase time. siRNA transfection was performed using HiPerfect transfection Reagent (Qiagen) according to manufacturer's protocol.

Antibodies

For immunofluorescence and Immuno-EM labeling: Rabbit-anti-Vps8 (Sigma), Mouse anti-HA (Covance), Goat anti-HA (Genscript), Rabbit anti-GFP (Acris), Mouse anti GM130 (BD). Rabbit anti-goat IGG (NORDIC) or rabbit anti-mouse IGG (Dako) was used to bridge between goat or mouse antibodies and protein-A gold (65). Fluorescent secondary antibodies were obtained from Invitrogen. For Immunoprecipitation and western blot we used Mouse anti-GFP (Roche), Mouse-anti-FLAG (M2, Sigma), Mouse anti-HA (Covance), Mouse-anti-Rab11 (clone47, BD) and Rabbit anti-GFP (Abcam). Fluorescent secondary antibodies were obtained from Li-Cor.

Reagents

5nm gold particles coupled to bovine serum albumin (BSA-Au5) and 10nm or 15nm gold particles conjugated to Protein-A were made on site (Cell Microscopy Core, UMC Utrecht, The Netherlands). HA-Vps8, Vps8-V5 and Vps8-GFP, untagged Vps33B were cloned from Vps8 cDNA purchased from Origen. Rab11-GFP and Rab11-mCherry were made on site. Vps8, Vps3, Vps11 and Vps41 SMARTPool siRNAs were purchased from Dharmacon. Nocodazole was purchased from Sigma.

Western blot

Cells were washed in ice cold PBS and scraped in E1A lysisbuffer (40mM TRIS pH7.4, 100mM NaCl, 0.1%TX-100, 5mMEDTA supplemented with cOMplete protease inhibitors (Roche)). Cells were lysed for 30min at 4°C followed by 15min centrifugation at max speed at 4°C to remove cell debris. Proteins were eluted using 1.5x sample buffer for 30min at 37°C, separated on a 7.5 or 10% SDS-PAGE and transferred to Immobilon-FL PVDF membrane (Millipore). Membranes were blocked at room temperature using Odyssey blocking buffer in PBS (1:1) for 1 hour and incubated with selected primary antibodies diluted in Odyssey blocking buffer in PBST 0,2% (1:1). Membranes were washed in PBST 0,1% and incubated with desired secondary antibodies diluted in Odyssey blocking buffer in PBST 0,2% (1:1) for 1 hour at room temperature. Finally membranes were washed and imaged on an Odyssey imaging system (Li-Cor).

Immunofluorescence microscopy

Cells grown on sterile glass coverslips were washed with ice-cold PBS and fixed with 4% paraformaldehyde (PFA) in PBS for 20 minutes at RT (room temperature). Then, cells were permeabilized using 0,1% Triton-X100 in PBS for 5 minutes and blocked for 15 minutes using PBS supplemented with 1% BSA. Cells were labeled with primary antibodies diluted in blocking buffer at RT for 1 hour, washed, and labeled with fluorescent secondary antibodies for 30 minutes in the dark. After labeling the cells were washed and mounted using Prolong Gold antifade reagent with DAPI. MDCK cells grown in Matrigel on chamberslides were processed the same except these alterations: Primary antibody was added overnight instead of 1 hour, secondary antibody was added for 3 hours instead of 30 minutes, Prolong Gold antifade reagent with DAPI was pipetted on top. Cells were imaged on a Deltavision wide field microscope using a 100x/1.4A immersion objective or a Zeiss LSM700 confocal microscope using a 63X/1.4 immersion objective. 3D MDCK cells were imaged using the 20x 20X/0.8 objective on the LSM700. Widefield pictures were deconvolved using Softworx software and analyzed using FIJI.

Immuno-electron microscopy

Sample preparation, ultrathin cryosectioning and immunolabeling were performed as in (65). In brief, cells were grown on 60mm dishes and fixed by the addition of freshly prepared 4% wt/vol paraformaldehyde (PFA) in 0.1M Phosphate buffer pH7.4 to an equal volume of culture medium for 10 min, followed by postfixation with fresh 4%PFA overnight at 4°C. Fixed cells were washed in PBS containing 0.05M glycine and gently scraped in PBS containing 1% gelatin. Cells were pelleted in 12% gelatin in PBS which was then left to solidify on ice and cut into small blocks. The blocks were infiltrated overnight in 2.3M sucrose at 4°C, mounted on alluminium pins and frozen in liquid nitrogen. 70nm ultrathin cryosections were cut on a Leica ultracut UCT ultracryomicotome and picked up in a freshly prepared 1:1 mixture of 2.3M sucrose and 1.8% methylcellulose. Sections were then immunogold labeled with antibodies and protein-A gold and examined on a JEOL TEM 1010 electron microscope.

Wound healing assay

HeLa cells were grown to 90% confluency, after which they were treated with 10 µg/ml of Mitomycin C (Sigma) for 3 hours to inhibit proliferation. Three hours after addition of Mitomycin C, cells were washed twice with 1X PBS and a linear scratch was made on the plate using a yellow tip. The cells were washed one more time with 1X PBS. The cells were then returned to complete medium and observed under an Inverted microscope fitted with a stage maintained at 37°C and 5% CO₂. Cells were observed for 20 hr. Migration was measured using ImageJ software. The wound was photographed at three positions across the length of the wound. Migration is the difference between wound width at time 0 hr and time 20 hr.

Golgi reorientation assay

HeLa Cells knocked down for target proteins were seeded in a glass bottom 35mm to a confluency of 90%. A linear scratch wound is made in the confluent monolayer with a pipette tip. Cells were fixed at 0 and 5-6 h following wounding. The Golgi was stained with an antibody directed against the Golgi-specific membrane protein GM130 and the nucleus stained with DAPI. To measure Golgi orientation, 120° angles were drawn (Image J) from the center of the nucleus on cells that lined the edge of the wound, creating three sectors. The angles were drawn such that one of the 120° sectors faced the edge of the wound (sector A). If the Golgi encompassed a sector away from the wound edge or spanned any two sectors, it was categorized as polarized in a different direction away from the wound edge. Golgi found within all three sectors were classified as non-polarized. All of the cells at the wound edge in three fields were categorized (120–150 total cells) per siRNA treatment and per time point.

Cytokinesis Imaging

HeLa cells knocked down for target proteins were treated overnight with thymidine to block cells in the G₁ phase. Cells were washed 3 times with warm 1XPBS and placed in complete medium and imaged for 16 hours under an Inverted microscope fitted with a stage maintained at 37°C and 5% CO₂. All cells going through cell division were counted manually to score the defect per stage of cell division.

Acknowledgments

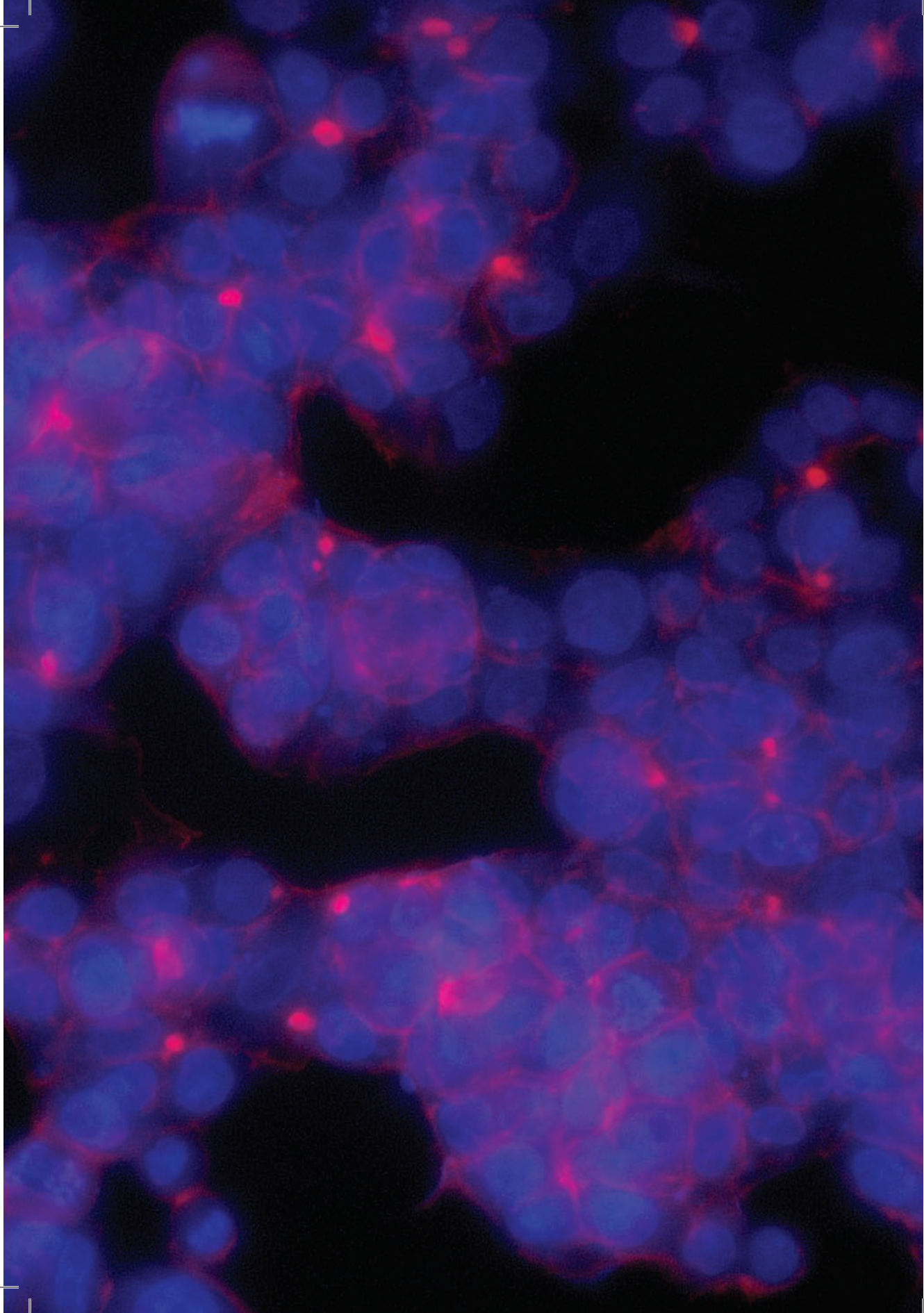
We thank Timo Kuijt for assistance with cytokinesis imaging, Lucas Bruurs and Hans Bos for kindly providing the LS174T-W4 cells, Peter van der Sluijs for valuable constructs and René Scriwanek for preparation of EM figures.

References

1. Drubin DG, Nelson WJ. Origins of cell polarity. *Cell*. 1996 Feb 9;84(3):335–344.
2. Balda MS, Matter K. Tight junctions. *J Cell Sci*. 1998 Mar;111 (Pt 5):541–547.
3. Sheff DR, Kroschewski R, Mellman I. Actin dependence of polarized receptor recycling in Madin-Darby canine kidney cell endosomes. *Mol Biol Cell*. 2002 Jan;13(1):262–275.
4. Wang E, Brown PS, Aroeti B, Chapin SJ, Mostov KE, Dunn KW. Apical and basolateral endocytic pathways of MDCK cells meet in acidic common endosomes distinct from a nearly-neutral apical recycling endosome. *Traffic*. 2000 Jun;1(6):480–493.
5. Golachowska MR, Hoekstra D, van IJzendoorn SC. Recycling endosomes in apical plasma membrane domain formation and epithelial cell polarity. *Trends Cell Biol*. 2010 Oct;20(10):618–626.
6. Apodaca G, Katz LA, Mostov KE. Receptor-mediated transcytosis of IgA in MDCK cells is via apical recycling endosomes. *J Cell Biol*. 1994 Apr;125(1):67–86.
7. Brown PS, Wang E, Aroeti B, Chapin SJ, Mostov KE, Dunn KW. Definition of distinct compartments in polarized Madin-Darby canine kidney (MDCK) cells for membrane-volume sorting, polarized sorting and apical recycling. *Traffic*. 2000 Feb;1(2):124–140.
8. Mostov K, Su T, ter Beest M. Polarized epithelial membrane traffic: conservation and plasticity. *Nat Cell Biol*. 2003 Apr;5(4):287–293.
9. Weisz OA, Rodriguez-Boulan E. Apical trafficking in epithelial cells: signals, clusters and motors. *J Cell Sci*. 2009 Dec 1;122(Pt 23):4253–4266.
10. Mellman I, Nelson WJ. Coordinated protein sorting, targeting and distribution in polarized cells. *Nat Rev Mol Cell Biol*. 2008 Nov;9(11):833–845.
11. Roland JT, Bryant DM, Datta A, Itzen A, Mostov KE, Goldenring JR. Rab GTPase-Myo5B complexes control membrane recycling and epithelial polarization. *Proc Natl Acad Sci U S A*. 2011 Feb 15;108(7):2789–2794.
12. Roland JT, Kenworthy AK, Peranen J, Caplan S, Goldenring JR. Myosin Vb interacts with Rab8a on a tubular network containing EHD1 and EHD3. *Mol Biol Cell*. 2007 Aug;18(8):2828–2837.
13. Lapierre LA, Kumar R, Hales CM, Navarre J, Bhartur SG, Burnette JO, et al. Myosin vb is associated with plasma membrane recycling systems. *Mol Biol Cell*. 2001 Jun;12(6):1843–1857.
14. Perez Bay AE, Schreiner R, Mazzoni F, Carvajal-Gonzalez JM, Gravotta D, Perret E, et al. The kinesin KIF16B mediates apical transcytosis of transferrin receptor in AP-1B-deficient epithelia. *EMBO J*. 2013 Jul 31;32(15):2125–2139.
15. Goldenring JR, Smith J, Vaughan HD, Cameron P, Hawkins W, Navarre J. Rab11 is an apically located small GTP-binding protein in epithelial tissues. *Am J Physiol*. 1996 Mar;270(3 Pt 1):G515–G525.
16. Babbey CM, Ahktar N, Wang E, Chen CC, Grant BD, Dunn KW. Rab10 regulates membrane transport through early endosomes of polarized Madin-Darby canine kidney cells. *Mol Biol Cell*. 2006 Jul;17(7):3156–3175.
17. Schuck S, Gerl MJ, Ang A, Manninen A, Keller P, Mellman I, et al. Rab10 is involved in basolateral transport in polarized Madin-Darby canine kidney cells. *Traffic*. 2007 Jan;8(1):47–60.
18. Tzaban S, Massol RH, Yen E, Hamman W, Frank SR, Lapierre LA, et al. The recycling and transcytotic pathways for IgG transport by FcRn are distinct and display an inherent polarity. *J Cell Biol*. 2009 May 18;185(4):673–684.
19. Cullinane AR, Straatman-Iwanowska A, Zaucker A, Wakabayashi Y, Bruce CK, Luo G, et al. Mutations in VIPAR cause an arthrogyriposis, renal dysfunction and cholestasis syndrome phenotype with defects in epithelial polarization. *Nat Genet*. 2010 Apr;42(4):303–312.
20. Smith H, Galmes R, Gogolina E, Straatman-Iwanowska A, Reay K, Banushi B, et al. Associations among genotype, clinical phenotype, and intracellular localization of trafficking proteins in ARC syndrome. *Hum Mutat*. 2012 Dec;33(12):1656–1664.
21. Van der Kant R, Jonker CT, Wijdeven RH, Bakker J, Janssen L, Klumperman J, et al. Characterization of the mammalian CORVET and HOPS complexes and their modular restructuring for endosome specificity. *J Biol Chem*. 2015 Oct 13;
22. Tornieri K, Zlatich SA, Mullin AP, Werner E, Harrison R, L'hernault SW, et al. Vps33b pathogenic mutations preferentially affect VIPAS39/SPE-39-positive endosomes. *Hum Mol Genet*. 2013 Dec 20;22(25):5215–5228.
23. Gissen P, Johnson CA, Morgan NV, Stapelbroek JM, Forshew T, Cooper WN, et al. Mutations in VPS33B, encoding a regulator of SNARE-dependent membrane fusion, cause arthrogyriposis-renal dysfunction-cholestasis (ARC) syndrome. *Nat Genet*. 2004 Apr;36(4):400–404.

24. Pols MS, ten Brink C, Gosavi P, Oorschot V, Klumperman J. The HOPS proteins hVps41 and hVps39 are required for homotypic and heterotypic late endosome fusion. *Traffic*. 2013 Feb;14(2):219–232.
25. Galmes R, Ten Brink C, Oorschot V, Veenendaal T, Jonker C, van der Sluijs P, et al. Vps33B is required for delivery of endocytosed cargo to lysosomes. *Traffic*. 2015 Dec;16(12):1288–1305.
26. Uhlén M, Fagerberg L, Hallström BM, Lindskog C, Oksvold P, Mardinoglu A, et al. Proteomics. Tissue-based map of the human proteome. *Science*. 2015 Jan 23;347(6220):1260419.
27. Perini ED, Schaefer R, Stöter M, Kalaidzidis Y, Zerial M. Mammalian CORVET is required for fusion and conversion of distinct early endosome subpopulations. *Traffic*. 2014 Dec;15(12):1366–1389.
28. Van IJendoorn SC, Hoekstra D. The subapical compartment: a novel sorting centre? *Trends Cell Biol*. 1999 Apr;9(4):144–149.
29. Van IJendoorn SC, Hoekstra D. (Glyco)sphingolipids are sorted in sub-apical compartments in HepG2 cells: a role for non-Golgi-related intracellular sites in the polarized distribution of (glyco)sphingolipids. *J Cell Biol*. 1998 Aug 10;142(3):683–696.
30. Zegers MM, Zaal KJ, van IJendoorn SC, Klappe K, Hoekstra D. Actin filaments and microtubules are involved in different membrane traffic pathways that transport sphingolipids to the apical surface of polarized HepG2 cells. *Mol Biol Cell*. 1998 Jul;9(7):1939–1949.
31. Klumperman J, Raposo G. The complex ultrastructure of the endolysosomal system. *Cold Spring Harb Perspect Biol*. 2014 Oct;6(10):a016857.
32. Ohgaki R, Matsushita M, Kanazawa H, Ogihara S, Hoekstra D, van IJendoorn SC. The Na⁺/H⁺ exchanger NHE6 in the endosomal recycling system is involved in the development of apical bile canalicular surface domains in HepG2 cells. *Mol Biol Cell*. 2010 Apr 1;21(7):1293–1304.
33. Van der Wouden JM, van IJendoorn SC, Hoekstra D. Oncostatin M regulates membrane traffic and stimulates bile canalicular membrane biogenesis in HepG2 cells. *EMBO J*. 2002 Dec 2;21(23):6409–6418.
34. Van IJendoorn SC, Hoekstra D. Polarized sphingolipid transport from the subapical compartment changes during cell polarity development. *Mol Biol Cell*. 2000 Mar;11(3):1093–1101.
35. Roberts M, Barry S, Woods A, van der Sluijs P, Norman J. PDGF-regulated rab4-dependent recycling of alphavbeta3 integrin from early endosomes is necessary for cell adhesion and spreading. *Curr Biol*. 2001 Sep 18;11(18):1392–1402.
36. Powelka AM, Sun J, Li J, Gao M, Shaw LM, Sonnenberg A, et al. Stimulation-dependent recycling of integrin beta1 regulated by ARF6 and Rab11. *Traffic*. 2004 Jan;5(1):20–36.
37. Caswell PT, Norman JC. Integrin trafficking and the control of cell migration. *Traffic*. 2006 Jan;7(1):14–21.
38. Nabi IR. The polarization of the motile cell. *J Cell Sci*. 1999 Jun;112 (Pt 12):1803–1811.
39. Kupfer A, Dennert G, Singer SJ. Polarization of the Golgi apparatus and the microtubule-organizing center within cloned natural killer cells bound to their targets. *Proc Natl Acad Sci U S A*. 1983 Dec;80(23):7224–7228.
40. Riggs B, Fasulo B, Royou A, Mische S, Cao J, Hays TS, et al. The concentration of Nuf, a Rab11 effector, at the microtubule-organizing center is cell cycle regulated, dynein-dependent, and coincides with furrow formation. *Mol Biol Cell*. 2007 Sep;18(9):3313–3322.
41. Pelissier A, Chauvin JP, Lecuit T. Trafficking through Rab11 endosomes is required for cellularization during *Drosophila* embryogenesis. *Curr Biol*. 2003 Oct 28;13(21):1848–1857.
42. Hickson GR, Matheson J, Riggs B, Maier VH, Fielding AB, Prekeris R, et al. Arfophilins are dual Arf/Rab 11 binding proteins that regulate recycling endosome distribution and are related to *Drosophila* nuclear fallout. *Mol Biol Cell*. 2003 Jul;14(7):2908–2920.
43. Skop AR, Bergmann D, Mohler WA, White JG. Completion of cytokinesis in *C. elegans* requires a brefeldin A-sensitive membrane accumulation at the cleavage furrow apex. *Curr Biol*. 2001 May 15;11(10):735–746.
44. Prekeris R, Gould GW. Breaking up is hard to do- membrane traffic in cytokinesis. *J Cell Sci*. 2008 May 15;121(Pt 10):1569–1576.
45. Barr FA, Gruneberg U. Cytokinesis: placing and making the final cut. *Cell*. 2007 Nov 30;131(5):847–860.
46. Gromley A, Yeaman C, Rosa J, Redick S, Chen CT, Mirabelle S, et al. Centriolin anchoring of exocyst and SNARE complexes at the midbody is required for secretory-vesicle-mediated abscission. *Cell*. 2005 Oct 7;123(1):75–87.
47. Boucrot E, Kirchhausen T. Endosomal recycling controls plasma membrane area during mitosis. *Proc Natl Acad Sci*

- U S A. 2007 May 8;104(19):7939–7944.
48. Wilson GM, Fielding AB, Simon GC, Yu X, Andrews PD, Hames RS, et al. The FIP3-Rab11 protein complex regulates recycling endosome targeting to the cleavage furrow during late cytokinesis. *Mol Biol Cell*. 2005 Feb;16(2):849–860.
 49. Leung SM, Ruiz WG, Apodaca G. Sorting of membrane and fluid at the apical pole of polarized Madin-Darby canine kidney cells. *Mol Biol Cell*. 2000 Jun;11(6):2131–2150.
 50. Ullrich O, Reinsch S, Urbé S, Zerial M, Parton RG. Rab11 regulates recycling through the pericentriolar recycling endosome. *J Cell Biol*. 1996 Nov;135(4):913–924.
 51. Odorizzi G, Pearse A, Domingo D, Trowbridge IS, Hopkins CR. Apical and basolateral endosomes of MDCK cells are interconnected and contain a polarized sorting mechanism. *J Cell Biol*. 1996 Oct;135(1):139–152.
 52. Hoekstra D, Tyteca D, van IJendoorn SC. The subapical compartment: a traffic center in membrane polarity development. *J Cell Sci*. 2004 May 1;117(Pt 11):2183–2192.
 53. Gissen P, Tee L, Johnson CA, Genin E, Caliebe A, Chitayat D, et al. Clinical and molecular genetic features of ARC syndrome. *Hum Genet*. 2006 Oct;120(3):396–409.
 54. Bayram Y, Karaca E, Coban Akdemir Z, Yilmaz EO, Tayfun GA, Aydin H, et al. Molecular etiology of arthrogryposis in multiple families of mostly Turkish origin. *J Clin Invest*. 2016 Feb 1;126(2):762–778.
 55. Dow LE, Humbert PO. *Polarity Regulators and the Control of Epithelial Architecture, Cell Migration, and Tumorigenesis*. Elsevier; 2007. p. 253–302.
 56. Danen EH, van Rheenen J, Franken W, Huvencuers S, Sonneveld P, Jalink K, et al. Integrins control motile strategy through a Rho-cofilin pathway. *J Cell Biol*. 2005 May 9;169(3):515–526.
 57. Petrie RJ, Doyle AD, Yamada KM. Random versus directionally persistent cell migration. *Nat Rev Mol Cell Biol*. 2009 Aug;10(8):538–549.
 58. White DP, Caswell PT, Norman JC. α v β 3 and α 5 β 1 integrin recycling pathways dictate downstream Rho kinase signaling to regulate persistent cell migration. *J Cell Biol*. 2007 May 7;177(3):515–525.
 59. Fielding AB, Schonteich E, Matheson J, Wilson G, Yu X, Hickson GR, et al. Rab11-FIP3 and FIP4 interact with Arf6 and the exocyst to control membrane traffic in cytokinesis. *EMBO J*. 2005 Oct 5;24(19):3389–3399.
 60. Schiel JA, Childs C, Prekeris R. Endocytic transport and cytokinesis: from regulation of the cytoskeleton to midbody inheritance. *Trends Cell Biol*. 2013 Jul;23(7):319–327.
 61. Schiel JA, Simon GC, Zaharris C, Weisz J, Castle D, Wu CC, et al. FIP3-endosome-dependent formation of the secondary ingression mediates ESCRT-III recruitment during cytokinesis. *Nat Cell Biol*. 2012 Oct;14(10):1068–1078.
 62. Chesneau L, Dambournet D, Machicoane M, Kouranti I, Fukuda M, Goud B, et al. An ARF6/Rab35 GTPase cascade for endocytic recycling and successful cytokinesis. *Curr Biol*. 2012 Jan 24;22(2):147–153.
 63. Kouranti I, Sachse M, Arouche N, Goud B, Echard A. Rab35 regulates an endocytic recycling pathway essential for the terminal steps of cytokinesis. *Curr Biol*. 2006 Sep 5;16(17):1719–1725.
 64. Bruurs LJ, Donker L, Zwakenberg S, Zwartkruis FJ, Begthel H, Knisely AS, et al. ATP8B1-mediated spatial organization of Cdc42 signaling maintains singularity during enterocyte polarization. *J Cell Biol*. 2015 Sep 28;210(7):1055–1063.
 65. Slot JW, Geuze HJ. Cryosectioning and immunolabeling. *Nat Protoc*. 2007;2(10):2480–2491.
 66. Uhlen M, Oksvold P, Fagerberg L, Lundberg E, Jonasson K, Forsberg M, et al. Towards a knowledge-based Human Protein Atlas. *Nat Biotechnol*. 2010 Dec 1;28(12):1248–1250.



The Smad4 chaperone and CORVET subunit TGFBRAP1/Vps3 has a dual role in TGF β receptor signalling and trafficking

Caspar TH Jonker¹, A.R. Lourenço², C. ten Brink¹, C. de Heus¹, M.C. Rotteveel¹, R. Baas², M. Timmers², P. Coffier², J. Klumperman¹.

¹ Department of Cell Biology, Center for Molecular Medicine, University Medical Center Utrecht, the Netherlands.

² Regenerative Medicine Center, University Medical Center Utrecht, The Netherlands.

Chapter 5

Abstract

The TGF β signaling pathway regulates the expression of target genes through a downstream cascade of Smad proteins. Activated TGF β receptors phosphorylate a complex of Smad2 and Smad3, which require Smad4 to transfer to the nucleus to modulate target gene expression. Recruitment of Smad4 to the TGF β receptor and Smad2/3 complexes is chaperoned by TGFBRAP1, which was recently identified as the TGFBRAP1/Vps3 subunit of the early endosomal class-C core vacuole endosome transport (CORVET) tethering complex. Suggesting a dual role in trafficking and signaling. Since the trafficking role of TGFBRAP1/Vps3 requires recruitment to endosomes, we investigated whether the signaling role of TGFBRAP1/Vps3 also depends on its endosomal localization. We find that TGFBRAP1/Vps3 together with its interaction partner Vps8 facilitates the endosomal recruitment of Smad4. Additionally, we find that TGFBRAP1/Vps3 and Vps8 are required for recycling of TGF β receptor II from endosomes to the plasma membrane. Moreover, TGFBRAP1/Vps3 or Vps8 overexpression decreases TGF β -induced downstream target gene transcription. Together our findings identify TGF β receptors as cargo for a recently discovered Vps3/8-regulated recycling pathway, and imply a role for TGFBRAP1/Vps3 and Vps8 in TGF β signaling, which depends on their endosomal localization.

Introduction

5 Transforming growth factor-beta (TGF β) is a cytokine belonging to the TGF- β superfamily of growth factors, which includes Bone Morphogenetic Proteins (BMPs) and Growth and differentiation factors (GDFs). TGF β -family members regulate cell proliferation, tissue homeostasis and cell motility by modulating the expression of hundreds of genes in a cell type specific manner (1,2). Disruption of these factors or their downstream pathways are associated with many severe human diseases like cancer, diabetes, immunity disorders, Parkinson's disease, tissue fibrosis and heart disease (3–8). TGF β signaling starts with binding of TGF β to type II cell surface receptors (TGFBR II), which induces complex formation with type I (TGFBR I) receptors. The Ser/Thr kinase TGFBR II then phosphorylates TGFBR I , which triggers the association and phosphorylation of Receptor-regulated Smad proteins Smad2 and Smad3 (R-Smads). The phosphorylated R-Smads then bind the co-Smad Smad4, after which the Smad2/3/4 complex shuttles to the nucleus. There they act as transcriptional regulators that modulate the expression of an extensive amount of genes (1,9–11).

Endocytosis provides a mechanism to up or downregulate signaling from cell surface receptors. For example, the availability of positively regulating effector proteins on endosomes can enhance signaling. Alternatively, endocytosis can negatively regulate signaling by separating receptors from cytosolic effectors, inducing receptor-ligand dissociation, and ultimately, by receptor degradation (12–16). Receptors that are not degraded can be recycled to the plasma membrane (PM) to participate in an additional round of signaling (17–19). These regulatory mechanisms provide a tight association between the endocytic pathway and receptor mediated signaling.

TGFBR I and TGFBR II are constitutively internalized (20–22), although endocytosis can also be triggered by ligand binding. (23–25). After transport to early endosomes (EEs), activated receptor complexes associate with Smad Anchor for Receptor Activation (SARA), which is recruited to EEs by binding phosphatidylinositol-3-phosphate (PI3P) (26). SARA recruits Smad2 to the activated

TGF β receptor complex on endosomes, thereby facilitating the phosphorylation of Smad2 by the receptor complex (26–28). Since SARA-mediated Smad activation can only occur at EEs, endocytosis is a crucial step in TGF β signaling (22,28,29).

Transforming growth factor-beta receptor associated protein 1 (TGFBRAP1) was initially identified as a Smad4 chaperone in the TGF β signaling cascade. TGFBRAP1 binds Smad4 and TGF β receptor 2 (TGFBR2), mediating the transfer of Smad4 to the phosphorylated Smad2/3 complex (30). Interestingly, TGFBRAP1 was recently identified as a subunit of the mammalian EE class-C core vesicle endosome tethering (CORVET) complex (31,32). This highly conserved multisubunit tethering complex consists of Vps3, Vps8, Vps11, Vps16, Vps18 and Vps33a. As part of the CORVET complex, TGFBRAP1/Vps3 mediates the homotypic fusion of EEs (32). Independent from CORVET, TGFBRAP1/Vps3 and are required for vesicular transport from EEs to REs (chapter 3). The identification of TGFBRAP1 as the Vps3 subunit of CORVET raises a number of interesting questions. The model of Wurthner et. al. (30) describes the function of TGFBRAP1 before the connection with CORVET was made. Therefore it is unknown if any of the other CORVET subunits are involved in the Smad4 chaperone function. Moreover, since TGFBRAP1/Vps3 is recruited to EEs and recycling vesicles for its role in membrane trafficking (31,32), this poses the question whether an endosomal localization is also required for its chaperone function.

Here, we examine the function of TGFBRAP1/Vps3 as a Smad4 chaperone in relation to its localization on EEs. In our studies we include Vps8, which is required for endosomal localization of TGFBRAP1/Vps3. We find that both TGFBRAP1/Vps3 and Vps8 affect TGF β signaling by regulating the endosomal recruitment of Smad4, as well as by regulating the endosomal recycling of TGFBR2. Our data directly link the vesicular transport function of TGFBRAP1/Vps3 to its role in signalling.

Results

TGF β pathway activation downregulates TGFBRAP1/Vps3 expression while not altering its localization

The model of Wurthner et. al. (30) postulates that TGFBRAP1/Vps3 is a chaperone that binds to Smad4 for presentation to the phosphorylated Smad2/3 complex at the TGF β receptor complex (30). In steady state, the majority the TGF β RIII localizes at the PM (33), and TGF β stimulation can induce Smad4 association with the PM (34). Localization microscopy of TGFBRAP1/Vps3 by both immunofluorescence (IF) and immuno-electron microscopy (IEM) however, showed that TGFBRAP1/Vps3 is recruited to EEs and recycling vesicles, but not the PM (chapter3) (31,32). This raises the questions at which site TGFBRAP1/Vps3 binds Smad4, and if TGF β stimulation can induce relocalization of TGFBRAP1/Vps3 from EEs to the PM. HeLa cells are a commonly used model system for endocytosis studies and known responders to TGF β stimulation (35). We determined the TGF β responsiveness of our HeLa cell line by expressing a construct containing the Smad3 consensus site GACAGA coupled to a luciferase reporter. Using an established luciferase reporter assay (36), we showed that our HeLa cell line responded significantly and reproducibly to TGF β stimulation (fig. 1a). Next, we studied the localization of TGFBRAP1/Vps3 upon TGF β stimulation by IF microscopy. HeLa cells expressing HA-Vps3 were stimulated with TGF β for 24 hours and immunolabeled for HA. In non-stimulated cells, HA-Vps3 localized to the cytosol and EEs as shown before (31,32). Notably, addition of TGF β did not induce re-localization of HA-Vps3 towards the PM (fig. 1b). We then performed identical experiments for Vps8, which interacts with TGFBRAP1/Vps3 and is needed for recruitment of TGFBRAP1/Vps3 to EEs (32). Similar to TGFBRAP1/Vps3, the localization of HA-Vps8 was not altered upon TGF β stimulation (fig. 1b). These data show that both TGFBRAP1/Vps3 and its interaction partner Vps8 show a strict endosomal localization pattern and are not recruited to the PM upon TGF β stimulation.

Induction of TGF β signalling results in modulation of the expression of hundreds of genes. To establish whether TGF β signaling affects the expression levels of TGFBRAP1/Vps3 we performed qPCR analysis. We used the immortalized non-tumorigenic human mammary epithelial (HMLE) cell line in which the transcriptional response to TGF β stimulation is well documented (37,38). This assay showed that upon TGF β stimulation TGFBRAP1/Vps3 mRNA levels decreased significantly. By contrast, Vps8 mRNA levels remained unaltered (fig. 1c). These results indicate TGFBRAP1/Vps3 as a direct downstream target of the TGF β signaling pathway. To test this we used Smad3 chromatin-IP sequencing analysis on the whole genome of HMLE cells. We found that binding of Smad3 to the start of the TGFBRAP1 gene is increased after stimulation of the cells with TGF β (fig. 1d.), indicating that TGFBRAP1/Vps3 is a direct target of the TGF β signaling pathway.

Together these results show that TGFBRAP1/Vps3 expression levels are downregulated by TGF β stimulation, possibly as a direct effect of Smad3 binding to the upstream region of the TGFBRAP1 start site. The downregulation is specific for TGFBRAP1/Vps3 since expression of its binding partner Vps8 is not altered upon TGF β stimulation. The membrane localizations of TGFBRAP1/Vps3 or Vps8 remain endosomal in response to TGF β treatment, suggesting that a role for TGFBRAP1/Vps3 as Smad4 chaperone would take place at EEs, not the PM.

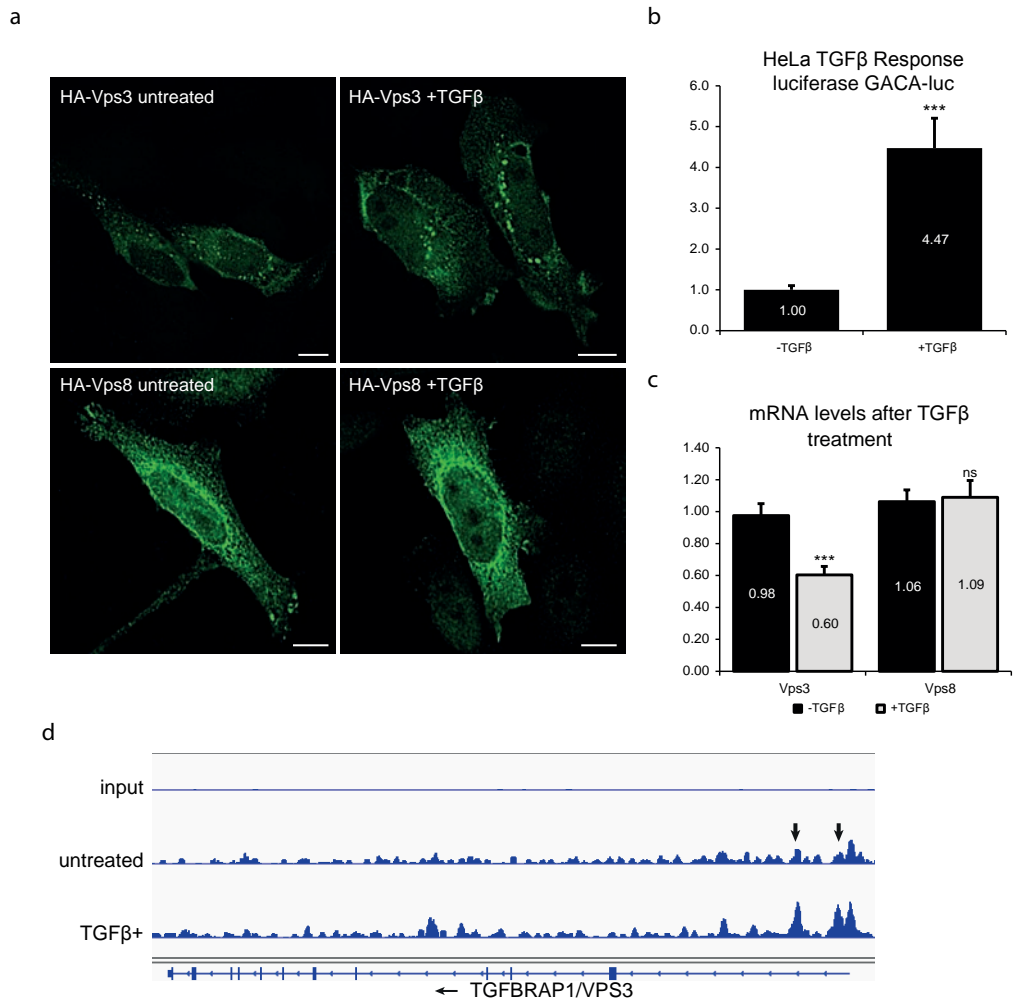


Figure 1. (a) HeLa cells overexpressing HA-Vps3 or HA-Vps8 were stimulated with TGF β for 24 hours and labeled with anti-HA. TGF β stimulation did not alter HA-Vps3 or HA-Vps8 localization. Bars 10 μ m. (b) Luciferase assay of HeLa cells expressing a CAGA-luciferase reporter shows activation of the reporter after addition of TGF β to the growth medium, indicating an intact TGF β signaling pathway. Error bars represent the standard deviation of the mean (SD). (c) qPCR analysis of TGFBRAP1/Vps3 and Vps8 expression shows that TGF β stimulation of HMLE reduces TGFBRAP1/Vps3 transcription. Vps8 mRNA levels are unaffected. Error bars represent SD. (d) Visualization of Smad3 Chromatin IP sequencing profiles in the genomic region of the TGFBRAP1/VPS3 locus in TGF β treated or unstimulated conditions. Upon TGF β treatment binding of Smad3 to the start site of the TGFBRAP1/VPS3 gene is increased.

Vps3 and Vps8 are required for Smad4 localization to early endosomes

Endocytosis of TGF β receptors is a constitutive process that occurs independently from ligand binding (17,25,39). However, endocytosis is a prerequisite for TGF β signaling (22,28,29). At EEs the TGF β receptor complex interacts with SARA, which mediates phosphorylation of Smad2 by the TGF β receptor complex (27,28,40,41). SARA is an endosome associated protein, endocytosis of the TGF β receptor complex is therefore required for stimulation of the pathway. Since TGFBRAP1/Vps3 retains a strict EE localization after TGF β stimulation (fig. 1a), the proposed Smad4 chaperone function of TGFBRAP1/Vps3 is likely to take place at EEs. To establish if TGFBRAP1/Vps3 and Smad4 colocalize on EEs after TGF β stimulation we expressed HA-Vps3 in a stable Smad4-GFP expressing HeLa cell line. IF microscopy revealed that both in TGF β stimulated and unstimulated conditions Smad4 and TGFBRAP1/Vps3 colocalize on endosomes (fig. 2a, 2b). These endosomes were also positive for Vps8 (fig. 2a, 2b), consistent with previous colocalization studies of TGFBRAP1/Vps3 and Vps8. Strikingly, we found more Smad4-GFP punctae in cells expressing TGFBRAP1/Vps3 or Vps8 than in cells expressing Smad4-GFP alone (fig. 2a, 2b, marked with *). This indicates that TGFBRAP1/Vps3 and Vps8 stimulate recruitment of Smad4 to EEs. To test this hypothesis we knocked down TGFBRAP1/Vps3 and Vps8 in the stable Smad4-GFP expressing HeLa cell line and calculated the percentage of cells that show significant (>5 punctae) endosomal Smad4 localization (fig. 3). This revealed that after knockdown of TGFBRAP1/Vps3 or Vps8, significantly less cells contain endosomal Smad4 (fig. 3).

Together these results show that TGFBRAP1/Vps3 and Vps8 colocalize with Smad4 on EEs, independent of TGF β stimulation. Moreover, increased levels of TGFBRAP1/Vps3 and Vps8 stimulate the endosomal recruitment of Smad4.

5

Overexpression of TGFBRAP1/Vps3 inhibits TGF β target gene expression

Our data show that knockdown of TGFBRAP1/Vps3 or its binding partner Vps8 reduces recruitment of Smad4 to EEs. To establish if this reduced EE localization of Smad4 affects TGF β signaling, we performed qPCR analysis of several of the TGF β target genes on HMLE cells after TGFBRAP1/Vps3 or Vps8 knockdown. This showed that neither knockdown of TGFBRAP1/Vps3 nor of Vps8 significantly reduces Serpin1, N-cadherin or TGF β RNA levels after TGF β stimulation (fig. 4a). By contrast, we found a slight increase in target gene expression (fig. 4a) although this was not statistically significant. Thus, although endosomal Smad4 levels are reduced upon TGFBRAP1/Vps3 or Vps8 knockdown (fig. 3), the signaling capacity of the pathway remains intact. We then studied the effect of overexpression of TGFBRAP1/Vps3 or Vps8 on TGF β signaling. Strikingly, overexpression of HA-Vps3 or HA-Vps8 significantly reduced the expression of TGF β target genes (fig. 4b). These results suggest that overexpression of TGFBRAP1/Vps3 or Vps8 inhibits the TGF β -induced Smad-mediated signaling cascade. Inhibition of signaling by TGFBRAP1/Vps3 or Vps8 overexpression could either be caused by inhibition of the translocation of Smad4 from EEs to the nucleus, or by another negative feedback mechanism, possibly involving the role of TGFBRAP1/Vps3 and Vps8 in trafficking.

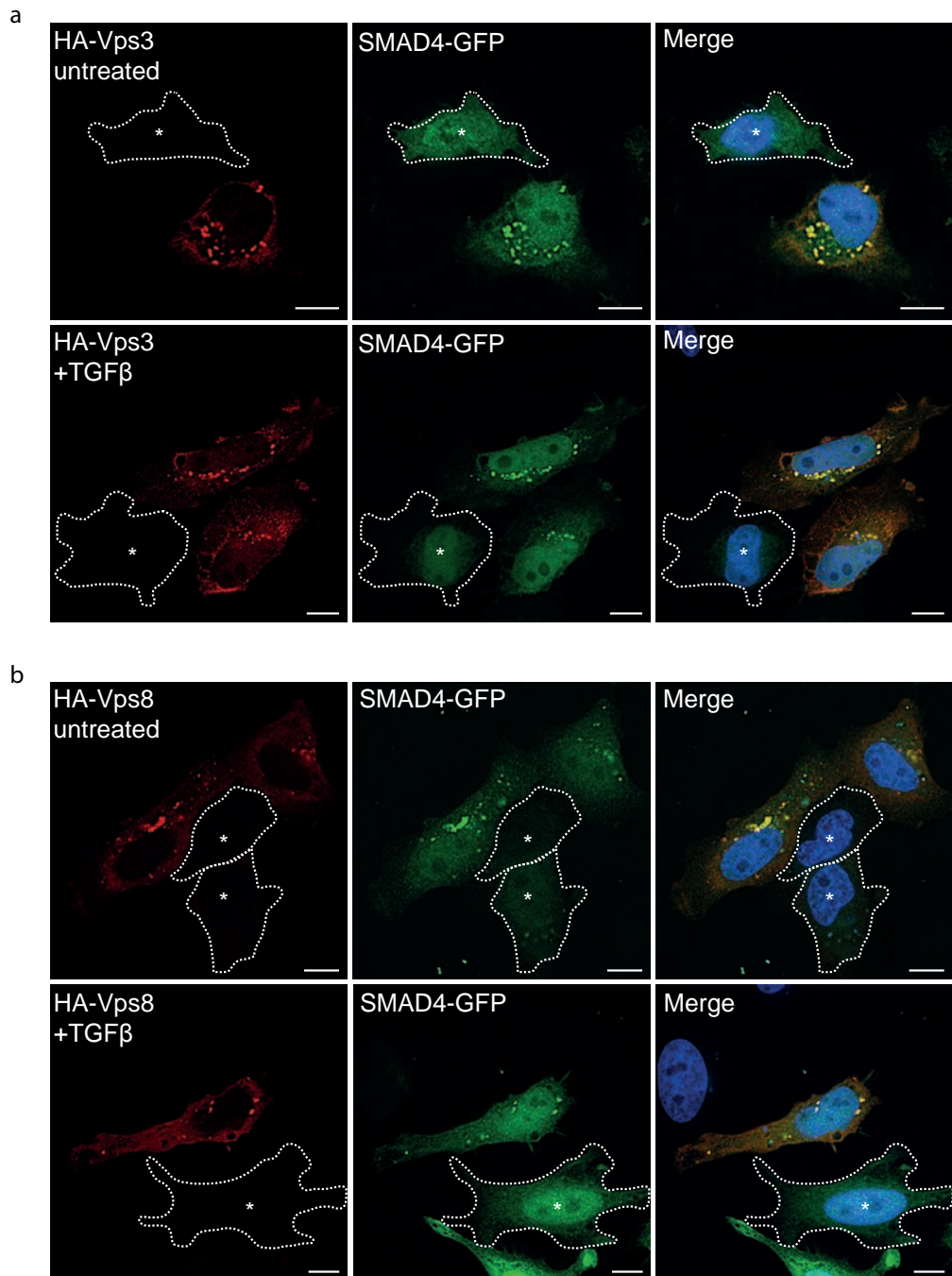


Figure 2. IF microscopy of HeLa cells expressing Smad4-GFP and HA-Vps3 (**a**) or HA-Vps8 (**b**) in the presence or absence of TGF β . Both HA-Vps3 and HA-Vps8 clearly overlap with Smad4. These colocalization punctae represent endosomal localization of Smad4. Notably, TGFBRAP1/Vps3 or Vps8 overexpressing cells show more endosomal Smad4 compared to cells expressing Smad4-GFP alone (marked with *). Bar 10 μ m.

a

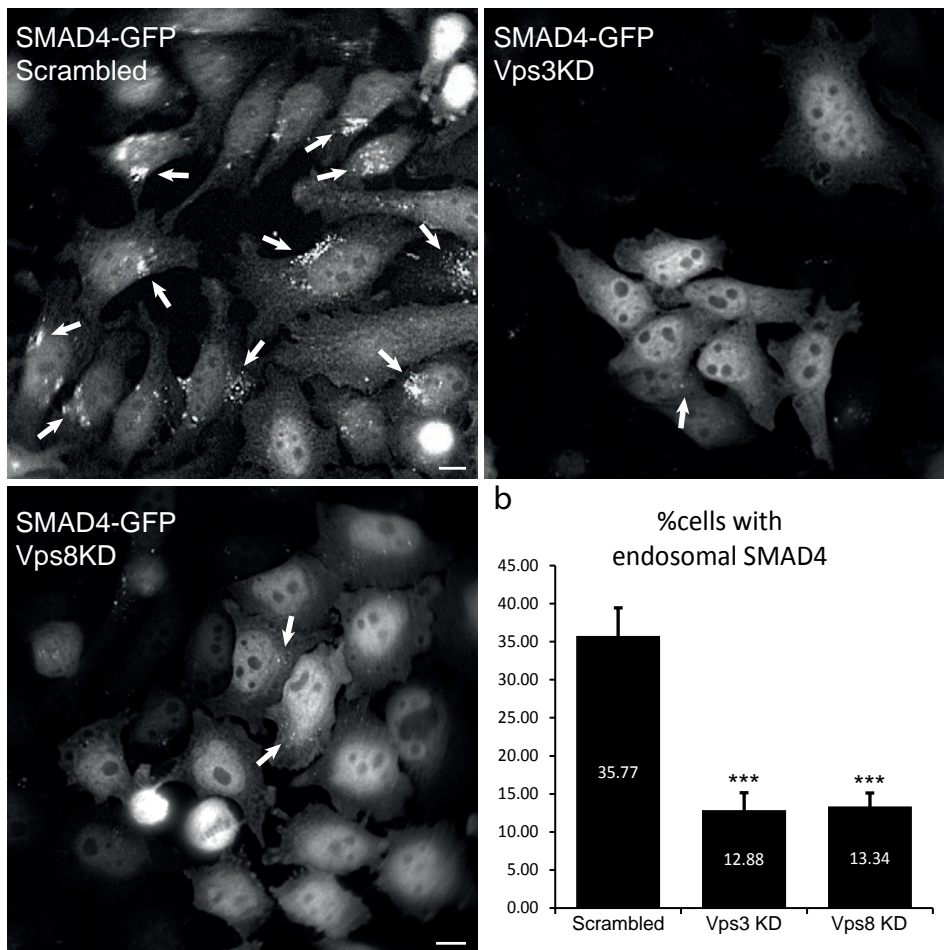


Figure 3. (a) IF microscopy of HeLa cells expressing Smad4-GFP. Knockdown of TGFBRAP1/Vps3 or Vps8 results in a marked decrease of Smad4-GFP punctae representing EE-associated Smad4 (white arrows). (b) Quantification of (a) by calculating the percentage of cells with >5 endosomal Smad4 punctae. The number of cells with more than 5 Smad4-GFP punctae was significantly reduced after TGFBRAP1/Vps3 or Vps8 knockdown. Bars 10 μ m. Error bars represent SD.

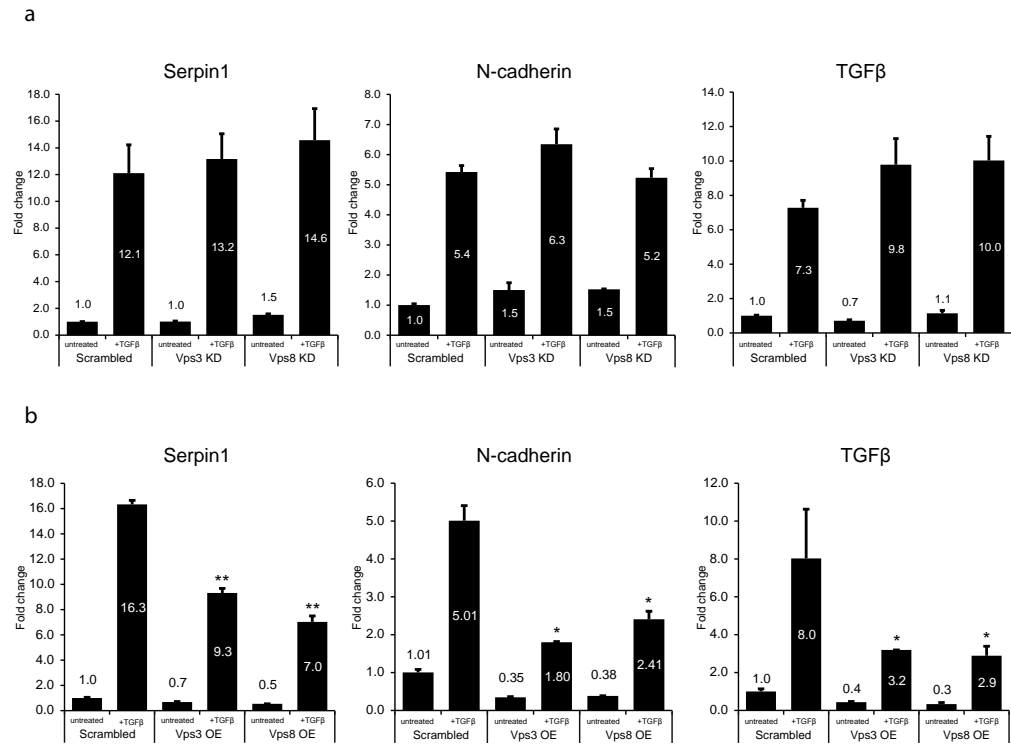


Figure 4. (a) qPCR analysis showing that TGF β stimulation of HMLE cells knocked down for TGFBRAP1/Vps3 or Vps8 does not decrease transcription of TGF β pathway target genes. (b) HMLE cells overexpressing (OE) HA-Vps3 or HA-Vps8 show significantly reduced transcription of target genes upon TGF β treatment. Error bars represent SD.

Vps3 and Vps8 knockdown induces intracellular accumulation of TGFBRII

Previously it was shown that TGFBRAP1/Vps3 and Vps8 function in EE-EE fusion as part of the CORVET complex (32), and independent from the CORVET complex in EE to recycling endosome (RE) transport (chapter 3). The latter pathway is required for transport of β 1 and α 5 integrin recycling, but not transferrin recycling. Vps3/8 dependent recycling involves transport through Rab4 and Rab11 positive compartments. Since TGF β receptor I and II recycling is also Rab4 and Rab11 dependent (18), this prompted us to investigate whether TGFBRAP1/Vps3 and Vps8 are required for TGF β receptor recycling. To measure an effect on TGFBRII recycling, we expressed TGFBRII-FLAG in HeLa cells knocked down for TGFBRAP1/Vps3 or Vps8. By IF microscopy, TGFBRII-FLAG in control cells was mainly found on the PM, with some intracellular punctae. Knockdown of TGFBRAP1/Vps3 or Vps8 reversed this pattern resulting in a marked intracellular accumulation of TGFBRII-FLAG (fig. 5). Since endocytosis continues after TGFBRAP1/Vps3 or Vps8KD (chapter 3) (32), we postulate that TGFBRAP1/Vps3 and Vps8 are required for recycling of TGFBRII.

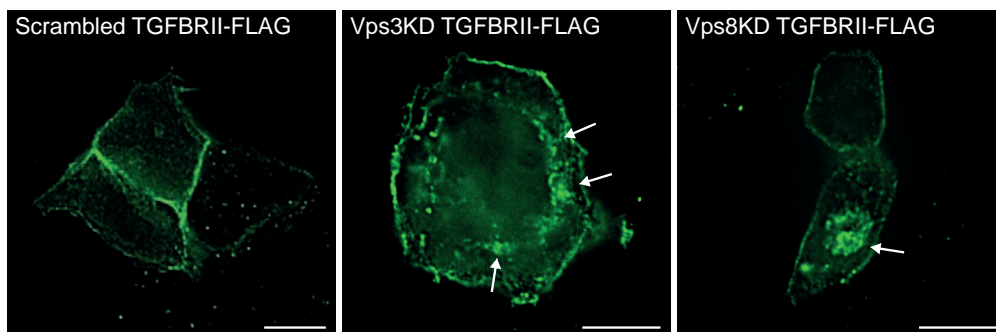


Figure 5. Knockdown of TGFBRAP1/Vps3 or Vps8 in HeLa cells expressing TGFBRII-FLAG results in intracellular accumulation of TGFBRII (arrows), indicating a block in recycling of the receptor. Bars 10 μ m.

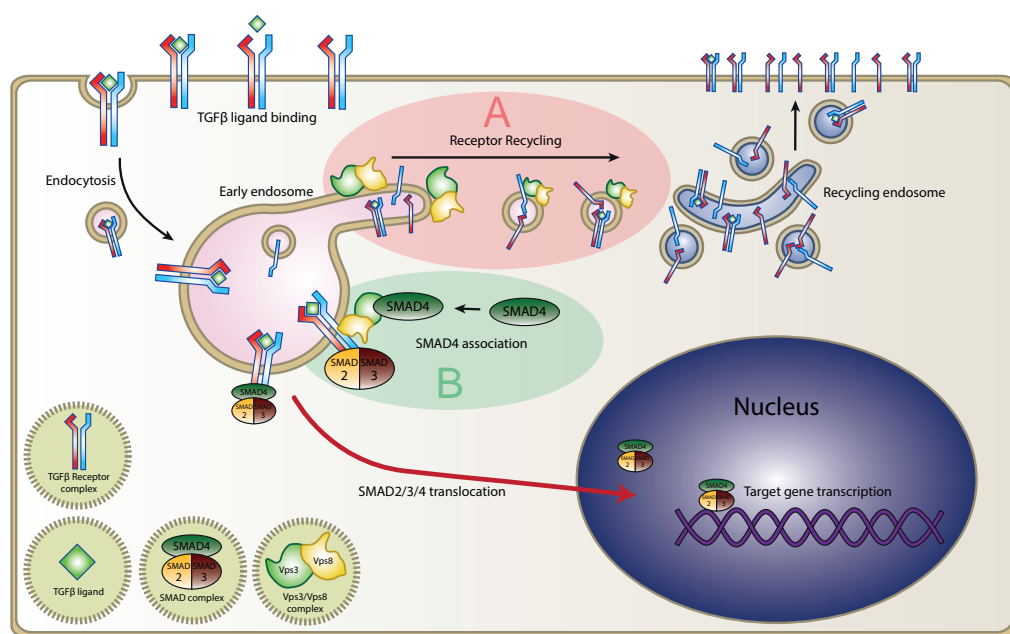


Figure 6. Model of the proposed functions of TGFBRAP1/Vps3 and Vps8 in the TGF β pathway. TGFBRAP1/Vps3 and Vps8 localize to EEs where they participate in the constitutive recycling of TGF β receptors (**A-region**). Additionally, TGFBRAP1/Vps3 and Vps8 facilitate the endosomal localization of Smad4, possibly in conjunction with the CORVET complex (**B-region**). This allows interaction of Smad4 with the activated Smad2/3 complex, nuclear translocation of the Smad2/3/4 complex and target gene activation.

Discussion

In this study we investigated the role of TGFBRAP1/Vps3 as a Smad4 chaperone in the context of the endolysosomal system and as a part of the CORVET complex. We find that TGFBRAP1/Vps3 is implicated in the TGF β pathway by 2 separate mechanisms (fig. 6). Firstly, we show that TGFBRAP1/Vps3, as well as its binding partner Vps8, mediate the recruitment of Smad4 to endosomes, pinpointing EEs as the site of the proposed chaperone function of TGFBRAP1/Vps3 (fig. 6, highlighted in A). Secondly, we show that TGFBR2 accumulates intracellularly upon knockdown of TGFBRAP1/Vps3 or Vps8 identifying TGF β receptors as additional cargo for the specialized Vps3/8-dependent recycling pathway (chapter 3) (fig. 6, highlighted in B). In addition we show that TGFBRAP1/Vps3 expression is affected by TGF β signaling, indicating that TGFBRAP1/Vps3, but not Vps8, is part of a feedback mechanism in the TGF β pathway. Our data show that the proposed role of TGFBRAP1/Vps3 in the TGF β signaling pathway is dependent on its EE localization and at least in part performed in conjunction with Vps8.

Both TGFBRAP1/Vps3 and Vps8 overexpression increases EE recruitment of Smad4, and both their knockdowns reduce EE localization of Smad4. Since no direct interactions between Vps8 and Smad4 have been detected to date, the role of Vps8 in Smad4 localization is likely indirect, via TGFBRAP1/Vps3. Concomitantly, we find that TGF β pathway activation downregulates TGFBRAP1/Vps3 but not Vps8. Together these data suggests that the chaperone function of TGFBRAP1/Vps3 requires Vps8 for recruitment to endosomes. Vps8 and TGFBRAP1/Vps3 reside together on EEs as part of the CORVET complex and on REs independently of CORVET (32) (chapter 3). Further studies are required to establish whether TGFBRAP1/Vps3 binds Smad4 in either or both settings.

We revealed that TGFBRAP1/Vps3 and Vps8 dependent recruitment of Smad4 to EEs is independent of TGF β pathway activation. Moreover, TGF β stimulation did not alter TGFBRAP1/Vps3 localization, which remained EE-associated. This suggests that Smad4 is continuously recruited to EEs, independent of pathway activation. This raises the question why Smad4 recruitment occurs independent from pathway activation. A plausible explanation is that pathway activation induces SARA-dependent phosphorylation of Smad2, which is restricted at EEs. Smad2 phosphorylation disrupts the binding between TGFBRAP1/Vps3 and Smad4 (30), allowing Smad4 to bind the Smad2/3 complex and translocate to the nucleus. If the chaperone role of TGFBRAP1/Vps3 would require TGF β activation, it would simultaneously induce and disrupt the interaction between TGFBRAP1/Vps3 and Smad4. Thus, we propose that Smad4 is constitutively recruited to endosomes by TGFBRAP1/Vps3 and that activation of the TGF β pathway is needed to allow nuclear translocation.

Knockdown of Vps8 or TGFBRAP1/Vps3 decreased Smad4 recruitment to EEs but had no effect on TGF β signaling. A possible explanation is that Smad4 is also recruited to EEs by other proteins. Endofin, a FYVE-domain containing protein, localizes to EEs and interacts with Smad4 and TGFBR1. Knockdown of Endofin or deletion of its FYVE domain reduces Smad2 phosphorylation and Smad2-Smad4 complex formation (42). Since TGFBRAP1/Vps3 interacts with TGFBR2 (30), and Endofin interacts with TGFBR1 (42), TGFBRAP1/Vps3 and Endofin could present Smad4 to Smad2 at EEs in a cooperative manner. Further studies on the interplay of TGFBRAP1/Vps3 and Endofin are needed to clarify the exact mechanism in Smad4 presentation on endosomes.

Although TGFBRAP1/Vps3 or Vps8 knockdown did not affect TGF β signaling, we found a major

effect on TGFBR11 localization, resulting in the intracellular accumulation of the receptor (fig. 5b). As transport machinery proteins, TGFBRAP1/Vps3 and Vps8 are required for EE fusion (1) and transport from EEs to REs (chapter 3). Until now, only integrins are an established cargo for the EE to RE pathway mediated by TGFBRAP1/Vps3 and Vps8. The TGFBR11 accumulation phenotype resembles that of integrin recycling defects, suggesting that TGF β receptor recycling also depends on the TGFBRAP1/Vps3 and Vps8 mediated pathway. Accumulation of intracellular TGFBR11 after TGFBRAP1/Vps3 or Vps8 knockdown could prolong endosomal localization of the activated receptor complex, thereby positively modulating TGF β signaling. This scenario would explain the slight increase in TGF β signaling shown in fig. 4a, which is in agreement with earlier observations (30). However, additional studies are required to confirm that TGF β receptors are cargo for the Vps3/8-dependent recycling pathway.

Remarkably, we observed a significant reduction of TGF β signaling after overexpression of TGFBRAP1/Vps3 or Vps8. This could be attributed to increased recycling of TGF β receptors, resulting in reduced signaling from endosomes. Alternatively, or additionally, increased recruitment and prolonged localization of Smad4 to EEs caused by TGFBRAP1/Vps3 overexpression could inhibit translocation of the Smad2/3/4 complex to the nucleus. These findings are in contrast with earlier observations showing that overexpressing of TGFBRAP1/Vps3 does not decrease TGF β signaling (30). However, overexpression of a truncated TGFBRAP1/Vps3 mutant that irreversibly binds Smad4 does downregulate TGF β signaling (30). Possibly, higher TGFBRAP1/Vps3 overexpression in our cell system was able to mimic the dominant negative effect of truncated Vps3.

In conclusion, we show that TGFBRAP1/Vps3 acts as a Smad4 chaperone in the TGF β signaling pathway by recruiting Smad4 to EEs. In addition, we propose a role for TGFBRAP1/Vps3 in TGF β receptor recycling. The role of TGFBRAP1/Vps3 in TGF β signaling thus depends on a tight balance between Smad4 recruitment and receptor recycling. Finally, since TGFBRAP1/Vps3 exerts its signaling function in conjunction with Vps8, our data link the CORVET tethering complex to the TGF β signaling cascade, which is a completely new role for this complex.

Materials & Methods

Cell culture and transfection

All cell lines were grown at 37°C and 5% CO₂. HeLa cells (ATCC clone ccl-2) and stable HeLa cells with inducible Smad4-GFP expression were cultured in Dulbecco's modified Eagle's medium (DMEM) supplemented with 10% heat inactivated Fetal Bovine Serum (FBS), 2mM L-Glutamin, 100U/mL penicillin and 100 μ g/mL streptomycin. The inducible HeLa-Smad4-GFP line was grown in medium supplemented with 5 μ g/mL blasticidin S and 250 μ g/mL hygromycin B (Roche Diagnostics, Mannheim, Germany). Non-transformed human mammary epithelial cells (classified as HMLE hTERT) were cultured in a 1:1 ratio of DMEM/F12 glutaMAX medium (Invitrogen) supplemented with insulin (Sigma), EGF (Lonza), hydrocortisone (Sigma), penicillin-streptomycin (Invitrogen) and MEGM medium (Lonza) supplemented with growth factors according to manufacturer's protocol. The stable doxycycline inducible Smad4-GFP HeLa cell line was created by co-transfecting pOG44 Flp-Recombinase expression vector along with pCDNA5/FRT/TOSmad4-GFP expression vectors into HeLa FRT cells using polyethyleneimine (PEI). 48 hours after transfection growth medium was to select for the Tet repressor and expression vector integration. HeLa cells were transfected with cDNA using Effectene transfection reagent (Qiagen) according to the manufacturer's protocol. HMLE cells and were transfected using Polyethylenimine (PEI) in a ratio of 1/5 cDNA/PEI. SMARTPool siRNAs were purchased from Dharmacon and siRNA transfection was performed using HiPerfect transfection Reagent (Qiagen) according to manufacturer's protocol. TGF β treatment was performed by supplementing the normal culture medium with 2.5ng/ml of TGF- β 1 (Sigma-Aldrich-Aldrich, Missouri, USA).

Antibodies and constructs

For immunofluorescence labeling: Mouse anti-HA (Covance), Mouse-anti-FLAG clone M2 (Sigma), Rabbit-anti-TGFBRII (Santa Cruz). Fluorescent secondary antibodies were obtained from Invitrogen. For Western blot: Rabbit-anti-Vps8 (Sigma), Rabbit-anti-TGFBRAP1 (sigma), Mouse-anti- α tubulin (Sigma). For chIP: Rabbit-anti-Smad3 (ab28379, abcam). HA-VPS8 was purchased from Origene and inserted into pcDNA3.2-HA/DEST vector (Invitrogen) using Gateway recombination cloning. TGFBRAP1-HA was a generous gift from J. Neefjes (NKI, Amsterdam, The Netherlands), Smad4 cDNA IMAGE clone was purchased from Dharmacon and cloned into pENTR vector using Gateway cloning. To obtain a HeLa FRT compatible expression vector, the pENTR vector containing Smad4 was recombined using the Gateway system into pCDNA5/FRT/TO/N-GFP according to manufacturer's protocol (Thermo Fischer Scientific, Waltham, MA).

Western Blotting

Cells were washed with PBS and lysed in Laemmli buffer [0.12 mol/L Tris-HCL (pH 6.8), 4% SDS and 20% glycerol]. Samples were analyzed by Sodium dodecyl sulfate polyacrylamide gel electrophoresis (SDS-PAGE) and electrophoretically transferred to polyvinylidene difluoride membrane (Milipore). The membranes were blocked with 5% milk protein in TBST (0.3% Tween, 10 mM Tris pH8 and 150 mM NaCl in H₂O) and probed with primary antibodies. Immunocomplexes were detected using ECL and exposure to Kodak XB films (Rochester, NY)

Luciferase Assays

HeLa cells were knocked down for 48 hours in 24 wells-plate (Nunc) and transfected overnight with CAGA-luciferase reporter and TK Renilla-luciferase constructs. After 24 hours of transfection, cells were washed twice with PBS and lysed in 50 μ L of passive lysis buffer (Promega) for 20 minutes. 20 μ L of the cell lysate was assayed for luciferase activity using Dual-Luciferase Reporter Assay System (Promega).

Immunofluorescence microscopy

Cells grown on sterile glass coverslips were washed with ice-cold PBS and fixed with 4% paraformaldehyde (PFA) in PBS for 20 minutes at RT (room temperature). Then, cells were permeabilized using 0,1% Triton-X100 in PBS for 5 minutes and blocked for 15 minutes using PBS supplemented with 1% BSA. Cells were labeled with primary antibodies diluted in blocking buffer at RT for 1 hour, washed, and labeled with fluorescent secondary antibodies for 30 minutes in the dark. After labeling the cells were washed and mounted using Prolong Gold antifade reagent with DAPI. Cells were imaged on a Deltavision wide field microscope using a 100x/1.4A immersion objective or a Zeiss LSM700 confocal microscope using a 63X/1.4 immersion objective. Widefield pictures were deconvolved using Softworx software and analyzed using FIJI. Quantification of Smad4 punctae was performed using FIJI. Cells containing >5 punctae with an intensity of 3 times the cytosolic intensity were scored manually.

Quantification of RNA Expression

mRNA was extracted from HeLa and HMLE cells using a Rneasy mini Isolation Kit (Qiagen). According to the manufactures protocol for single-stranded cDNA synthesis, 500 ng of total RNA was reverse transcribed using iScript cDNA synthesis kit (BIO-Rad). cDNA samples were amplified using SYBR green supermix (BIO-Rad), in a MyiQ single-color real time PCR detection system (BIO-Rad) according to the manufacturés protocol. To quantify the data, the comparative Ct method was used. Relative quantity was defined as $2^{-\Delta\Delta Ct}$ and $\beta 2$ -Microglobulin was used as reference gene.

Antibody uptake

HeLa cells were incubated at 4°C for 1hr with Rabbit-anti-TGFBRII (Santa Cruz) diluted in serum free DMEM to a final concentration of 10 μ g/ml. Excess antibody was removed by 2 washes with cold DMEM. Cells were transferred to pre-warmed complete DMEM, and endocytosis was allowed for 2hrs at 37°C. Surface-bound antibodies that were not endocytosed were removed with 2 acid washes (0.5% Acetic acid, 0.5M NaCl) at 4°C. Cells were fixated and preparation for immunofluorescence microscopy as described above.

Chromatin Immuno-precipitation (ChIP)

ChIP was performed as previously described (43). HMLE cells were crosslinked with 2 mM disuccinimidyl glutarate (Thermo Fisher Scientific) and 1% formaldehyde, cells were lysed in pre-immunoprecipitation buffer (10 mM Tris, 10 mM NaCl, 3 mM MgCl₂ and 1 mM CaCl₂). Chromatin was prepared and ChIP was performed according to the Millipore online protocol using 5 μ g of rabbit-anti-Smad3 (ab28379, abcam) or rabbit IgG as a control.

The Smad4 chaperone and CORVET subunit TGFBRAP1/Vps3 has a dual role in TGF β receptor signalling and trafficking

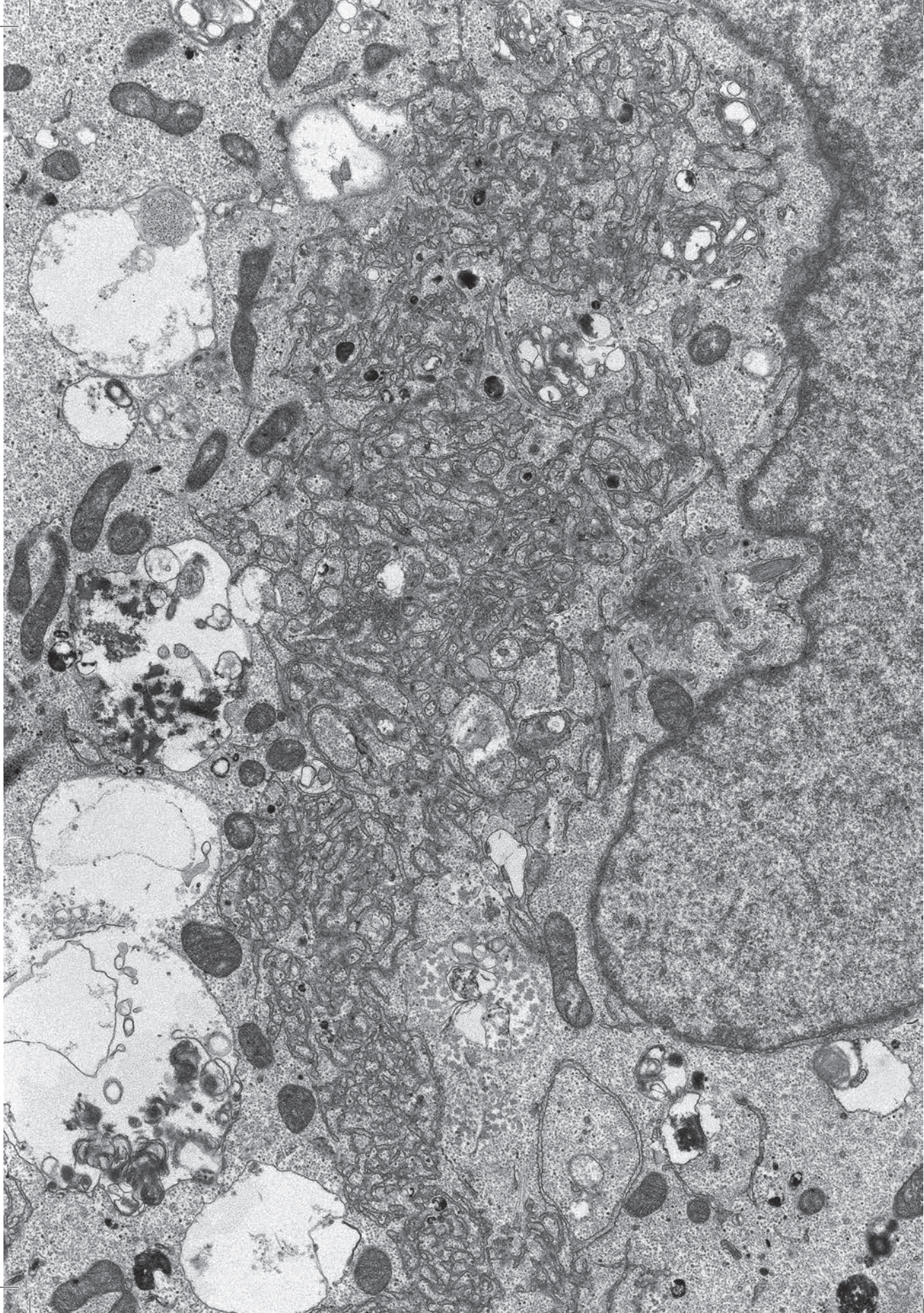
Acknowledgments

We thank Stephin Vervoort for assistance with the ChipSeq experiments, Janneke Peeters for assistance with ChipSeq data analysis and Peter ten Dijke for valuable constructs.

References

1. Derynck R, Zhang YE. Smad-dependent and Smad-independent pathways in TGF-beta family signalling. *Nature*. 2003 Oct 9;425(6958):577–584.
2. Le Roy C, Wrana JL. Clathrin- and non-clathrin-mediated endocytic regulation of cell signalling. *Nat Rev Mol Cell Biol*. 2005 Feb;6(2):112–126.
3. Ten Dijke P, Arthur HM. Extracellular control of TGFbeta signalling in vascular development and disease. *Nat Rev Mol Cell Biol*. 2007 Nov;8(11):857–869.
4. Miyazono K, Suzuki H, Imamura T. Regulation of TGF-beta signaling and its roles in progression of tumors. *Cancer Sci*. 2003 Mar;94(3):230–234.
5. Massagué J, Blain SW, Lo RS. TGFbeta signaling in growth control, cancer, and heritable disorders. *Cell*. 2000 Oct 13;103(2):295–309.
6. Blobe GC, Schiemann WP, Lodish HF. Role of transforming growth factor beta in human disease. *N Engl J Med*. 2000 May 4;342(18):1350–1358.
7. Massagué J. TGFβ signalling in context. *Nat Rev Mol Cell Biol*. 2012 Oct;13(10):616–630.
8. Waite KA, Eng C. From developmental disorder to heritable cancer: it's all in the BMP/TGF-beta family. *Nat Rev Genet*. 2003 Oct;4(10):763–773.
9. Feng XH, Derynck R. Specificity and versatility in tgf-β signaling through Smads. *Annu Rev Cell Dev Biol*. 2005;21:659–693.
10. Wrana JL. Regulation of Smad activity. *Cell*. 2000 Jan 21;100(2):189–192.
11. Shi Y, Massagué J. Mechanisms of TGF-beta signaling from cell membrane to the nucleus. *Cell*. 2003 Jun 13;113(6):685–700.
12. Ceresa BP, Schmid SL. Regulation of signal transduction by endocytosis. *Curr Opin Cell Biol*. 2000 Apr;12(2):204–210.
13. Platta HW, Stenmark H. Endocytosis and signaling. *Curr Opin Cell Biol*. 2011 Aug;23(4):393–403.
14. Von Zastrow M, Sorkin A. Signaling on the endocytic pathway. *Curr Opin Cell Biol*. 2007 Aug;19(4):436–445.
15. Conner SD, Schmid SL. Regulated portals of entry into the cell. *Nature*. 2003 Mar 6;422(6927):37–44.
16. González-Gaitán M. Signal dispersal and transduction through the endocytic pathway. *Nat Rev Mol Cell Biol*. 2003 Mar;4(3):213–224.
17. Mitchell H, Choudhury A, Pagano RE, Leof EB. Ligand-dependent and-independent transforming growth factor-beta receptor recycling regulated by clathrin-mediated endocytosis and Rab11. *Mol Biol Cell*. 2004 Sep;15(9):4166–4178.
18. Li H, Li HF, Felder RA, Periasamy A, Jose PA. Rab4 and Rab11 coordinately regulate the recycling of angiotensin II type I receptor as demonstrated by fluorescence resonance energy transfer microscopy. *J Biomed Opt*. 2008 Jun;13(3):031206.
19. Maxfield FR, McGraw TE. Endocytic recycling. *Nat Rev Mol Cell Biol*. 2004 Feb 1;5(2):121–132.
20. Ehrlich M, Shmueli A, Henis YI. A single internalization signal from the di-leucine family is critical for constitutive endocytosis of the type II TGF-beta receptor. *J Cell Sci*. 2001 May;114(Pt 9):1777–1786.
21. Lu Z, Murray JT, Luo W, Li H, Wu X, Xu H, et al. Transforming growth factor beta activates Smad2 in the absence of receptor endocytosis. *J Biol Chem*. 2002 Aug 16;277(33):29363–29368.
22. Di Guglielmo GM, Le Roy C, Goodfellow AF, Wrana JL. Distinct endocytic pathways regulate TGF-beta receptor signalling and turnover. *Nat Cell Biol*. 2003 May;5(5):410–421.
23. Anders RA, Doré JJ, Arline SL, Garamszegi N, Leof EB. Differential requirement for type I and type II transforming growth factor beta receptor kinase activity in ligand-mediated receptor endocytosis. *J Biol Chem*. 1998 Sep 4;273(36):23118–23125.
24. Anders RA, Arline SL, Doré JJ, Leof EB. Distinct endocytic responses of heteromeric and homomeric transforming growth factor beta receptors. *Mol Biol Cell*. 1997 Nov;8(11):2133–2143.
25. Garamszegi N, Doré JJ, Penheiter SG, Edens M, Yao D, Leof EB. Transforming growth factor beta receptor signaling and endocytosis are linked through a COOH terminal activation motif in the type I receptor. *Mol Biol Cell*. 2001

- Sep;12(9):2881–2893.
26. Tsukazaki T, Chiang TA, Davison AF, Attisano L, Wrana JL. SARA, a FYVE domain protein that recruits Smad2 to the TGF β receptor. *Cell*. 1998 Dec 11;95(6):779–791.
 27. Itoh F, Divecha N, Brocks L, Oomen L, Janssen H, Calafat J, et al. The FYVE domain in Smad anchor for receptor activation (SARA) is sufficient for localization of SARA in early endosomes and regulates TGF- β /Smad signalling. *Genes Cells*. 2002 Mar;7(3):321–331.
 28. Hayes S, Chawla A, Corvera S. TGF β receptor internalization into EEA1-enriched early endosomes: role in signaling to Smad2. *J Cell Biol*. 2002 Sep 30;158(7):1239–1249.
 29. Rajagopal R, Ishii S, Beebe DC. Intracellular mediators of transforming growth factor beta superfamily signaling localize to endosomes in chicken embryo and mouse lenses in vivo. *BMC Cell Biol*. 2007 Jun 25;8:25.
 30. Wurthner JU, Frank DB, Felici A, Green HM, Cao Z, Schneider MD, et al. Transforming growth factor- β receptor-associated protein 1 is a Smad4 chaperone. *J Biol Chem*. 2001 Jun 1;276(22):19495–19502.
 31. Van der Kant R, Jonker CT, Wijdeven RH, Bakker J, Janssen L, Klumperman J, et al. Characterization of the mammalian CORVET and HOPS complexes and their modular restructuring for endosome specificity. *J Biol Chem*. 2015 Oct 13;290(41):24811–24821.
 32. Perini ED, Schaefer R, Stöter M, Kalaidzidis Y, Zerial M. Mammalian CORVET is required for fusion and conversion of distinct early endosome subpopulations. *Traffic*. 2014 Dec;15(12):1366–1389.
 33. Gilboa L, Wells RG, Lodish HF, Henis YI. Oligomeric structure of type I and type II transforming growth factor beta receptors: homodimers form in the ER and persist at the plasma membrane. *J Cell Biol*. 1998 Feb 23;140(4):767–777.
 34. Yang Y, Wolfram J, Shen J, Zhao Y, Fang X, Shen H, et al. Live-cell single-molecule imaging reveals clathrin and caveolin-1 dependent docking of SMAD4 at the cell membrane. *FEBS Lett*. 2013 Dec 11;587(24):3912–3920.
 35. Maliekal TT, Anto RJ, Karunakaran D. Differential activation of Smads in HeLa and SiHa cells that differ in their response to transforming growth factor- β . *J Biol Chem*. 2004 Aug 27;279(35):36287–36292.
 36. Dennler S, Itoh S, Vivien D, ten Dijke P, Huet S, Gauthier JM. Direct binding of Smad3 and Smad4 to critical TGF β -inducible elements in the promoter of human plasminogen activator inhibitor-type 1 gene. *EMBO J*. 1998 Jun 1;17(11):3091–3100.
 37. Taube JH, Herschkowitz JI, Komurov K, Zhou AY, Gupta S, Yang J, et al. Core epithelial-to-mesenchymal transition interactome gene-expression signature is associated with claudin-low and metaplastic breast cancer subtypes. *Proc Natl Acad Sci U S A*. 2010 Aug 31;107(35):15449–15454.
 38. Vervoort SJ, Lourenço AR, van Boxtel R, Coffey PJ. SOX4 mediates TGF- β -induced expression of mesenchymal markers during mammary cell epithelial to mesenchymal transition. *PLoS ONE*. 2013 Jan 3;8(1):e53238.
 39. Zwaagstra JC, Kassam Z, O'Connor-McCourt MD. Down-regulation of transforming growth factor- β receptors: cooperativity between the types I, II, and III receptors and modulation at the cell surface. *Exp Cell Res*. 1999 Nov 1;252(2):352–362.
 40. Panopoulou E, Gillooly DJ, Wrana JL, Zerial M, Stenmark H, Murphy C, et al. Early endosomal regulation of Smad-dependent signaling in endothelial cells. *J Biol Chem*. 2002 May 17;277(20):18046–18052.
 41. Runyan CE, Schnaper HW, Poncelet AC. The role of internalization in transforming growth factor β 1-induced Smad2 association with Smad anchor for receptor activation (SARA) and Smad2-dependent signaling in human mesangial cells. *J Biol Chem*. 2005 Mar 4;280(9):8300–8308.
 42. Chen YG, Wang Z, Ma J, Zhang L, Lu Z. Endofin, a FYVE domain protein, interacts with Smad4 and facilitates transforming growth factor- β signaling. *J Biol Chem*. 2007 Mar 30;282(13):9688–9695.
 43. Van der Vos KE, Eliasson P, Proikas-Cezanne T, Vervoort SJ, van Boxtel R, Putker M, et al. Modulation of glutamine metabolism by the PI(3)K-PKB-FOXO network regulates autophagy. *Nat Cell Biol*. 2012 Aug;14(8):829–837.



An adapted protocol to overcome endosomal damage caused by polyethylenimine (PEI) mediated transfections

Caspar TH Jonker¹, L. Faber¹, C. de Heus¹, C. ten Brink¹, L. Potze¹, J. Klumperman¹

¹ Department of Cell Biology, Center for Molecular Medicine, University Medical Center Utrecht, the Netherlands.

Chapter 6

Manuscript in preparation

Abstract

Transfection of cells using polyethylenimine (PEI) polymers is a widely used technique for gene insertion and exogenous protein expression that offers several advantages over virus or lipid based transfection methods. PEI facilitates endocytosis of DNA into the cell, release of DNA from the endolysosomal system and protection from nucleases. Although PEI is extensively investigated for application in research and therapy, the mechanism of release from the endosomal system has remained a point of debate. The most prevailing model states that PEI causes endosomal rupture, resulting in release of PEI-DNA complexes into the cytosol. Hence, the use of PEI transfection should be applied with great care in studies on the endosomal system, since PEI transfection could induce endosomal artefacts. Here we study the effect of PEI transfections on the endolysosomal system. Using fluorescent and electron microscopy we find a decrease in early endosomes after PEI transfection. Adapting the PEI transfection protocol by including a chase time after initial uptake of the PEI-DNA polyplexes rescues this phenotype without affecting the efficiency of PEI transfection. Our data result in an adapted protocol for PEI transfection that can be used in studies involving the endolysosomal system.

Introduction

Exogenous expression of (tagged) proteins is a commonly used method in Life Sciences studies. For example, to localize proteins using fluorescence or electron microscopy when endogenous protein levels are too low for detection or when there are no specific antibodies available. Also numerous functional assays, for example luciferase assays or co-immunoprecipitations, often require over-expression of (tagged) proteins to obtain sufficient levels for quantitative measurements. Clearly, the transfection method used to express the protein of interest should have minimal effect on the cells, to allow unbiased measurements. However, transfection protocols pose a number of strains onto cells in order to deliver foreign DNA to the nucleus and to escape the cells natural defense mechanisms against incorporation of non-self DNA (1). A common technique is the use of viruses and utilize their efficient mechanisms to overcome the obstacles raised by the cell. Alternative non-viral methods are based on lipid carriers or polymers which copy viral entry pathways and have the advantage that the safety regulations involving the work with viruses are not required (2).

Polyethylenimine (PEI) is a synthetic polymer agent for nucleic acid delivery *in vitro* and *in vivo*. Since its initial discovery as a transfection agent (3) it has become one of the most widely used gene transfer agents. The reasons for PEI's popularity are numerous: i) PEI is not expensive and can be stored for several years. ii) PEI is able to transfect many different cell lines with high efficiency. iii) The protocol to use PEI is simple. iv) PEI can be chemically modified to adapt it for special transfection procedures. These advantages make PEI a favored reagent for gene transfections in biochemistry and cell biology research (Reviewed in (4)), as well as a research target for the application of gene therapy (5,6).

The efficiency of PEI in gene delivery relies on its chemical characteristics. PEI is a cationic polymer that efficiently binds to nucleic acids via charged amino groups (3). Despite extensive research, however, the details on the mechanism by which PEI transfects cells is still unclear. The PEI-DNA complexes, called polyplexes, condense into particles with a cationic surface, which can interact with anionic proteoglycans that are abundantly present on the cell surface (7–9). These

particles are endocytosed via clathrin dependent as well as clathrin independent endocytosis (10). After endocytosis the polyplexes need to escape from the endocytic system to the cytosol in order to reach the nucleus. The generally accepted mechanism for endosomal release is the “proton sponge” hypothesis (11), which refers to the buffering capacity of the cationic polymer. Endocytosis encompasses the transfer of endocytosed cargo from early endosome (EEs) to late endosomes (LEs) and finally lysosomes. Progression from EEs to LEs is indicated as endosomal maturation. During endosomal maturation the pH inside endosomes is lowered by resident ATPase proton pumps that actively translocate protons into the endosomes. This causes the polymers to be protonated, inhibiting acidification of the endosomal lumen. With no change in pH, the ATPase proton pumps will continue to translocate protons into the endosomes, resulting in an accumulation of protons inside endosomes causing an influx of water and chloride ions. This causes osmotic swelling of endosomes leading to disruption of their membrane and consequent release of the PEI-DNA polyplexes to the cytosol (12,13) (fig. 1). In the cytosol a portion of the PEI-DNA polyplexes enter the nucleus either via the nuclear pore complex or after dismantling of the nuclear envelope during cell division (14). Although the general mechanism is well-studied and most difficulties are known, the practical efficiency of polymer transfections depends heavily on cell type and the type of polymer that is used (10).

Studies involving the endolysosomal system are often combined with protein expression to label distinct compartments, for example with fluorescent Rab5 or RAB7 to label EEs or LEs, respectively (15,16). However, since PEI transfections may cause endosomal membrane rupture, this imposes a problem for studying the endolysosomal system in combination with PEI-mediated transfection.

Here we test to what extent the endolysosomal system is affected by PEI-mediated transfections. We show that PEI transfections specifically affect EEs and provide a protocol to overcome these PEI-induced artefacts.

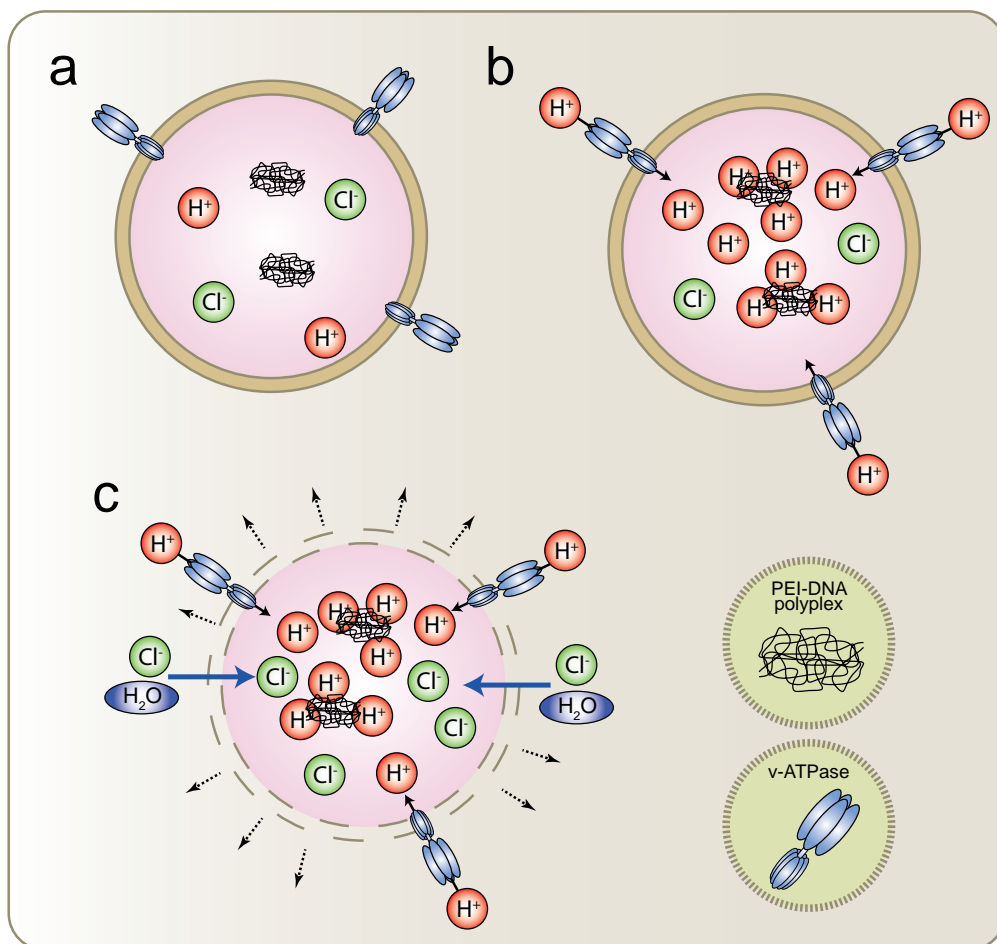


Figure 1. Model depicting the proton sponge hypothesis. (a) DNA-PEI polyplexes are endocytosed and transported to endosomes. **(b)** During endosomal maturation resident v-ATPases on the endosomal limiting membrane pump protons into the lumen of endosomes resulting in a lower pH. Consequently PEI is protonated, which blocks the acidification of endosomes, resulting in more protons that are pumped into the lumen to lower the pH. **(c)** The proton accumulation is followed by passive influx of chloride ions, which increasing the ionic concentration, causing water influx. The resulting osmotic pressure causes swelling and rupture of endosomes, which releases their luminal content, including the DNA-PEI polyplexes, into the cytosol.

Results

Transfected PEI-DNA polyplexes accumulate in the endosomal system

Endocytosis starts with vesicles that bud off from the plasma membrane (PM) and fuse with an early endosome (EE) (17). From EEs, endocytosed cargo can be recycled to the PM via recycling endosomes (REs) (18) or proceed to late endosomes (LEs) and lysosomes for degradation (19–21). To track PEI-DNA polyplexes throughout the endolysosomal system, we transfected HeLa cells overnight with a GFP construct using a well-established PEI-based transfection protocol (22) with a DNA:PEI ratio of 1:5, which we further refer to as protocol A. After overnight transfection, cells were fixed and prepared for electron microscopy (EM) to assess the cellular localization of the PEI-DNA polyplexes, which by EM are visible as dense aggregates of approximately 60-100 nanometers (23). Using this protocol we could readily identify PEI-DNA polyplexes in EEs (fig. 2a, panel A), LEs and lysosomes (fig. 2a, panel B-D). The polyplexes appeared as individual particles (fig. 2a, Panel A, arrows), or larger accumulations consisting of multiple particles (fig. 2a, panel B-D). Only in very few cases did we encounter PEI-DNA polyplexes in the cytoplasm or nucleus (not shown).

PEI-mediated transfection is believed to cause endosomal swelling prior to polyplex release. To identify an effect of PEI-mediated transfection on the ultrastructure of the endolysosomal compartments, we quantified the size of endosomes after PEI-mediated transfection and control cells. Endocytosed PEI polyplexes prevent accurate determination of endosome subtype by morphology (fig. 2a), therefore all endosomes in a given cell were measured. This revealed a significant increase in endosome size after transfection, indicating endosomal swelling occurred (fig. 2b).

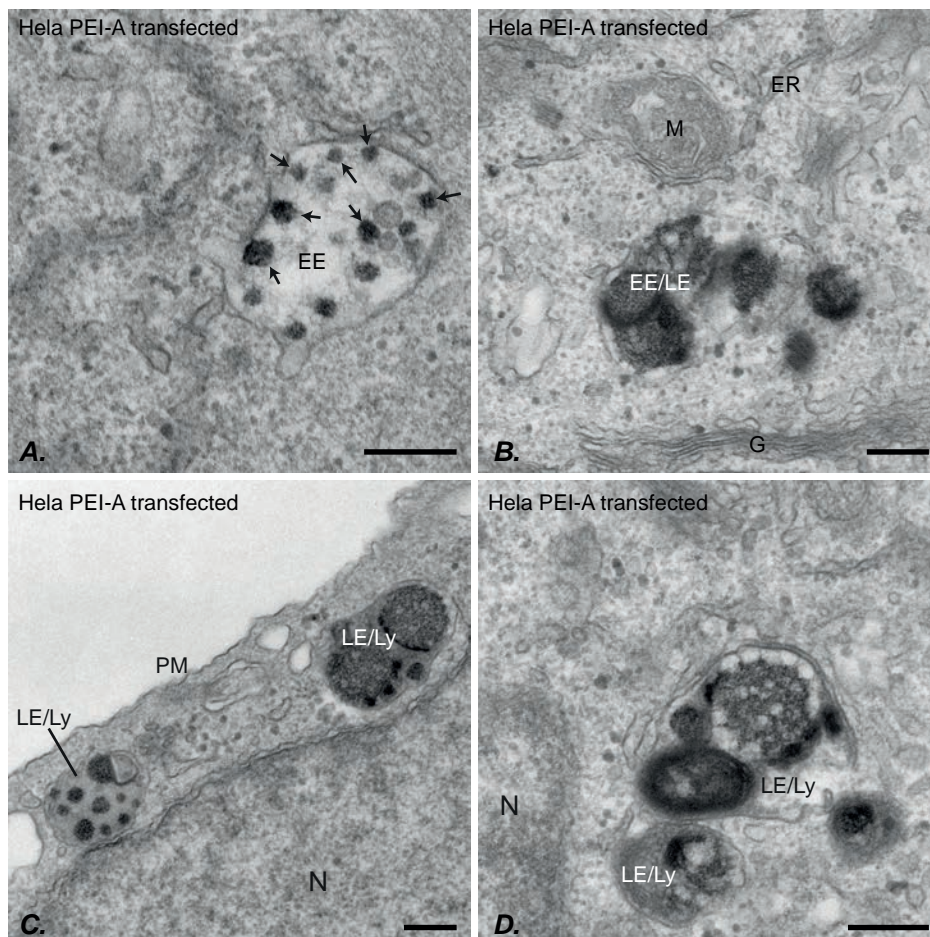
These data show that endocytosed PEI-DNA polyplexes traverses the entire endolysosomal to lysosomes and induce swelling of endosomes. Therefore, PEI-mediated endosomal rupture could occur at both early and late stages of endosomal maturation.

PEI transfection leads to a reduced early endosomal population

To test whether PEI-mediated transfection affects the composition of the endolysosomal system we used markers for endosomal compartments that are commonly applied in immunofluorescence microscopy (IF) and quantified their distribution after PEI-mediated transfection. HeLa cells were transfected using protocol A with GFP overnight, after which cells were fixed and labeled for the early endosomal marker EEA1 or the LE/lysosomal marker LAMP-1. In addition, cells were incubated with the fluorescent endocytic marker dextran for 2 hours before fixation to mark the entire endolysosomal system. Subsequent analysis of fluorescence area per cell revealed that EEA1 and dextran fluorescence area per cell was decreased in the transfected GFP-positive cells compared to the non-transfected cells, whereas LAMP-1 area was not affected (fig. 3a, 3b). Quantification confirmed that EEA1 and dextran levels were reduced 2-fold in transfected cells compared to non-treated cells, while LAMP-1 levels did not change significantly (fig. 3b). Decreased EEA1 fluorescence indicates a reduction in the number of early endosomes. By contrast, LAMP-1-positive LEs/lysosomes were not affected by the transfection. Reduced levels of dextran indicates that either endocytosis is decreased in transfected cells or disruption of endosomal membranes causes leaking of fluorescent dextran out of the compartment.

Together these results indicate that the endolysosomal system is disrupted after PEI-mediated transfection and primarily affects EEs.

a



b

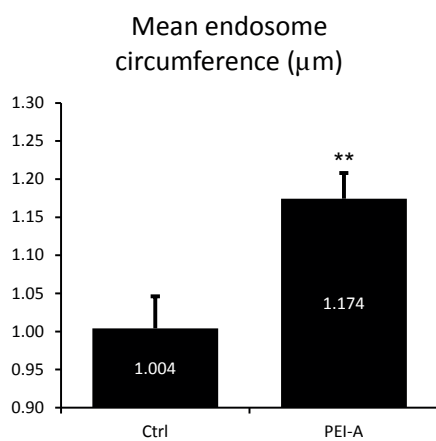
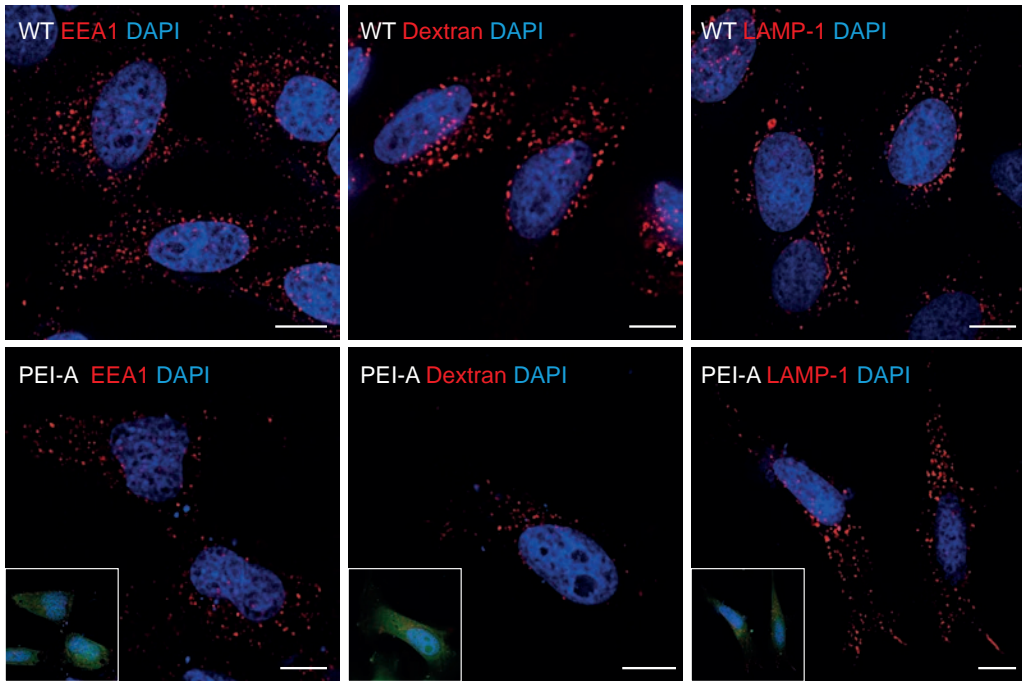


Figure 2. (a) DNA-PEI polyplexes are visible as dense particles (arrows in A.). EEs are recognized by a lucent content, presence of tubular regions and a clathrin coat (A.). Late endosomes/lysosomes are more electron dense and contain multiple internal membranes (21) (B-C.). Since the dense DNA-PEI polyplexes partially obscure luminal content, the distinction between EEs, LEs and lysosomes cannot always be made in these samples (B-C.). EE= early endosome, LE= late endosome, Ly= lysosome, N= nucleus, M= mitochondrion, PM= plasma membrane, ER= endoplasmic reticulum G= Golgi. Bars 200nm. **(b)** Endosome size quantification using pictures taken from >20 randomly selected cells. Endosome size is significantly increased after PEI-mediated transfection using protocol A. Error bars represent the standard error of the mean (SEM).

a



b

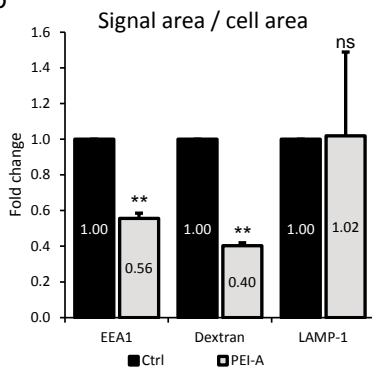


Figure 3 (a) Immunofluorescence analysis of HeLa cells labeled for endogenous EEA1 or LAMP-1 or treated with dextran-Alexa568 for 2 hours. Non-transfected (upper panels) or PEI transfection with protocol A (lower panels). Insets show the GFP signal after transfection. Bars 10 μ m. **(b)** Quantification of (a) using fluorescence signal area corrected for cell area. Error bars represent the standard deviation of the mean (SD).

6

Lysosome integrity is not affected after PEI-mediated transfection

According to the proton sponge hypothesis, PEI-DNA polyplexes escape the endolysosomal pathway through endosomal membrane rupture. Permeabilization of the lysosomal membrane can lead to release of lysosomal enzymes from the lysosomal lumen to the cytoplasm, which ultimately can cause cell death (24,25). To study lysosomal integrity after PEI-mediated transfection, we used a galectin3-mCherry based assay that detects lysosomal membrane permeabilization as described in (26). In short, the stably transfected mCherry conjugated galectin3 protein is localized to the cytoplasm and nucleus in steady state conditions. However, upon disruption of the lysosomal membrane, galectin3, which has a high affinity for β -galactosides, translocates

into the lysosome to interact with β -galactosides in the glycocalyx. This process can be visualized by the appearance of fluorescent galectin3-mCherry puncta, which correspond to damaged lysosomes. We used stably transfected galectin3-mCherry HeLa cells to test lysosomal membrane permeabilization (LMP) after PEI-mediated transfection of a GFP-construct using protocol A. As a positive control for LMP we used a 5-times higher than recommended dose of Effectene transfection reagent, which under these conditions induces lysosomal leakage. Both in control cells and cells transfected overnight, the galectin3-mCherry localization was primarily cytosolic. In contrast, clearly visible puncta were observed in the positive control (fig. 4a). Quantification of mCherry-galectin3 confirmed that PEI transfection does not increase the number or size of galectin-mCherry punctae (fig. 4b). We conclude from these data that PEI transfection does not cause significant lysosomal membrane permeabilization.

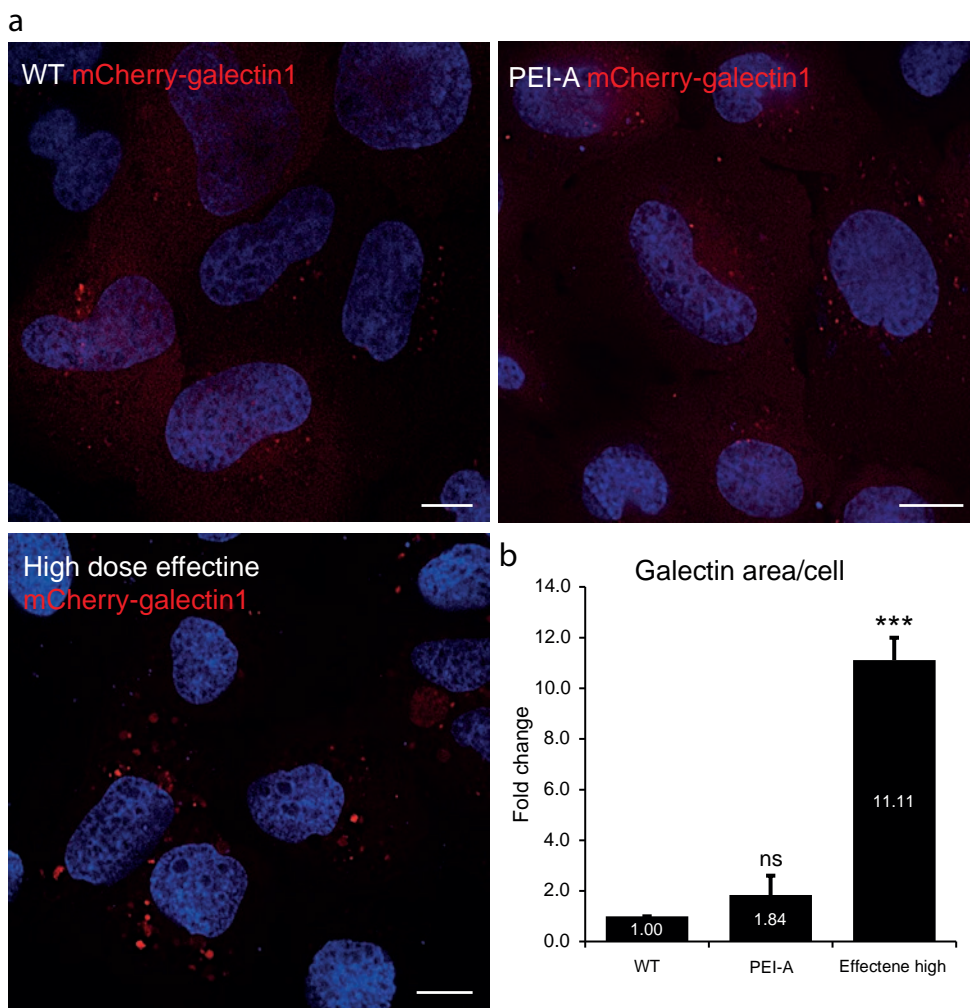


Figure 4. (a) HeLa cells stably expressing Galectin3-mCherry were transfected using PEI or a high dose effectene as positive control. Non-treated or PEI transfected cells show a predominantly cytosolic staining for mCherry, with only a few puncta. Positive control cells show many intense puncta of galectin3 indicating lysosomal permeabilization. Bars 10 μ M. **(b)** Quantification shows a significant increase of Galectin puncta in the positive control, but not in PEI transfected cells. Error bars represent SD.

The early endosome population recovers after a pulse chase PEI transfection protocol

Our findings show that after overnight PEI transfection the population of EEA1-marked EEs is decreased. Since EEs are critical compartments for sorting and signaling of a wide variety of proteins, distortion of EE function is a highly unwanted side-effect in studies that require transfection. We reasoned that the impact of PEI on EE function might be restored over time and therefore developed a pulse-chase transfection protocol to increase the recovery time after transfection. To this end, cells were transfected for 8 hours, washed to remove surplus PEI-DNA polyplexes and chased overnight with fresh medium, we refer to this protocol as protocol B. Cells were then fixed and prepared for EM analysis or IF microscopy. By EM, PEI-DNA polyplexes were observed throughout the endolysosomal system after this pulse chase protocol B (fig. 5a), which reflects the data obtained using protocol A. Analysis of the endosomal size using protocol B revealed a slight decrease in endosomal swelling compared to protocol A (fig. 5b). Moreover, quantification of the EEA1 signal by IF identical to as shown in fig. 3a showed that protocol B restored EEA1 fluorescence area to control levels (fig. 5c).

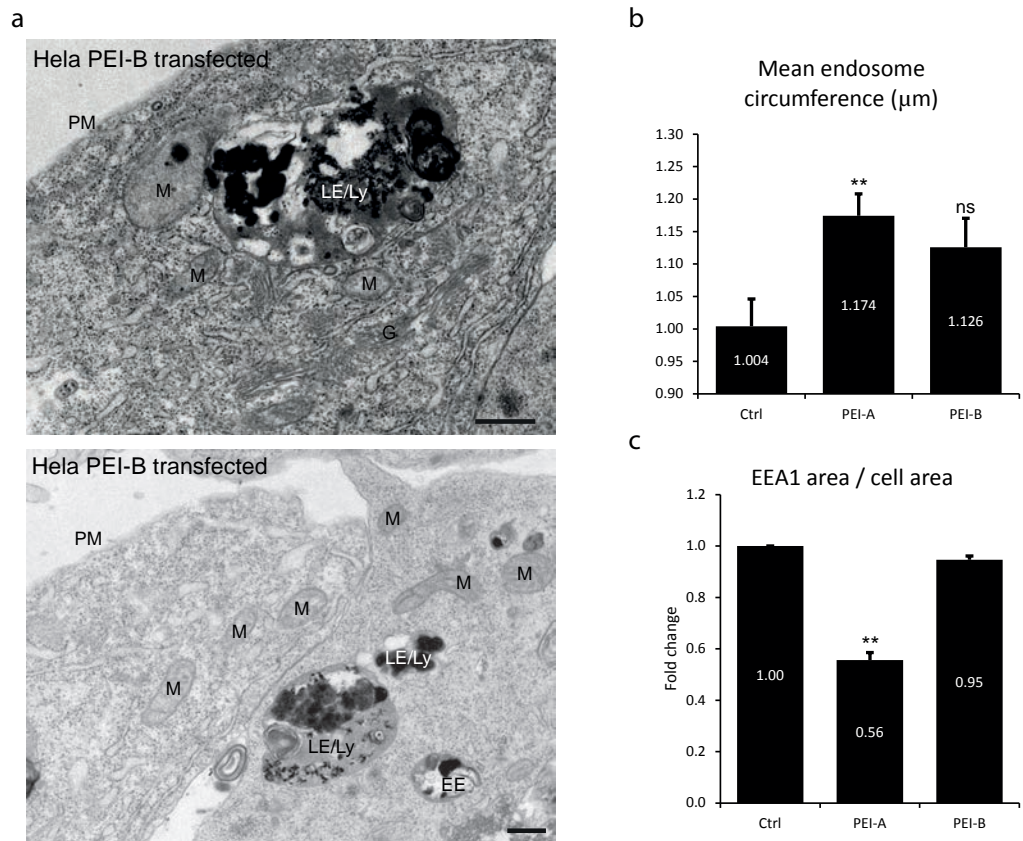


Figure 5 (a) Electron micrographs showing cells transfected with PEI using the adapted protocol B. DNA-PEI polyplexes are present in EEs, LEs and lysosomes. EE= early endosome, LE= late endosome, Ly= lysosome, N= nucleus, M= mitochondrion, PM= plasma membrane, G= Golgi. Bars 200nm. **(b)** Endosome size quantification using pictures taken from >20 randomly selected cells. Endosome size is slightly decreased in protocol B compared to protocol A. Error bars represent SEM. **(c)** Using the adapted protocol B shows a rescue in the early endosomal population compared to the standard protocol A. The adapted protocol B restores the EEA1 signal to control levels. Error bars represent SD.

The pulse chase protocol has identical transfection efficiency

A prerequisite to our adapted pulse-chase transfection protocol B is a comparable efficient transfection yield. To test this we used FACS analysis to determine GFP expression (fig. 6a). This showed that the transfection efficiency of HeLa cells was identical in the original (A) and adapted (B) protocol (fig. 6a, 6b). These data show that the effect of the PEI on the endolysosomal system is temporary and that cells are able to restore their endosomal system. Our adapted transfection protocol incorporates time for restoring endosome function while maintaining high expression levels of the transfected protein.

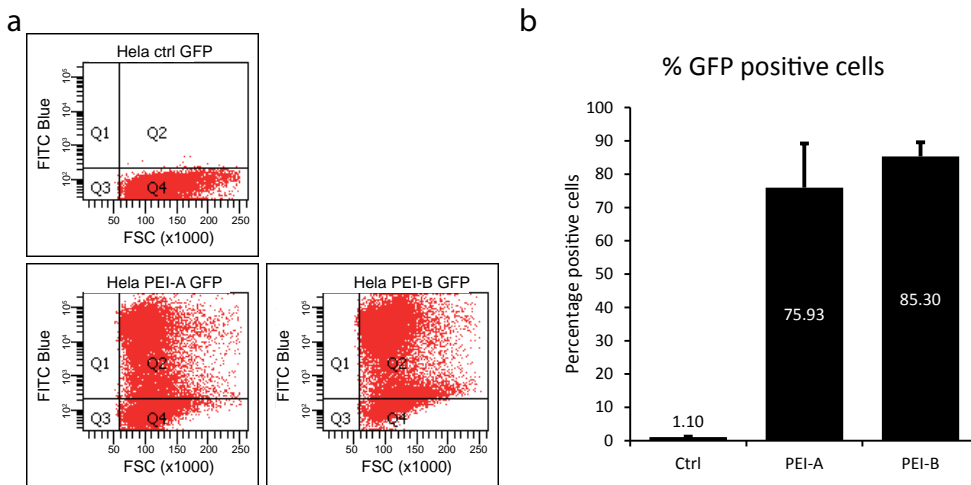


Figure 6 (a) FACS analysis of the GFP signal in the PEI transfected HeLa cells shows that transfection efficiency is similar using the standard protocol (PEI-A) or adapted protocol (PEI-B). **(b)** Quantification of GFP positive (Q2) versus total cells shows a transfection efficiency of ~75% using protocol A, which is equal to the adapted protocol B. Error bars represent SD.

Discussion

In this study we use fluorescence and electron microscopy to study the effect of PEI transfection on the endolysosomal system, using HeLa cells as model system. We show that a widely used transfection protocol for PEI (22) caused a significant decrease in EEA1-positive EE numbers. By contrast, LAMP-1-positive LE/lysosome numbers and integrity were unaffected. Importantly, adapting the standard overnight transfection protocol to a pulse-chase protocol restored the number of EEs to wild-type levels while retaining a high level of transfection activity. From these data we conclude that PEI-mediated transfections particularly affect EEs but that this effect is temporary and can be reversed. We therefore recommend an adapted transfection protocol for studies that require an intact endolysosomal system in PEI transfected cells.

Escape from the endolysosomal system is an essential step for successful transfection (27). For cationic polymers such as PEI the proton sponge model for endosomal escape indicates that rupture of endosomal membranes is needed for transfer from the endosomal lumen to cytoplasm. By EM we found PEI-DNA polyplexes in all compartments of the endolysosomal system up to lysosomes. This is in agreement with earlier observations (11,13). Notably, despite the presence of PEI-DNA polyplexes in lysosomes, we observed no change in LE/lysosome number and no lysosomal membrane permeabilization could be detected. This indicates that lysosomes are unaffected by the presence of PEI, implicating that PEI-DNA polyplexes will be degraded rather than transferred to the cytosol. An explanation for this is that lysosomes have more stable, heavily glycosylated limiting membranes that protect them from hydrolase activity (20,21) that may protect from rupture.

We revealed a significant decrease EEA1 fluorescence signal area after PEI-mediated transfection. This indicates that the number of EEA1-positive EEs is decreased. If osmotic rupture disrupts endosomal membranes, it is likely that damaged endosomes are cleared from the cytosol by autophagy, a mechanism that is known to clear damaged endosomes and lysosomes (28,29). Alternatively, or additionally, disruption of the endosomal membrane could prevent recruitment of fusion proteins such as EEA1 to EEs to avoid erroneous fusion with damaged compartments. Future studies on the induction of autophagy by PEI-mediated transfection could distinguish between these mechanisms of EE clearance.

In addition to decreased levels of EEA1, we found a significant decrease in dextran levels after PEI-mediated transfection. This can be explained by either a decrease in endocytosis or by leaking of dextran from damaged endosomes to the cytosol. Since PEI-DNA polyplexes are endocytosed themselves, and we could detect polyplexes in EEs after transfection (fig. 2), it is likely that the latter explanation causes the decrease in dextran fluorescence. Dextran leaking into the cytosol is diluted, resulting in disappearance of the fluorescent signal under the threshold that was set to identify endosomal punctae, causing a decrease in dextran fluorescence area per cell.

Surprisingly, we identified only a minor increase in endosomal size after overnight PEI-mediated transfection. The proton sponge hypothesis states membrane rupture is caused by endosomal swelling, while we observed only a 17% increase in endosome size. Although we cannot exclude that minor swelling induces membrane rupture, other inhibitors of endosomal acidification, such as chloroquine or ammonium chloride can induce over 10-fold increase in endosome size in the same timeframe (30,31). One explanation for this is that endosome and consecutive rupture occurs rapidly and is therefore undetectable after overnight treatment. This is in agreement with

earlier observations where a 3-fold increase in endosome size was measured after 1 hour (32). Alternatively, other mechanisms for polyplex release other than the proton sponge hypothesis should be investigated. For example, membrane instability caused by the direct interaction of PEI with the endosomal membrane could induce permeabilization (33).

Other commonly used transfection methods that require endosomal escape are the use of lipid-based reagents or calcium phosphate precipitates (CCPs). CCPs induce endosomal damage, upregulating autophagy resulting in major alterations of the endolysosomal system after transfection (28). CCP-based transfection protocols could therefore also potentially profit from a protocol that includes a chase period. By contrast, the destabilizing effect of the lipid complexes on the endolysosomal system is less damaging since they do not cause osmotic swelling or membrane rupture, but back-fuse with the limiting membrane of endosomal compartments (34–36), causing only minor disruptive effects on endosomal membrane integrity. However, in studies that require an intact endolysosomal system the use of any transfection method that requires endosomal escape could potentially benefit from a protocol that includes a chase period to allow restoration of endosome numbers.

In summary, our data show that PEI-induced alterations to the endolysosomal system are limited to the early endocytic compartments and transient in nature. Application of an adapted protocol that includes a chase period is an easy tool to circumvent this disruption.

Materials & Methods

Cell culture

HeLa cells (ATCC clone ccl-2) were cultured in Dulbecco's modified Eagle's medium (DMEM) supplemented with 10% heat inactivated Fetal Bovine Serum (FBS), 2mM L-Glutamin, 100U/mL penicillin and 100µg/mL streptomycin (complete DMEM) at 37°C and 5% CO₂.

Antibodies and reagents

Mouse-anti-human EEA1 (BD Transduction Lab), mouse-anti-human LAMP-1 CD107a (BD Pharmingen), Fluorescent secondary antibodies were obtained from Invitrogen, Fluorescent 10.000MW dextran-Alexa Fluor 568 (Invitrogen), linear 40kDa polyethylenimine (PEI) (Polysciences inc.), effectene transfection reagent (Qiagen).

Transfection protocols

HeLa cells were transfected with Pcdna3.2-GFP cDNA using linear 40kDa polyethylenimine (Polysciences inc.) with a DNA:PEI ratio of 1:5 using protocol described in (22). In the standard protocol the transfection mix was added to the HeLa cells for 16 hours. In the adapted protocol cells were washed 3 times and chased for 16 hours with 37°C complete DMEM after being subjected to the PEI-DNA mixture for 8 hours. Effectene transfection reagent (Qiagen) was used as a positive control for lysosomal leakage assay using a 5 times higher concentration of effectene than the manufacturer's protocol.

Immunofluorescence microscopy

HeLa cells grown on sterile glass coverslips were washed with ice-cold PBS and fixed with 4% paraformaldehyde (PFA) in PBS for 20 minutes at RT (room temperature). Then, cells were permeabilized using 0,1% Triton-X100 in PBS for 5 minutes and blocked for 15 minutes using PBS supplemented with 1% BSA. Cells were labeled with primary antibodies diluted in blocking buffer at RT for 1 hour, washed, and labeled with fluorescent secondary antibodies for 30 minutes in the dark. After labeling the cells were washed and mounted using Prolong Gold antifade reagent with DAPI. Cells were imaged on a Deltavision wide field microscope using a 100x/1.4A immersion objective. Widefield pictures were deconvolved using Softworx software and analyzed using FIJI.

Electron microscopy

Cells grown on 6cm dishes were fixed in 2% wt/vol PFA, 2.5% wt/vol GA in Na-cacodylate buffer (Karnovsky fixative) for 2 h at RT. Subsequently, the Karnovsky fixative was replaced for 0.1 M Na-cacodylate buffer, pH 7.4. Post fixation before Epon embedding was performed with 1% wt/vol OsO₄, 1.5% wt/vol K₃Fe(III)(CN)₆ in 0.065 M Na-cacodylate for 2 h at 4°C. Subsequently the cells were stained with 0.5% uranyl acetate for 1 h at 4°C, dehydrated with ethanol, and embedded in Epon. Ultrathin sections were stained with uranyl acetate and lead citrate. Images were taken on a TECNAI T12 electron microscope.

Lysosomal membrane permeabilization assay

Galectin-mCherry based lysosomal leakage assay as described in (26). In short, galectin3-

mCherry is localized to the cytosol and nucleus in unaffected cells. Upon lysosomal membrane permeabilization (LMP) Galectin3 is able to bind N-acetyllactosamine-containing glycans present on the inner membrane of lysosomes, leading to an accumulation selectively in damaged lysosomes.

FACS analysis

Transfection efficiency was measured by FACS using the GFP signal after PEI transfection of PCDNA3.2-GFP in HeLa cells using 20.000 cells analyzed on a BD CANTO-II FACS.

Acknowledgments

We thank Nalan Liv, Job Fermie, Ann De Mazière and George Posthuma for assistance with the electron micrographs and René Scriwanek for preparation of EM figures.

References

1. Ruponen M, Honkakoski P, Rönkkö S, Pelkonen J, Tammi M, Urtti A. Extracellular and intracellular barriers in non-viral gene delivery. *J Control Release*. 2003 Dec 5;93(2):213–217.
2. Thomas CE, Ehrhardt A, Kay MA. Progress and problems with the use of viral vectors for gene therapy. *Nat Rev Genet*. 2003 May;4(5):346–358.
3. Boussif O, Lezoualc’h F, Zanta MA, Mergny MD, Scherman D, Demeneix B, et al. A versatile vector for gene and oligonucleotide transfer into cells in culture and in vivo: polyethylenimine. *Proc Natl Acad Sci U S A*. 1995 Aug 1;92(16):7297–7301.
4. Neuberg P, Kichler A. Recent developments in nucleic acid delivery with polyethylenimines. *Adv Genet*. 2014;88:263–288.
5. Yin H, Kanasty RL, Eltoukhy AA, Vegas AJ, Dorkin JR, Anderson DG. Non-viral vectors for gene-based therapy. *Nat Rev Genet*. 2014 Aug;15(8):541–555.
6. Kay MA. State-of-the-art gene-based therapies: the road ahead. *Nat Rev Genet*. 2011 May;12(5):316–328.
7. Mislick KA, Baldeschwieler JD. Evidence for the role of proteoglycans in cation-mediated gene transfer. *Proc Natl Acad Sci U S A*. 1996 Oct 29;93(22):12349–12354.
8. Paris S, Burlacu A, Durocher Y. Opposing roles of syndecan-1 and syndecan-2 in polyethyleneimine-mediated gene delivery. *J Biol Chem*. 2008 Mar 21;283(12):7697–7704.
9. Kopatz I, Remy JS, Behr JP. A model for non-viral gene delivery: through syndecan adhesion molecules and powered by actin. *J Gene Med*. 2004 Jul;6(7):769–776.
10. Von Gersdorff K, Sanders NN, Vandenbroucke R, De Smedt SC, Wagner E, Ogris M. The internalization route resulting in successful gene expression depends on both cell line and polyethylenimine polyplex type. *Mol Ther*. 2006 Nov;14(5):745–753.
11. Benjaminsen RV, Matthebjerg MA, Henriksen JR, Moghimi SM, Andresen TL. The possible “proton sponge” effect of polyethylenimine (PEI) does not include change in lysosomal pH. *Mol Ther*. 2013 Jan;21(1):149–157.
12. Bieber T, Meissner W, Kostin S, Niemann A, Elsasser HP. Intracellular route and transcriptional competence of polyethylenimine-DNA complexes. *J Control Release*. 2002 Aug 21;82(2-3):441–454.
13. Merdan T, Kunath K, Fischer D, Kopecek J, Kissel T. Intracellular processing of poly(ethylene imine)/ribozyme complexes can be observed in living cells by using confocal laser scanning microscopy and inhibitor experiments. *Pharm Res*. 2002 Feb;19(2):140–146.
14. Brunner S, Fürtbauer E, Sauer T, Kursa M, Wagner E. Overcoming the nuclear barrier: cell cycle independent nonviral gene transfer with linear polyethylenimine or electroporation. *Mol Ther*. 2002 Jan;5(1):80–86.
15. Sönnichsen B, De Renzis S, Nielsen E, Rietdorf J, Zerial M. Distinct membrane domains on endosomes in the recycling pathway visualized by multicolor imaging of Rab4, Rab5, and Rab11. *J Cell Biol*. 2000 May 15;149(4):901–914.
16. Rink J, Ghigo E, Kalaidzidis Y, Zerial M. Rab conversion as a mechanism of progression from early to late endosomes. *Cell*. 2005 Sep 9;122(5):735–749.
17. Doherty GJ, McMahon HT. Mechanisms of endocytosis. *Annu Rev Biochem*. 2009;78:857–902.
18. Grant BD, Donaldson JG. Pathways and mechanisms of endocytic recycling. *Nat Rev Mol Cell Biol*. 2009 Sep;10(9):597–608.
19. Huotari J, Helenius A. Endosome maturation. *EMBO J*. 2011 Aug 31;30(17):3481–3500.
20. Saftig P, Klumperman J. Lysosome biogenesis and lysosomal membrane proteins: trafficking meets function. *Nat Rev Mol Cell Biol*. 2009 Sep;10(9):623–635.
21. Klumperman J, Raposo G. The complex ultrastructure of the endolysosomal system. *Cold Spring Harb Perspect Biol*. 2014 Oct;6(10):a016857.
22. Longo PA, Kavran JM, Kim MS, Leahy DJ. Transient mammalian cell transfection with polyethylenimine (PEI). *Meth Enzymol*. 2013;529:227–240.
23. Choosakoonkriang S, Lobo BA, Koe GS, Koe JG, Middaugh CR. Biophysical Characterization of PEI/DNA Complexes. *J Pharm Sci*. 2003 Aug;92(8):1710–1722.
24. Aits S, Jäättelä M. Lysosomal cell death at a glance. *J Cell Sci*. 2013 May 1;126(Pt 9):1905–1912.
25. Ellegaard AM, Groth-Pedersen L, Oorschot V, Klumperman J, Kirkegaard T, Nylandsted J, et al. Sunitinib and

- SU11652 inhibit acid sphingomyelinase, destabilize lysosomes, and inhibit multidrug resistance. *Mol Cancer Ther.* 2013 Oct;12(10):2018–2030.
26. Aits S, Krickler J, Liu B, Ellegaard AM, Hämälistö S, Tvingsholm S, et al. Sensitive detection of lysosomal membrane permeabilization by lysosomal galectin puncta assay. *Autophagy.* 2015;11(8):1408–1424.
 27. El Ouahabi A, Thiry M, Pector V, Fuks R, Ruyschaert JM, Vandenbranden M. The role of endosome destabilizing activity in the gene transfer process mediated by cationic lipids. *FEBS Lett.* 1997 Sep 8;414(2):187–192.
 28. Chen X, Khambu B, Zhang H, Gao W, Li M, Chen X, et al. Autophagy induced by calcium phosphate precipitates targets damaged endosomes. *J Biol Chem.* 2014 Apr 18;289(16):11162–11174.
 29. Hung YH, Chen LM, Yang JY, Yang WY. Spatiotemporally controlled induction of autophagy-mediated lysosome turnover. *Nat Commun.* 2013;4:2111.
 30. Bacac M, Fusco C, Planche A, Santodomingo J, Demaurex N, Leemann-Zakaryan R, et al. Securin and separase modulate membrane traffic by affecting endosomal acidification. *Traffic.* 2011 May;12(5):615–626.
 31. Florey O, Gammoh N, Kim SE, Jiang X, Overholtzer M. V-ATPase and osmotic imbalances activate endolysosomal LC3 lipidation. *Autophagy.* 2015;11(1):88–99.
 32. Sonawane ND, Szoka FC, Verkman AS. Chloride accumulation and swelling in endosomes enhances DNA transfer by polyamine-DNA polyplexes. *J Biol Chem.* 2003 Nov 7;278(45):44826–44831.
 33. Choudhury CK, Kumar A, Roy S. Characterization of conformation and interaction of gene delivery vector polyethylenimine with phospholipid bilayer at different protonation state. *Biomacromolecules.* 2013 Oct 14;14(10):3759–3768.
 34. Zelphati O, Szoka FC. Mechanism of oligonucleotide release from cationic liposomes. *Proc Natl Acad Sci U S A.* 1996 Oct 15;93(21):11493–11498.
 35. Xu Y, Szoka FC. Mechanism of DNA release from cationic liposome/DNA complexes used in cell transfection. *Biochemistry.* 1996 May 7;35(18):5616–5623.
 36. Zhou X, Huang L. DNA transfection mediated by cationic liposomes containing lipopolylysine: characterization and mechanism of action. *Biochimica et Biophysica Acta (BBA) - Biomembranes.* 1994 Jan;1189(2):195–203.



Summarizing discussion

Caspar TH Jonker¹ & J. Klumperman¹

¹ Department of Cell Biology, Center for Molecular Medicine, University Medical Center Utrecht, the Netherlands.

Chapter 7

Mammalian HOPS and CORVET in the endolysosomal system

Transport of internalized cargo through the endolysosomal system is a tightly controlled process that ultimately results in cargo degradation or recycling. Cargo fate is determined by passage through different compartments of the endolysosomal system, which requires multiple protein sorting and membrane fusion steps. Membrane fusion depends on dedicated fusion machinery, which comprises SNARE proteins, Rab-GTPases and tethering factors. Tethering factors establish the first contact between membranes, which ultimately can lead to fusion. The multi-subunit tethering complexes CORVET and HOPS are important for fusion between endolysosomal compartments. Mammalian CORVET and HOPS consist of a core of 4 proteins (Vps11, Vps16, Vps18, Vps33A) and two complex-specific subunits, Vps8 and Vps3 for CORVET and Vps41 and Vps39 for HOPS (1). In higher eukaryotes, a third complex exists consisting of VIPAS39 and Vps33B, which are highly homologous to core subunits Vps16 and Vps33A respectively. In this thesis we investigate the role of Vps tethering proteins in endolysosomal transport, as part of a complex and as individual subunits.

In chapter 2 we provide a detailed analysis of the interactions within the mammalian CORVET and HOPS complexes, and show that VIPAS39 and VPS33B form a separate complex. We show that interactions within CORVET and HOPS are largely conserved from yeast to mammals, but that the membrane-targeting mechanism in HOPS has evolved by binding of individual HOPS subunits to the mammalian-specific Rab7-interacting lysosomal protein (RILP). Via RILP the HOPS complex is connected to other processes than tethering. For example, RILP binds the dynein motor complex which mediates retrograde transport of late endosomes (LEs) to the perinuclear area (2). Interestingly, the HOPS specific protein Vps41 in addition to RILP also interacts with Arl8b, which together with its effector protein SKIP regulates anterograde transport (3). This shows that LE movement is connected to HOPS and the fusion machinery. Since the HOPS and CORVET complexes are highly similar, comparable mechanisms are believed to exist for the CORVET complex.

The high level of similarity between HOPS and CORVET raises the question how they can interact with distinct sets of interactor proteins present on different membranes (i.e. on early and late endosomes respectively). For example, the CORVET complex does not interact with RILP. In chapter 2 we show that Vps11, a subunit of core complex shared by CORVET and HOPS, acts as a molecular switch to regulate binding to RILP. Binding of Vps3 to Vps11 prevents interaction of RILP with Vps11, thereby regulating the selective targeting of CORVET and HOPS to early- or late endosomes. This shows how dynamic interactions within the complex result in a different interactome and contributes to the emerging view that multisubunit tethering complexes can regulate multiple transport pathways by locally distinct subunit compositions.

The versatile nature of CORVET subunits: Vps3 and Vps8 in endocytic recycling and polarity

As part of the CORVET complex, Vps3 and Vps8 mediate the homotypic fusion between early endosomes (EEs) (4,5). In addition to this established function, in chapter 3 we define a novel complex consisting of Vps3 and Vps8 only (i.e without requiring the core subunits) that localizes to Rab4-positive, EE-associated recycling vesicles and regulates vesicular transport from EEs to recycling endosomes (REs). The formation of a distinct Vps3/8 complex independent of the CORVET/ HOPS core components underlines the dynamic nature of multisubunit tethering complexes and exemplifies the individual roles that subunits can have outside the complex.

In analogy herewith, it was previously shown that Vps41 independently of the HOPS complex regulates the vesicular transport of lysosomal membrane proteins from the TGN to LEs (6).

The Vps33B/VIPAS39 complex binds to Rab11 on REs (5,7–9). Using colP we show in Chapter 3 that the Vps3/8 and Vps33B/VIPAS39 complexes interact with each other and that both complexes are required for transport of β 1 integrins from EEs to REs. Impairment of the pathway delayed integrin recycling, resulting in defects in cell adhesion, spreading, migration and focal adhesion formation. By contrast, depletion of Vps3/8 or Vps33B/VIPAS39 did not affect transferrin recycling, indicating that recycling through this pathway is for selected cargo's only. The Vps33B/VIPAS39 complex is only found in higher eukaryotes (10). Similarly, integrin-mediated processes such as substrate dependent migration are only found in higher eukaryotes. We therefore speculate that the Vps33B/VIPAS39 complex as well as the role of Vps3 and Vps8 in recycling co-evolved with the need for specialized recycling pathways, such as for integrin. The Vps3/8-Vps33B/VIPAS39 pathway shares machinery like Rab4 and Rab11 with other recycling pathways, but likely defines a subset of membranes or specialized membrane subdomains to regulate the PM expression of specific cargo's. In case of integrins PM levels determine migration capacity of metastasizing cancer cells, illustrating the importance of a specialized recycling pathway to regulate PM levels. In polarized cells, Vps33B and VIPAS39 are required for transport of apical and junctional proteins (7,8), a process that is also specific for higher eukaryotes. Mutations in Vps33B or VIPAS39 cause Arthrogyryposis-Renal dysfunction-Cholestasis (ARC) syndrome, a multisystem disorder that is characterized by neurogenic arthrogyryposis, renal dysfunction and neonatal cholestasis (7,8,11). Interestingly, a recent study revealed that a subset of patients with an ARC-like phenotype carried a mutation in Vps8 (12), linking Vps8 to apical trafficking and reinforcing the connection between Vps3/8 and Vps33B/VIPAS39 that we found in non-polarized cells.

Apical recycling pathways in polarized epithelial cells requires specialized apical recycling endosomes (AREs) to regulate transport to the apical PM (13–15). Since we showed that the Vps3/8 complex together with VIPAS39/Vps33B controls transport from EEs to REs in non-polarized cells, we investigated in chapter 4 whether the Vps3/8 complex is also involved in apical recycling. We showed that Vps8 localized to EEA1-positive EEs as well as Rab11-positive AREs. Strikingly, overexpression of Vps8 induced recruitment of EEs to the ARE, suggesting a role for Vps8 in membrane tethering between these compartments. Furthermore, knockdown of Vps8 resulted in perturbation of apical-basal cell polarity, prevented completion of cytokinesis, and impaired front-rear polarization of cells during directed cell migration. Similarly, depletion of Vps33B or VIPAS39 result in the loss of polarization in renal cell lines (7). These findings reinforce the notion that Vps3/8 and VIPAS39/Vps33B act together on the same recycling pathway, which in polarized cells has developed into a specialized pathway from EEs to the ARE.

Integrin recycling is intimately connected to the correct polarization of a migrating cell. Specialized protein complexes that establish front-rear polarization are localized on the leading edge of the cell and are activated by integrins (16,17). This connects the role of Vps8 in integrin recycling to that of front-rear polarization in migrating cells. A similar connection can be made between integrin recycling and cell division. Completion of cytokinesis requires abscission of the intercellular bridge (ICB) near the midbody, a process that requires input from Rab11 positive REs (18–21). During the late stages of cytokinesis, β 1 integrins are transported to the ICB to assist in the abscission process (22). Although the exact function remains unclear, it is speculated that integrins mediate the attachment of the ICB to the matrix and assist in the assembly of the

contractile ring (22,23). This indicates that the defect after Vps8 knockdown could be caused by disturbed integrin transport. In most polarized epithelial cells however, the majority of integrins is localized to the basal membrane where they initiate apical-basal polarity (24,25). This raises the question whether in polarized cells the Vps3/8-dependent recycling pathway is truly conserved. In polarized cells, integrins are mainly recycled basolateral, not apical (24), suggesting a different cargo for the Vps3/8-dependent recycling pathway in these cells. Further identification of cargo specific for Vps3/8-positive recycling vesicles in different cell types would help to clarify the connection between the Vps3/8-dependent integrin recycling pathway and the processes of epithelial polarity, cytokinesis and front-rear polarity.

Vps3 and Vps8 as modulators of the TGF β pathway

The TGF β signaling pathway regulates the expression of target genes through a signaling cascade of Smad proteins. A complex of Smad2 and Smad3 is phosphorylated by activated TGF β receptors and requires Smad4 to travel the nucleus (26–29). Transforming growth factor-beta receptor associated protein 1 (TGFBRAP1) is a Smad4 chaperone that mediates transfer of Smad4 to the phosphorylated Smad2/3 complex (30). Recently, TGFBRAP1 was identified to be the CORVET subunit Vps3 (4,5), suggesting a role for TGFBRAP1/Vps3 in both signaling (by binding Smad4 in the TGF β signaling pathway) and trafficking (by mediating EE fusion and EE to RE transport in and outside the CORVET complex respectively). Since TGFBRAP1/Vps3 localizes to EEs and recycling vesicles, we investigated in chapter 5 whether this membrane localization is required for its chaperone function and if any of the other CORVET subunits are involved in the Smad4 chaperone function. We find that TGFBRAP1/Vps3 expression induces endosomal recruitment of Smad4, pinpointing EEs as the site of the proposed chaperone function of TGFBRAP1/Vps3. Similar results were found after Vps8 expression, indicating a role for the binding partners of TGFBRAP1/Vps3 in Smad4 binding. A likely explanation therefore is that Vps8 recruits TGFBRAP1/Vps3 to EE membranes. Our findings are in agreement with the concept that the dynamic composition of multisubunit tethering complexes allows them to engage various endosomal processes, such as signaling.

Additionally, we find that TGFBRAP1/Vps3 and Vps8 knockdown results in the intracellular accumulation of TGF β receptor II (TGFBRII). This indicates that TGFBRAP1/Vps3 and Vps8 are required for the recycling of TGFBRII and identify TGF β receptors as a potential cargo for the Vps3/8-regulated recycling pathway. Together these results reveal a potential role for the CORVET complex in TGF β signaling from endosomes, a new function for this complex. Moreover, it shows that Vps3 and Vps8 have a dual role in the TGFBR signaling pathway, as signaling molecules and as regulators of TGFBR transport.

The impact of polymer based transfection methods on the endolysosomal system

Studying the endolysosomal system using fluorescence and electron microscopy techniques often requires exogenous expression of (tagged) proteins. Overexpression is used when endogenous protein levels are too low or when there are no suitable antibodies available. In addition, numerous functional assays such as luciferase reporter assays require overexpression. Transfection should have minimal effect on the homeostasis of cells, but in practice often poses a number of strains on cells (31). Transfection of cells using polyethylenimine (PEI) polymers is a widely used method. The current model states that PEI polymers are internalized by endocytosis,

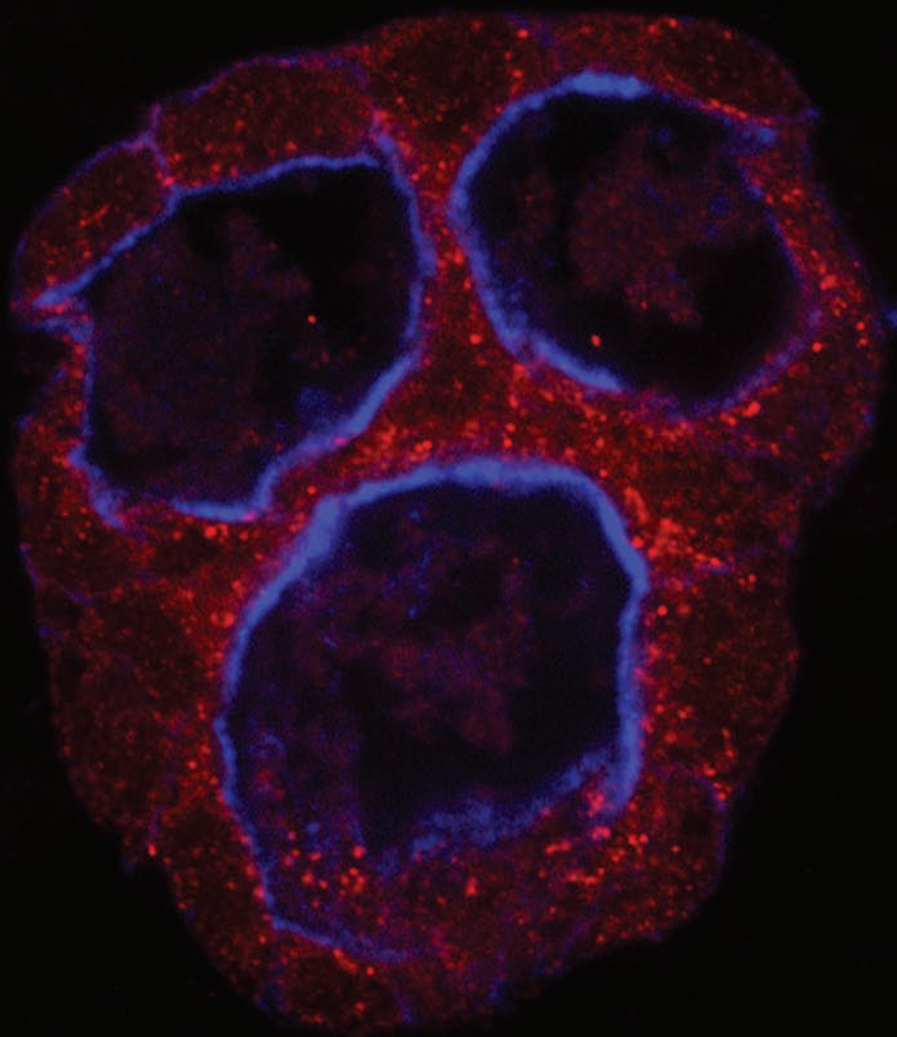
which then cause endolysosomal rupture, releasing the PEI-DNA complexes into the cytosol (32). In chapter 6 we test the impact of PEI transfections on the endolysosomal system using fluorescent and electron microscopy techniques. We find a decrease in the number of EEs after PEI transfection, while the number and integrity of lysosomes stay intact. Importantly, we reveal that the disruption of the endolysosomal system is reversible by implementing a chase period after transfection that allows the endosomal system to recover.

Together our studies highlight multisubunit tethering complexes as dynamic molecular regulators with multiple functions in vesicular transport, organelle dynamics and signaling. By relatively minor changes in subunit composition or by the formation of subcomplexes, a single subunit can regulate various transport steps. Our data thus depict CORVET, HOPS, Vps33B/VIPAS39 and the here defined subcomplex Vps3/8 as active regulatory components of the cellular protein machinery. They can act in general pathways, like EE fusion, as well as specialized pathways, such as integrin recycling. The importance of these protein complexes for human health is illustrated by the increasing number of diseases that is caused by mutations in individual subunits, such as ARC syndrome, but also cancer and neurodegenerative diseases (33–38). A challenge for future studies will be to understand the precise role of each subunit in intracellular trafficking, and establish whether disease-causing mutations are due to disruption of a complex or by complex-independent activities.

References

1. Klinger CM, Klute MJ, Dacks JB. Comparative genomic analysis of multi-subunit tethering complexes demonstrates an ancient pan-eukaryotic complement and sculpting in Apicomplexa. *PLoS ONE*. 2013 Sep 27;8(9):e76278.
2. Van der Kant R, Fish A, Janssen L, Janssen H, Krom S, Ho N, et al. Late endosomal transport and tethering are coupled processes controlled by RILP and the cholesterol sensor ORP1L. *J Cell Sci*. 2013 Aug 1;126(Pt 15):3462–3474.
3. Khatter D, Raina VB, Dwivedi D, Sindhwani A, Bahl S, Sharma M. The small GTPase Arl8b regulates assembly of the mammalian HOPS complex on lysosomes. *J Cell Sci*. 2015 May 1;128(9):1746–1761.
4. Perini ED, Schaefer R, Stöter M, Kalaidzidis Y, Zerial M. Mammalian CORVET is required for fusion and conversion of distinct early endosome subpopulations. *Traffic*. 2014 Dec;15(12):1366–1389.
5. Van der Kant R, Jonker CT, Wijdeven RH, Bakker J, Janssen L, Klumperman J, et al. Characterization of the mammalian CORVET and HOPS complexes and their modular restructuring for endosome specificity. *J Biol Chem*. 2015 Oct 13;190(26):16111–16121.
6. Pols MS, van Meel E, Oorschot V, ten Brink C, Fukuda M, Swetha MG, et al. hVps41 and VAMP7 function in direct TGN to late endosome transport of lysosomal membrane proteins. *Nat Commun*. 2013;4:1361.
7. Cullinane AR, Straatman-Iwanowska A, Zaucker A, Wakabayashi Y, Bruce CK, Luo G, et al. Mutations in VIPAR cause an arthrogryposis, renal dysfunction and cholestasis syndrome phenotype with defects in epithelial polarization. *Nat Genet*. 2010 Apr;42(4):303–312.
8. Smith H, Galmes R, Gogolina E, Straatman-Iwanowska A, Reay K, Banushi B, et al. Associations among genotype, clinical phenotype, and intracellular localization of trafficking proteins in ARC syndrome. *Hum Mutat*. 2012 Dec;33(12):1656–1664.
9. Tornieri K, Zlatich SA, Mullin AP, Werner E, Harrison R, L'hernault SW, et al. Vps33b pathogenic mutations preferentially affect VIPAS39/SPE-39-positive endosomes. *Hum Mol Genet*. 2013 Dec 20;22(25):5215–5228.
10. Gissen P, Johnson CA, Gentle D, Hurst LD, Doherty AJ, O'Kane CJ, et al. Comparative evolutionary analysis of VPS33 homologues: genetic and functional insights. *Hum Mol Genet*. 2005 May 15;14(10):1261–1270.
11. Gissen P, Johnson CA, Morgan NV, Stapelbroek JM, Forshew T, Cooper WN, et al. Mutations in VPS33B, encoding a regulator of SNARE-dependent membrane fusion, cause arthrogryposis-renal dysfunction-cholestasis (ARC) syndrome. *Nat Genet*. 2004 Apr;36(4):400–404.
12. Bayram Y, Karaca E, Coban Akdemir Z, Yilmaz EO, Tayfun GA, Aydin H, et al. Molecular etiology of arthrogryposis in multiple families of mostly Turkish origin. *J Clin Invest*. 2016 Feb 1;126(2):762–778.
13. Golachowska MR, Hoekstra D, van IJzendoorn SC. Recycling endosomes in apical plasma membrane domain formation and epithelial cell polarity. *Trends Cell Biol*. 2010 Oct;20(10):618–626.
14. Apodaca G, Katz LA, Mostov KE. Receptor-mediated transcytosis of IgA in MDCK cells is via apical recycling endosomes. *J Cell Biol*. 1994 Apr;125(1):67–86.
15. Brown PS, Wang E, Aroeti B, Chapin SJ, Mostov KE, Dunn KW. Definition of distinct compartments in polarized Madin-Darby canine kidney (MDCK) cells for membrane-volume sorting, polarized sorting and apical recycling. *Traffic*. 2000 Feb;1(2):124–140.
16. Osmani N, Peglion F, Chavrier P, Etienne-Manneville S. Cdc42 localization and cell polarity depend on membrane traffic. *J Cell Biol*. 2010 Dec 27;191(7):1261–1269.
17. Etienne-Manneville S, Hall A. Integrin-Mediated Activation of Cdc42 Controls Cell Polarity in Migrating Astrocytes through PKC ζ . *Cell*. 2001 Aug;106(4):489–498.
18. Fielding AB, Schonteich E, Matheson J, Wilson G, Yu X, Hickson GR, et al. Rab11-FIP3 and FIP4 interact with Arf6 and the exocyst to control membrane traffic in cytokinesis. *EMBO J*. 2005 Oct 5;24(19):3389–3399.
19. Wilson GM, Fielding AB, Simon GC, Yu X, Andrews PD, Hames RS, et al. The FIP3-Rab11 protein complex regulates recycling endosome targeting to the cleavage furrow during late cytokinesis. *Mol Biol Cell*. 2005 Feb;16(2):849–860.
20. Schiel JA, Childs C, Prekeris R. Endocytic transport and cytokinesis: from regulation of the cytoskeleton to midbody inheritance. *Trends Cell Biol*. 2013 Jul;23(7):319–327.
21. Schiel JA, Simon GC, Zaharris C, Weisz J, Castle D, Wu CC, et al. FIP3-endosome-dependent formation of the secondary ingression mediates ESCRT-III recruitment during cytokinesis. *Nat Cell Biol*. 2012 Oct;14(10):1068–1078.
22. Pellinen T, Tuomi S, Arjonen A, Wolf M, Edgren H, Meyer H, et al. Integrin trafficking regulated by Rab21 is necessary for cytokinesis. *Dev Cell*. 2008 Sep;15(3):371–385.
23. Caswell PT, Vadrevu S, Norman JC. Integrins: masters and slaves of endocytic transport. *Nat Rev Mol Cell Biol*. 2009

- Dec;10(12):843–853.
24. Lee JL, Streuli CH. Integrins and epithelial cell polarity. *J Cell Sci.* 2014 Aug 1;127(Pt 15):3217–3225.
 25. Rodriguez-Boulan E, Macara IG. Organization and execution of the epithelial polarity programme. *Nat Rev Mol Cell Biol.* 2014 Apr;15(4):225–242.
 26. Derynck R, Zhang YE. Smad-dependent and Smad-independent pathways in TGF-beta family signalling. *Nature.* 2003 Oct 9;425(6958):577–584.
 27. Feng XH, Derynck R. Specificity and versatility in tgf- β signaling through Smads. *Annu Rev Cell Dev Biol.* 2005;21:659–693.
 28. Wrana JL. Regulation of Smad activity. *Cell.* 2000 Jan 21;100(2):189–192.
 29. Shi Y, Massagué J. Mechanisms of TGF-beta signaling from cell membrane to the nucleus. *Cell.* 2003 Jun 13;113(6):685–700.
 30. Wurthner JU, Frank DB, Felici A, Green HM, Cao Z, Schneider MD, et al. Transforming growth factor-beta receptor-associated protein 1 is a Smad4 chaperone. *J Biol Chem.* 2001 Jun 1;276(22):19495–19502.
 31. Ruponen M, Honkakoski P, Rönkkö S, Pelkonen J, Tammi M, Urtti A. Extracellular and intracellular barriers in non-viral gene delivery. *J Control Release.* 2003 Dec 5;93(2):213–217.
 32. Benjaminsen RV, Matthebjerg MA, Henriksen JR, Moghimi SM, Andresen TL. The possible “proton sponge” effect of polyethylenimine (PEI) does not include change in lysosomal pH. *Mol Ther.* 2013 Jan;21(1):149–157.
 33. Suzuki T, Oiso N, Gautam R, Novak EK, Panthier JJ, Suprabha PG, et al. The mouse organellar biogenesis mutant buff results from a mutation in Vps33a, a homologue of yeast vps33 and Drosophila carnation. *Proc Natl Acad Sci U S A.* 2003 Feb 4;100(3):1146–1150.
 34. Peng C, Yan S, Ye J, Shen L, Xu T, Tao W. Vps18 deficiency inhibits dendritogenesis in Purkinje cells by blocking the lysosomal degradation of Lysyl Oxidase. *Biochem Biophys Res Commun.* 2012 Jul 13;423(4):715–720.
 35. Peng C, Ye J, Yan S, Kong S, Shen Y, Li C, et al. Ablation of vacuole protein sorting 18 (Vps18) gene leads to neurodegeneration and impaired neuronal migration by disrupting multiple vesicle transport pathways to lysosomes. *J Biol Chem.* 2012 Sep 21;287(39):32861–32873.
 36. Zhang J, Lachance V, Schaffner A, Li X, Fedick A, Kaye LE, et al. A Founder Mutation in VPS11 Causes an Autosomal Recessive Leukoencephalopathy Linked to Autophagic Defects. *PLoS Genet.* 2016 Apr 27;12(4):e1005848.
 37. Edvardson S, Gerhard F, Jalas C, Lachmann J, Golan D, Saada A, et al. Hypomyelination and developmental delay associated with VPS11 mutation in Ashkenazi-Jewish patients. *J Med Genet.* 2015 Nov;52(11):749–753.
 38. Chi C, Zhu H, Han M, Zhuang Y, Wu X, Xu T. Disruption of lysosome function promotes tumor growth and metastasis in Drosophila. *J Biol Chem.* 2010 Jul 9;285(28):21817–21823.



Addendum

Nederlandse samenvatting

Inleiding tot intracellulair transport en het endo-lysosomaal systeem

Het menselijk lichaam is opgebouwd uit miljoenen cellen die samen de verschillende organen vormen. Het samenspel van de cellen is belangrijk voor het vormen van weefsels en orgaanstructuren. De taak van een orgaan wordt voor het overgrote deel uitgevoerd binnen in de cellen waaruit het is opgebouwd. Een cel is het toneel voor de duizenden verschillende chemische reacties die nodig zijn voor onderhoud van de cel en het uitvoeren van haar functies. Deze reacties zijn soms tegenstrijdig aan elkaar, zo is het in een cel bijvoorbeeld nodig om eiwitten te produceren, maar ook om eiwitten af te breken. Om deze processen toch in goede banen te laten lopen worden ze onderverdeeld in verschillende compartimenten die omsloten zijn met een lipide membraan, de organellen. Binnen de organellen wordt een optimaal micromilie gecreëerd voor de processen die zich daar afspelen. De organellen in een cel zijn dus van elkaar afgesloten, maar kunnen toch met elkaar communiceren en stoffen uitwisselen. Dit gebeurt voornamelijk door middel van transport via kleine blaasjes die uit het lipide membraan van het organel vormen, zich afsnoeren en vervolgens fuseren met een ander organel. Op deze manier worden eiwitten en lipiden aan- en afgevoerd en kunnen signalen overgebracht worden van het ene naar het andere organel. Deze processen vormen de basis van intracellulair transport in een cel.

Het opnemen van voedingsstoffen, signaal- en membraaneiwitten uit het extracellulair milieu gebeurt door endocytose, het vormen van blaasjes aan het plasmamembraan die zich naar binnen afsnoeren. De blaasjes fuseren met het vroege endosoom waar de geëndocyteerde lading gesorteerd wordt. Vanaf het vroege endosoom kunnen eiwitten weer terug naar het plasmamembraan getransporteerd worden, dit is de recycling-route. De recycling-route wordt bijvoorbeeld gebruikt bij veel plasmamembraan eiwitten met een signaleringsfunctie. Deze worden doorlopend geëndocyteerd en gerecycled zodat ze nog een ronde kunnen signaleren. Het recyclen van eiwitten begint met het afsnoeren van blaasjes van het vroege endosoom. Deze blaasjes kunnen vervolgens óf direct fuseren met het plasmamembraan óf fuseren met een speciaal recycling endosoom. Vanaf het recycling endosoom worden de eiwitten vervolgens alsnog naar het plasmamembraan getransporteerd. De niet gerecyclede eiwitten blijven in het vroege endosoom achter. Het vroege endosoom ondergaat daaropvolgend een verandering die er voor zorgt dat recycling niet meer mogelijk is. Dit gaat gepaard met verzuring van het endosoom, de verplaatsing naar het centrum van de cel en het vormen van blaasjes die afsnoeren naar de binnenkant van het endosoom. Dit proces heet endosomale rijping en resulteert in een laat endosoom. Het late endosoom ontvangt enzymen die nodig zijn voor afbraak van eiwitten en lipiden via transportblaasjes, en is in staat om met een lysosoom te fuseren. Het lysosoom heeft een erg zuur milieu en is volgepakt met een arsenaal aan enzymen die de inhoud van het endosoom/lysosoom afbreken. Het product van de enzymen kan vervolgens weer gebruikt worden om nieuwe eiwitten of lipiden te produceren. De voltallige route vanaf plasmamembraan-blaasjes tot lysosomen vertegenwoordigt het endo-lysosomale systeem.

Het transport via blaasjes en fusie van endosomen is van groot belang voor de functie van het endo-lysosomale systeem. Om er voor te zorgen dat alleen de juiste blaasjes met de juiste compartimenten fuseren, wordt het fuseren van membranen streng gereguleerd en

gecontroleerd. Eén van de eiwitten van fundamenteel belang voor dit proces is de tether, ook wel de lasso genoemd. De tether verzorgt het eerste contact tussen membranen voordat de fusie plaatsvindt. In dit proefschrift spitsen wij ons toe op twee tethers in het endo-lysosomale systeem, het HOPS complex en het CORVET complex. Het HOPS en CORVET zijn overeenkomstige eiwitcomplexen die elk opgebouwd zijn uit zes componenten. Van deze zes eiwitten zijn er vier (Vps11, Vps16, Vps18 en Vps33A) aanwezig in beide complexen. Het CORVET bevat daarnaast Vps3 en Vps8, en het HOPS heeft Vps39 en Vps41 als complex-specifieke eiwitten. Het CORVET complex doet dienst op vroege endosomen, waar het de fusie tussen vroege endosomen reguleert. HOPS reguleert de fusie tussen late endosomen en tussen late endosomen en lysosomen.

De vraagstelling van dit proefschrift richt zich op de functie van het CORVET en HOPS complex in het endo-lysosomale systeem. Enkele vraagstukken zijn: Wat is de samenstelling van de complexen? Is de samenstelling statisch of dynamisch? In welke cellulaire processen en transportroutes functioneren deze complexen? De eiwitten die de basis vormen van beide complexen zijn gering beschreven, wat het verklaren van de fenotypes van sommige gevonden mutaties van deze genen ernstig bemoeilijkt. Een gedegen fundamentele kennis over de functie van deze eiwitten is daarmee ook belangrijk voor toekomstig “translationeel onderzoek”.

Samenvatting van het proefschrift

In **hoofdstuk 2** richten wij ons op de moleculaire architectuur van HOPS en CORVET. Wij stellen de interacties tussen de eiwitten binnen de complexen vast en sluiten uit dat Vps33B en VIPAS39, die gerelateerd zijn aan Vps33A en Vps16, zich in één van de complexen bevinden. In plaats daarvan vormen Vps33B en VIPAS39 een apart complex. Daarnaast onthullen wij dat HOPS en CORVET van elkaar verschillen in hun vermogen met RILP een interactie aan te gaan. RILP is een laat endosomaal eiwit dat van belang is voor het koppelen van een endosoom aan motor-eiwitten die het endosoom verplaatsen naar het centrum van de cel. De interactie van Vps3 met Vps11 in het CORVET complex zorgt er voor dat Vps11 niet meer in staat is om met RILP een interactie aan te gaan. In het HOPS complex verbreekt de interactie van Vps39 met Vps11 deze binding met RILP niet. Deze vindingen laten zien dat deze gelijkende complexen genoeg van elkaar verschillen om hun functie op verschillende endosomen uit te voeren. Bovendien laat het zien dat een tether betrokken bij membraan fusie ook is verbonden met het transport van endosomen binnen de cel.

In **hoofdstuk 3** verdiepen wij ons in onze vondst dat Vps3 en Vps8 zich op recycling blaasjes bevinden, naast hun plaats op het vroege endosoom in het CORVET. We laten zien dat Vps3 en Vps8 een apart complex vormen wat het transport van vroege naar recycling endosomen reguleert. In samenwerking met het Vps33B/VIPAS39 complex en het SNARE eiwit VAMP3 reguleren ze het transport van integrines naar het recycling endosoom. Integrines zijn eiwitten die verantwoordelijk zijn voor de hechting van de cel aan zijn omgeving. Het specifiek verstoren van de productie van Vps3, Vps8, Vps33B of VIPAS39 heeft dan ook tot gevolg dat cellen zich minder goed kunnen hechten, spreiden en migreren. Ook wordt de vorming van de aanhechtingsstructuren van de cel, de focale adhesies, geremd. Deze route is specifiek voor integrines aangezien transferines, eiwitten waarvan bekend zijn dat ze via recycling endosomen worden getransporteerd, niet in de Vps3 en Vps8 gemarkeerde blaasjes voorkomen. Bovendien is het transport van transferines niet verstoord na inhibitie van Vps3, Vps8, Vps33B of VIPAS39. Deze bevindingen laten zien dat de

eiwitten waaruit het CORVET complex is opgebouwd ook buiten het complex een functie kunnen uitvoeren, het complex is dus dynamisch in zijn samenstelling.

In gepolariseerde cellen is het endo-lysosomale systeem anders ingericht dan in niet-gepolariseerde cellen. Gepolariseerde cellen, bijvoorbeeld epitheelcellen, vormen specifieke apicale en basolaterale plasmamembranen. Van deze membranen is gescheiden endocytose mogelijk en kunnen eiwitten afzonderlijk gerecycled worden. In gepolariseerde cellen is het complex van Vps33B en VIPAS39 belangrijk voor transport van apicale eiwitten. Mutaties in Vps33B of VIPAS39 kunnen de ziekte ARC-syndroom veroorzaken wat onder andere de lever en nieren aantast. Aangezien we de rol van Vps3 en Vps8 hebben kunnen koppelen aan de rol van het Vps33B/VIPAS39 complex, bestuderen we in **hoofdstuk 4** de rol van Vps8 in gepolariseerde cellen. We laten zien dat Vps8 verhoogd tot expressie komt in gepolariseerde cellen en lokaliseren Vps8 op gespecialiseerde apicale recycling endosomen. Het verhoogd tot expressie brengen van Vps8 heeft tot gevolg dat vroege endosomen zich opeenstapelen nabij de apicale recycling endosomen. Dit is een indicatie dat Vps8 een transportfunctie uitoefent tussen vroege endosomen en apicale recycling endosomen. Het verstoren van de Vps8 productie in de cel heeft tot gevolg dat HepG2 cellen verminderde apicaal-basolateraal polariteit vertonen en dat HeLa cellen een verminderde voor-achter polarisatie vertonen tijdens het migreren. Tevens verstoort Vps8 inhibitie het losmaken van de dochtercellen tijdens de celdeling, een proces waarvan bekend is dat het berust op de functie van het recycling endosoom. Uit deze resultaten concluderen wij dat Vps8 in gepolariseerde cellen een rol speelt in het transport van vroege endosomen naar apicale recycling endosomen.

Voordat de functie van Vps3 in het CORVET complex werd vastgesteld, was dit eiwit al eerder beschreven onder de naam TGF β Receptor Associated Protein 1 (TGFBRAP1). Het TGF β netwerk is van belang voor het reguleren van honderden genen in verschillende cellulaire processen zoals celdeling, weefsel homeostase en cel migratie. In **hoofdstuk 5** onderzoeken wij daarom de rol van Vps3/TGFBRAP1 in het TGF β signaleringsnetwerk. Vps3 bindt aan Smad4, wat na activatie van het TGF β netwerk naar de nucleus wordt getransporteerd om genen te reguleren. Wij wilden eten hoe de rol van Vps3 in het TGF β netwerk zich verhoudt tot de rol van endosomale tether. Wij laten we zien dat Vps3 en Vps8 verantwoordelijk zijn voor het rekruteren van Smad4 naar endosomen. We identificeren het endosoom als de lokatie in de cel waar Vps3-Smad4 binding plaats vindt en tonen aan dat ook andere Vps genen dan Vps3 betrokken zijn bij TGFbeta signaling. Het verstoren van de Vps3 of Vps8 productie in de cel heeft tot gevolg dat de TGF β receptor II zich in de cel ophoopt, wat wijst op verstoorte recycling. Dit is de eerste keer dat Vps3, in de context van het CORVET complex, gekoppeld wordt aan een moleculaire signalerings route.

Tijdens ons onderzoek naar het endo-lysosomale systeem vonden wij dat een veelvuldig gebruikte methode om eiwit expressie te verhogen in cellen, schade geeft aan endosomen. In **hoofdstuk 6** laten wij zien dat DNA transfectie-methodes die gebaseerd zijn op het polymeer polyethylenimine (PEI) het aantal vroege endosomen in een cel vermindert. PEI transfectie geeft echter geen meetbaar effect op de conditie van of het aantal lysosomen. De vermindering van het aantal vroege endosomen is tijdelijk. Invoering van een hersteltijd na toevoeging van het PEI polymeer resulteert in herstel van het endo-lysosomalesysteem. Voor het bestuderen van intracellulair transport en het endo-lysosomale systeem is het van belang om deze aanpassing in acht te nemen voor DNA transfectie-methodes die gebaseerd zijn op PEI.

In **hoofdstuk 7** worden de resultaten van het gehele proefschrift samengevat en bediscussieerd.

Acknowledgements/Dankwoord

Hier is het dan, eindelijk af! Het heeft een tijdje geduurd, maar dan heb je ook wat. Er is nu nog maar één ding te schrijven, het dankwoord. Het moeilijkste gedeelte om te schrijven, maar het leukste om te lezen. Ik hoop het niet, maar ik zal ongetwijfeld iemand vergeten in dit stuk te zetten, daarvoor alvast mijn excuses, in mijn volgend dankwoord zal je de eerste zijn.

To those reading this in English, I know most of you skipped here to see if I included you in the acknowledgements, of course you are! But even if you do not find your name below, know that you mean a lot to me and I couldn't have done it without you.

Allereerst wil ik **Judith** bedanken. Ik heb me tijdens mijn promotietraject altijd erg prettig gevoeld onder jouw leiding. In het begin vond ik het moeilijk om de vrijheid die je me gaf goed te benutten, maar gedurende de eerste jaren heb ik me daardoor juist snel kunnen ontwikkelen en heb ik ook nooit een 'nee' gekregen als ik nieuwe technieken wilde proberen. Dit heeft mij ontzettend veel geleerd en gaf me de motivatie om te blijven lezen, vragen en proberen. Om deze redenen heb ik ook erg uiteenlopend projecten gehad, wat ik misschien wel het leukste vond aan mijn AIO tijd. Om deze projecten bij elkaar in een proefschrift te brengen was qua schrijfwerk wel lastig en het heeft ook de nodige tijd gekost. De eerste fases van het schrijven van artikelen of hoofdstukken waren voor mij erg moeizaam, vooral omdat ik van mening was dat je het me allemaal maar veel te moeilijk maakte met alle comments. Naderhand en vooral tegen het einde was het me gelukkig allemaal duidelijk en was het schrijven iets geworden wat me voldoening bracht, dat had ik nooit kunnen bedenken. Deze lessen, vrijheid en het gevoel dat je aan mijn kant stond hebben mijn promotietraject tot een mooie en productieve tijd gemaakt en daar wil ik je dan ook ontzettend voor bedanken.

At the time of writing I do not know yet how difficult you will make my life at the defence, but I would like to thank all the committee members: **Marc Timmers, Rik Korswagen, Sven van IJzendoorn, Catherine Rabouille, Jaques Neeffes** and **Fulvio Reggiori** for your interest in my thesis and for taking part in this (for me) special event.

The department of cell biology at the UMC has been my home away from home for a couple of years now. To make the department what it is I would like to thank all the PI's **Judith, Madelon, Peter, Catherine, Paul, Fulvio** and **Ger** for their excellent choice in hiring such a great group of people and above all for the scientific conversations and assistance you offered. I want to give special thanks to **Catherine**, thank you very much for your interest in my projects and the many comments and questions that helped shape my thinking. You also taught me the important lesson never to thank someone for "allowing me to be in your lab/group", come up with something better to thank them for. Very useful information while writing acknowledgements. Also **Fulvio**, your comments during the progress report meetings were always right on the spot and I was sad to see you move so far away to Groningen. I enjoyed the time when you were still playing in the UMC football team, we never had a better defence. I also want to thank you for your support in all the movies we made over the year, you were a great tree. **Peter van der Sluijs**, bedankt voor

alle hulp met de biochemische experimenten, niks heeft mij zo goed troubleshooting geleerd als een colP die maar niet wil lukken. Ik denk niet dat ik ooit een blotje heb kunnen laten zien die aan jouw hoge kwaliteitseisen voldeed, maar dat geeft me iets om naar toe te werken.

Of course I want to thank all the people from the Klumperman group! It was a great experience working in the lab with all of you. I had an unbelievably great time with each and every one of you and I will miss you all when leave! Most importantly, I would have never made it to this point if it was not for you all. **Corlinda**, bedankt voor alle hulp in het lab in mijn hele AIO tijd en voor alle hulp met de Deltavision, mijn favoriete stuk werktuig in de hele afdeling. De Deltavision en ik hadden elkaar nooit ontmoet zonder jou. **Suzanne**, bedankt voor de noodhulp met EM gerelateerde vraagstukken, ik heb je zelfs in het weekend thuis nog kunnen bellen omdat de Jeol weer eens op tilt sloeg (dat was toen nog nieuw voor mij). **Ann**, voor morfologie vraagstukken kon ik altijd bij jou terecht, en ik voelde me altijd geweldig opgelucht als jij ook niet wist wat het was. Want als jij het niet weet, dan bestaat het niet. **Tineke**, ik vond het heel gezellig om met jou samen te werken. Je hebt me ontzettend geholpen door mij niet altijd zelf te laten aanploeteren, dat heeft me denk ik wel een jaar extra tijd gegeven en heeft een hoop mooie data opgeleverd. **George**, ook bij jou kon ik altijd terecht, als het nou ging om een luchtsluis die verkeerd stond in de EM, of een ringsleutel om mijn fiets te repareren, je hebt overal wel een oplossing voor. **Cilia**, ook al ben je er voor mijn gevoel nog maar net, het is alsof je al jaren meedraait. Heel erg bedankt voor ook jouw hulp met de EM en alle gezelligheid die je in de groep hebt gebracht. **René**, wat kan ik zeggen, jij bent de DJ geweest van mijn hele AIO periode. Ik heb zo veel nieuwe (oude) muziek leren kennen en dat maakt het eindeloos kwantificeren van oneindig veel cellen toch leuk. Ik kijk altijd uit naar jouw mailtjes met muzieklinkjes er in, misschien dat ik eens een verzamel CD ga maken van alle muziek die je me hebt gestuurd. Ook bedankt voor alle hulp met het afdrucken en inscannen en de hulp met illustrator, photoshop en indesign, dat heeft echt heel erg geholpen bij het in elkaar zetten van dit proefschrift en de artikelen. **Reini**, de altijd gelukkige, vrolijke en optimistische tornado die door de afdeling waait. Ik vind het echt geweldig om met je samen te werken, het is jammer dat ik de laatste tijden niet meer zo vaak in het lab sta, want het is supergezellig met jou in het lab. Jouw PhD wordt een mooie, je verzet nu al zo veel goed werk, dat kan alleen maar goed gaan, maar laat het werk je goede humeur nooit afpakken! Daarnaast wil ik je ook echt bedanken voor de koffiepauze, die je eigenhandig in oude glorie hebt hersteld, chapeau! **Nalan**, you also brought an amazing change to the group. Because of your expertise that lead to so many new techniques (which I never had a chance to use unfortunately ☹), and most of all because of your nice smile, optimism and kindness that always makes everyone happy. **Lisette**, bedankt voor alle goede zorgen en hulp die je altijd voor iedereen aanbied. Ik ben blij dat ik jou ook heb kunnen helpen met al die velocity data. **Job**, het was fijn om weer een man te hebben in deze groep met zo veel (lieftallige) dames. Bedankt voor je EM expertise die je in een mum van tijd hebt opgebouwd en veel succes met de laatste helft van je PhD. **Despina**, ik zou niet weten in welke groep jij nu precies thuishoort, je bent overal en zorgt voor iedereen. Het was gezellig boven in het lab, beneden in het lab en in het kantoor beneden, we hebben overal wel samen ergens gewerkt.

In the last couple of years I was evicted from the H-wing and went to an office in the notorious G-wing, home of those weird Wnt people. Luckily they took me in and I had a great time being the only H in the G. So thanks to the whole G-side: **Madelon, Ingrid, Peter van Kerkhof, Manja, Eline, Cara, Nicola, Tomica, Huiying** and **Mario**. Lieve **Ingrid**, bedankt voor alle hulp in het lab en ook vooral voor alle gezelligheid in het lab en ook daar buiten. Ik vond het super in de activiteitencommissie met jou, samen de borrels opzetten en dan tot het allerlaatst blijven om te zorgen dat alle drank op is. Je hebt het altijd zo druk, maar je maakt altijd tijd om mensen te helpen, en om bij alle gezellige bezigheden te zijn, zo'n postdoc wil ik ook zijn. **Eline**, je maakt de lunch altijd gezellig met al je verhalen over van alles en nog wat, en je hebt de periode overleefd waarin het vooral vieze mannenpraat was tijdens de lunch. Ookal kun je er zelf ook best wat van. Veel succes met het afronden straks! **Peter van Kerkhof**, bedankt voor de hulp met de virussen en de gradiënten, de oldschool technieken moeten niet verloren gaan, ik zal ze blijven gebruiken. **Nicola**, you brought a nice amount of liveliness in the hallways. I have learned a lot of recipes from you, and even more which recipes are not allowed to exist. Make sure you patrol around lunchtime as the pastapolic every now and then. **Manja**, I'm really glad you chose to join the department. Thanks for all the nice times around the office but also for all our nice arguments outside the lab, I know you secretly enjoy those too (say goodbye to your dragongate!!!). **Cara**, although I might not always agree with your pronunciation, you are a lot of fun to have around and I hope you will have a good time in the department. **Huiying**, thanks for the pen trick; I will keep working on it! **Mario**, the adopted child after the divorce, thanks for your punctuality. It was your disciplined regime that allowed us to eat on set times even in a lab full of mediterraneans and slavs that have no perception of time. Without you some of them probably would have starved to death. Also thanks for supporting the grapefruit cause, together we stand strong. And of course **Tomica!** my new neighbor. Thanks for all the illustration input and advice. I was afraid that nobody would be able to replace Maui as my office buddy, but you did very well, you just need to work on the looks. Have fun during your PhD and don't get diabetes, you chocolate addict.

In 2013 our department was overrun by a bunch of stem cell loving foxes with soxes. Everything was done to make sure the integration of this group went well. I thoroughly agreed with this and I think I integrated more than anyone. **Paul**, although you didn't decide to stay long, I can't thank you enough for bringing your lab over, for obvious reasons. The integration went very well and I want to thank all of the Cofferlab people for being such a good addition and for all the good times. So thanks **Enric, Cata, Sanne, Guy, Cindy, Jorg, Koen Braat, Koen Schepers, Luca, Magdalena, Cornelieke, Sandra, Anita, Stephin, Desiree, Janneke** and... **Ana** ☺. **Cata**, you were a great office buddy, thanks for all the laughs and advice, I would never have tried to eat fizzy vitamin tablets if it wasn't for you. **Enric** and **Miriam**, thanks for the science career advice but especially the G&T advice. I'm not sure it will ever be my favourite, but if you make it, I will have it. Let's have another soon! **Guy**, ondanks de kinderen toch bij alle "buitenschoolse" activiteiten van het lab aanwezig. Ik vind het jammer dat ik het lasergamen met Halloween had gemist, dit jaar hopelijk weer! **Cindy**, bedankt voor de goede hulp in de activiteitencommissie, het was leuk om weer aan alle activiteiten mee te kunnen doen toen jij het had overgenomen. Vooral de bierproeverij was erg leuk, wat jammer dat ik tweede was, ik dacht echt dat ik misschien wel had kunnen winnen (**Sanne!!!**). Alle andere office buddies, **Janneke, Anita, Stephin** en **Desiree**,

het was druk met z'n zessen maar wel heel erg gezellig, wij waren duidelijk het betere AIO hok van de twee. Ook **Jorg**, niet van de chipseq PC af te slaan, je was even onze 7de kantoorgenoot, maar ook met zoveel was het heel gezellig daar! And **Luca**, thanks for all the great times inside and outside the lab. It was great to have someone to share all the frustrations with that has such a similar view on things. You're a legend, don't forget to chill when you're wrapping up as well soon. Coocumbear.

Then our downstairs colleagues, **David, Daphne** and **Wienand**. I was mostly by myself in the lab downstairs, so it was great to have you around for good company. **Daphne**, sorry voor al het klagen over de klanten, jij kon er ook niets aan doen, maar ik had jarenlang het rijk voor mezelf alleen daar beneden, ik kon het moeilijk delen. Ik vond het heel gezellig beneden met jou. Bedankt voor alle hulp met onze rare burens, van ontplofte bierkratjes tot bedorven taarten, ik kon altijd op je rekenen om ze weer eens op het matje te roepen. **Wienand**, bedankt voor het gezelschap als ik weer eens beneden eindeloos op de PC beneden zat.

Dan terug naar boven naar alle ondersteuning. Het secretariaat: **Wieke** en **Betty**, en de teaching staff: **Rita, Maggy** en **Annemarie**. Bedankt voor alle gezelligheid in de afdeling. **Wieke** en **Betty** heel erg bedankt voor de jarenlange ondersteuning. Alle hulp met formulieren, creditcards en pakketjes verzenden, het zou niks zijn geworden zonder jullie. Ik kom altijd met vragen en moeilijke problemen, maar het is altijd gezellig bij jullie.

Then there is a very large group of people that I would like to thank: The people who left before I was finished; PhD students that finished before me, groups that moved, postdocs that found other jobs, people that retired and students that finished. So thank you: **Viola, Janice, Maaïke, Prajakta, Romain, Jan, Ineke, Francesca, Maui, Malik, Marc, Tobi, Emma, Adam, Guliani, Fabrizio, Muriel, Romina, Anneloes, Lieke, Nienke, Andri, Ruben, Susana, Eduardo, Jana, Rodrigo and Remko**. A very special thanks of course to my old supervisor, the person who brought me into the lab, my buddy, **Romain**. Thanks for everything man, you were a good supervisor (I will always apply your unique scoring system) and an even better friend. We had a lot of fun throughout the years in the lab and I know we will always be in touch. But now that the student has become the master, it's time that you fetch ME a beer. **Maui**, mijn kamergenootje, heel erg bedankt voor de gezelligheid maar ook voor de hulp met allerlei vreemde biochemische vragen en vragen over promotie dingen. Ik vond het heel leuk om naast jouw chaos te zitten en om met jouw eindeloze voorraden chocola en drop mee te genieten. Jouw speciale antistress methodes en de happylamp die ik van je heb geërft hebben me er doorheen geholpen, ik zal hem traditiegetrouw doorgeven aan de volgende stresser. **Malik**, my friend, I am very happy you were there in the department. We had some good science discussions and also a lot of non-science related discussions. Overall we had many, many, many discussions (e.g. the great pomelo debate of 2014), and most of them ended with the question if we wanted one more. Thanks for inviting us to Paris, it was amazing, I hope we can have a trip to (Kafé) België as well soon ☺. **Adam**, we had great time in the tiny lab downstairs, we would make great singers. We also would make great barefoot snooker players, hope to play with you again one day. **Jan**, thanks for all the humour and also the serious science conversations. We will see each other around for a while in Lombok. **Francesca**, it was great to have an Italian around that didn't have so much trouble

with everyone's cooking. Thanks for inviting us to your hometown, it was really amazing. **Muriel**, I really enjoyed our time in the lab and in the office together. We always had a laugh and joked around a lot. I also learned some valuable lessons from you on how not to comment on a lady's new clothes. I still feel guilty.

Natuurlijk had ik ook hulp in het lab in de vorm van studenten. Het is een mooie ervaring om mensen te trainen en daarna samen te kunnen werken. Daarom wil ik **Luke, Martijn en Jesse** bedanken voor de hulp in het lab. Ik hoop dat ik jullie de wetenschap interessant blijven vinden en dat jullie het ver schoppen. Succes!

Then a shout out to the incredible UMC football team. There were a lot of players over the years so I might forget some but thanks to **Arjan, Teun, Peter, Roberto, Salvatore, Arnold, Stefano, Dennis, Doron, Oliver, Cees, Alejo (& Ana), other Alejo** and **Alvaro**. It was great to be able to let go and just play some relaxed football every Thursday. Special thanks to **Arjan**, de organisator van het team. Ik kan niemand bedenken die zo goed dingen kan regelen terwijl je zo'n hekel aan dingen regelen hebt. Ook je hulp met de FACS, je bezoeken in het kantoor en de avondjes in België hebben me door de AIO tijd heen geholpen. En dan natuurlijk **Teun**, goede vriend en de allerbeste huisgenoot die je je kan wensen. Ik ben echt heel blij dat je in het huis kon trekken. Ik heb enorm respect voor je musicale enthousiasme en het is jammer dat onze band nooit van de grond is gekomen, maar je nieuwe band is veel beter en daarmee gaat het helemaal lukken. En dat allemaal naast je baan ben je een inspiratiebron van hoe je zoveel dingen tegelijkertijd kan doen, dat zal mij nooit lukken, want ik heb meer slaap nodig.

I would not have even made it to starting a PhD if it wasn't for some great internship supervisors. I did many internships that allowed me to really experience different fields of research and thereby choose my own path. So thanks to **Sandra Kling, Stephan Rudiger, Rutger Douma, Lodewijk de Jonge, Wouter van der Star, Brenda Vonk, Mahbub Rahman** and **Otto Schmidt**. **Sandra**, I spent the longest of all with you, I learned a lot from you and we had a lot of fun in the lab. I want to thank you for your inspiring laudatio at my master diploma ceremony.

Then I want to thank all **my fellow AIO's from the institute of biomembranes**. The IB AIO-evenings we had together were great. I learned a lot from your presentations and the comments you gave me for my presentations. There are too many fantastic people to name here, but if you read this, you know who you are. A special shout out to **Dorothee, Michiel** en **Raimond** samen met wie ik de intercity young scientist meeting heb mogen organiseren, het was een leuke ervaring en ik was trots op het resultaat.

Then to the **BMOL crew**. The group that stuck together after the master and shared the pleasure and pain of our jobs in science. We are now all starting to flock out, but it was great to have such a close group of friends undergoing similar situations to hang out with. So thanks **Tessa, João, Marcelo, Timo, Steven, Marti, Sacha** and **Ian** for all the great times, I know we will be in contact forever. **Tessa**, bedankt voor alle moeite om de hele groep altijd bij elkaar te krijgen. Jouw bent een fantastisch wetenschapper en je laat het er allemaal zo makkelijk uit zien, wat het natuurlijk niet altijd is. Ik weet zeker dat je het groot gaat maken daar in Cambridge, en ik

zal echt eens komen buurten, ook al zeg ik dat al jaren. **João**, its crazy how many Portuguese people I have met in Utrecht. Always the life of the party, mostly sober, you too made it seem so easy. I hope my defense will be close to that of yours. **Marcelo**, the man I learned the most Portuguese swearwords from. You are going to be the best integrated Portuguese in this country soon. Maybe this is caused by your enthusiastic affection for the locals here.. Now in Enschede, you will be Dutch soon man! **Timo**, bedankt voor het delen van lief en leed en etentjes en eindeloze Citadels-avonden. Ook voor hulp met microscopen en andere technieken kon ik bij je aankloppen. Daarnaast ook onze koffie@3 met mr de Maat was altijd een welkome afleiding. Ik ben blij dat je mijn paranimf bent. Speaking of Koffie@3, **Steven**, altijd gezellig met jou een praatje te maken. Jouw praktische kijk op zaken is vaak anders dan die van mij, maar je flikt het wel allemaal gewoon. Je klaagde altijd fijn mee over problemen op het lab, maar terwijl Timo en ik klagen over 3 keer op rij mislukte experimenten en andere problemen, waren jouw problemen meer: "Ik heb zo veel goede data, ik weet niet hoe ik het allemaal in mijn high impact paper kan krijgen". **Marti**, nu ben je veel op en neer aan het reizen en ben je er niet vaak meer bij, maar we hebben veel lol gehad in Utrecht. Met jouw enthousiasme hebben we veel gezellige uitgaansavondjes en bokbierfestivals meegepakt. **Ian**, although you left quite early for London, we had a great time in Utrecht. Your awesome place where we discussed football, science and religion, a mix for a guaranteed great evening. **Sacha**, het was goed om een mede Delftenaar tegen te komen in de master tussen al die rare Utrechters. Bedankt voor alle gezellige avondjes en feestjes waar we terecht kwamen.

Dan ook nog de andere mede Utrechters en pre-master collega's: **Lisette, Marijn, Vera** en **Hans**, het was heel gezellig in de premaster dankzij jullie. **Lisette**, bedankt voor het introduceren van Lombok, ik ben me er thuis gaan voelen, ik zie je wel weer eens rondfietsen.

Dan is het echt tijd om naar het support team uit Delft te gaan. Onze leuke vriendengroep en slingersvereniging: **Gudo, Nol, Tom, Imke, Lae, Eva** en **Maarten**. Jullie zijn allemaal fantastisch en zonder jullie was ik hier nooit gekomen. Bedankt voor de morele ondersteuning en het begrip om elke keer weer rare celbiologie-dingen aan te horen en die te begrijpen, of niet. **Gudo**, mijn broeder en vriend en nu ook paranimf, ik ben blij dat jij straks naast me staat tijdens de verdediging. Van je familie moetje het hebben en ik ben blij dat wij zo'n sterke band hebben. Speaking of family, **Lae**, bedankt voor al je aanmoedigingen en steun. Ook voor taaladviezen kon ik op je rekenen, ik hoop dat je geen taalvoutjes kunt vinden. **Nol**, je bent een van de weinigen die zich altijd kan herinneren waar ik aan werk in het lab, dat geeft de burger moed. Natuurlijk bedankt voor alle lol door de jaren heen, de band, de LAN, Napo en alle keren dat ik op je bank kon blijven crashen. **Tom**, ik heb met jou en een beetje dankzij jou mijn andere passie gevonden, het drummen (Heb je wel gut geüfnend?). Ik hoop dat we het ooit als ouwelullenband gaan maken, met jouw motivatie moet dat wel lukken. Dat geldt ook voor de rest van **HAPPY ACCIDENT**, we doen het niet voor de roem, maar we blijven het wel mooi doen (daar zit een liedje in). Met jullie in deze band spelen blijft een van de leukste dingen in het leven. **Eva**, jouw interesse en enthousiasme is aanstekelijk, het lijkt altijd wel of je overal mee bezig bent. Dat werkt motiverend voor anderen, ook al heb je dat misschien zelf niet door. Ook bedankt voor je geregeld in de uitjes en natuurlijk voor de groepsreisjes naar Frankrijk. **Imke**, ik was wel een beetje droevig toen je uit Utrecht verdween, het was gezellig om bij je te kunnen komen buurten

bij de daklava bijvoorbeeld. Het blijft leuk om met iemand nog de lomboknieuwtsjes te kunnen delen, ook al ben je zelfs nu soms beter op de hoogte dan ik. **Maarten**, bedankt voor het helpen terugvinden van mijn inner-nerd. Ook voor je whisky-adviezen, goede whisky is onmisbaar voor goed onderzoek.

Natuurlijk zijn er nog veel meer mensen uit Delft en omstreken te bedanken. **David, Jurren, Theo, Maylon, Nina, Wouter** en **Niki. Theo**, wij hebben elkaar gestimuleerd te blijven leren vanaf huiswerkklassen tot nu. Ik ben blij dat je ook geïnteresseerd bent in de biologie en het was leuk dat je in het lab langs bent geweest. Bedankt voor de voorstellingen van het koor, ik hoop je snel weer te zien zingen. **David**, bedankt voor de vele conceptuele discussies die wij tot laat voerden, dat heeft mijn denken echt gestimuleerd. **Maylon**, thanks for the great evenings in Den Haag and online. You tried to talk me into industry life instead of academia and me vice versa, but I guess we are both at a good place now.

Als het gaat om steun en motivatie is er niets dat je zo lang heeft gesteund als je familie. **Mam en pap**, dank jullie wel voor alles. Ik zou hier niet staan zonder al jullie hulp, steun en gedrevenheid. Als het om opvoeden en levenslessen gaat zijn jullie een perfect paar en vullen jullie elkaar helemaal aan. **Pap**, ik vond het altijd geweldig om mee te gaan naar de TU en het robotlab om daar te zien wat jullie deden. Ik heb me daardoor altijd heel erg aangetrokken gevoeld tot de sfeer van de academische wereld in de universiteit. Ik wist daarom al vroeg dat ik AIO wilde worden, ook al wist ik nog niet welk vakgebied. Jouw gehamer op cijfers en het meetrekken naar open dagen heeft me geholpen om te vinden wat ik zocht en ik ben je daar ontzettend dankbaar voor. **Mam**, jouw praktische kijk op moeilijke problemen van elke aard heeft me geholpen om alles met een gezonde psyche gedaan te krijgen. Om iets af te krijgen moet je gewoon beginnen. Als ik jou niet had gehad, was ik er nooit als een mornaal persoon uit gekomen. Ook jouw onverzettelijke steun waar ik altijd op kan vertrouwen laat me altijd tot rust komen. **Juliëtte**, lieve grote zus, ik ben blij dat ik met jou kan praten over mijn onderzoek omdat jij het tenminste begrijpt. Ik ben altijd trots geweest om zo'n slimme zus te hebben en daardoor ben je ook altijd een voorbeeld voor me geweest. Temeer omdat je altijd zoveel hebt gedaan en nog steeds doet, ook al zijn er momenten waarop het allemaal te veel is, je bent mentaal de sterkste persoon die ik ken. Samen met onze broers hebben we de grootste lol en ik kijk er altijd naar uit als we weer met z'n allen zijn. **Filip**, ook jij bent altijd een voorbeeld geweest en ik heb ontzettend veel van je geleerd. Dat is ook een beetje de rol van de oudste broer, het zal niet makkelijk zijn geweest, maar je deed en doet het perfect. Soms was je een voorbeeld van wat je juist niet moet doen, maar meestal ben je het beste voorbeeld voor wat je allemaal kan bereiken als je er gewoon voor gaat en het gewoon doet. Al dit praktisch en logisch denken moet ergens vandaan komen, en ik denk dat het mede van **oma** kwam. Oma, je wilde me niet beloven om bij mijn verdediging te zijn, uit praktisch oogpunt, een logisch denker ten top. Ik wil natuurlijk ook de rest van mijn ontzettend grote families bedanken aan zowel de **Kolstee** en **Jonker** kant, waar ik me altijd thuis bij heb gevoeld. Speciaal ook **oom Stefan**, bedankt voor alle hulp met de organische chemie in de vroege stadia van mijn master, ik vond het leuk om bij je komen buurten in het Went gebouw.

De seguida, gostaria de agradecer a minha outra família, **José e Maria Rita**. Obrigado por me acolherem de braços abertos na vossa casa e vida. Apesar de, por vezes, a comunicação ser

dificultada pela barreira linguística, sempre me senti otimamente acolhido por vocês e gosto sempre imenso de vos visitar em Portugal.

And lastly I would like to thank you mijn liefje, meu amor da minha vida, my everything, mijn **lieve Ana**. I cannot thank you enough for all the support you gave me. Tu estas sempre lá quando eu preciso-te. We are a perfect team, we even share a project in this thesis, together we can do anything! You have made me feel safe, loved, happy and supported throughout all the highs and lows of PhD life, which made it an endlessly better experience. I can't wait to start our next adventures together!

Curriculum Vitae

Caspar Theodorus Hugo Jonker was born on the 18th of May 1986 in Delft, The Netherlands. In 2003 Caspar finished the higher general secondary education at St. Stanislas college with the course profiles Nature & Technology and Nature & Biology. In 2004 he started his Bachelor of Applied Sciences degree in Biotechnology (BA Sc) at Inholland University in Delft. He realized that classic biotechnology techniques in industry were not his main interest and he therefore enrolled in many extra internships to work in biochemistry, microbiology and cell biology in academia. In 2004 he worked as a student assistant as an Atomic Force Microscope (AFM) technician following an internship at the Quantative Imaging group provided by prof. Ted Young at the Technical University Delft, faculty of Applied Sciences. In 2005 he completed an internship at the Insect Molecular Biology Research group of prof. Otto Schmidt at Adelaide university, School of Agriculture, Food and Wine in Australia, Investigating LPS-induced coagulation of lipophorin particles in the cell free immune response of *E. Kuehniella*. In 2006 he worked as an intern at the Environmental Biotechnology research group of dr. Cristian Piciooreanu at the Technical university of Delft in the department of Biotechnology investigating anaerobic ammonium oxidation in *Brocadia anammoxidans* and assessing hydrazine metabolism stages in the oxidation reaction. In 2007 he did an internship at DSM Food Specialties, R&D genetics department in the group of dr. Gerard C.M. Selten on a project that focused on PrsA overexpression in *Bacillus Subtilis* to enhance Amylase secretion for large scale production. In 2008 Caspar finished his Bachelor of Applied Sciences degree after a final internship at the Bioprocess Technology group of prof. J.J. Heijnen at the Technical University of Delft, department of Biotechnology investigating new possibilities for rapid sampling techniques used for intracellular metabolite analysis of *Penicillium Chrysogenum*. The many internships in academia motivated Caspar to apply for a Master of Science (MSc) degree in Biomolecular Sciences at Utrecht University. In 2008 he started the pre-master program and started the Master program in 2009. Before completing the master degree in 2011, he worked as an intern at the Cellular Protein Chemistry group of dr. Stefan Rüdiger at Utrecht University. There he investigated the interaction of molecular chaperone Hsp90 with oncogenic kinases. Additionally he worked as an intern at the group of prof. Judith Klumperman at the University Medical Center Utrecht (UMCU) investigating the role of the CORVET component Vps8 in intracellular trafficking. The projects and techniques used in this lab peaked his interest and he applied for a PhD position in the same lab in 2011. The projects focused on the role of multisubunit tethering complexes in the mammalian endolysosomal system. During his PhD Caspar organized a 2 day conference for PhD students across the Netherlands in the field of cell biology, the Intercity Young Scientist Meeting (IYSM). He also attended the 2013 conference of the European study group on lysosomal disease conference in Leibnitz, Austria, where he won the ESGLD Young Scientist Award. In 2015 he attended EMBO conference: The multidisciplinary era of endocytic mechanics and functions in Mandelieu-la-Napoule, France where he won the poster award for his work on the CORVET tethering complex. The results of his work on the CORVET multisubunit tethering complex are described in this thesis.

Publications

- **Jonker CT**, van der Kant R, Wijdeven RH, Bakker J, Janssen L, Klumperman J, Neefjes J (2015) Characterization of the Mammalian CORVET and HOPS Complexes and Their Modular Restructuring for Endosome Specificity. *J Biol Chem.* 2015 Dec 18;290(51):30280-90. doi: 10.1074/jbc.M115.688440. Epub 2015 Oct 13. PMID:26463206
- Galmes R, ten Brink C, Oorschot V, Veenendaal T, **Jonker CT**, van der Sluijs P, Klumperman J (2015) Vps33B is required for delivery of endocytosed cargo to lysosomes. *Traffic.* 2015 Dec;16(12):1288-305. doi: 10.1111/tra.12334. Epub 2015 Oct 21. PMID: 26403612
- Douma RD, de Jonge LP, **Jonker CT**, Seifar RM, Heijnen JJ, van Gulik WM (2010) Intracellular metabolite determination in the presence of extracellular abundance: Application to the penicillin biosynthesis pathway in *Penicillium chrysogenum*. *Biotechnol Bioeng.* 2010 Sep 1;107(1):105-15. doi: 10.1002/bit.22786. PMID: 20506508
- (Thesis) Sandra Kling (2010). "Helping Hands – Molecular chaperones for Protein Kinases"; Chapter2: Destabilisation of c-Src is insufficient to induce Hsp90 binding